

**Investigation of DNA adducts formed in cells and  
clinical tumour biopsies following exposure to  
platinum-containing anticancer drugs**

**Ian William Harry Jarvis**



Thesis submitted to Newcastle University for the degree of  
Doctor of Philosophy

January 2011

Northern Institute for Cancer Research

Faculty of Medical Sciences

Newcastle University

# Acknowledgements

I would like to extend a massive thank you to my supervisors Dr. Mike Tilby and Dr Gareth Veal for their advice and support during the course of my Ph.D., and I am especially grateful for their hard work during my write-up period. My time with Mike and Gareth has been extremely enjoyable and I have been inspired and encouraged by both of them to embark on a career in science.

I am eternally grateful to all the staff at Durham University who have assisted me with both their technical expertise and time. Special thanks go to Dr Chris Ottley and Professor D. Graeme Pearson for their assistance with ICP-MS. I am also grateful to all the supervisors and staff at Newcastle University who assisted me with both their technical expertise and time. Special thanks go to Dr Joe Gray and Mr Robert Liddell for their MALDI-TOF work and to Professor Bernard Golding and Professor William McFarlane for their assistance with NMR.

I would also like to thank the members of the NICR who have been helpful in the lab, in particular the molecular pharmacology team, and all the staff who have all taught me techniques or been especially helpful in the laboratory. Thanks also to the friends I have made over the past four years at the NICR who are too exhaustive to list – we've had some good times and I shall miss you all.

I would also like to thank my sponsors, Cancer Research UK, for providing funding for this project. I thank the BACR for providing funding to attend conferences both at home and international.

Finally, I am grateful to both my family and my wonderful girlfriend Sarah for their constant love and support, both financially and emotionally, especially during the tense write up period. I can never thank them sufficiently and I love you all.

## Abstract

Platinum-based anticancer drugs are believed to exert their action through chemical reactions with genomic DNA, forming adducts with DNA bases. Although the pharmacology of such adducts has been widely studied, the cytotoxic mechanism remains unclear. The possibility that non-DNA molecules have the potential to alter the types of adducts formed has received very little attention, and limited information is available on the levels of adducts formed in clinical tumours. Further understanding of platinum-DNA adduct formation may be important in explaining the efficacy of platinum-based drugs in different tumour types, providing insights into both the cytotoxic mechanism and the development of clinical resistance.

The aims of the work described in this thesis were: a) to analyse the nature of DNA adducts formed by three clinically used platinum-based anticancer drugs and to investigate the potential intracellular formation of additional types of adducts to those previously characterised on pure DNA; b) to determine platinum-DNA adduct levels formed in solid ovarian cancer tissue following treatment of patients with carboplatin and test the hypothesis that these levels are comparable to the levels of DNA adducts formed in blood cells; and c) to determine whether sodium thiosulfate (STS), which is currently in clinical trials to protect against cisplatin-induced normal tissue toxicity, impacts on DNA adduct formation.

Analysis of the properties of all DNA adducts formed in cells was made possible by analysing enzymatically digested DNA using anion exchange chromatography together with inductively-coupled plasma mass spectrometry (ICP-MS). Putative adducts involving deoxyguanosine monophosphate cross-linked via cisplatin to glutathione were prepared and the chromatographic properties determined. Studies were carried out to characterise the types of adducts formed following incubations of cisplatin with four cancer cell lines. No additional types of adducts were observed compared to those formed by the reaction of cisplatin with pure DNA. The chromatographic behaviour of adducts formed in cells incubated with carboplatin and oxaliplatin were comparable to those formed by cisplatin.

This study is the first to investigate carboplatin-DNA adduct levels induced in solid tumours during therapy in patients. Total DNA adduct levels in tumour biopsies and blood cells were measured using ICP-MS with thallium as an internal standard. Tumour biopsies from all four patients studied showed clearly detectable levels of treatment-induced DNA adducts ranging from 1.9 - 4.2 nmoles Pt/g DNA. Blood cell adduct levels ranged from 0.15 – 3.5 nmoles Pt/g DNA. Both tumour and blood cell adduct levels were significantly above background measurements. No correlation was observed between adduct levels in DNA from biopsies and levels in DNA from peripheral blood cells.

Concurrent incubation of four human tumour cell lines with cisplatin and STS caused greater than 2-fold decreases in total DNA adducts. Delayed administration of STS had no effect of adducts levels. STS did not appear to affect the chromatographic behaviour of DNA adducts formed in cells following incubation with cisplatin.

# Declaration

I certify that no part of the material documented in this thesis has previously been submitted for a degree or other qualification in this or any other university and that all of the work described in this thesis has been carried out by me with the following exceptions:

1. MALDI-TOF mass spectrometry was carried out by Mr Robert Liddell and Dr Joe Gray, Pinnacle Lab, Newcastle University.
2. NMR spectrometry was carried out by Professor William McFarlane, School of Chemistry, Newcastle University.
3. Patient pharmacokinetic analysis was carried out by Dr Gareth Veal, NICR, Newcastle University.

# Abbreviations

(w/v)	Weight per Volume
(v/v)	Volume per Volume
A	Adenine
AAS	Atomic Absorption Spectrometry
AG	Adenine-Guanine
AL <sub>50</sub>	Adduct level required to achieve 50% growth inhibition
dAMP	5'-Deoxyadenosine Monophosphate
ATP	Adenine Triphosphate
BER	Base Excision Repair
c/s	Cycles per second
C	Cytosine
CBDCA	cyclobutane dicarboxylate
CPS	Counts-per-second
dCMP	5'-Deoxycytidine Monophosphate
DACH	1,2-diaminocyclohexane
DB	DNA Buffer
DMSO	Dimethyl Sulfoxide
DNA	Deoxyribonucleic Acid
EDTA	Ethylenediaminetetraacetic Acid

FCS	Foetal Calf Serum
FDA	Food and Drug Administration
FPLC	Fast Protein Liquid Chromatography
G	Guanine
GG	Guanine-Guanine
GI <sub>50</sub>	Concentration required causing 50% Growth Inhibition
dGMP	5'-Deoxyguanosine Monophosphate
GSH	Glutathione
GSSG	Glutathione Disulphide
GST	Glutathione-S-transferase
HA	Hydroxyapatite
HPLC	High Performance Liquid Chromatography
i.a.	Intra-arterial
ICP-MS	Inductively-Coupled Plasma Mass Spectrometry
i.v.	Intravenous
kDa	Kilodaltons
KP	Potassium Phosphate
MALDI	Matrix Assisted Laser Desorption/Ionisation
MDR	Multidrug Resistance
MHz	Megahertz

MMR	Mismatch Repair
MRP	Multidrug Resistance Associated Protein
MS	Mass Spectrometry
MT	Metallothionein
MW	Molecular Weight
NER	Nucleotide Excision Repair
NICR	Northern Institute for Cancer Research
NMR	Nuclear Magnetic Resonance
OD	Optical Density
PB	Phosphate Buffer
PB-MNC	Peripheral Blood MonoNuclear Cells
PBL	Peripheral Blood Lymphocytes
PBS	Phosphate-Buffered Saline
PD	Pharmacodynamics
PK	Pharmacokinetics
PPB	Parts per billion
PPM	Parts per million
PPT	Parts per Trillion
Rb	Retinoblastoma Protein
RNA	Ribonucleic Acid

RPM	Revolutions per Minute
RPMI	Roswell Park Memorial Institute
SD	Standard Deviation
SRB	Sulphorhodamine B
STS	Sodium Thiosulfate
T	Thymine
TCA	Trichloroacetic Acid
TMP	5'-Thymidine Monophosphate
TOF	Time of Flight
TS	Thiosulfate
UV	Ultraviolet

# Table of Contents

## Chapter 1

<b>Introduction</b>	<b>1</b>
<b>1.1: Cancer and Cancer Treatment</b>	<b>1</b>
1.1.1: Cancer	1
1.1.1.1: The origin of the word cancer	1
1.1.1.2: What is cancer?	2
1.1.2: Cancer treatment	7
1.1.2.1: Surgery	7
1.1.2.2: Radiotherapy	7
1.1.2.3: Chemotherapy	8
<b>1.2: Platinum Complexes</b>	<b>12</b>
1.2.1: Discovery of cisplatin	12
1.2.2: Cisplatin – from bench to bedside	14
1.2.3: Carboplatin	16
1.2.4: Oxaliplatin	18
<b>1.3: Molecular mechanism of action of platinum complexes</b>	<b>20</b>
1.3.1: Identification of genomic DNA as the principle target for platinum complexes	20
1.3.2: Behaviour of platinum complexes in cells and tissues	21
1.3.3: Platinum-DNA (Pt-DNA) adducts formed by platinum complexes	23
<b>1.4: Resistance to Platinum Complexes</b>	<b>31</b>
1.4.1: Decreased Drug Accumulation	33
1.4.2: Inactivation of Platinum Complexes	35
1.4.3: DNA Repair	36
	10

1.4.4: Defective Apoptosis Response	40
<b>1.5: Cell death induced by platinum complexes</b>	<b>41</b>
<b>1.6: Adduct levels in clinical samples of cancer patients</b>	<b>43</b>
<b>1.7: Glutathione</b>	<b>45</b>
1.7.1: Intracellular chemistry and redox state of glutathione	45
1.7.2: GSH and platinum drug resistance	47
1.7.3: Evidence for potential GSH-Pt-DNA cross-links	48
1.7.4: Potential clinical implications of GSH-Pt-DNA cross-links	54
<b>1.8: Sodium thiosulfate</b>	<b>56</b>
1.8.1: Sodium thiosulfate as a chemo-protective agent	56
<b>1.9: Aims of this study</b>	<b>60</b>

## **Chapter 2**

### **Materials and Methods 62**

<b>2.1: Materials</b>	<b>62</b>
2.1.1: Reagents	62
2.1.2: Solutions and Buffers	63
2.1.3: Enzymes	66
<b>2.2: Tissue Culture</b>	<b>67</b>
2.2.1: Equipment	67
2.2.2: Cell lines	67
2.2.3: Maintenance of cell lines	68
2.2.4: Counting cells	68
2.2.5: Cryogenic storage and resuscitation of frozen cells	69
<b>2.3: Exposure of cells to cytotoxic drugs</b>	<b>70</b>
<b>2.4: Sulphorhodamine B colorimetric assay</b>	<b>71</b>

<b>2.5: DNA extraction</b>	<b>72</b>
2.5.1: DNA extraction using hydroxyapatite	72
2.5.2: DNA extraction using QIAGEN Blood and Cell Culture DNA midi kit	74
2.5.3: Measurement of DNA concentration	76
<b>2.6: Enzymatic digestion of platinated DNA</b>	<b>78</b>
<b>2.7: Reactions of cisplatin with nucleic acids</b>	<b>80</b>
2.7.1: Reaction of cisplatin with highly purified calf thymus DNA in the presence or absence of GSH or STS	80
2.7.2: Reaction of cisplatin with deoxyguanosine monophosphate (dGMP) in the presence or absence of GSH or STS	81
<b>2.8: Gel filtration chromatography</b>	<b>82</b>
<b>2.9: Anion exchange chromatography</b>	<b>84</b>
<b>2.10: Graphite furnace Atomic Absorption Spectrometry (AAS)</b>	<b>87</b>
<b>2.11: Inductively-Coupled Plasma Mass Spectrometry (ICP-MS)</b>	<b>90</b>
<b>2.12: Matrix-Assisted Laser Desorption/Ionisation Time-of-Flight Mass Spectrometry (MALDI-TOF)</b>	<b>100</b>
<b>2.13: Nuclear Magnetic Resonance Spectrometry (NMR)</b>	<b>102</b>
<b>2.14: Statistical analysis</b>	<b>104</b>

## **Chapter 3**

### **In vitro characterisation of potential new Pt-DNA adducts formed in the presence of glutathione** **105**

<b>3.1: Introduction</b>	<b>105</b>
<b>3.2: Chromatographic system</b>	<b>109</b>
<b>3.3: Results</b>	<b>110</b>
3.3.1: Characterisation of the chromatographic system using mononucleotides	110

3.3.2: Anion exchange separation of enzymatically digested calf thymus DNA	115
3.3.3: Identification of products formed in the reaction of cisplatin with 5'-deoxyguanosine monophosphate	119
3.3.3.1: Preliminary Identification of products formed between cisplatin and dGMP	120
3.3.3.2: Determination of the chemical nature of the products formed between cisplatin and dGMP	125
3.3.3.3: Timecourse of the formation of products between cisplatin and dGMP	130
3.3.3.4: MALDI-TOF mass spectrometric analysis of products formed in the reaction of cisplatin and dGMP	133
3.3.4: Identification of products formed in the reaction of platinated dGMP with GSH	138
3.3.4.1: Incubation of cisplatin with GSH	139
3.3.4.2: Identification of products formed in the reaction of cisplatin-dGMP with GSH	141
3.3.4.3: Analysis of the three peaks identified in the reaction of GSH with platinated dGMP	144
3.3.5: Structural analysis of products formed in the reaction of platinated dGMP with GSH	148
<b>3.4: Discussion</b>	<b>149</b>

## **Chapter 4**

### **Analysis of Pt-DNA adducts formed in cells 151**

<b>4.1: Introduction</b>	<b>151</b>
<b>4.2: Results</b>	<b>153</b>
4.2.1: Sensitivity of human tumour cells to Pt-drugs	153
4.2.1.1: Determination of optimal seeding density	153

4.2.1.2: Determination of sensitivity to Pt drugs	155
4.2.1.3: Total Pt-DNA adducts formed in cells	164
4.2.2: Chromatographic Analysis of Pt-DNA adducts formed in cells	171
4.2.2.1: DNA adducts formed in cells exposed to cisplatin for 24hr	172
4.2.2.2: DNA adducts formed in cells exposed to carboplatin for 24hr	176
4.2.2.3: DNA adducts formed in cells exposed to oxaliplatin for 24hr	179
4.2.2.4: DNA adducts formed in LoVo cells exposed to drugs for 2hr	183
4.2.3: Pt-DNA adducts formed on purified DNA in the presence of GSH	187
4.2.3.1: The effect of GSH on overall Pt-DNA adduct level	189
4.2.3.2: Effect of GSH on total Pt-DNA adduct level	191
4.2.3.3: Effect of GSH on the formation of specific types of Pt-DNA adducts	194
<b>4.3: Discussion</b>	<b>205</b>

## **Chapter 5**

### **Characterisation of cisplatin-DNA adducts formed in the presence of sodium thiosulfate 212**

<b>5.1: Introduction</b>	<b>212</b>
<b>5.2: Results</b>	<b>215</b>
5.2.1: Overall Adduct Level	216
5.2.1.1: Effect of STS on total Pt-DNA adduct level	218
5.2.1.2: Reaction of cisplatin with STS	221
5.2.2: Effect of STS on the formation of Pt-DNA adducts in pure DNA	223
5.2.3: Effect of STS on the reaction of cisplatin with dGMP	226
5.2.4: Effect of STS on the antiproliferative activity of cisplatin in human tumour cell lines	229

5.2.5: Effect of STS on growth inhibition by cisplatin	231
5.2.6: Effect of STS on total Pt-DNA adduct formation	236
<b>5.3: Discussion</b>	<b>240</b>

## **Chapter 6**

### **Investigation of adducts formed in biopsies from ovarian cancer patients following treatment with carboplatin 244**

<b>6.1: Introduction</b>	<b>244</b>
<b>6.2: Study Methods</b>	<b>248</b>
6.2.1: Patient Details	248
6.2.2: Treatment Schedule and Sampling Time	250
6.2.3: Preparation of blood samples at the Queen Elizabeth Hospital	251
6.2.4: Sample Handling in the NICR	252
6.2.5: Samples for checking the techniques and reagents to be used	253
6.2.6: ICP-MS analysis	253
6.2.7: Data Analysis	254
<b>6.3: Results</b>	<b>256</b>
6.3.1: Patient Pharmacokinetics	256
6.3.2: Determination of background Pt levels in control samples	259
6.3.3: Analysis of Pt-DNA adducts levels in patient blood samples	263
6.3.4: Analysis of Pt-DNA adducts in patient tumour biopsies	266
<b>6.4: Comparison of patient pharmacokinetic parameters with adduct levels</b>	<b>269</b>
<b>6.5: Comparison of adduct levels in blood cells and tumour</b>	<b>271</b>
<b>6.6: Discussion</b>	<b>273</b>

## **Chapter 7**

<b>Final Discussion</b>	<b>277</b>
<b>7.1: Introduction</b>	<b>277</b>
<b>7.2: Effects of GSH and STS on cisplatin-DNA adduct formation in cells</b>	<b>278</b>
<b>7.3: Can GSH and STS be cross-linked to DNA by cisplatin?</b>	<b>279</b>
<b>7.4: Nature of Pt-DNA adducts formed in cells</b>	<b>283</b>
<b>7.5: Effect of STS on the antiproliferative activity of cisplatin in human tumour cell lines</b>	<b>286</b>
<b>7.6: Analysis of Pt-DNA adducts in relation to growth inhibition data</b>	<b>288</b>
<b>7.7: Analysis of Pt-DNA adducts formed in tumour biopsies and blood cells of ovarian cancer patients treated clinically with carboplatin</b>	<b>290</b>
<b>7.8: Overall Conclusions</b>	<b>293</b>
<b>References</b>	<b>294</b>
<b>Appendix</b>	<b>337</b>

# List of Figures

Figure 1.1	Acquired Capabilities of Cancer cells	2
Figure 1.2	The chemical structure of diamminedichloroplatinum in cis- and trans isomers	12
Figure 1.3	Scanning electron micrograph of E.coli	13
Figure 1.4	The chemical structure of carboplatin	17
Figure 1.5	The chemical structure of oxaliplatin	19
Figure 1.6	Different chemical species of cisplatin	22
Figure 1.7	Diagrams of the known adducts formed by the reaction of cisplatin with DNA	28
Figure 1.8	Postulated mechanisms of resistance to cisplatin	32
Figure 1.9	The chemical structure of reduced glutathione	45
Figure 1.10	MonoQ elution profile for digested calf thymus DNA and Mor/p DNA incubated with cisplatin from Azim-Araghi 2003	50
Figure 1.11	MonoQ elution profile for digested calf thymus DNA incubated with cisplatin and GSH from Azim-Araghi 2003	51
Figure 1.12	Trans-labilisation of cis-DDP and trans-DDP by GSH	55
Figure 1.13	The chemical structure of sodium thiosulfate	56
Figure 2.1	Enzymatic hydrolysis of DNA to mono- and di-nucleotides	78
Figure 2.2	Typical standard curve used for AAS	89
Figure 2.3	Typical standard curve used on the Sciex Elan ICP-MS	94
Figure 2.4	Typical standard curve used on the Element2 ICP-MS	99
Figure 3.1	Typical MonoQ elution profiles for individual mononucleotides	111
Figure 3.2	Typical MonoQ elution profile for a mixture of the four mononucleotides	112
Figure 3.3	Analysis of absorbance of dAMP, dCMP, dGMP and TMP in the UV region 210-320 nm	113
Figure 3.4	Typical MonoQ elution profile for enzymatically digested calf thymus DNA incubated with or without cisplatin	117

Figure 3.5	Typical MonoQ elution profile for cisplatin	122
Figure 3.6	Typical MonoQ elution profile for cisplatin incubated with dGMP	123
Figure 3.7	Typical MonoQ elution profile for 1mM cisplatin incubated with 1 mM dGMP for 24hr	124
Figure 3.8	Typical MonoQ elution profile for cisplatin-dGMP incubated with dGMP	127
Figure 3.9	Typical MonoQ elution profile for cisplatin-dGMP incubated with NaCl	128
Figure 3.10	Typical MonoQ elution profile for cisplatin-dGMP incubated with NaOH	129
Figure 3.11	Timecourse of the decrease in free dGMP in the reaction of equimolar cisplatin and dGMP	131
Figure 3.12	Timecourse of the formation of four products during the reaction of equimolar cisplatin and dGMP	132
Figure 3.13	Typical MALDI-TOF mass spectrometry analysis of products formed in the reaction of equimolar cisplatin and dGMP after a 24hr incubation	135
Figure 3.14	Typical MALDI-TOF mass spectrometry analysis of products formed in the reaction of equimolar cisplatin and dGMP after a 24hr incubation	136
Figure 3.15	Typical MonoQ elution profile for cisplatin incubated with GSH	140
Figure 3.16	Typical MonoQ elution profile for cisplatin incubated with dGMP then incubated with GSH	142
Figure 3.17	Typical MonoQ elution profile for cisplatin-dGMP incubated with GSH for 24hr	143
Figure 3.18	Analysis of the changes in peak area for the four products identified in the reaction of equimolar cisplatin with dGMP	146
Figure 3.19	Analysis of the changes in peak area for the products identified in the reaction of equimolar cisplatin with dGMP followed by further incubation with GSH	147

Figure 4.1	Typical analysis of growth of 833K, A2780, LoVo and MorCPR cells	154
Figure 4.2	The effect of cisplatin on growth inhibition in human tumour 833K, A2780, LoVo and Mor/CPR cells	157
Figure 4.3	The effect of carboplatin on growth inhibition in human tumour 833K, A2780, LoVo and Mor/CPR cells	158
Figure 4.4	The effect of oxaliplatin on growth inhibition in human tumour 833K, A2780, LoVo and Mor/CPR cells	159
Figure 4.5	Total Pt-DNA adducts levels formed in human tumour 833K, A2780, LoVo and Mor/CPR cells following incubation with various concentrations of cisplatin	165
Figure 4.6	Total Pt-DNA adducts levels formed in human tumour 833K, A2780, LoVo and Mor/CPR cells following incubation with various concentrations of carboplatin	166
Figure 4.7	Total Pt-DNA adducts levels formed in human tumour 833K, A2780, LoVo and Mor/CPR cells following incubation with various concentrations of oxaliplatin	167
Figure 4.8	Typical MonoQ elution pattern for 833K, A2780, LoVo and Mor/CPR cells incubated with cisplatin for 24hr	174
Figure 4.9	Typical MonoQ elution pattern for 833K, A2780, LoVo and Mor/CPR cells incubated with carboplatin for 24hr	177
Figure 4.10	Typical MonoQ elution pattern for 833K, A2780, LoVo and Mor/CPR cells incubated with oxaliplatin for 24hr	180
Figure 4.11	Typical MonoQ elution pattern for LoVo cells incubated with cisplatin, carboplatin or oxaliplatin for 2hr	185
Figure 4.12	Typical Sephadex G-75 gel elution profiles of calf thymus DNA incubated with cisplatin and GSH	190
Figure 4.13	Effect of increasing GSH concentration on total adducts formation of cisplatin-DNA adducts	193
Figure 4.14	Typical MonoQ elution pattern for calf thymus DNA incubated with cisplatin for 2hr	195
Figure 4.15	Typical MonoQ elution pattern for calf thymus DNA incubated with cisplatin and GSH	196

Figure 4.16	Typical MonoQ elution pattern for calf thymus DNA incubated with cisplatin for 1hr	201
Figure 4.17	Typical MonoQ elution pattern for calf thymus DNA incubated with cisplatin for 1hr followed by incubation with GSH	202
Figure 5.1	Typical Sephadex G-75 gel elution profiles of calf thymus DNA incubated with cisplatin and STS	217
Figure 5.2	Effect of increasing STS concentration on the level of total adducts formed on DNA by cisplatin	220
Figure 5.3	Typical MonoQ elution profile for cisplatin incubated with STS	222
Figure 5.4	Typical MonoQ elution profile for enzymatically digested calf thymus DNA digested after reaction with cisplatin	224
Figure 5.5	Typical MonoQ elution profiles for enzymatically digested calf thymus DNA digested after reaction with cisplatin and STS	225
Figure 5.6	MonoQ elution profile for equimolar cisplatin and dGMP incubated for 24hrs and with STS for 24hrs	228
Figure 5.7	Incubation schedule for exposure of human tumour cell lines to cisplatin in the presence and absence of STS	230
Figure 5.8	The effect of concurrent administration of STS on growth inhibition by cisplatin in 833K, A2780, LoVo and Mor/CPR cells	232
Figure 5.9	The effect of sequential administration of STS on growth inhibition by cisplatin in 833K, A2780, LoVo and Mor/CPR cells	233
Figure 5.10	The effect of delayed administration of STS on growth inhibition by cisplatin in 833K, A2780, LoVo and Mor/CPR cells	234
Figure 5.11	Changes in total Pt-DNA adducts formed in 833K, A2780, LoVo and Mor/CPR cells following incubation with cisplatin	237

Figure 5.12	Analysis of total cisplatin-DNA adduct level in 833K, A2780, LoVo and Mor/CPR cells following incubation with cisplatin and STS	238
Figure 6.1	Concentrations of unbound Pt in the plasma of four patients after a 30 minute infusion of carboplatin	258
Figure 6.2	Summary of the source of the 13 biopsy pieces used in this study for measuring Pt-DNA adducts in patient tumours following carboplatin administration	267
Figure 6.3	Relationship between patient AUC and Pt-DNA adduct levels in PB-MNCs and human tumour biopsies	270
Figure 6.4	Relationship between in vivo Pt-DNA adducts levels in PBLs and human tumour biopsies	272

## List of Tables

Table 2.1	Chromatographic gradient used for selective elution of mono- and di-nucleotides from the MonoQ column	86
Table 2.2	Furnace program used for determination of Pt concentration	88
Table 2.3	Standards used for calibration of the Element2 ICP-MS	96
Table 2.4	Isotopes detected by the Element2 ICP-MS	97
Table 3.1	Average retention times on MonoQ column for the four mononucleotides	114
Table 3.2	Chromatographic separation of enzymatically digested pure DNA reacted with cisplatin	118
Table 4.1	GI <sub>50</sub> values for 833K, A2780, LoVo and Mor/CPR human tumour cells exposed to cisplatin, carboplatin and oxaliplatin for 2hr, 6hr and 24hr	160
Table 4.2	GI <sub>50</sub> ratios for 833K, A2780, LoVo and Mor/CPR cells incubated with cisplatin, carboplatin or oxaliplatin	161
Table 4.3	GI <sub>50</sub> ratios for 833K, A2780, LoVo and Mor/CPR cells incubated with carboplatin or oxaliplatin compared to cisplatin	162
Table 4.4	Ratio of GI <sub>50</sub> values for A2780, LoVo and Mor/CPR cells to 833K GI <sub>50</sub> values	163
Table 4.5	Pt-DNA adduct levels in human tumour 833K, A2780, LoVo and Mor/CPR cells following incubation with various concentrations of cisplatin for 2hr and 24hr	168
Table 4.6	Pt-DNA adduct levels in human tumour 833K, A2780, LoVo and Mor/CPR cells following incubation with various concentrations of carboplatin for 2hr and 24hr	169
Table 4.7	Pt-DNA adduct levels in human tumour 833K, A2780, LoVo and Mor/CPR cells following incubation with various concentrations of oxaliplatin for 2hr and 24hr	170

Table 4.8	Mean retention times for the products detected by UV absorbance and ICP-MS in DNA extracted from cisplatin-treated cells	175
Table 4.9	Mean retention times for the products detected by UV absorbance and ICP-MS in DNA extracted from carboplatin-treated cells	178
Table 4.10	Mean retention times for the products detected by UV absorbance and ICP-MS in DNA extracted from oxaliplatin-treated cells	181
Table 4.11	Pt content of each of the four main peaks of Pt-containing material recovered from anion exchange chromatographic analysis of enzymatic hydrolysates of DNA extracted from drug-treated cells	182
Table 4.12	Pt content of each of the four main peaks of Pt-containing material recovered from anion exchange chromatographic analysis of enzymatic hydrolysates of DNA extracted from drug-treated LoVo cells	186
Table 4.13	Pt-DNA adduct levels for calf thymus DNA mixed with GSH, then incubated with cisplatin for 2hrs and 24hrs	192
Table 4.14	Mean retention times for the products detected by UV absorbance and ICP-MS in purified DNA exposed to cisplatin in the presence and absence of GSH	197
Table 4.15	Percentage of the Pt in peaks formed in calf thymus DNA incubated with cisplatin and GSH for 2hr and 24hr	198
Table 4.16	Mean retention times for the products detected by UV absorbance and ICP-MS in purified DNA exposed to cisplatin in the presence and absence of GSH	203
Table 4.17	Percentage of the Pt in peaks formed in calf thymus DNA incubated with cisplatin then GSH for 2hr and 24hr	204
Table 4.18	AL <sub>50</sub> values for 833K, A2780, LoVo and Mor/CPR cells exposed to cisplatin, carboplatin or oxaliplatin	210
Table 4.19	Ratios of 2hr and 24hr GI <sub>50</sub> and AL <sub>50</sub> values for 833K, A2780, LoVo and Mor/CPR cells exposed to cisplatin, carboplatin or oxaliplatin	211

Table 5.1	Overall Pt-DNA adducts levels formed by the reaction of cisplatin with pure DNA in the presence of varied concentrations of STS	219
Table 5.2	GI <sub>50</sub> values for 833K, A2780, LoVo and Mor/CPR cells incubated with cisplatin and STS	235
Table 5.3	Effect of STS of cisplatin-DNA adducts formation in four cell lines exposed to cisplatin	239
Table 6.1	Pt concentration and total adduct level in control mouse kidney tissues	261
Table 6.2	Pt concentration and total adduct level in control human blood	262
Table 6.3	Pt concentrations and adduct level in patient pre-carboplatin blood samples	264
Table 6.4	Pt concentrations and adduct level in patient post-carboplatin blood samples	265
Table 6.5	Pt concentration and adduct level in patient biopsies	268

# **Chapter 1**

## **Introduction**

### **1.1: Cancer and Cancer Treatment**

#### **1.1.1: Cancer**

##### **1.1.1.1: The origin of the word cancer**

The Edwin Smith papyrus (*c*1600 B.C.) and the Ebers papyrus (*c*1550 B.C.) are believed to be two of the oldest surgical documents, and the first to describe tumours of the breast and uterus respectively. Furthermore, they are based on material from a thousand years earlier. The term cancer however is credited to the Greek physician Hippocrates (460-370 B.C.) who used the terms *carcino's* and *carcinoma* to describe non-ulcer-forming and ulcer-forming tumours. In Greek terminology these words refer to the crab, probably applied describing the spreading projections from a cancer in a similar manner to that of the shape of the crab (Diamandopoulos 1996). Some of the earliest direct evidence of cancer was found in bone tumours in ancient Egyptian mummies.

### 1.1.1.2: What is cancer?

Cancer is a non-specific term that describes a group of diseases characterized by deregulated growth mechanisms. Normal cells acquire the ability to proliferate abnormally to form tumours, which can be benign or malignant. This “transformation” from normal to cancerous cells is a multi-stage process, and major advances have been made in demonstrating that many of the steps involved reflect genetic alterations or abnormalities. Normal cells acquire tumorigenic potential as a result of an initiating factor causing mutations, for example chemicals or radiation. Mutations can also occur through spontaneous DNA damage. Hanahan and Weinberg proposed that the transformation of cells to a cancerous genotype involves six hallmark characteristics, shown in Figure 1.1 (Hanahan and Weinberg 2000). A brief description of each proposed acquired potential is given below.

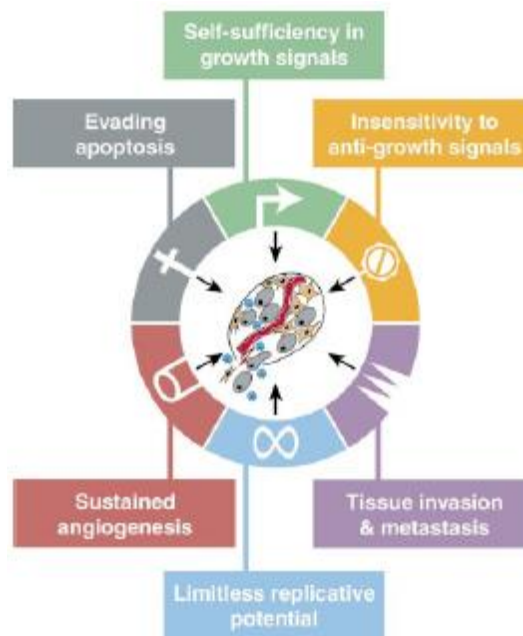


*Figure 1.1: Acquired capabilities of cancer cells (Hanahan and Weinberg 2000).*

*Acquired Capability: Self-sufficiency in growth signalling*

In normal cells, mitogenic growth signal cascades control the progression from a quiescent state into an active proliferative state. Oncogenes are mutated forms of proto-oncogenes usually involved in the positive regulation of this progression. Activation of proto-oncogenes can occur through point mutations, amplification, translocation and/or epigenetic up-regulation, causing normal cells to grow uncontrollably and giving them a selective growth advantage. Examples of these include growth factors such as platelet-derived growth factor and tumour growth factor  $\alpha$  (Fedi et al 1997) and growth factor receptors such as EGF-R/*erb2* and HER2/*neu*, both up-regulated in stomach and breast cancers (Yarden and Ullrich 1988, Slamon et al 1987). Growth signalling autonomy can also arise through alterations in the downstream signalling circuitry that processes growth signalling, such as the SOS-Ras-Raf-MAPK cascade. The Ras protein has been found to be structurally altered in approximately 25% of human tumours, allowing continuous signalling without stimulation from their normal upstream regulators (Medema and Bos 1993).

*Acquired Capability: Insensitivity to anti-growth signalling*

Normal cells and tissues receive multiple anti-proliferative signals which act to either force cells into the quiescent ( $G_0$ ) state of the cell cycle, or to permanently relinquish their proliferative capabilities. Tumour suppressor genes code for proteins that function in the opposite manner to that of oncogenes, with a primary function of slowing cell division and maintaining genetic stability. At the molecular level, many, if not all anti-proliferative signals are processed by the retinoblastoma protein (pRb) (Hanahan and Weinberg 1996), which in its hyperphosphorylated form, blocks progression from  $G_1$  to S phase in the cell cycle (Weinberg 1995). Functional impairment of tumour suppressor

gene signalling can be a result of reduced expression, mutation or deletion and leads to uncontrolled cellular growth and genetic instability. The anti-proliferative signalling circuit that acts through pRb is disrupted in a majority of human cancers (Dyson et al 1989, Fyran and Reiss 1993, Markowitz et al 1995, Schutte et al 1996, Chin et al 1998).

*Acquired Capability: Evasion of apoptosis*

Programmed cell death (apoptosis) is a process that maintains the healthy development of multi-cellular organisms, and evidence suggests the apoptotic program is present in virtually all cell types found throughout the body. The ability of tumour cell populations to expand is determined both by the ability of the population to maintain proliferation, and also to evade apoptosis. Acquired resistance to apoptosis is a hallmark of most types of cancer and can occur through a variety of mechanisms. The most commonly occurring loss of pro-apoptotic regulation involves mutation of the p53 protein, and inactivation of p53 is found in greater than 50% of human cancers (Anthoney et al 1996, Harris 1996, Soussi and Wiman 2007), although not all cancers are hallmarked by p53 mutations (Peng et al 1993). Loss of the tumour suppressor pTEN has been linked to mitigating apoptosis (Cantley and Neel 1999), and mechanisms for avoiding death signals conveyed through the FAS receptor have been found in lung and colon cancers (Pitti et al 1998).

*Acquired Capability: Limitless replicative potential*

Cellular senescence is a phenomenon that stops cells from proliferating indefinitely, effectively giving cells a finite lifespan. Immortality genes allow cells to proliferate indefinitely. Cancer cells are often described as immortal, and this may be attributed to

up-regulation of telomerase, an enzyme that adds specific DNA repeats (3'-TTAGGG-5') to the ends of telomeres (Zakian 1995). Telomeric DNA comprises tandem repeats that protect the chromosome from degradation. During replication DNA is shortened and in normal dividing cells critical shortening of telomeres can cause cells to stop replicating and senesce (Harley et al 1990, Hastie et al 1990). Up-regulation of telomerase enables cancer cells to overcome telomere shortening by continually synthesising the repeat sequence, effectively immortalizing the cells. This has been demonstrated in many different tumour types (Kim et al 1994, Hiyama et al 1995 (a), Hiyama 1995 et al (b), Langford et al 1995, Hiyama et al 1996, Shay and Wright 1996, Wright et al 1996).

*Acquired Capability: Sustained angiogenesis*

Cell function and survival is critically dependent on a constant supply of oxygen and nutrients provided by the vasculature. This dependence on supply obliges virtually all cells to reside within 100 µm of a capillary blood vessel (Hanahan and Weinberg 1996). This closeness is maintained during organogenesis, and the process of angiogenesis is closely regulated. It was initially assumed therefore that proliferating cells were intrinsically able to stimulate blood vessel development, but the evidence suggested otherwise. Proliferating cells initially lack angiogenic signalling capacity, and the ability to induce and sustain angiogenesis is therefore a critical step in tumour development. This ability is believed to be acquired during tumour development through an “angiogenic switch”, and this was found to be activated in mid-stage lesions, prior to full tumour appearance, although the mechanisms involved are poorly understood (Reviewed in Hanahan and Folkman 1996). Angiogenesis inhibitors have been found to impair the growth of human tumour cells inoculated into mice (Folkman

1997) and tumours in cancer-prone transgenic mice have demonstrated susceptibility (Bergers et al 1999), further supporting the essential role of angiogenesis in tumour development.

*Acquired Capability: Tissue invasion and metastasis*

In addition to the alterations described above, full malignancy is associated with the spread of tumour cells outside of the site of origin, invading neighbouring tissues and allowing the tumours to metastasise. Metastasis describes the movement and subsequent re-development of cancer cells from their primary site to secondary locations around the body, facilitated by transport through the vasculature. Metastasis is a defining event in cancer and is believed to account for 90% of human cancer deaths (Sporn 1996). Invasion and metastasis are complex mechanisms, and the genetics and biochemical processes involved are incompletely understood.

### **1.1.2: Cancer treatment**

Early detection of cancerous cells significantly improves outcome for patients, increasing the potential for complete elimination of the malignant population. However, in many cases by the time of diagnosis the tumour has already metastasised and invaded vital organs, complicating treatment and resulting in poorer prognosis. Cancer therapy is therefore often multi-modal, involving surgery, radiotherapy and/or chemotherapy.

#### **1.1.2.1: Surgery**

For established solid cancers, removal of the tumour by surgery is the preferred approach to treatment. In the early stages of tumour development surgery can be curative, as can cyto-reduction surgery followed by chemotherapy. However surgery has many limitations and excision of the full tumour from essential organs such as the brain or lungs is often not possible. For most haematological cancers, such as leukaemia, lymphoma and myeloma, surgery is not an option. Furthermore for cancers that have spread through metastasis, surgery is mainly of palliative value to patients.

#### **1.1.2.2: Radiotherapy**

There are three main divisions of radiotherapy used clinically: external beam radiotherapy, brachytherapy (sealed source radiotherapy) and systemic radioisotope therapy (unsealed source radiotherapy). Conventional external beam radiotherapy consists of a single beam of ionising radiation, often in the form of x-rays, being

delivered to the patient from several directions but is limited by collateral damage to surrounding tissues. Stereotactic and 3-D conformal radiotherapy were developed in an attempt to reduce the collateral damage, and involve focusing directed beams of radiation to the tumour using well defined scans and images of the tumour. Particle therapy is another form of external beam radiotherapy that involves directing energised particles (protons or carbon ions) to the tumour. Brachytherapy is delivered by placing the radiation source directly at the site of treatment, which limits the irradiation to a localized area and minimises surrounding tissue damage, allowing for higher doses of radiation to be used. Brachytherapy is commonly used in the treatment of cervical, prostate and breast cancer (Gaffney et al 2007, Morris et al 2009, Polgar and Major 2009). Systemic radioisotope therapy generally involves infusion of isotopes either alone, or coupled to another molecule or antibody to target specific tissues. A major use of systemic radiotherapy is in the treatment of bone metastasis (Lin and Ray 2006). Radiotherapy however is not effective as a single modality treatment for cancer, and as with surgery, radiotherapy has limited application in haematological malignancies. For advanced metastatic cancers, radiotherapy is mainly of palliative value.

### **1.1.2.3: Chemotherapy**

One of the major advantages of chemotherapy over alternative treatments is the potential to treat tumours that have metastasised or which are in surgically inaccessible locations. Chemotherapy is generally divided into two categories; cytotoxic chemotherapy and targeted chemotherapy. Cytotoxic chemotherapy kills cancer cells through the inhibition of replication and mitotic division. There are numerous classes of cytotoxic chemotherapeutic agents that elicit their effect in a number of ways and show

varying efficacy against different tumour types. The cytotoxic agents were amongst the earliest anticancer drugs to be discovered at a time when the underlying biology of cancer was poorly understood. The first cytotoxic agents to demonstrate anti-tumour activity were the mustards, developed after the discovery that soldiers exposed to “mustard gas” (1,5-dichloro-3-thiapentane) during World War One often presented with leukopaenia (Reviewed in Hall and Tilby 1992). Although treatment of superficial tumours with small quantities of liquid sulfur mustard was possible, damage to surrounding tissue was severe and administration was a hazard for both patient and clinician. During the Second World War, in an effort to create improved chemical warfare agents, the sulfur atom of mustard gas was replaced by an amine. These new “nitrogen mustards” were less reactive than their sulfur counterpart, and were entered into clinical trials in 1942, although no data was published until 1946 due to wartime secrecy constraints. Many derivatives of the nitrogen mustards were synthesised and tested in animal tumour systems, and it was shown that having a benzene ring coupled to the nitrogen mustard reduced the reactivity of the chloroethyl groups of the mustard. This increase in the chemical half life of the drug allowed more effective distribution throughout the body. After nitrogen mustard itself (mechlorethamine), chlorambucil was the first analogue of this type to be successful in clinical practice, and is still used today in the treatment of chronic lymphocytic leukaemia (CLL) (Begleiter et al 1994, Begleiter et al 1996). During the second half of the 20<sup>th</sup> century a number of major cytotoxic drugs were discovered through screening programmes.

The vast majority of cytotoxic agents act to kill cells by disrupting DNA function and synthesis, with the notable exceptions of the vinca alkaloids and the taxanes which disrupt microtubule dynamics. Cytotoxic agents may act through chemical reactions

with DNA to form adducts (alkylating and platinating agents), blocking synthesis of DNA precursors (anti-metabolites), blocking enzymes that control DNA structure (topoisomerase poisons), or by affecting microtubule metabolism (tubulin binding agents). The platinum-based chemotherapy drugs are sometimes described as being “alkylating-like” agents as they form adducts on DNA but they do not contain an alkyl group.

It is generally thought that dividing cells are more susceptible to cytotoxic chemotherapy. Rapidly dividing cells, such as cells in bone marrow, hair follicles and the intestinal lining are frequent sites of toxicity (Corrie 2004). Dysregulation of cell growth and cell cycle checkpoints, both common hallmarks of many cancers, could potentially explain why cancer cells can be more susceptible to cytotoxic drugs compared to normal tissues.

The cytotoxic agents have generally been used clinically with limited or no understanding of their mechanism of action. This contrasts to targeted agents, which are being developed strategically to target a specific characteristic of a tumour. The first successful small molecule drug of this class was the tyrosine kinase inhibitor Imatinib (Glivec). This works by blocking the active site of the fused bcr-abl protein, a product of the rearranged genes in the Philadelphia chromosome. It is used for chronic myeloid leukaemia (CML) and gastrointestinal stromal tumours (GISTs) (Kantarjian et al 2001, Kantarjian and Talpaz 2001, Eisenberg et al 2003). Trastuzumab (Herceptin) is a monoclonal antibody that was designed to target the HER2/*neu* receptor, amplified in breast cancer. It has had a significant impact in the treatment of metastatic HER2<sup>+</sup> breast cancer (Baselga et al 1998, Baselga et al 1999). Although there have been

important advances in targeting tumours for many types of cancer, cytotoxic chemotherapy is likely to remain the most effective treatment for the immediate future, and seems likely to continue to play an important role in combination with new targeted agents, particularly drugs that inhibit DNA repair, such as inhibitors of PARP (Calabrese et al 2004, Curtin 2005) and DNA PK (Salles et al 2006, Zhao et al 2006, Bolderson et al 2009). It is therefore important to continue to improve our understanding of the precise mechanisms involved in the anticancer activity of both newer and more established agents.

## 1.2: Platinum Complexes

### 1.2.1: Discovery of cisplatin

Diamminedichloroplatinum (DDP) is an inorganic compound with platinum (II) atom co-ordinated to two ammonia molecules and two chlorine atoms. It was first described by Michel Peyrone in 1845 and originally known as Peyrone's salt (Peyrone 1845). The chemical structure was elucidated in 1893 by Alfred Werner (Werner 1893) and is shown in Figure 1.2.

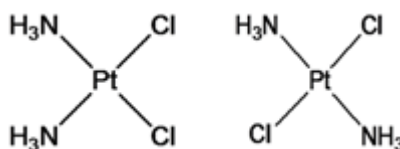


*Figure 1.2: The chemical structure of diamminedichloroplatinum (II) in cis- and trans-isomers*

Diamminedichloroplatinum (II) was re-discovered in 1965 at Michigan State University by Dr Barnett Rosenberg (Rosenberg et al 1965). Rosenberg was investigating the effects of electric fields on growth processes of *Escherichia coli* cells. Experiments were carried out in a continuous culture chamber in a chemically defined medium. Importantly this growth medium contained ammonium chloride. The electric current was applied using an audio oscillator generating between 50 and  $10^5$  c/s frequency (alternating current). Platinum electrodes were chosen as they were believed to be chemically inert and alternating current chosen to eliminate the effects of electrolysis and electrode polarization.

Microscopic examination of the *E. coli* cells showed that cell division ceased after 1-2 hours of exposure to the electric field. However the bacteria continued to elongate, growing unusually long and filamentous, to up to 300 times their normal length of between 2 – 5  $\mu\text{m}$  as shown in Figure 1.3 (Rosenberg et al 1965). Further investigation concluded that the reason for the inhibition of bacterial cell division was not the action of the electric field directly on the cells, but platinum-containing chemical species formed between the platinum electrodes and the bacterial growth medium containing ammonium chloride. Many platinum-containing complexes were discovered in the media, with the most biologically active being the chemically neutral diamminedichloroplatinum (II) (Rosenberg et al 1965, Rosenberg 1967 et al (a). Rosenberg further concluded that it was the *cis*- conformation (*cis*-DDP) and not the *trans*- conformation that was the active species (Rosenberg 1967 et al (a), Rosenberg et al 1967 (b)).

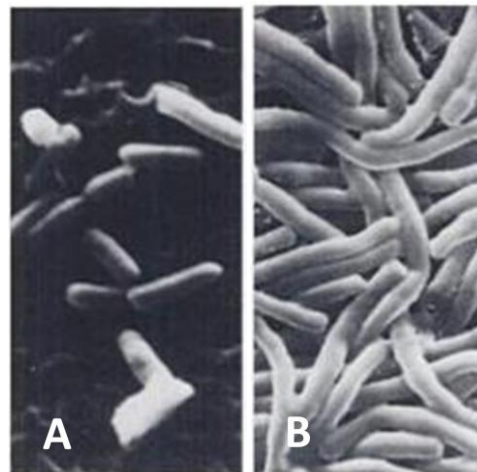


*Figure 1.3: Scanning electron micrograph of E. coli grown in normal media (A) and in normal media containing low levels of cis-DDP (B). Figure taken from Lippert 1999*

### 1.2.2: Cisplatin – from bench to bedside

Following on from the interesting results found in bacteria, Rosenberg hypothesised that *cis*-DDP might be effective at inhibiting cell division in mammalian cells, and investigated the effects on two murine cell lines implanted into mice (Sarcoma 180 and Leukaemia L1210). *Cis*-DDP was injected i.p. at 0.5 – 2.0 mg/kg daily and 1.25 – 10.0 mg/kg daily for mice implanted with Sarcoma 180 and L1210 cells respectively. There was a marked difference between the treated groups compared with the untreated, with *cis*-DDP causing tumour regression, and a complete cure in mice which were kept alive for 6 months (Rosenberg et al 1969). Following confirmatory *in vivo* investigations which were carried out at the Chester Beatty Institute (UK), *cis*-DDP was entered into clinical trials in 1970, with encouraging results obtained despite toxic side effects (Kelland 2007). The first patients were treated with *cis*-DDP in 1971, and the drug was approved for clinical use by the Food and Drug Administration (FDA) against metastatic testicular and metastatic ovarian cancer in 1978, under the generic name cisplatin.

Cisplatin is currently used clinically in the treatment of a variety of different cancers as a single agent, or more commonly, as part of combination therapies. Administration is generally intravenous, and adults typically receive doses of 50 – 100 mg/m<sup>2</sup> repeated every 3 to 4 weeks (McKeage 1995). Prior to the introduction of cisplatin, the cure rate for testicular cancer was approximately 10%. However, currently more than 90% of patients are cured after undergoing surgery and chemotherapy, and this improvement was mainly due to the introduction of cisplatin in combination therapy. Ovarian cancer response rate to chemotherapy prior to the introduction of cisplatin was between 30-

60%, with 5 year survival less than 10% (Young et al 1974). Use of cisplatin as a single agent showed a response rate of 50% in previously untreated patients, and in combination with doxorubicin this rose to between 55-96% (Cvitkovic et al 1977). Cisplatin use in ovarian cancers however has been widely superseded by carboplatin (discussed in section 1.2.3). Cisplatin is also an important drug in combination therapy for treatment of bladder cancer (Noguchi et al 1992, Keane et al 1994, Hussain et al 2001), and in other cancers such lung and neuroblastoma (Meczes et al 2002, Lee et al 2004, Mishima et al 2004, Hirose et al 2006, Feliu et al 2009).

Clinically, despite its broad spectrum of activity, cisplatin is very toxic and causes severe side effects in some patients even following single doses  $\geq 50 \text{ mg/m}^2$ . These include nephrotoxicity, ototoxicity, myelosuppression, neurotoxicity, and also nausea and vomiting (McKeage 1995). Less common side effects that have been linked to cisplatin include pancreatitis, seizures and vision loss (Loehrer and Einhorn 1984). Nephrotoxicity is potentially the most severe side effect encountered in cisplatin-treated patients, and involves cumulative damage to both tubules and glomeruli (Weiner and Jacobs 1983, McKeage 1995). Saline hydration can be used to decrease nephrotoxicity, but it does not completely prevent the damage (Hayes et al 1977, Al-Sarraf et al 1982). Cisplatin induced ototoxicity is cumulative with treatment, and causes irreversible damage to the inner ear cells (Rybak et al 2005, Thomas et al 2006). Myelosuppression is considered a mild toxicity which allows combination of cisplatin with other highly myelosuppressive agents (McKeage 1995). Cisplatin causes leukopaenia in up to 50% of patients, with a typical onset of between 6-26 days, and recovery occurring between days 21-45 (Von Hoff et al 1979). Cisplatin also causes thrombocytopaenia in nearly half of all patients, with a typical onset between 10 to 26 days, whilst recovery occurs

between days 22 to 45 (Von Hoff et al 1979). Anaemia has also been reported in some patients (Von Hoff et al 1979). Neurotoxicity presents often in the form of peripheral neuropathy, seizures and muscle cramps (Cersosimo 1989, Harmers et al 1991). Nausea and vomiting can last up to 24 hours after treatment, though is easily treatable with anti-emetics. Toxicity limits administration of higher doses of cisplatin and can result in early cessation of therapy.

### **1.2.3: Carboplatin**

In an effort to improve the efficacy of platinum drugs and decrease the severe toxicities associated with cisplatin, other platinum-containing compounds were screened for anticancer activity (Kelland 2007). One of the most successful of these compounds was *cis*-diammine-[1,1-cyclobutanedicarboxylato] platinum (II), (*cis*-Pt(NH<sub>3</sub>)<sub>2</sub>CBDCA-*O,O'*) (Figure 1.4) developed in an industry-academia collaboration between the Institute of Cancer Research (ICR) in London, and Johnson-Matthey Plc (Reviewed in Kelland 1993 and Kelland 2007). *Cis*-Pt(NH<sub>3</sub>)<sub>2</sub>CBDCA-*O,O'* proved significantly less toxic than cisplatin, particularly to the kidneys and nervous system (McKeage 1995, Ozols et al 2003), whilst maintaining comparable anti-tumour activity, especially in ovarian cancer (Aabo et al 1998, Sandercock et al 2002, Ozols et al 2003). It is thought that the more stable bound CBDCA leaving group is the reason for greater stability of the compound and the decrease in toxicity compared to cisplatin.

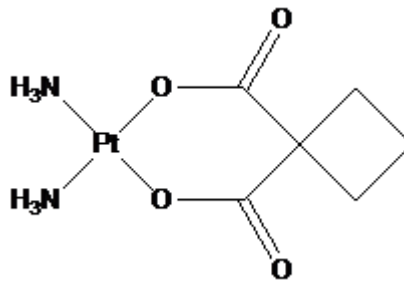


Figure 1.4: The chemical structure of carboplatin

*Cis*-Pt(NH<sub>3</sub>)<sub>2</sub>CBDCA-*O,O'* was approved by the FDA for palliative treatment of ovarian cancer following previous chemotherapy in 1989, and as a first-line agent against ovarian cancer in 1991, under the generic name carboplatin. Currently, carboplatin is widely used in the treatment of advanced ovarian cancer in combination with paclitaxel (Sandercock et al 2002). Carboplatin has also been used in combination treatments for hormone refractory prostate cancer (Urakami et al 2002), nephroblastoma (Kremens et al 2002) and non-small cell lung cancer (Vieitez et al 2003).

Long-term follow up studies of renal function in patients treated with carboplatin showed no significant effects on renal function (Mason 1991), although carboplatin at doses higher than 1200 mg/m<sup>2</sup> has been associated with reductions in glomerular filtration rate in over 50% of patients (Gore 1987). Typical doses for adults receiving carboplatin are between 250-400 mg/m<sup>2</sup> (McKeage 1995) or doses based on individual patient GFR (Calvert et al 1989). Haematological toxicity is the major dose-limiting toxicity associated with carboplatin, with thrombocytopenia a greater problem than leukopenia at conventional doses (Calvert et al 1982, Curt et al 1983). Carboplatin is often used in high-dose chemotherapy (greater than 1200 mg/m<sup>2</sup>) due to its lack of non-haematological toxicities, although more than 90% of patient's present grade IV

neutropaenia and thrombocytopaenia in these regimes. Carboplatin has also been linked with ototoxicity in humans and animals (Kennedy 1990, McAlpine and Johnstone 1990) but this is only dose-limiting when carboplatin dosing is greater than 2000 mg/m<sup>2</sup> (Kennedy et al 1990, McAlpine and Johnstone 1990, Neuwelt et al 1996). Compared to cisplatin, carboplatin is associated with greatly reduced neurological toxicity (Shea et al 1989) and is considerably less emetogenic (Harvey et al 1991).

#### **1.2.4: Oxaliplatin**

Oxaliplatin (1R,2R-diaminocyclohexane)oxalatoplatinum(II) (Figure 1.5) was originally discovered in 1976 at Nagoya City University, Japan (Kidani et al 1978). It was licensed to Debiopharm for development as a treatment for advanced colorectal cancer. Sanofi-Avensis gained the license in 1994, and oxaliplatin became licensed for clinical use in Europe in 1996 under the trade name Elaxotin. The FDA initially approved oxaliplatin for treatment of metastatic colorectal cancer (second line) in 2002, and as a first line agent in 2004 (Kelland 2007). Oxaliplatin is based on the 1,2-diaminocyclohexane carrier ligand (DACH), and is a more water soluble derivative of the failed drug tetraplatin (Kelland 2007). DACH compounds were thought to be promising as drugs development targets due to their lacking of the major toxicities of cisplatin and carboplatin (Burchenal et al 1979, Hoeschele et al 1994, Monti et al 2005). Also, of particular importance, cells resistant to cisplatin have demonstrated a lack of cross-resistance with oxaliplatin (Fukuda et al 1995, Rixe et al 1996).

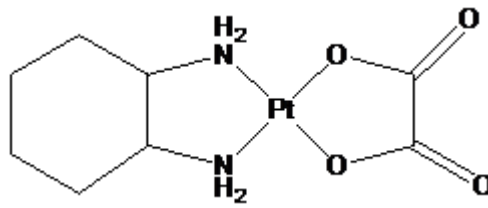


*Figure 1.5: The chemical structure of oxaliplatin*

Oxaliplatin has demonstrated modest activity when used as a single agent in the treatment of colorectal cancer (Machover et al 1996) but greater activity when used in combination with 5-fluorouracil and folinic acid (Levi et al 1992). Neither cisplatin nor carboplatin demonstrate any significant clinical activity against colorectal cancer. Oxaliplatin has also been reported to have activity as both a single agent (Misset et al 1991) and in combination with cisplatin and/or paclitaxel (Soulie et al 1997, Faivre et al 1999, Delalogue et al 2000, Piccart et al 2000) in the treatment of ovarian cancer.

The major dose limiting toxicity with oxaliplatin is peripheral neuropathy, associated with acute paraesthesia of the lips and extremities, and peripheral sensory neuropathy can develop with repeated treatment (Extra et al 1990). Other toxicities associated with oxaliplatin include myelosuppression, emesis and gastrointestinal tract toxicity. Nephrotoxicity observed following oxaliplatin treatment is far less severe than that associated with cisplatin allowing administration of oxaliplatin without hydration (Cassidy and Misset 2002).

### **1.3: Molecular mechanism of action of platinum complexes**

#### **1.3.1: Identification of genomic DNA as the principle target for platinum complexes**

Platinum complexes can react with many molecules in the intracellular environment including DNA, RNA, proteins, membrane phospholipids and cytoskeletal microfilaments (Akaboshi et al 1992, Kopf-Maier and Muhlhausen 1992, Speelmans et al 1996, Speelmans et al 1997). It is commonly accepted that platinum binding to DNA is responsible for the major cytotoxic effects of platinum complexes (Jamieson and Lippard 1999, Wong and Giandomenico 1999) although only 5-10% of the total platinum binding is to DNA, with the majority (85-90%) binding to proteins (Fuertes et al 2003).

Some of the earliest evidence that identified DNA as the principal cellular target was the filamentous growth of bacteria induced by cisplatin (Rosenberg et al 1965, Witkin 1967). This is a common attribute to DNA damaging agents such as UV and ionising radiation. DNA damaging agents also cause lysis of *E. coli* cells containing bacteriophage  $\lambda$ , and this phenomenon was demonstrated with cisplatin (Reslova 1971). Most of this initial evidence was obtained in bacteria. Investigation of DNA, RNA and protein synthesis using radiolabelled precursors provided early indications that DNA was also the target for cisplatin in mammalian cells. DNA synthesis was inhibited when cells were exposed to cisplatin, but there was no effect on RNA or protein synthesis (Harder and Rosenberg 1970, Howle and Gale 1970), further implicating DNA as the principle target. Additional studies investigating the mechanisms are discussed in

greater detail in section 1.3.3, providing further evidence supporting DNA as the principle target (Roberts and Pascoe 1972, Fichtinger-Schepman et al 1985).

### **1.3.2: Behaviour of platinum complexes in cells and tissues**

Once administered into the bloodstream, cisplatin is believed to remain in its non-aquated form due to the high chloride ion ( $\text{Cl}^-$ ) concentration. Cisplatin uptake into cells and tissues is a much debated issue and is addressed in section 1.4. It is proposed that a lower intracellular chloride ion concentration facilitates the aquation of cisplatin to its active form, but this is a debated topic. The effects of intracellular chloride ion on the pharmacodynamics of cisplatin are reviewed in Jennerwein and Andrews 1995.

Cisplatin reacts with biological molecules by substitution of one or both of the chlorine atoms. Cisplatin in its dichloro form (Figure 1.6, structure A) is not believed to be reactive with molecules such as DNA, and it appears that initially one or both of the chlorine atoms must be replaced by water molecules (Riley et al 1983, el Khateeb et al 1999) (Figure 1.6, structures B and D). This is kinetically favourable because of the high concentration of water ( $\sim 55 \text{ M}$ ). The resulting positively charged mono- or di-aqua derivatives of cisplatin are the species which are believed to react with DNA. The reaction with DNA involves the substitution of a water molecule, and investigation with free nucleobases and short oligo-nucleotides provided evidence that platinum binds to the N7 atom of guanine, the N7 and N1 atoms of adenine, and the N3 atom of cytosine (Marcelis et al 1984, Hambley 1997, Wang and Lippard 2005). In polymeric DNA however it has been shown that the substitution of a water molecule occurs primarily at the N7 position of guanine and adenine. In DNA, the N7 atoms of the purines are

exposed on the surface of the major groove of DNA, making them very accessible to metal binding (Sherman and Lippard 1987). The aquated cisplatin molecule can also undergo ionisation to yield neutral hydroxy derivatives (Figure 1.6, Structures C, E and F), thought to be non-reactive with DNA. It seems likely that two factors contribute to the reactivity of the aquated form of cisplatin with DNA. Firstly, the Pt-O bond is less stable than Pt-Cl (Zhou et al 1994), and secondly, the overall positive charge on the molecule will result in electrostatic interaction to DNA. As discussed above, it is believed that DNA bases are unable to directly attack the non-aquated molecule.

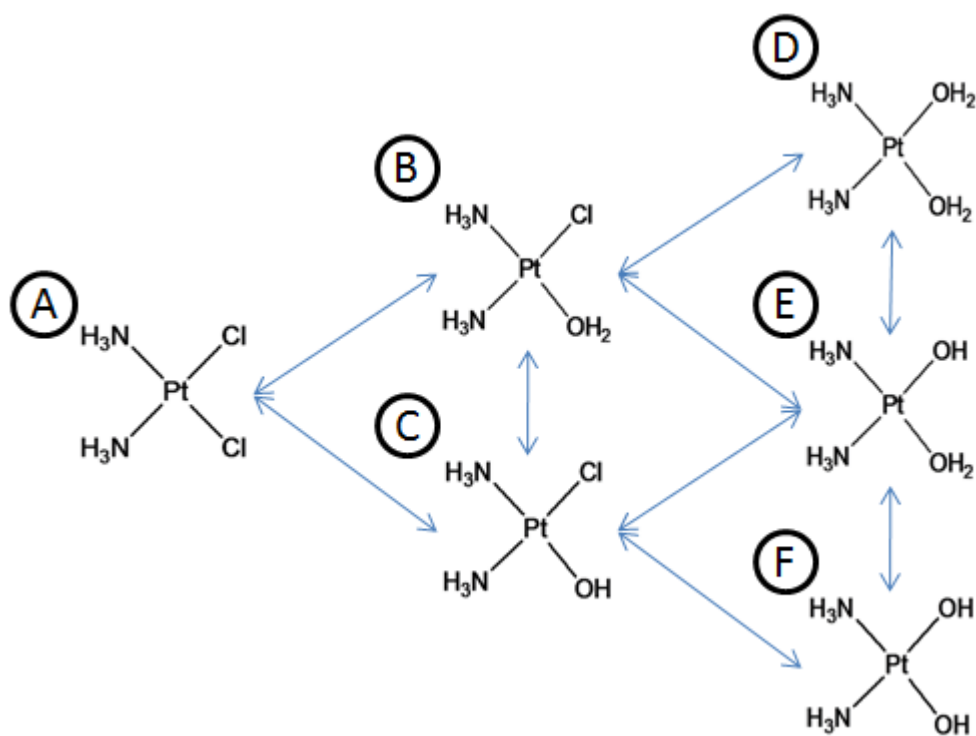


Figure 1.6: Different chemical species of cisplatin. Cisplatin can potentially form six species from aquation with water or ionisation: A,  $\text{cis-Pt}(\text{NH}_3)_2\text{Cl}_2$ ; B,  $\text{cis-Pt}(\text{NH}_3)_2(\text{Cl})(\text{OH}_2)$ ; C,  $\text{cis-Pt}(\text{NH}_3)_2(\text{Cl})(\text{OH})$ ; D,  $\text{cis-Pt}(\text{NH}_3)_2(\text{OH}_2)_2$ ; E,  $\text{cis-Pt}(\text{NH}_3)_2(\text{OH})(\text{OH}_2)$  and F,  $\text{cis-Pt}(\text{NH}_3)_2(\text{OH})_2$ . These species occur in equilibrium in solution.

### 1.3.3: Platinum-DNA (Pt-DNA) adducts formed by platinum complexes

The establishment of DNA as the major target for cisplatin led to further investigations to characterise the nature of platinum binding to DNA. The interaction with DNA is believed to be a multi-step process which involves formation of monofunctional lesions with the mono-aquated complex, followed by aquation of the second arm and closure to a bifunctional adduct. Cisplatin and carboplatin form the same bifunctional complexes with DNA of the general structure  $cis\text{-Pt}(\text{NH}_3)_2(\text{R})_2$  where R represents individual bases of DNA. However, their intermediate complexes differ, with  $cis\text{-[Pt}(\text{NH}_3)_2\text{Cl}(\text{OH}_2)]^+$  for cisplatin and  $cis\text{-[Pt}(\text{NH}_3)_2\text{CBDCA}(\text{OH}_2)]^+$  for carboplatin. The diaqua form  $cis\text{-[Pt}(\text{NH}_3)_2(\text{OH}_2)_2]^{2+}$  is the same for both compounds but is much less prevalent (Kozelka et al 1999, McGowan et al 2005). As expected, aquation has been shown to be much slower for carboplatin than cisplatin (Knox et al 1986). The intracellular mechanism of removal of the oxalate ligand from oxaliplatin is unknown, but it is probable that, like cisplatin and carboplatin, it involves aquation.  $\text{Pt}(\text{DACH})\text{Cl}_2$  had been proposed previously as a potential intermediate product, and there is evidence that  $\text{Pt}(\text{DACH})\text{Cl}_2$  causes formation of two-fold more adducts than oxaliplatin in mammalian cells at equimolar concentrations (Luo et al 1998). However, further investigation showed that with  $\text{Pt}(\text{DACH})\text{Cl}_2$  there was a 30-fold higher intracellular platinum level, so the conversion from oxaliplatin to  $\text{Pt}(\text{DACH})\text{Cl}_2$  seems to make only a minor contribution to oxaliplatin cytotoxicity.

Before the development of chromatographic methods to separate and characterise Pt-DNA products the only specific adducts that could be detected were cross-links between two opposite strands of DNA. Roberts et al used a caesium chloride density

gradient centrifugal technique based on 5-bromo-2'-deoxyuridine (bUDR) incorporation to separate and study cross-linking of “light” and “heavy” strands of DNA (Roberts and Pascoe 1972). When incubated with cisplatin, a third chain of “hybrid” DNA consisting of both strands of DNA was detected. The study further investigated the formation of these cross-links by using concomitant radioactive and density labelling of DNA to achieve radiolabelled heavy chain DNA. The extent of formation of hybrid DNA was found to be dependent on the concentration of platinum.

Early techniques to study Pt-DNA cross-links however were unable to investigate the formation of specific adducts. Interstrand cross-links could be analysed, but based on the size of DNA have been shown to account for less than 1% of the total Pt-DNA adducts (Roberts and Friedlos 1981). Atomic absorption spectrometry (AAS) has been used to study total Pt-DNA adducts, but due to its inherent lack of sensitivity for platinum has limited application for studying specific adducts. Pt-DNA adducts have also been shown to block DNA synthesis *in vitro* (Pinto and Lippard 1985) but such methods don't address the nature or proportions of such adducts. Pt-DNA adducts have also been shown to block *Taq* polymerase primer extension in PCR reactions (Ponti et al 1991).

A major step forward in understanding the nature of Pt-DNA adducts other than interstrand cross-links was the development of suitable chromatographic techniques. Several studies investigated the nature of Pt-DNA complexes using chromatographic separation methods, with three main strategies employed for these investigations. Approaches involving enzymatic digestion of platinated DNA were deployed by Eastman (Eastman 1983, Eastman 1985, Eastman 1986) and Fichtinger-Schepman et al

(Fichtinger-Schepman et al 1985, Fichtinger-Schepman et al 1987). A major difference between the two techniques was differing end-points of enzymatic digestion, and the results obtained were determined by the specificity of the enzymes used in the digestion. The third strategy involved removal of platinum-modified adenine and guanine bases from DNA by acid depurination, followed by separation of free and platinum-bound nucleobases by cation exchange chromatography (Johnson 1982, Johnson et al 1985). The latter technique was found to be less informative as it involved removal of the sugar-phosphate linkages between platinated bases.

Fichtinger-Schepman et al enzymatically digested salmon sperm DNA that had been incubated with cisplatin using deoxyribonuclease 1 and nuclease P1. These enzymes cut 3' phosphate bonds resulting in the formation of 5' deoxyribonucleotides. It is suggested that these enzymes were unable to cut the deoxyribose-3'-phosphate bond between two adjacent platinum cross-linked deoxynucleotides. Anion exchange chromatography was used based on the use of DEAE-Sephacel and MonoQ columns to separate negatively charged nucleotides. The amount of DNA-bound platinum in collected fractions was determined by AAS (Fichtinger-Schepman et al 1985, Fichtinger-Schepman et al 1987). Eastman employed a method that involved digestion with alkaline phosphatase, resulting in deoxyribonucleosides, which were separated using reverse-phase chromatography (Eastman 1983, Eastman 1985, Eastman 1986).

Analyses by Fichtinger-Schepman et al (Fichtinger-Schepman et al 1985) showed the separation of four major products after the reaction of pure DNA with cisplatin. They found that the major cross-link formed was the 1,2-intrastrand cross-link involving adjacent guanine bases (*cis*-Pt(NH<sub>3</sub>)<sub>2</sub>d(GpG)), with a 1,2-intrastrand cross-link

involving adjacent guanine and adenine bases (*cis*-Pt(NH<sub>3</sub>)<sub>2</sub>d(ApG)) also identified. Analysis by <sup>1</sup>H-NMR analysis showed the product to be *cis*-Pt(NH<sub>3</sub>)<sub>2</sub>d(ApG) and not *cis*-Pt(NH<sub>3</sub>)<sub>2</sub>d(GpA). A third identified product was *cis*-Pt(NH<sub>3</sub>)<sub>2</sub>(dGMP)<sub>2</sub>. This was attributed to cross-links formed between guanines on opposite strands of DNA or between non adjacent guanines on the same strand of DNA (*cis*-Pt(NH<sub>3</sub>)<sub>2</sub>d(GpXpG)). The fourth product was found to be *cis*-Pt(NH<sub>3</sub>)<sub>3</sub>dGMP, proposed to form as a result of the monofunctional reaction of cisplatin with the N7 position of guanine. In the above mentioned work the second arm of monofunctionally bound cisplatin was inactivated by addition of ammonium bicarbonate before enzymatic digestion. Further studies revealed that the 1,2-intrastrand *cis*-Pt(NH<sub>3</sub>)<sub>2</sub>d(GpG) adducts accounted for approximately 60-65% of the total adducts formed. The 1,2-intrastrand *cis*-Pt(NH<sub>3</sub>)<sub>2</sub>d(ApG) adduct accounted for 20-25%, and the 1,3-intrastrand *cis*-Pt(NH<sub>3</sub>)<sub>2</sub>d(GpXpG) adduct accounted for 5-10%. Only a very small percentage (less than 1%) was comprised of interstrand cross-links or monofunctional lesions. If cisplatin reacted randomly with all the guanines in DNA, only 37% of the total adducts formed would be expected to be 1,2-d(GpG) (Fichtinger-Schepman et al 1985). The fact that over 60% of the total adducts are of this type suggests that cisplatin has a strong binding preference for adjacent guanines.

Comparative analyses to the above were performed by Eastman, analysing DNA modified by [<sup>3</sup>H]-*cis*-dichloro(diethylenediammine)platinum (II) (*cis*-DEP). This gave similar results (Eastman 1986). Eastman showed that the major product formed was a cross-link between two deoxyguanosines connected by a phosphodiester linkage (dGpdG), followed by a similar adduct between adjacent deoxyadenine and deoxyguanosine (dApdG), with adenine always 5' to the guanine. A minor product

involving two deoxyguanosines with no phosphate (dG-Pt-dG) was also observed. A similar spectral distribution was obtained.

However, the extension of analyses to DNA from drug-treated cells was not possible due to the low sensitivity of AAS for detecting platinum. The development of immunochemical (Fichtinger-Schepman et al 1987, Tilby et al 1991, Meczes et al 2005, Liedert et al 2006) and  $^{32}\text{P}$  post-labelling assays (Blommaert and Saris 1995, Welters et al 1997, Pluim et al 1999) enabled investigation of adducts in DNA extracted from cells where the levels of platinum were too low to detect by AAS.

The first antibodies used in immunochemical studies (Fichtinger-Schepman et al 1987) were raised against dinucleotide cross-links in collected fractions eluted chromatographically and used in immunoassays to detect specific Pt-DNA cross-links. Unfortunately there are two major problems with this approach: firstly, the antibodies are raised against specific dinucleotide cross-links and would be incapable of detecting alternative cross-links, and secondly they wouldn't work on high molecular weight DNA. Antibodies that detect Pt-DNA cross-links on high molecular weight DNA have also been developed for use in immunoassays (Tilby et al 1991, Meczes et al 2005, Liedert et al 2006), but again are limited to detection of the cross-link antigen they are raised against and may not recognise new cross-links altogether.  $^{32}\text{P}$  post-labelling techniques have also been used to study cross-links (Blommaert and Saris 1995, Welters et al 1997, Pluim et al 1999). Briefly, in these assays Pt-DNA adducts are separated by strong cation exchange chromatography after enzymatic digestion, then deplatinated with sodium cyanide. The resulting dinucleotides are labelled with [ $\gamma$ - $^{32}\text{P}$ ] ATP, then further separated by thin-layer or high-performance liquid chromatography.

Radioactivity is detected by scintillation counting.  $^{32}\text{P}$  post-labelling techniques have demonstrated high sensitivity for analysis of low levels of 1,2-intrastrand *cis*-Pt(NH<sub>3</sub>)<sub>2</sub>d(GpG) adducts, and a less sensitive analysis of low levels of 1,2-intrastrand *cis*-Pt(NH<sub>3</sub>)<sub>2</sub>d(ApG) adducts. However, these assays are unable to detect interstrand and monofunctional products due to their lack of a 3' phosphate bond.

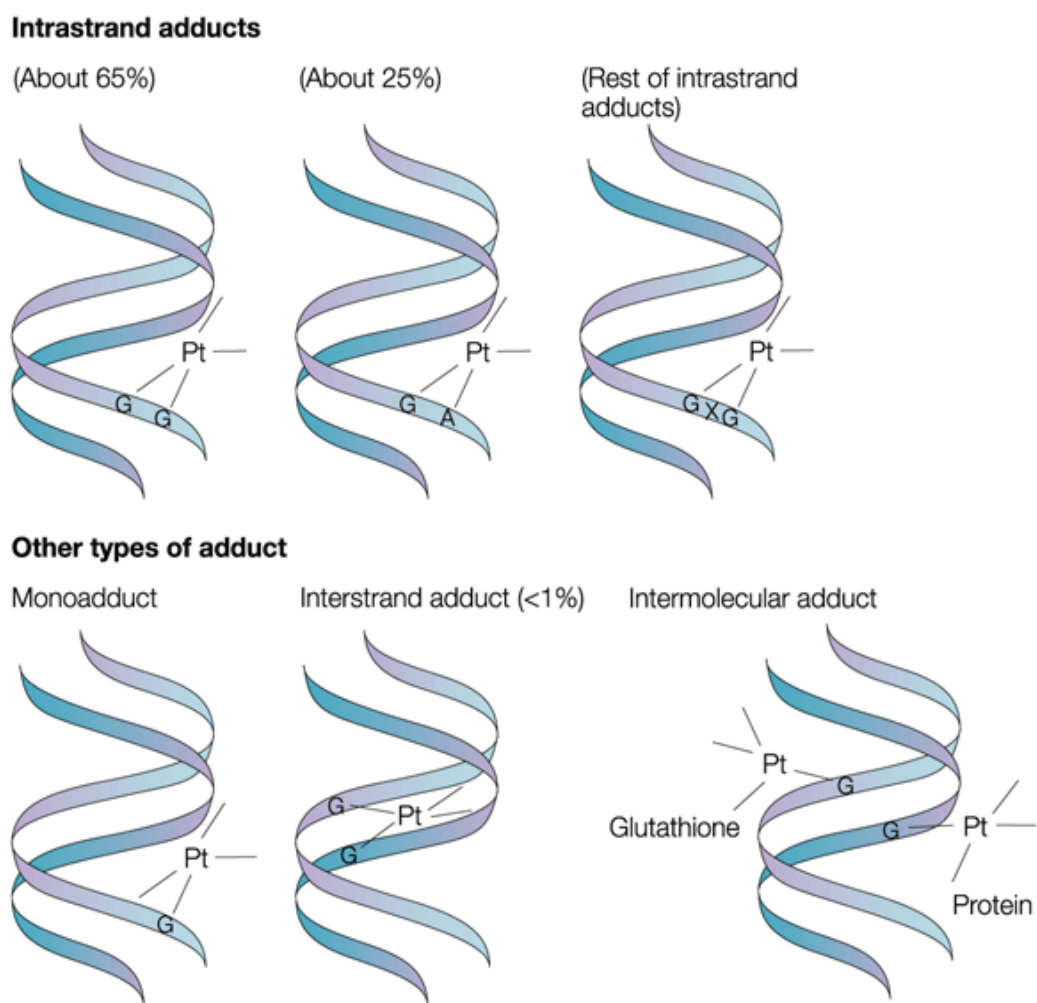


*Figure 1.7: Diagrams of the known adducts formed following the reaction of cisplatin with DNA. The majority of adducts formed are intrastrand (greater than 90%). Adducts can also form between DNA and non-DNA molecules. Diagram modified from Masters and Koberle 2003*

The formation of Pt-DNA cross-links structurally distorts DNA and binding of cisplatin has been shown to unwind the helix and to disrupt helical stability (Maeda et al 1990). This destabilisation is more predominant with 1,2-intrastrand *cis*-Pt(NH<sub>3</sub>)<sub>2</sub>d(GpG) adducts and flanking base sequences have been demonstrated to alter the levels of destabilisation (Poklar et al 1996). Cisplatin binding has been shown to induce a bend in the helix towards the major groove, widening the minor groove with the 1,2-intrastrand *cis*-Pt(NH<sub>3</sub>)<sub>2</sub>d(GpG) and *cis*-Pt(NH<sub>3</sub>)<sub>2</sub>d(ApG) adducts inducing approximately a 30-35° bend in the helix (Bellon and Lippard 1990, Bellon et al 1991). As the major and minor grooves are important in protein binding and recognition, and are sites of functional group presentation, helical disturbance can hinder the ability of proteins to interact with DNA.

Carboplatin is believed to form the same types of cross-links as cisplatin (Knox et al 1986). Blommaert et al incubated salmon sperm DNA with carboplatin, and demonstrated a similar profile of Pt-DNA adduct formation to that of cisplatin, with the 1,2-intrastrand *cis*-Pt(NH<sub>3</sub>)<sub>2</sub>d(GpG) adducts accounting for approximately 58% of the total Pt-DNA adducts, the 1,2-intrastrand *cis*-Pt(NH<sub>3</sub>)<sub>2</sub>d(ApG) adducts accounting for approximately 11% of the total Pt-DNA adducts, 9% 1,3-intrastrand *cis*-Pt(NH<sub>3</sub>)<sub>2</sub>d(GpXpG) adducts and 22% monofunctionally bound lesions (Blommaert et al 1995). Platinum was detected using AAS. However, in the same study when Chinese hamster ovary cells were incubated with carboplatin and platinum levels determined by ELISA, the ratio of adducts was different, with 30% 1,2-intrastrand *cis*-Pt(NH<sub>3</sub>)<sub>2</sub>d(GpG) adducts, 16% 1,2-intrastrand *cis*-Pt(NH<sub>3</sub>)<sub>2</sub>d(ApG) adducts, 40% 1,3-intrastrand *cis*-Pt(NH<sub>3</sub>)<sub>2</sub>d(GpXpG) adducts and 14% monofunctionally bound lesions. These data suggest that unlike cisplatin, carboplatin does not show an intrinsic

preference for formation of 1,2-intrastrand *cis*-Pt(NH<sub>3</sub>)<sub>2</sub>d(GpG) adducts. Similar data was also provided by Fichtinger-Schepman et al (Fichtinger-Schepman et al 1995). In this study only the levels of 1,2-intrastrand *cis*-Pt(NH<sub>3</sub>)<sub>2</sub>d(ApG) adducts were comparable. It is interesting to note that a much higher concentration of carboplatin is required to achieve comparable platination levels to cisplatin (Blommaert et al 1995, Fichtinger-Schepman et al 1985). This may be reflective of differences in the rate of aquation (Knox et al 1986).

Oxaliplatin is also believed to form the same types of adducts as cisplatin, albeit with a DACH ligand in the place of two ammonia molecules. Jennerwein et al analysed DNA incubated with oxaliplatin and separated by reverse-phase chromatography, and identified the same types of adducts as cisplatin at similar ratios (Jennerwein et al 1989). Platinum was detected by AAS and the chemical nature of the products was confirmed by <sup>1</sup>H-NMR. Oxaliplatin has demonstrated equal cytotoxicity to cisplatin (Saris et al 1996), and experiments have shown that the levels of adducts for oxaliplatin compared to cisplatin were significantly lower, both at equimolar and equitoxic concentrations (Saris et al 1996, Woynarowski et al 1998, Woynarowski et al 2000). The structural differences of oxaliplatin adducts appear to be biologically significant and appear to make them more toxic than similar levels of cisplatin adducts.

#### **1.4: Resistance to Platinum Complexes**

Platinum-based drugs are one of the most commonly prescribed classes of anticancer agents in clinical use. Whilst patients can show good initial responses to platinum drug chemotherapy, resistance develops in most cases and is a major factor in therapeutic failure. Resistance to platinum drugs can be either intrinsic, i.e. a property of the tumour at the start of treatment, or may be acquired as a result of repeated exposure to the drug. When tumour cells become resistant to a platinum drug, they can also become cross-resistant to other drugs, and this has been demonstrated with other classes of cytotoxic drugs including melphalan, etoposide, adriamycin, mitoxantrone and taxol (Hamaguchi et al 1993). Cisplatin and carboplatin have also demonstrated cross-resistance (Hamaguchi et al 1993). Resistance has been attributed to a number of different molecular mechanisms through studies involving cell lines (Figure 1.8). However, the underlying mechanisms that lead to development of resistance in clinical tumours are poorly understood.

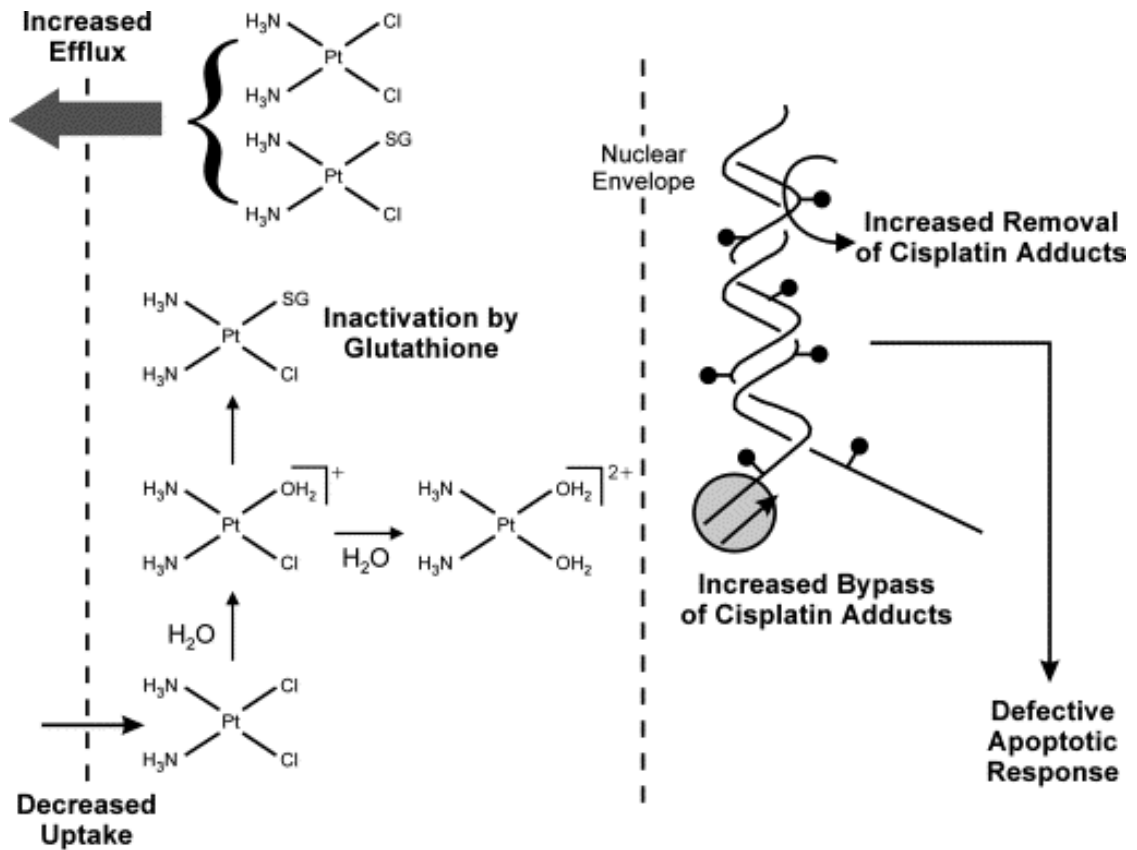


Figure 1.8: Postulated mechanisms of resistance to cisplatin: Resistance could result from decreased uptake or increased efflux of the drug, both leading to decreased drug accumulation; inactivation by cytoplasmic thiols such as glutathione, or through an enhanced capacity for repair of or tolerance to Pt-DNA adducts. Taken from Kartalou and Essigman 2001

### **1.4.1: Decreased Drug Accumulation**

Drug accumulation is critical for therapeutic efficacy and has been studied in many cell lines, including human ovarian, testicular, head and neck, lung and murine L1210 cells (Strandberg et al 1982 (a), Strandberg et al 1982 (b), Andrews et al 1987, Richon et al 1987, Teicher et al 1987, Waud 1987, Eastman and Schutte 1988, Hospers et al 1988, Parker et al 1991 (a), Dabholkar et al 1992, Kelland et al 1992). The majority of cell lines that are selected for resistance display a decreased accumulation phenotype, and this is generally considered to be a result of decreased uptake into the cell as opposed to increased efflux.

The exact mechanism of uptake of platinum drugs is poorly understood and passive diffusion appears to be the main route, with evidence of some active transport (Fuentes et al 2003). Cells which are resistant to cisplatin often display resistance to copper (Katano et al 2002), and reduced uptake of cisplatin has been shown in cells deficient in the copper transporter CTR1 (Ishida et al 2002, Lin et al 2002). Human CTR1 has been shown to be localised to both the plasma membrane, and also in intracellular vesicle perinuclear compartments (Klomp et al 2002). CTR1 deficient cells have also been linked with reduced uptake of carboplatin and oxaliplatin (Lin et al 2002) and there is growing evidence linking the expression and function of the human copper transporter CTR1 with uptake of platinum complexes (Lin et al 2002, Holzer et al 2004 (a), Holzer et al 2004 (b), Safaei et al 2004 (a), Safaei et al 2004 (b), Safaei and Howell 2005, Chen et al 2008, Larson et al 2009). In particular, strong evidence linking an increase in cisplatin and copper uptake with increased expression of CTR1 came from experiments with human ovarian cancer cells transfected to over-express CTR1 (Holzer et al 2004).

However, it is noteworthy that, the increased uptake was not accompanied by an increase in Pt-DNA adducts compared to cells transfected with empty vector. It remains unclear whether reduced accumulation of platinum could result from reduced expression of CTR1 or impaired function of CTR1, but it is possible that varying levels of CTR1 expression in different tumours might contribute to the variable responses observed to platinum complexes.

Resistance to platinum complexes has also been associated with increased efflux both from cells (Mann 1990) and from the nucleus into the cytoplasm (Wang et al 2004). The copper exporter pumps ATP7A and ATP7B have been linked with efflux of platinum complexes (Katano et al 2003, Samimi et al 2003, Samimi et al 2004 (a), Samimi et al 2004 (b), Safaei et al 2008) and over-expression of ATP7B has been linked with poor outcome in both squamous cell head and neck (Miyashita et al 2003) and esophageal (Higashimoto et al 2003) cancers. The clinical significance of variations in uptake and efflux in solid tumours has yet to be fully addressed, with most information arising from studies in tissue culture monolayers.

### 1.4.2: Inactivation of Platinum Complexes

Inactivation of platinum complexes through co-ordination to sulfur-containing molecules has been proposed as a potential mechanism of resistance. Thiol (-SH) containing molecules are implicated in inactivation of platinum complexes, of which the most abundant intracellular thiol is glutathione (GSH) (Meister 1983). There are many studies linking resistance to increased interaction of drug with GSH, and this is addressed in detail in section 1.7. The thiol-containing  $\alpha$ -amino acid cysteine has also been implicated with co-ordination and inactivation of platinum complexes (Bose 1995, Bose et al 1997, Sadowitz et al 2002, Volckova et al 2002). Metallothioneins are cysteine-rich proteins involved in zinc homeostasis that have been associated with resistance to cisplatin (Andrews et al 1987, Endo et al 2004), although there is conflicting evidence (Masters et al 1996) and their contribution to resistance, if any, is unclear. Biomolecules containing thioethers (-C-S-C-), such as the amino-acid methionine, have also been investigated. There is limited evidence supporting a proposed role in forming a reservoir for platinum complexes that mediates the transfer of platinum to DNA (van Boom and Reedijk 1993, Barnham et al 1995). However, there is also evidence that they act in a similar manner to thiol-containing molecules and inactivate platinum complexes (Reedijk 1999, Reedijk and Teuben 1999).

### 1.4.3: DNA Repair

Formation of adducts with DNA is considered to be a major part of the mechanism of platinum complexes, with increased tolerance and an improved ability to repair DNA seen as potentially important factors in the development of drug resistance. Tolerance to platinated DNA is a phenotype demonstrated in resistant cells from chemotherapy refractory patients (Johnson et al 1997), and also in cells selected for resistance *in vitro* (Johnson et al 1994 (a), Johnson et al 1994 (b)). Interstrand cross-links are believed to inhibit DNA replication as they block the unwinding of the DNA helix and strand separation. Intrastrand Pt-DNA adducts have been linked with stalling of DNA replication, although there is evidence that the replication mechanism can bypass the lesion by recruiting alternative DNA polymerases to the damaged site, and synthesising new DNA post-lesion (Reviewed by Prakash et al 2005).

Following Pt-DNA adducts formation, repair systems intrinsic to cells are activated to recognize the damage and where possible to repair the DNA restoring normal structure and function. Several major repair processes have been implicated as determinants of cellular sensitivity to platinum-induced DNA modifications; nucleotide excision repair (NER), mismatch repair (MMR) and homologous recombination (HR)/ interstrand cross-link repair.

The biochemical mechanism of nucleotide excision repair has been extensively studied, and is described in detail elsewhere (de Laat et al 1999, Costa et al 2003). NER is subdivided into two categories, global genome (GG-NER) and transcription coupled (TC-NER), which are believed to recognise DNA damage through different mechanisms,

although the underlying repair mechanism is the same. GG-NER is believed to be initiated following recognition of DNA damage by the XPC-HR23B complex (Sugasawa et al 1998), although there is also evidence for involvement of the XPE protein (Kusumoto et al 2001). TC-NER initiation is believed to arise as a result of blockage of transcription elongation by RNA polymerase II when lesions are encountered (de Laat et al 1999). It is not known whether the stalled RNA polymerase II is displaced and/or dissociated from DNA to allow the NER machinery access to the damaged site. Cockayne Syndrome proteins A (CSA) and B (CSB) are believed to be involved, though their exact functions are not yet known.

After initial recognition of DNA damage, TFIIH, XPA and RPA are the first set of NER proteins to assemble at the damaged site, followed by XPB and XPD helicases, which unwind the DNA helix allowing XPG and XPF-ERCC1 to bind to the unwound DNA. XPG makes an incision 3' to the damage (approximately 2-10 bases from the damage) and XPF-ERCC1 makes another incision 5' to the damage (approximately 15-24 bases from the damage). The excised oligonucleotide containing the damaged section is released from the DNA leaving an exposed hydroxy (-OH) group at the 3' terminus of the gap, believed to act as a primer for DNA polymerases to synthesise the new DNA fragment. DNA polymerases delta and epsilon are implicated as the NER polymerases, with PCNA and RFC cofactors working as a complex to facilitate polymerase assembly. The last step in the process is the ligation of the newly synthesised DNA into the gap by DNA ligase I.

There is strong evidence linking defects in NER with sensitivity to Pt-DNA damage, and NER-deficient cell lines have shown greater sensitivity to cisplatin than proficient

lines (Beck and Brubaker 1973, Drobnik and Horacek 1973, Markham and Brubaker 1980, Brouwer et al 1981, Beck et al 1985, Fram et al 1985, Popoff et al 1987). Cells lacking specific components of the NER machinery have been shown to be 5- to 10-fold more sensitive to cisplatin (Furuta et al 2002) and cells resistant to cisplatin have displayed greater than 2-fold increases in levels of proteins such as XPA, XPC and ERCC1 (Weaver et al 2005). Extracts of tissues from ovarian patients who have demonstrated resistance to cisplatin and carboplatin have also been shown to exhibit elevated levels of XPC and ERCC1 (Dabholkar et al 1994) and it has been suggested that the sensitivity of testicular tumours to cisplatin may be a direct result of decreased levels of NER proteins such as XPA, XPC and ERCC1 (Koberle et al 1997, Koberle et al 1999, Welsh et al 2004).

The effect of NER on excision of individual cisplatin-DNA adducts however is poorly understood, with limited direct evidence of repair derived from studies investigating synthetic fragments of DNA *in vitro* (Szymkowski et al 1992, Huang et al 1994, Zamble et al 1996). Initial studies indicated that the 1,2-d(GpG) intrastrand cross-link was refractory to NER. Further studies however suggested that it is removed by NER, although at a lower efficiency than the 1,3-(GpXpG) intrastrand cross-link (Huang et al 1994, Zamble et al 1996, Moggs et al 1997). No excision repair was identified for interstrand cross-links. (Zamble et al 1996). XPF and ERCC1, both components of the NER machinery, have previously been shown to have a potential role in the early stages of NER, possibly contributing to the excision of ICLs, but no further role in the repair process (de Silva et al 1999, de Silva et al 2000, McHugh et al 2000). However, it is important to note that the attribution of NER in the removal of Pt-DNA damage is

mainly inferred from studies of cellular sensitivity to platinum complexes, with very limited data on direct removal of Pt-DNA adducts.

Defects in mismatch repair (MMR) have been shown to be associated with resistance to cisplatin. MMR is a post-replicative DNA repair system that corrects single base mismatches (Parsons et al 1993, Chu 1994). Proteins of the MMR system have been shown to recognise Pt-DNA cross-links (Duckett et al 1996, Yamada et al 1997), although MMR is not believed to directly repair such adducts. Studies using MMR defective cell lines have demonstrated that inactivation of MMR genes confer resistance to cisplatin (Aebi et al 1996, Anthony et al 1996, Drummond et al 1996). Similarly, restoration of MMR function in yeast lacking the hMLH1 protein has been shown to restore sensitivity to cisplatin (Durant et al 1999). However, the underlying mechanism of cell death induction by MMR proteins remains unclear. There are two predominant hypotheses for MMR involvement in sensitivity to cisplatin. The first hypothesis is that proteins of the MMR system bind to damaged DNA and cell death is initiated by downstream pro-death molecules (Chu 1994, Fink et al 1996). The second is a repair-dependent hypothesis, where mismatches arise in the daughter strand of DNA as a result of translesion DNA synthesis. However, the damage remains on the parent strand and 'futile' cycles of repair and re-synthesis of the daughter strand occur, believed to ultimately lead to double strand breaks (DSB) and induction of cell death (Karran and Bignami 1994, Mello et al 1996, Vaisman et al 1998). These hypotheses suggest that MMR defects confer resistance as a result of failure to recognise DNA damage and induce apoptosis, enabling resistant cells to acquire and tolerate damage that would otherwise be lethal.

Interstrand cross-links are not believed to be repaired by NER, but homologous recombination (HR) has been proposed to be involved. HR defective mammalian cells have shown greater sensitivity to cisplatin than wild type (Raaphorst et al 2005). HR is involved in repair of DSB and there is evidence of DSB occurring following incubation with cisplatin (Sorenson and Eastman 1988 (a)). However, there is conflicting evidence suggesting that cisplatin does not induce DSB (Frankenberg-Schwager et al 2005). It has been suggested that that HR may be important in repair of DSB caused as a result of interstrand cross-linking by cisplatin (Eastman and Schutte 1988), although it is important to distinguish that DSB result from cross-link repair as a specific mechanism from those that occur as a result of apoptotic degradation.

#### **1.4.4: Defective Apoptosis Response**

Cisplatin resistance has been linked with a decreased apoptotic response in ovarian carcinoma and lymphoma cells, and cisplatin-resistant ovarian cells have been shown to need higher levels of cisplatin to elicit a response (Fan et al 1994, Fajac et al 1996, Perego et al 1996). Alterations in expression of apoptotic regulators have also been linked to differences in sensitivity of cells to cisplatin. Decreased levels of Bax, an apoptosis promoter, have been shown in resistant ovarian cancer cells (Fajac et al 1996, Perego et al 1996, Sakakura et al 1997). Other reports have linked increased levels of Bax to the inherent increased sensitivity of testicular cancer cells to cisplatin and Lutzker and Levine 1996), although there is contradictory data to this (Burger et al 1999). It is important to consider defects in apoptosis and drug resistance since, as described in the next section, apoptosis is involved in cell death following Pt-drug treatment.

### **1.5: Cell death induced by platinum complexes**

Apoptosis is the process of programmed cell death that normally occurs during development and aging as a homeostatic mechanism involved in maintaining the normal health and development of multicellular organisms. Apoptosis also occurs as a defence mechanism when cells are damaged by disease or noxious agents (Norbury and Hickson 2001). Apoptosis is triggered by a variety of physiological signals and consists of a series of genetically programmed biochemical processes. Conversely necrosis refers to the disintegration of damaged cells, with the release of products of cellular degradation which have inflammatory effects *in vivo*.

During the early stages of apoptosis, cells decrease in size making the cytoplasm denser and compacting organelles. Chromatin becomes irreversibly condensed in the nucleus (pyknosis), one of the most characteristic features of apoptosis (Kerr et al 1972, Wyllie et al 1980). On histologic examination the cell appears as a round/oval mass with a dark cytoplasm and dense chromatin fragments (see Elmore 2007). Extensive plasma membrane blebbing, nuclear fragmentation (karyorrhexis) and separation of cell fragments follows, forming apoptotic bodies which consist of a tightly packed cytoplasm, often with no visible signs of a nuclear compartment. Organelle integrity is retained as the plasma membrane remains intact. These apoptotic bodies are subsequently phagocytosed by macrophages. There is no inflammatory response involved with apoptosis, as unlike necrosis, no intracellular components are released into the surrounding tissues and the apoptotic bodies are quickly phagocytosed preventing secondary necrosis (Savill and Fadok 2000, Kurosaka et al 2003).

Studies using murine leukaemia L1210 and Chinese hamster ovarian cells provided the first details about the mechanism of cisplatin-induced cell death, with cells incubated with cisplatin shown to arrest in the G<sub>2</sub> phase of the cell cycle. Cells incubated with low levels of cisplatin were able to recover from this arrested state, but cells incubated with increasing concentrations of cisplatin showed decreasing numbers of surviving cells (Sorenson and Eastman 1988 (a), Sorenson and Eastman 1988 (b)). The appearance of DSB in the DNA was the first detectable sign of cell death, and further investigation utilising gel electrophoresis studies identified these breaks as occurring in the nucleosome spacer region of the DNA. Cleavage of genomic DNA is a major part of the apoptotic process and is hallmarked by the appearance of nucleosome ladders of fragmented DNA in these studies. The appearance of nucleosome ladders has been shown after cisplatin treatment in murine leukaemia L1210 cells (Sorenson et al 1990), implicating apoptosis in the mechanism of cell death. The same study also showed a decrease in cell volume and the occurrence of surface blebbing, additional common hallmarks observed in cells undergoing apoptosis. These observations were also seen in Chinese hamster ovary cells (Barry et al 1990). However, it is not known to what extent apoptosis is essential for cytotoxicity, particularly in clinical tumours. Also, it is not understood how various types of DNA damage trigger apoptosis.

## 1.6: Adduct levels in clinical samples of cancer patients

Platinum-based anticancer drugs are believed to exert their anti-tumour effect by reacting with DNA, and there have been many studies investigating adduct formation *in vitro* with purified DNA and human tumour cells (Roberts and Pascoe 1972, Johnson 1982, Eastman 1983, Eastman 1985, Fichtinger-Schepman et al 1985, Johnson 1985, Eastman 1986, Fichtinger-Schepman et al 1987, Roberts and Friedlos 1987). However, it is inherently more complicated to study adduct formation in animals and in cancer patients because of the inability to repeatedly sample the tumour mass, the small sample sizes and numbers, and the low levels of Pt-DNA adducts requiring highly sensitive assays. Formation of Pt-DNA adducts in peripheral blood leukocytes (PBLs) has been correlated with clinical response and toxicity, suggesting that adduct formation in normal cells may be reflective of adduct formation in tumour tissue (Reed et al, 1988, Reed et al 1990, Parker et al 1991 (b), Schellens et al 1996). Correlations between adduct levels in PBLs of patients receiving cisplatin chemotherapy and adduct formation in PBLs from the same patients incubated with cisplatin *in vitro* have also been published (Fichtinger-Schepman et al 1990, Oshita et al 1995), but contradictory data has also been published (Bonetti et al 1996). Unfortunately pharmacokinetic parameters were not investigated. This means the data published may not reflect the effects on Pt-DNA adduct formation, but might be a result of differences in pharmacokinetics rather than differences in drug/DNA access. More recent studies have measured pharmacokinetics as well as Pt-DNA adducts formation in patients treated with cisplatin and carboplatin. Ghazal-Aswad et al showed that pharmacokinetic-based dosing of carboplatin accurately predicted the required dose to achieve a target AUC resulting in consistent patient exposure to active drug (Ghazal-Aswad et al 1999). The

same study also showed that Pt-DNA adduct levels in PBLs were positively related to carboplatin dose and AUC. However, similar studies that also investigated pharmacokinetics (Peng et al 1997, Veal et al 2001, Veal et al 2007) showed a poor correlation between the AUC of active drug and Pt-DNA adduct levels. The conclusion from these studies was that whilst pharmacokinetic monitoring is important to maintain a consistent AUC value in patients receiving cisplatin or carboplatin, variation in Pt-DNA adduct formation cannot simply be attributed to the dose administered or drug exposure in patients. It is more likely therefore that differences in Pt-DNA adduct formation are attributable to host-specific characteristics such as variations in drug uptake in PBLs, differences in intracellular inactivation of the drugs or differences in factors in the blood that would affect drug availability (Veal et al 2001).

The studies referred to above involved measurement of Pt-DNA adducts in normal blood cells. There are very limited data available on Pt-DNA adduct formation in tumour tissue from patients receiving cisplatin or carboplatin. Recently, Pt-DNA adducts in tumour biopsies from head and neck squamous cell carcinomas have been investigated (Hoebbers et al 2006, Hoebbers et al 2008). Normal tissue samples (WBCs and buccal cells) and tumour biopsies were investigated using a  $^{32}\text{P}$  post-labelling assay to quantify adduct levels. Although adduct levels were found to be higher in tumour biopsies than normal tissue samples, no correlation in Pt-DNA adducts levels was observed. As described more fully in chapter 6, one of the aims of the work described in this thesis was to measure the levels of Pt-DNA adducts formed in a small number of tumour biopsies removed from solid tumours during therapy.

## 1.7: Glutathione

### 1.7.1: Intracellular chemistry and redox state of glutathione

Glutathione (L- $\gamma$ -glutamyl-L-cysteine-glycine) (GSH) is the most abundant non-protein thiol found in nearly all eukaryotic and prokaryotic cells at concentrations ranging between 0.5 and 10 mM (Meister 1983). GSH plays a major role in protecting cells from organic and inorganic xenobiotics by undergoing spontaneous or enzyme catalysed binding to form a conjugate with the toxic chemical species (Arrick and Nathan 1984). The resulting compounds are hydrophilic and readily excretable. GSH concentrations are highest in the liver, kidneys and spleen, probably due to the intrinsically high exposure of these organs to toxins. Many carcinogens and drug metabolites are excreted this way, although the pathway can also have the negative effect of inactivating reactive cytotoxic anticancer drugs before they reach DNA.

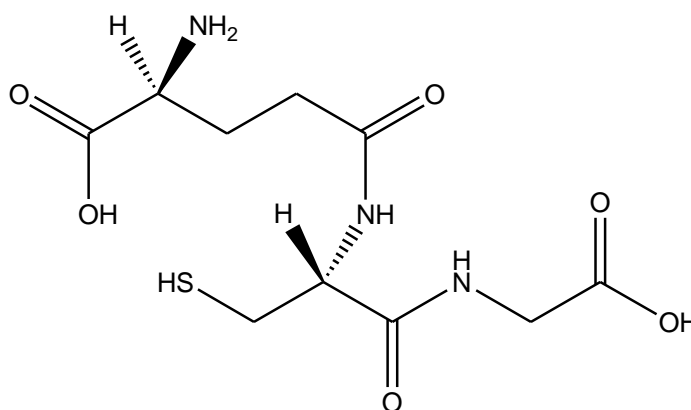


*Figure 1.9: Structure of reduced GSH. Oxidised GSH comprises two molecules joined by an S-S bond*

GSH is a tripeptide synthesised from three amino acid precursors (cysteine, glutamic acid and glycine) in a two step ATP-dependent manner (Meister 1983). The reactive sulfhydryl (-SH) group comes from the cysteine residue. Firstly,  $\gamma$ -glutamylcysteine is synthesised from L-glutamate and cysteine, catalysed by  $\gamma$ -glutamylcysteine synthetase. The enzyme  $\gamma$ -glutamylcysteine synthetase can be inhibited with D, L-buthionine-(S, R)-sulfoximine (BSO) and this has been widely used for investigating the role of GSH in cellular processes. The second step involves addition of glycine to the carboxyl group of the cysteine moiety via the enzyme GSH synthetase. In cells, GSH exists in the reduced form (GSH) and the oxidized or disulfide form (GSSG) (Arrick and Nathan 1984). The overall cellular ratio of GSH:GSSG ranges from 30:1 to 100:1 (Bass 2004). In mammalian cells approximately 90% of the GSH is contained in the cytosolic/nuclear compartments, with approximately 10% in mitochondria and a very small amount in the endoplasmic reticulum (ER) (Meredith and Reid 1982, Hwang et al 1992, Lu 1999). In the ER the ratio of GSH:GSSG differs to the normal cellular state in a range of 1:1 to 3:1, although it is not known how this oxidative state is maintained (Hwang et al 1992). Mitochondria are heavily dependent on GSH for prevention of oxidative damage as a result of aerobic respiration, although they cannot synthesise GSH *de novo* and require salvage from GSSG catalysed by GSH reductase and uptake of cytosolic GSH (Griffith and Meister 1985). GSH breakdown is initiated by  $\gamma$ -glutamyl transpeptidase.

### **1.7.2: GSH and platinum drug resistance**

As discussed in section 1.3.2, intracellular cisplatin aquates, forming a species that is believed to be reactive with DNA. However, the intracellular environment is rich in thiols such as cysteine and GSH which are known to bind readily to cisplatin. Interestingly, there is evidence that, unlike DNA which reacts with cisplatin in its aquated form, GSH can directly attack and inactivate the dichloro form of the drug (Dedon et al 1987). This raises the interesting question of how cisplatin is able to react with DNA in the presence of the very high molar ratio of intracellular GSH to cisplatin (Reedijk, 1999). There have been studies that propose platinum-sulfur binding is kinetically less favourable than platinum-nitrogen, suggesting a possible reason why platinum drugs bind the nitrogen residues of DNA (Deubel 2004). However, the data come from theoretical modelling and have limited relevance to the intracellular pharmacology of platinum binding. It is interesting to note that the mono-aqua and diaqua species of cisplatin were investigated. It is believed that the non-aquated form of cisplatin does not react with DNA, whereas it has been proposed that sulfur-containing molecules can attack the dichloro species of cisplatin.

Many studies have investigated the role of GSH in resistance to cisplatin. Differences in GSH levels have been correlated with sensitivity to cisplatin with increased levels of GSH observed in cisplatin resistant cell lines (Behrens et al 1987, Wolf et al 1987, Godwin et al 1992). Studies in colon cancer cells have found a 3-fold increase in GSH in cisplatin-resistant cells (Fram et al 1990). Conversely, no increase in GSH was seen in ovarian carcinoma cells and human testicular nonseminomatous germ cells resistant to cisplatin compared to parental lines (Kelland et al 1992).

Covalent binding of cisplatin and GSH leads to formation of a complex which is believed to be inactive and is exported from cells by the ATP-dependent GSH C-conjugate efflux pump (Dedon and Borch 1987, Ishikawa and Aliosman 1993). In addition, it has been proposed that GSH conjugated to monofunctionally platinated DNA inhibits the conversion to bifunctional cross-links, reducing the cytotoxic potential of the initial lesion (Eastman 1987). However, there is also the potential for conjugated *cis*-Pt(NH<sub>3</sub>)<sub>2</sub>(DNA)(GSH) cross-links to be cytotoxic as discussed below.

### **1.7.3: Evidence for potential *cis*-Pt(NH<sub>3</sub>)<sub>2</sub>(DNA)(GSH) cross-links**

Current knowledge of Pt-DNA cross-links stems from the discovery of interstrand (Roberts and Pascoe 1972) and intrastrand (Fichtinger-Schepman et al 1985) cross-links. In recent years evidence has been obtained that an additional class of DNA cross-link can be formed in cells, potentially accounting for up to 25% of the total Pt-DNA products (Azim-Araghi 2003). These data arose from the novel combination of anion-exchange chromatographic separation as described previously (Fichtinger-Schepman et al 1985), with the sensitive technique of inductively coupled plasma mass spectrometry (ICP-MS), to detect platinum in chromatographic fractions. ICP-MS is a technique principally developed for geochemical analyses and methodologies have been developed to allow detection limits of ~ 0.5 attomolar Pt levels, allowing for highly accurate and sensitive analysis of experimental samples at clinically relevant cross-link levels. This permitted the direct analysis of adducts present in DNA extracted from drug treated cells. As discussed in section 1.3.3, previous analyses relied on the use of antibodies or <sup>32</sup>P post-labelling to increase detection sensitivity. Both methods are established and highly sensitive for specific adducts, but equally both could fail to

detect additional types of Pt-DNA cross-links that are formed in cells. The introduction of ICP-MS for detecting low levels of platinum has made possible new investigations.

In the work referred to above (Azim-Araghi 2003) lung carcinoma cell lines were treated with cisplatin, DNA was extracted and enzymatically hydrolysed prior to analysis by anion exchange chromatography and ICP-MS. The results revealed the presence of additional products not detected when purified DNA was incubated with cisplatin (Figure 1.10). Comparison of calf thymus DNA incubated with cisplatin in the presence and absence of GSH confirmed these findings (Figure 1.11). Further analysis with increased nuclease concentrations confirmed these were not products of incomplete digestion of the DNA. Since these new cross-links had not been identified previously in purified DNA reacted with cisplatin (Fichtinger-Schepman et al 1985), or on single strand oligodeoxynucleotides (Meczes et al 2005), it was hypothesised that their formation was a result of platinum-mediated cross-linkage to a non-DNA molecule. The hypothesis underlying much of the work in this thesis is that this new type of cross-link is formed between GSH and Pt-DNA.

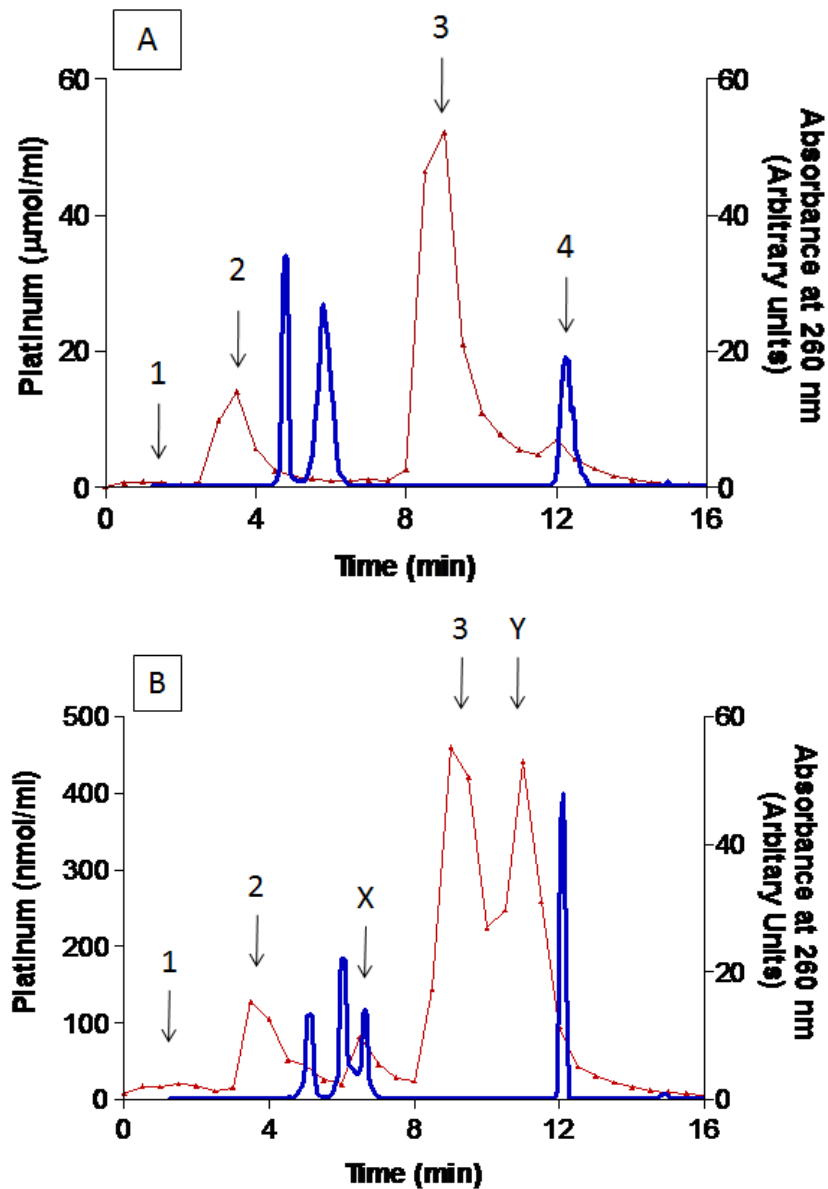


Figure 1.10: Mono-Q elution pattern for digested calf-thymus DNA (A) and Mor/P cell DNA (B) after incubation with cisplatin. DNA was enzymatically digested and eluted with increasing NaCl concentrations. Solid blue line: OD 260 nm (▲) Platinum levels measured in collected fractions using ICP-MS. (1):  $Pt(NH_3)_2(R)(dGMP)$ ; (2):  $cis-Pt(NH_3)_2d(ApG)$ ; (3):  $cis-Pt(NH_3)_2d(GpG)$ ; (4):  $cis-Pt(NH_3)_2(dGMP)_2$ ; (X): new product possibly involving thymine; (Y) new product possibly involving GSH. Adapted from Azim-Araghi 2003

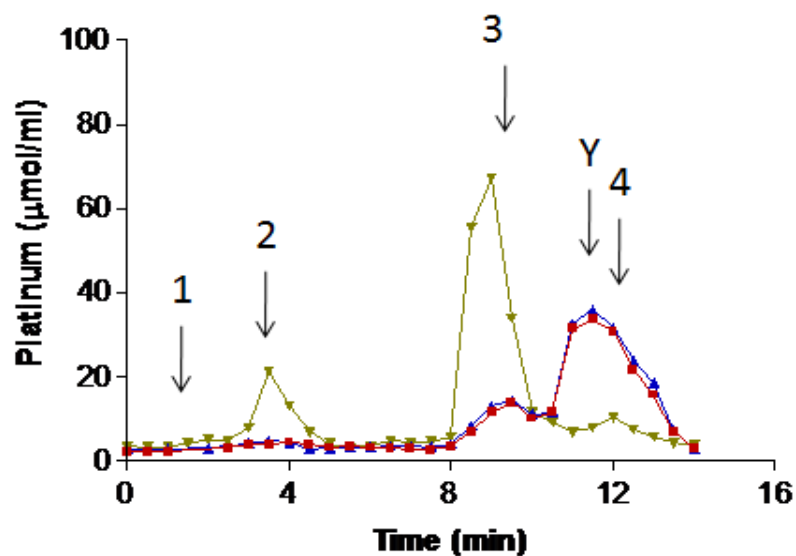


Figure 1.11: Mono-Q elution pattern for digested calf-thymus DNA incubated with cisplatin in the presence and absence of GSH. (▲): Platinum after 2-hour incubation of DNA with 50 mM GSH ( $\mu\text{mol/ml}$ ). (■): Platinum after 24 hour incubation of DNA with 50 mM GSH ( $\mu\text{mol/ml}$ ). (▼): Platinum after 24 hour incubation of DNA in the absence of GSH ( $\mu\text{mol/ml}$ ). (1):  $\text{Pt}(\text{NH}_3)_2(\text{R})(\text{dGMP})$ ; (2):  $\text{cis-Pt}(\text{NH}_3)_2\text{d}(\text{ApG})$ ; (3):  $\text{cis-Pt}(\text{NH}_3)_2\text{d}(\text{GpG})$ ; (4):  $\text{cis-Pt}(\text{NH}_3)_2(\text{dGMP})_2$ ; (Y): new product possibly involving GSH. Adapted from Azim-Araghi 2003

Evidence for the cross-linking of GSH to purified DNA in the presence of cisplatin was first published by Eastman over twenty years ago (Eastman 1987). Eastman enzymatically digested salmon testes DNA incubated with cisplatin with and without GSH and chromatographically separated the resulting products. GSH was found to be able to react with monofunctionally platinated DNA, but was unable to form complexes with DNA that had no monofunctionally bound platinum. Eastman proposed therefore that GSH can block the conversion of monofunctional Pt-DNA lesions to the toxic bifunctional cross-links. The possibility that GSH could quench monofunctional Pt-DNA adducts before rearrangement had been proposed previously (Micetich et al 1983). Micetich et al presented kinetic data comparing mouse leukaemia L1210 cells resistant to cisplatin (L1210/PAM) with its parent cell line (L1210/NCL). The data showed an increased resistance to cisplatin in the L1210/PAM cells and proposed that it may be due to increased thiol content in the cell line blocking conversion to bifunctional cross-links. Suzukake et al had previously found the L1210/PAM cell line to have elevated levels of GSH compared to its parental line and concluded that this may be the reason for its resistance to L-phenylalanine mustard (Suzukake et al 1982, Suzukake et al 1983).

Interestingly, the data described above made no suggestion that the formation of cross-links with GSH could generate potentially cytotoxic lesions. The cross-linking of GSH to DNA was proposed to stop the conversion of monofunctional Pt-DNA lesions to toxic bifunctional Pt-DNA cross-links, and GSH binding to cisplatin was proposed to detoxify the drug. Two possible mechanisms were suggested for this. The first mechanism involved cisplatin binding to the sulphhydryl residue in GSH, thereby blocking access of the drug to DNA (Eastman 1987). The second mechanism involved

binding to cisplatin monofunctionally bound to DNA, thereby detoxifying the lesion (Micetich et al 1983, Eastman 1987). Both mechanisms are plausible. Formation of monofunctional Pt-DNA lesions is believed to occur relatively rapidly, with conversion to bifunctional lesions occurring for up to 12 hours after drug removal (Zwelling et al 1978, Eastman 1986). Even though the reaction of GSH with monofunctional Pt-DNA adducts is slow (Eastman 1987), the lengthy time to form bifunctional adducts suggests this is a possibility. Binding to and inactivating cisplatin in the cytoplasm may be a more efficient method of detoxification, especially considering the molar excess of GSH to drug, although the limited time between cisplatin uptake and reacting with DNA may limit the extent to which this occurs (Eastman 1987). It has also been suggested that reaction of cisplatin with intracellular sulfur ligands may form a reservoir from which the platinum complex is slowly released (van Boom and Reedijk 1993) though this theory is not supported by more recent studies (Lau and Deubel 2005). It is conceivable that both mechanisms may in turn contribute to the modulation of platinum drug toxicity. However, should *cis*-Pt(NH<sub>3</sub>)<sub>2</sub>(DNA)(GSH) cross-links contribute to platinum drug cytotoxicity it seems unlikely that this would involve initial binding to GSH, although neither possibility can be totally ruled out.

Recent unpublished investigations at Newcastle have supported the possibility that GSH can cross-link to DNA in three ways. Firstly, in the presence of cisplatin, radioactively labelled GSH became bound to DNA. Secondly, the level of intrastrand 1,2-d(GpG) cross-links as a proportion of total Pt-DNA adducts was reduced when the reaction between cisplatin and DNA took place in the presence of GSH. In this work total platinum was measured by AAS and intrastrand 1,2-d(GpG) cross-links by immunoassay with monoclonal antibody CP9/19. Thirdly, studies on two lung cancer

cell lines (Mor/P and H69), again using AAS for total platinum and immunoassay for cross-links, indicated that cross-links formed in Mor/P cells showed a smaller proportion of 1,2 cross-links than those formed in H69 cells (Tilby and Twentyman, unpublished). If the existence of such a new class of cross-links were to be proven, it would have a significant impact on our understanding of platinum drug pharmacology.

#### **1.7.4: Potential clinical implications of *cis*-Pt(NH<sub>3</sub>)<sub>2</sub>(DNA)(GSH) cross-links**

It is well established that clinically active platinum complexes possess the *cis*-planar conformation and that *trans*-DDP, the structural isomer of cisplatin, is clinically ineffective (Roberts and Friedlos 1987). Investigations of the reactions of *trans*-DDP with DNA suggested that 85% of adducts formed are monofunctional, and the rate of conversion to bifunctional cross-links is very slow (Eastman 1987). Furthermore, it has been suggested that the lack of activity of *trans*-DDP may be attributable to its inability to form intrastrand 1,2- cross-links (Pinto and Lippard 1985).

Early investigations with *cis*-DDP used thiourea to block monofunctional lesions rearranging to bifunctional cross-links (Micetich et al 1983, Eastman 1986). This approach was deployed by Eastman to study *trans*-DDP adducts formed in DNA (Eastman 1987). However, rather than “trapping” monofunctional lesions, thiourea displaced the drug from DNA. Eastman concluded that this was not surprising as ‘*the strength of any ligand is markedly influenced by the ligand in a trans orientation*’. Sulfur is a stronger ligand than nitrogen, and hence when thiourea was bound to DNA, the opposing Pt-N (guanine) bond was sufficiently labilised to remove the drug. Eastman further concluded that the major reaction of monofunctionally bound *trans*-

DDP in cells would be with GSH (Eastman 1987). Andrews et al demonstrated that reducing GSH levels markedly enhanced toxicity to *trans*-DDP with little effect on cisplatin toxicity (Andrews et al 1985) supporting the possibility that GSH may act in a manner similar to that of thiourea in displacing *trans*-DDP from DNA. The *trans*-labilising effect is particularly strong for the bond between Pt and the sulfur of GSH (Lau and Deubel 2005). The presence of GSH would cause the labilisation of one of the usually stable ammonia moieties in cisplatin, thus becoming a potential leaving group. The resulting adduct could then possibly undergo delayed reactions with other molecules, with possible implications on cell survival and drug efficacy. The same mechanism for *trans*-DDP would lead to the dissociation from DNA (Figure 1.12).

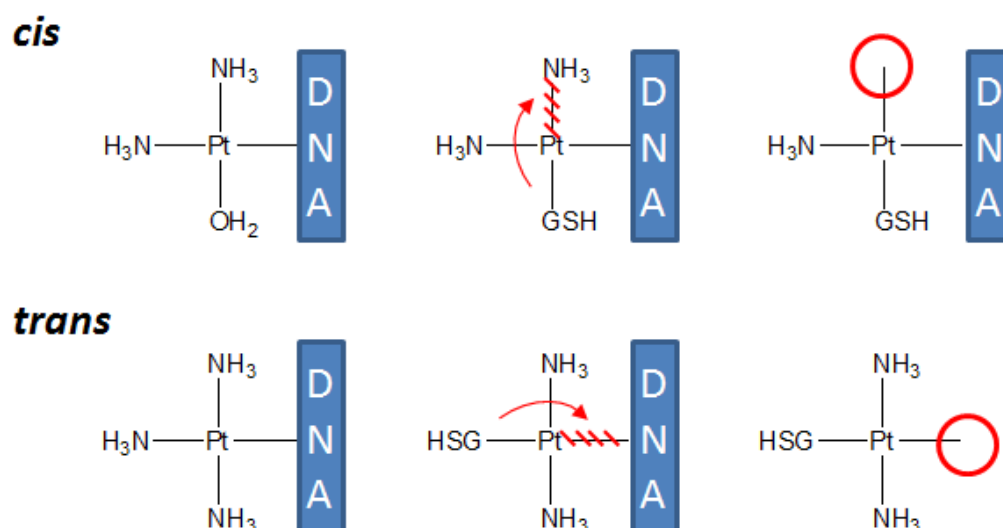


Figure 1.12: Trans-labilisation of *cis*-DDP and *trans*-DDP by GSH and subsequent effect on binding of molecule to DNA. Red circles indicate active bond

As described more fully in chapters 3 and 4, one of the aims of the work described in this thesis was to investigate whether or not *cis*-Pt(NH<sub>3</sub>)<sub>2</sub>(DNA)(GSH) cross-links can be formed in cells.

## 1.8: Sodium thiosulfate

### 1.8.1: Sodium thiosulfate as a chemo-protective agent

Cisplatin binds readily to sulfur-containing molecules. Thiourea is a sulfur-containing molecule that has previously been shown to reduce the toxicity and anti-tumoural activity of cisplatin (Burchenal et al 1978, Filipski et al 1979). It was proposed that sulfur-containing molecules may have a role in the selective protection from toxicity by reducing the amount of active drug in the circulation, although there was no data from animal or mouse studies at the time.

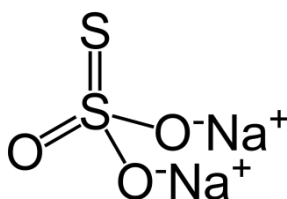


Figure 1.13: The chemical structure of sodium thiosulfate

Sodium thiosulfate ( $\text{Na}_2\text{S}_2\text{O}_3$ ) (STS) is a sulfur-containing molecule that is known to react with metals. It is used in the photographic industry as a fixative where it reacts with silver halides. It is also known to readily react with gold, and is often used in extraction as a replacement for cyanide. STS has also been used in patients as an antidote for cyanide poisoning. Howell et al proposed that like thiourea, STS could potentially have a role in modulating cisplatin toxicity (Howell and Taetle 1980). STS was shown to be toxic to CFU-C cells *in vitro* at concentrations above 10 mg/ml, whereas at 0.1 mg/ml STS significantly reduced the toxicity of cisplatin at

concentrations up to 10 µg/ml. The same study also showed STS to cause a dose-related decrease in nephrotoxicity in mice. Interestingly, simultaneous injection into mice reduced the antitumoural effect of cisplatin. STS has since been shown to bind and inactivate cisplatin and carboplatin *in vitro* (Abe et al 1986, Elferink et al 1986, Dedon et al 1988), and to reduce cisplatin-induced nephrotoxicity in animal models (Iwamoto et al 1984, Nagai et al 1995) and patients (Howell et al 1982, Pfeifle et al 1985). The exact mechanism by which STS protects against nephrotoxicity is unclear. There is evidence that STS binds and inactivates cisplatin in the kidneys, and high concentrations of thiosulfate have been found in urine during thiosulfate administration, suggesting that concentrations in kidney tissues are high (Shea and Howell 1984). At these high concentrations the reaction rate between cisplatin and STS is increased (Elferink et al 1986). Cisplatin nephrotoxicity is believed to be a result of cisplatin reacting with protein-bound thiol groups in the renal tubules (Weiner and Jacobs 1983), and this mechanism suggests that competition between the thiosulfate and thiol groups for binding cisplatin might explain the decreased nephrotoxicity. However, there is evidence that thiosulfate distribution remains extracellular (Gilman et al 1946), and that STS binds directly to inactive cisplatin in the systemic circulation, resulting in a decreased amount of cisplatin in the kidneys (Nagai et al 1995). This would suggest that the decrease in nephrotoxicity is attributable to cisplatin being inactivated before it reaches sites of potential toxicity. However, the exact mechanism through which STS protects against nephrotoxicity is still unknown.

Platinum-induced hearing loss (ototoxicity) is progressive and irreversible in patients, and is associated in animal models with loss of the inner and outer hair cells of the inner ear (Neuwelt et al 1996). Ototoxicity is a particularly significant problem in

children receiving platinum-based chemotherapy, with ototoxicity noted by Parsons et al in 9/11 (82%) of children treated with carboplatin for neuroblastoma (Parsons et al 1998). Hearing loss significantly affects quality of life and has been linked with delayed development of language and reading skills in children (Hindley 1997), and the development of depressive symptoms in elderly patients (Cacciatore et al 1999, Keller et al 1999).

High frequency hearing loss is a major form of ototoxicity, and was a key negative finding in a study investigating the effects of carboplatin on human brain tumours, with blood brain barrier disruption to optimise drug delivery (Williams et al 1995). The positive reports of STS protecting against cisplatin-induced nephrotoxicity suggested that STS may have a role in protection against ototoxicity. Although the mechanism for protection against nephrotoxicity is unknown, the available evidence suggests a role for STS as a scavenger of free cisplatin in the kidneys. In protection against ototoxicity, STS is hypothesised therefore to accumulate in the cells of the inner ear, and bind and inactivate free drug (Neuwelt et al 1996). Neuwelt et al investigated the effects of STS *in vitro* and *in vivo* in protecting against carboplatin-induced ototoxicity, and found that STS protected against carboplatin toxicity *in vitro* when incubated for up to 8 hours after carboplatin was added, but no protection was seen at 24 hours (Neuwelt et al 1996). In the same study, STS was found to be neurotoxic *in vivo* when administered immediately after blood brain barrier disruption, but no toxicity was seen at 30 minutes or 60 minutes after disruption, by which time the barrier is believed to have become re-established (Neuwelt et al 1996). Further *in vitro* studies and investigations in animals and patients have confirmed the findings that delaying administration of STS can be used to reduce ototoxicity and have also indicated that this occurs without

compromising the anti-tumour effects of either cisplatin or carboplatin (Neuwelt et al 1998, Muldoon et al 2000, Doolittle et al 2001, Harned et al 2008). STS is currently in a phase III clinical trial (SIOPEL 6) designed to investigate a potential role in reducing ototoxicity in paediatric patients receiving cisplatin for standard risk hepatoblastoma.

The hypothesis for protection against nephrotoxicity and ototoxicity involves STS accumulating in the kidneys and inner ears respectively, and potentially binding and inactivating free drug. However, the mechanism through which this protection occurs is unknown. STS has previously been shown to remain extracellular (Gilman et al 1946) although this data is based on whole body distribution in dogs. It is therefore unclear to what extent STS is able to enter cells in humans. More recent studies have demonstrated that the human sulfate transporter SLC13A1 (NaS1, previously known as SUT-1) a member of the SLC13 sulfate transporter family found on the plasma membranes of mammalian cells and located on the apical membrane of the renal proximal tubule, is involved in the active transport of thiosulfate ions across the cell membrane (Busch et al 1994, Lee et al 2000, Pajor 2006). There is limited information available on another member of the SLC13 transporter family, SLC13A4 (NaS2), found predominantly in human placenta, although it is believed to have similar substrate specificity to SLC13A1 (Pajor 2006). This suggests a potential mechanism through which STS can enter cells, and we hypothesise that intracellular STS has the potential to interact with intracellular platinum drugs and even modify platinated DNA. Potential mechanisms by which this may occur include removal of pre-formed Pt-DNA adducts or removal of bound platinum, inactivation of cytoplasmic platinum drugs and/or quenching of monofunctionally bound Pt-DNA lesions.

## **1.9: Aims of this study**

The work described in this thesis addresses three topics related to the quantity and quality of DNA adducts formed by platinum drugs.

### **1: To test the hypothesis that GSH can become cross-linked to DNA by platinum drugs**

Available evidence to support this hypothesis was described in section 1.7. If such adducts were to form in human tumour cells it would have broad implications in understanding the pharmacology of platinum-based anticancer drugs.

This study was approached in two ways:

1. To attempt to synthesise the putative *cis*-Pt(NH<sub>3</sub>)<sub>2</sub>(DNA)(GSH) cross-link using dGMP as a surrogate for DNA so as to identify its chromatographic behaviour
2. To combine the methods of HPLC and ICP-MS for the analysis of DNA from a number of human tumour cell lines that had been exposed to platinum drugs to seek evidence of additional adducts to those previously identified

### **2. To test the hypothesis that STS protects cancer cells by reduction of Pt-DNA interactions**

The effects of STS on modulating platinum drug toxicity were discussed in section 1.8. However, little is known about the mechanisms through which such protection occurs, or the effects of STS on Pt-DNA adduct formation.

This study was approached in two ways:

1. To investigate the potential of STS to interact with platinated DNA using dGMP as a surrogate for DNA so as to identify its chromatographic behaviour and to identify any additional products in pure DNA
2. To determine the effect of concurrent and delayed administration of STS on growth inhibition and total Pt-DNA adduct formation in human tumour cell lines exposed to cisplatin

**3. To assess the levels of Pt-DNA adducts achieved in human tumour biopsies compared to blood samples**

There is very limited data on the formation of Pt-DNA adducts in human tumours. The work described in the thesis aimed to establish the feasibility of analysing adducts in human tumour biopsies following treatment with carboplatin.

This study aimed to measure adducts levels in solid tumour biopsies and peripheral blood mononuclear cells from patients treated with carboplatin for advanced ovarian cancer. This was approached in two ways:

1. Determine the DNA adduct levels achieved in solid ovarian tumour tissue during therapy
2. To compare these levels to adduct levels formed in peripheral blood mononuclear cells from the same patients
3. To compare adducts levels to plasma pharmacokinetics for carboplatin

## **Chapter 2**

### **Materials and Methods**

#### **2.1: Materials**

##### **2.1.1: Reagents**

Unless otherwise stated all chemical reagents used were of analytical grade and purchased from Sigma-Aldrich Company Ltd. (UK).

Cisplatin was dissolved in sterile de-ionised water to a final concentration of 2 mM and stored at -20°C. Carboplatin (Johnson Mathey, UK) was dissolved in either full growth media or water immediately prior to use. Oxaliplatin was dissolved in sterile de-ionised water to a final concentration of 10 mM, then diluted in full growth medium immediately prior to use. Carboplatin and oxaliplatin were always prepared fresh for experiments. All handling of cytotoxic drugs for exposure to DNA was carried out in a BioMAT<sup>2</sup> class II pharmaceutical safety cabinet (Medical Air Technology Ltd, UK) . All drugs were filter-sterilised immediately before use in tissue culture.

### 2.1.2: Solutions and Buffers

Buffer C1 (QIAGEN)	1.28 M sucrose, 40 mM Tris-Cl, pH 7.5 containing 20 mM magnesium chloride and 4% Triton X-100
Buffer G2 (QIAGEN)	800 mM guanidine-HCl, 30 mM Tris-Cl, 30 mM disodium salt of ethylenediaminetetraacetate (EDTA), pH 8.0 containing 5% Tween-20 and 0.5% Triton X-100
Buffer QBT (QIAGEN)	750 mM sodium chloride, 50 mM 3-(N-morpholino)propanesulfonic acid (MOPS), pH 7.0 containing 15% isopropanol and 0.15% Triton X-100
Buffer QC (QIAGEN)	1 M sodium chloride, 50 mM MOPS, pH 7.0 containing 15% isopropanol
Buffer QF (QIAGEN)	1.25 M sodium chloride, 50 mM Tris-Cl, pH 8.5 containing 15% isopropanol
DNA buffer (DB)	50 mM sodium chloride, 50 mM sodium dihydrogen phosphate, 0.02% sodium azide, pH 7.0

DNA digest buffer	10 mM Tris, pH 7.2 containing 0.1 mM EDTA.
Freezing Solution	90% v/v foetal calf serum (FCS), 10% (v/v) dimethyl sulfoxide (DMSO)
HA lysis buffer	80 mM potassium phosphate, 1% (v/v) Sarkosyl NL30 detergent, 10 mM EDTA, pH 6.8
HPLC buffer A	12.5 mM Tris, pH 8.8
HPLC buffer B	12.5 mM Tris, pH 8.8 with 1 M sodium chloride
Kirby's Phenol	500 g phenol, 0.5 g 8-hydroxyquinoline, 55 ml de-ionised water, 70 ml m-cresol, pH 7.0. Prior to use Kirby's phenol was saturated with water by mixing with 80 mM KP buffer and centrifuged (150 x g, 5 minutes)
Phosphate buffer (PB)	50 mM sodium phosphate, 0.02% sodium azide, pH 7.0
10X PB	500 mM sodium phosphate, 0.02% sodium azide, pH 7.0

Phosphate Buffered Saline (PBS)	10 mM phosphate buffer, 2.7 mM potassium chloride, 137 mM sodium chloride, pH 7.4
80 mM potassium phosphate (KP)	80 mM potassium phosphate, pH 6.8
0.5 M KP	0.5 M potassium phosphate, pH 6.8
Ribonuclease A (RNAase A) buffer	10 mg/ml RNAase A from bovine pancreas in 1.2 g/l 10 mM Tris and 0.44 g/l 15 mM sodium chloride, pH 7.5.
30 mM sodium acetate	172 $\mu$ l glacial acetic acid in 100 ml water, adjusted to pH 5.3 with sodium hydroxide
SRB stain	0.4% sulphorhodamine B in 1% acetic acid
TE	10X Trypsin-EDTA (Gibco BRL) diluted 10-fold in warm PBS
Tissue culture media	Roswell Park Memorial Institute (RPMI-1640) tissue culture media with HEPES modification, supplemented with 10% (v/v) foetal calf serum (FCS) and 2 mM L-Glutamine, <i>Penicillin</i> (100 units/ml) and <i>Streptomycin</i> (100 $\mu$ g/ml) were also present in the media

10 mM Tris

10 mM Tris, no pH adjustment (pH ~ 9.6)

5 M Urea, 80 mM KP

80 mM KP buffer containing 5 M Urea, pH 6.8

6 M Urea, 80 mM KP

80 mM KP buffer containing 6 M Urea, pH 6.8

### **2.1.3: Enzymes**

Ribonuclease A (RNAase A) was dissolved at 10 mg/ml in Ribonuclease 1 buffer and incubated in a boiling water bath for 15 minutes to inactive deoxyribonucleases. Aliquots were stored at -20°C. Deoxyribonuclease 1 (DNAase 1) was dissolved at 20 Kunitz units/ml in DNA digest buffer immediately before use. Nuclease P1 was dissolved in 30 mM sodium acetate buffer at 200 units/ml and stored at -20°C.

## **2.2: Tissue Culture**

### **2.2.1: Equipment**

All tissue culture procedures were carried out in a BioMAT<sup>2</sup> class II pharmaceutical safety cabinet (Medical Air Technology Ltd, UK). Cells were incubated in an MCO-20AIC CO<sub>2</sub> incubator (Sanyo Biomedical, Japan) maintained at 37°C, 5% CO<sub>2</sub>. A VacuSafe Comfort aspirator (Integra Biosciences, UK) was used to aspirate all culture media and drugs. All tissue culture plastic ware were obtained from Nunc (Fisher Scientific, UK). Routine centrifugation was carried out using a CR-4-22 refrigerated centrifuge (Jouan, UK),

### **2.2.2: Cell lines**

Human testicular germ cell tumour cells (833K) and human colon adenocarcinoma cells (LoVo) were obtained from the American Type Culture Collection. Human ovarian carcinoma cells (A2780) were kindly donated by Dr Sally Coulthard, NICR. Cisplatin-resistant human lung adenocarcinoma cells (Mor/CPR) were obtained from the European Collection of Cell Cultures (now HPA cultures). All cell lines were cultured in Roswell Park Memorial Institute (RPMI-1640) tissue culture media and maintained at 37°C, 5% CO<sub>2</sub>.

### **2.2.3: Maintenance of cell lines**

All cell lines were cultured as adherent mono-layers in tissue culture flasks and were sub-cultured frequently (less than 90% confluence) to maintain continuous growth. For routine sub-culture of all cell lines, media was removed through aspiration and cells washed with 10 ml warm PBS. Following aspiration, 2 ml warm TE was added to the flask and passed across the cells. Excess TE was aspirated after 30 seconds exposure and the flasks incubated at 37°C until all cells had detached. Cells were protected from TE through addition of 10 ml fresh culture media and cells counted. An appropriate volume of cell suspension was added to fresh culture media and transferred to a new flask. Mycoplasma testing was carried out every 3 months using a Mycoplasma Detection Kit (Roche Diagnostics, UK) and cells were negative for contamination throughout.

### **2.2.4: Counting cells**

A haemocytometer comprises a glass slide containing chambers of a known depth with grids etched onto the surface. Each chamber is divided into 9 squares with surface areas of 1 mm<sup>2</sup>. When a glass cover slip is placed over the chambers and grid, the depth is 0.1 mm and hence the volume of solution for each 1 mm<sup>2</sup> is 10<sup>-4</sup> ml. Cell samples were loaded into the counting chamber through capillary action. Cells were counted using a microscope and the density of cells per ml = average cell count per mm<sup>2</sup> x 10<sup>4</sup>. To avoid overestimating the number of cells, any cells touching the upper and right hand perimeter lines were ignored.

## **2.2.5: Cryogenic storage and resuscitation of frozen cells**

### *Storage*

Cells were harvested using trypsin-EDTA as described in section 2.2.3 and collected by centrifugation (275 x g, 20°C for 5 minutes). Excess media was aspirated and cell pellets resuspended in freezing solution at a concentration of  $10^6$  cells/ml. Cell suspensions (1 ml) was transferred into a cryovial, and then frozen for 24hr at -80°C in an expanded polystyrene box to achieve a slow freezing rate. Slow freezing and the presence of DMSO in the freezing solution help to minimise the formation of ice crystals which could potentially damage the cells. After initial freezing, cells were transferred to liquid nitrogen.

### *Resuscitation*

Aliquots of frozen cells (1 ml), stored in liquid nitrogen, were thoroughly thawed to 37°C and immediately added to 9 ml fresh tissue culture media. Cells were washed by centrifugation (275 x g, 20°C for 5 minutes) before being inoculated into tissue culture flasks. Cells were not used for experimentation for at least one week to ensure recovery from the effects of cryopreservation.

### **2.3: Exposure of cells to cytotoxic drugs**

#### *Cell Lines – Incubations in flasks*

Cisplatin, carboplatin and oxaliplatin were prepared in medium at 5 to 10-fold higher initial concentrations and appropriate volumes added to cell cultures to achieve the desired final concentrations. For control experiments water without drug was added. Sterile sodium chloride was added to correct for osmotic changes as a result of adding water or aqueous drug solution. After exposure cells were washed three times with PBS, before harvesting by trypsinisation. Following centrifugation (275 x g, 20°C for 10 minutes), pellets were stored at -20°C.

#### *Cell Lines – Incubations in 96 well plates*

Cisplatin, carboplatin and oxaliplatin were prepared in medium at 2-fold higher initial concentrations, and 100 µl/well added to cell cultures to achieve the desired final concentrations. For control experiments medium without drug was added. Cells were incubated at 37°C for varying times dependent on the experimental setup.

#### *Volunter Human Blood*

Blood was collected in sterile heparinised tubes, and then incubated in tissue culture flasks with 2 mM carboplatin (dissolved in saline) or saline alone for 60 minutes. Immediately after incubation, 10 ml blood samples were layered onto Lymphoprep (Axis Shield, Norway) and centrifuged (800 x g, 20°C for 15 minutes). Peripheral blood lymphocytes were collected and washed twice in sterile PBS, then pellets frozen at -20°C. Prior written consent was obtained for all volunteer samples.

## **2.4: Sulphorhodamine B colorimetric assay**

### *Principle*

Sulphorhodamine B (SRB) is an aminoxanthine dye with two sulphonic groups that binds electrostatically to basic amino acids of cell proteins under mildly acidic conditions. The intensity of staining is proportional to the amount of cellular protein and therefore cell number, assuming cell size is consistent. As described previously (Skehan et al 1990) the SRB colorimetric assay can be used as a rapid and sensitive means of determining cellular growth rate and growth inhibition. The SRB assay was carried out using 96-well microtitre plates. The number of cells plated was dependent on growth rate of the cells, the confluent cell density and the duration of the experiment. Cells were inoculated only in the inner 60 wells on the plate to avoid “edge-effect”, a phenomena that can cause abnormal growth in the outer wells (Dr Rony Nuydens, Janssen Cilag Ltd, Belgium - personal communication).

### *Method: SRB Assay*

Cells were fixed by aspirating all media from the plates, followed by addition of 200  $\mu$ l cold PBS and then 50  $\mu$ l cold 50% trichloroacetic acid (TCA). After incubating at 4°C for 1hr, plates were washed with water and stored at 4°C ready for staining. To each well 100  $\mu$ l SRB stain was added and incubated at room temperature for 30 minutes. Excess dye was removed by rinsing 5 times with 1% acetic acid (VWR). Rinsing was performed quickly but gently to avoid dislodging cells and prevent desorption of the protein-bound dye. Stained plates were air-dried overnight before addition of 100  $\mu$ l 10 mM Tris to each well to solubilise the dye. Staining intensity was then analysed at 490 nm using a SpectraMAX 250 microplate reader (Molecular Devices).

## **2.5: DNA extraction**

### **2.5.1: DNA extraction using hydroxyapatite**

#### *Principle*

DNA extraction using hydroxyapatite was described previously (Tilby et al 1991) for preparation of cellular DNA for measurement of melphalan-DNA adducts by immunoassay. Hydroxyapatite is a calcium phosphate mineral that is believed to interact with phosphate groups on DNA. By manipulating phosphate concentration (i.e. low phosphate concentration in solution) it is possible to bind DNA to hydroxyapatite, allowing retention of DNA whilst washing away any remaining cellular material. Increasing phosphate ion concentration causes DNA to elute from the hydroxyapatite. This method can reliably produce a good yield of DNA from a relatively small number of cells and produces low molecular weight DNA free of alcohol, RNA and protein.

#### *Method: DNA extraction*

Frozen cell pellets were lysed by addition of 2 ml HA lysis buffer and then sonicated for 2 minutes at full power in a 600 W Vibracell ultrasonic processor equipped with a water-filled cup-horn (Roth Scientific, UK). After sonication 20 µl RNAase A was added to each lysate to digest RNA and samples were incubated at 37°C for 15 minutes. Following incubation, an additional 3 ml HA lysis buffer was added along with 5 ml water saturated Kirby's phenol, and samples mixed by rotation at room temperature for 20 minutes. Samples were centrifuged (700 x g, 4°C for 15 minutes) to separate the two phases. For each sample the aqueous upper phase (approximately 5ml) was collected and transferred to a fresh tube.

To each tube 25 ml of 6 M urea, containing 80mM KP buffer and 0.5 g DNA grade hydroxyapatite BioGel (BioRad, UK), was added to the DNA solution and mixed by rotation at room temperature for 20 minutes. The hydroxyapatite with DNA bound was collected above a filter in a spin column, which comprised a 10 ml syringe barrel (central Luer connection) with a piece of plastic gauze covering the bottom and a close-fitted glass fibre filter paper disc. The syringes were suspended inside 50 ml tubes. Excess liquid was removed by centrifugation (50 x g, 20°C for 5 minutes) and washed twice with 10 ml 5 M Urea containing 80 mM KP buffer to remove traces of proteins, phenol and detergent, followed by three further washes with 10 mM KP buffer to remove urea. After each volume of wash buffer had been added the columns were centrifuged (50 x g, 20°C for 5 minutes) and the eluate discarded. DNA was finally eluted from the hydroxyapatite by addition of 2 ml 0.5 M KP buffer followed by centrifugation (50 x g, 4°C for 5 minutes). Eluates were stored at -80°C.

*Method: Removal of salt and concentration of DNA*

Desalting of the DNA solution was carried out using Centricon Ultracel YM-10 centrifugal filter units (Millipore, UK). Initially the units were washed thoroughly with de-ionised water, then the DNA samples were added and centrifuged (5000 x g, 4°C) until the volume in the Centricon was approximately 60 µl. DNA was washed twice by addition of 1 ml DNA digest buffer and further centrifugation. 440 µl DNA digest buffer was added to the unit which was then left to stand at room temperature for one hour to allow DNA to dissociate from the filter. The resulting concentrated DNA solution was collected by placing a vial over the top of the Centricon, inverting, and centrifuging (500 x g, 4°C for 5 minutes). The DNA solution was stored at -80°C.

## **2.5.2: DNA extraction using QIAGEN Blood and Cell Culture DNA midi kit**

### *Principle*

The blood and cell culture DNA midi kit makes use of the QIAGEN ‘Genomic-tips’, which use an anion exchange resin to retain DNA, without use of phenol or chloroform. In this procedure cells were lysed and digested with protease enzyme and the lysates then added to the column and allowed to pass through by gravity flow. The pH and low salt conditions of the buffer caused DNA to bind to the QIAGEN resin whilst other cellular constituents passed through. Purified DNA was eluted in a high salt buffer. The type of kit used was limited to processing cellular samples with a maximum cell count of  $2 \times 10^7$  (see section 1A) or tissue samples up to approximately 100 mg (see section 1B). Section 2 was the same for both cellular and tissue preparations.

### *Method*

#### *Section 1A: Cell Pellets*

Frozen cell pellets were thawed fully, re-suspended in 1 ml PBS, and transferred to 15 ml centrifuge tubes (Sarstedt, Germany). Ice cold buffer C1 (2 ml) was added and mixed and then 6 ml ice cold de-ionised water added. Samples were placed on ice for 15 minutes, followed by centrifugation (1300 x g, 4°C for 15 minutes). Supernatants were discarded and pellets were each re-suspended in 1 ml ice cold buffer C1, mixed, and then 3 ml ice cold de-ionised water was added. They were again placed on ice for 10 minutes, followed by centrifugation (1300 x g, 4°C for 15 minutes). Supernatants were discarded and pellets re-suspended in 1 ml buffer G2 and samples were sonicated for 2 minutes at full power in a 600 W Vibracell ultrasonic processor equipped with a water-filled cup-horn (Roth Scientific, UK). After sonication, buffer G2 (4 ml) and

RNAase A solution (10 µl) were added and incubated at 37°C for 20 minutes, followed by addition of QIAGEN protease (95 µl) and incubation at 50°C for 1hr.

#### *Section 1B: Human or Mouse Tissue Samples*

Tissue samples up to 100 mg were initially homogenised with 100 µl buffer G2 in a 1.5 ml microtube using a plastic “pellet pestle” (Anachem, UK). A further 900 µl buffer G2 was added and the sample transferred to a 15 ml centrifuge tube (Sarstedt, Germany). A further 1 ml buffer G2 was added and samples were sonicated for 2 minutes at full power in a 600 W Vibracell ultrasonic processor equipped with a water-filled cup-horn (Roth Scientific, UK). After sonication 7.5 ml buffer G2 and 19 µl RNAase A were added and samples incubated at room temperature for 15 minutes, followed by addition of 500 µl QIAGEN protease and incubation at 50°C for 2hr.

#### *Section 2: Genomic Tip DNA Extraction*

During the incubation steps columns were equilibrated with 4 ml buffer QBT. After incubation samples were added to the columns. At this point DNA became bound to the column, and was washed twice with 7.5 ml of buffer QC. DNA was eluted into 15 ml centrifuge tubes (Sarstedt, Germany) by addition of 5 ml of buffer QF. Isopropanol (3.5 ml) was added to each DNA sample. The samples were centrifuged (5000 x g, 4°C for 25 minutes). Supernatant was carefully poured off and 2 ml cold 70% ethanol was added, followed again by centrifugation (5000 x g, 4°C for 15 minutes). Supernatant was carefully poured off and samples were air-dried. DNA was dissolved in 500 µl de-ionised water and stored at -80°C.

### **2.5.3: Measurement of DNA concentration**

The concentration of isolated DNA was quantified using either an NanoDrop ND-1000 spectrophotometer (Thermo Finnigan, USA) or a Lambda 2 UV/Vis Spectrophotometer (Perkin Elmer, USA). DNA maximally absorbs light at a wavelength of 260 nm. A sample of pure DNA has a ratio of optical density (OD) 260/280 which is empirically determined to be 1.8. The overall absorbance of DNA is a combination of the absorbance peaks of the four DNA bases. Sample contamination, with proteins for example, can cause the OD<sub>260/280</sub> ratio to vary. Samples with an OD<sub>260/280</sub> of less than 1.75 or greater than 1.90 were discarded.

#### *NanoDrop Spectrophotometer*

The NanoDrop is a rapid and simple method for measuring absorbance without the use of cuvettes. Samples (1 µl) are loaded onto a fibre optic cable (receiving fibre). Samples are maintained on the cable by surface tension. A second fibre optic cable (source fibre) is brought into contact with the sample, bridging the gap between the two fibres. The gap is controlled at 0.2 and 1 mm distances. A pulsed xenon flash lamp provides the light source, and a spectrophotometer with a linear CCD array used to analyse the light passing through the sample. The concentration of DNA is automatically calculated by the NanoDrop software, based on the principle that a sample of 50 µg/ml pure DNA has an absorbance of 1 AU at 260 nm in a 10 mm path length cuvette. This method was used for all samples of DNA isolated using Qiagen kits (section 2.5.2) and DNA concentrated from gel filtration (section 2.8)

### *Lambda 2 UV/Vis Spectrophotometer*

This method is much slower for determining DNA concentration, but possibly more reliable. The Lambda 2 uses double-beam optics for excellent long term stability, reference compensation and baseline correction, and can be used for measuring individual or multiple wavelengths, or for scanning wide wavelengths ranging from 190-1100 nm, with scan speeds between 7.5-2880 nm/min. The Lambda 2 was used for measuring DNA isolated using hydroxyapatite (section 2.5.1) using a 1 mm path length cuvette and for measuring dissolved pure DNA (section 2.7.1) or DNA in gel filtration fractions (section 2.8) using a 10 mm path length cuvette.

For DNA isolated by hydroxyapatite, approximately 500  $\mu$ l samples were added. DNA digest buffer was initially measured at OD<sub>254nm</sub> to provide a blank reading. OD<sub>280nm</sub> was also measured to test sample purity. Between each sample the cuvette was rinsed thoroughly with acetone and air dried. DNA concentration was determined using the equation below:

$$\text{DNA concentration } (\mu\text{g/ml}) = \text{Absorbance } 260\text{nm} * 50 * 10$$

DNA in collected gel filtration fractions was measured at OD<sub>254nm</sub>. Initially, OD<sub>254nm</sub> of 50 mM sodium phosphate buffer was measured to provide a blank reading. The cuvette was not rinsed between samples. DNA concentration was not calculated as all gel filtration plots in this thesis used OD<sub>254nm</sub> as a vertical Y2 axis.

## 2.6: Enzymatic digestion of platinated DNA

### *Principle*

Prior to chromatographic separation of Pt-DNA adducts DNA samples were enzymatically digested to form 5' mononucleotides and 5' dinucleotides, where adjacent nucleotides are joined by a Pt atom. DNAase1 was initially added to DNA samples and incubated. DNAase1 is a nuclease that cleaves DNA at phosphodiester linkages, preferentially adjacent to pyrimidine bases. This results in 5'-phosphate polynucleotides, with a free 3'-hydroxyl. Nuclease P1, which further cleaves DNA yielding 5'-monophosphate nucleotides, was added after incubation with DNAase1. Importantly, nuclease P1 cannot cleave dinucleotides linked by Pt, possibly due to steric hindrance. This allows for cleavage of Pt-DNA adducts from DNA with a terminal 5'-phosphate

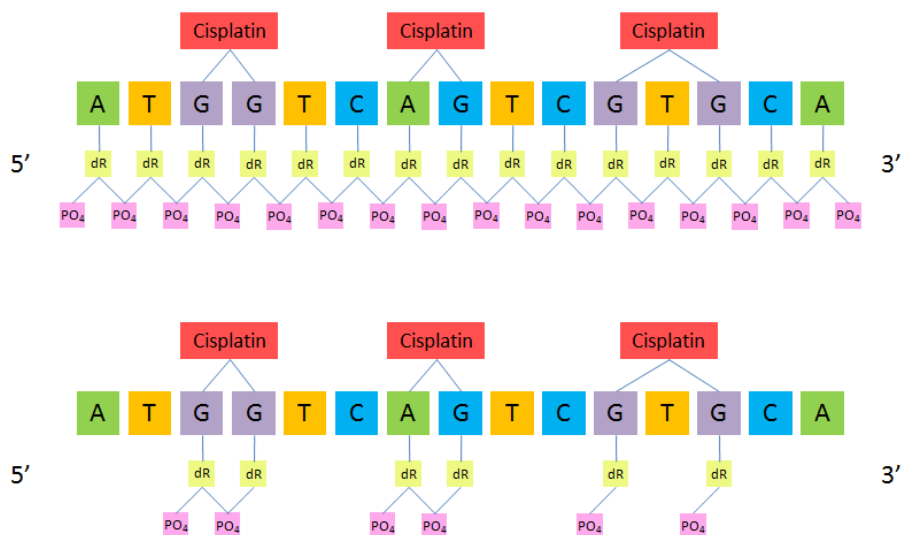


*Figure 2.1 Enzymatic hydrolysis of platinated DNA to mono- and di-nucleotides, which were subsequently separated by anion exchange chromatography under varying salt concentrations*

### *Method*

The volume of DNA solution required in each digest was calculated by dividing the required [DNA] from the measured [DNA], and multiplying this value by the total digest volume. The final concentration of DNA was 0.25 mg/ml, made up in a final volume of 200  $\mu$ l. 20 Kunitz units of DNAase1, 4.8  $\mu$ l 10 mM zinc sulfate and 3.2  $\mu$ l 250 mM magnesium chloride was added and incubated for an initial 2hr at 37°C. Nuclease P1 (200 units/ml) was added after the initial 2hr and incubated for a further 16hr at 37°C. After the incubation period the digested DNA samples were added to a Microcon YM-10 ultrafiltration unit (Millipore, UK) (nominal 10 kDa MW cut-off) and centrifuged (14000 x g, 4°C for 1hr) to remove proteins prior to chromatography. Ultrafiltrates were stored at -80°C.

## **2.7: Reactions of cisplatin with nucleic acids**

### **2.7.1: Reaction of cisplatin with highly purified calf thymus DNA in the presence or absence of GSH or STS**

Highly purified calf thymus DNA (Merck, USA) was dissolved in 5 mM sodium chloride over several days at 4°C. DNA concentration was determined at OD<sub>260nm</sub> using a Lambda 2 UV/VIS spectrophotometer as described in section 2.5.3. Cisplatin was diluted in de-ionised water from a 2 mM stock stored at -20°C. The final required concentration was achieved by diluting cisplatin in water and 10X PB. GSH and STS were dissolved in PB immediately prior to use, and pH adjusted with 10 M and 1 M sodium hydroxide.

Cisplatin was reacted with calf thymus DNA in the presence and absence of GSH or STS to give a final DNA concentration of 500 µg/ml. The DNA, GSH and STS solutions were prepared in PB. Cisplatin was added and the reaction vessels were immediately gassed with nitrogen to prevent oxidation. The mixture was then incubated at 37°C. Samples were stored at -80°C. Platinated DNA was separated by gel filtration chromatography as described in section 2.8.

### **2.7.2: Reaction of cisplatin with deoxyguanosine monophosphate (dGMP) in the presence or absence of GSH or STS**

dGMP was dissolved in de-ionised water to a concentration of 2 mM to match the concentration of cisplatin. Equal volumes of cisplatin and dGMP were mixed to achieve a final concentration of 1 mM, and incubated at 37°C. GSH and STS were dissolved in de-ionised water immediately prior to use, and pH adjusted with 10 M and 1 M sodium hydroxide. GSH and STS were added to the dGMP/cisplatin reaction mixture after 24hr incubation at 37°C. Reaction samples were stored at -80°C.

## **2.8: Gel filtration chromatography**

### *Principle*

Following reaction of calf thymus DNA with cisplatin in the presence or absence of GSH or STS, platinated DNA was separated from unreacted drug and other low molecular weight material by gel filtration chromatography. Gel filtration chromatography is a method that allows separation of molecules through a gel column on the basis of their molecular size. Molecules move through a bed of porous beads, diffusing into the beads based on size. Smaller molecules diffuse further and more often into the beads and therefore spend a greater proportion of time in the stationary phase compared to larger molecules, such as high molecular weight DNA, which are excluded from the pores of the stationary phase. Movement of solutes through the column is dependent on mobile phase flow rate and partitioning of molecules between the stationary and mobile phases based on molecular size. Molecules are eluted in the order of decreasing molecular size.

### *Method – Gel Filtration*

PB was used as the mobile phase, and Sephadex G-75 as the stationary phase. Sephadex G-75 is a porous gel with a fractionation range of 3000 – 80000 MW, and was prepared by swelling the beads in de-ionised water overnight at room temperature, and then boiling for an hour to remove air. Two XK26 gel columns (Pharmacia, Sweden), each with an approximate bed volume of 400 ml, were used to contain the gel. The apparatus comprised two P1 peristaltic pumps (Pharmacia, Sweden), both routed through a 1.5 mm bore Omnifit rotary valve (Kinesis, UK) allowing simultaneous separation and flushing of alternate columns. Samples were introduced

through a Valve V7 mixer (Pharmacia) into a 10 ml sample loop (Pharmacia, Sweden) and collected using a Frac 200 collector (Pharmacia, Sweden). Fractions were collected over 5 minutes at a flow rate of 2.0 ml/min. DNA was detected in collected fractions by measuring OD<sub>254nm</sub> using a Lambda 2 UV/VIS spectrophotometer as described in section 2.5.3. Pt content determined by atomic absorption spectrometry as described in section 2.10, using nitric acid standards containing sodium phosphate to replicate the phosphate concentration of the diluted samples.

*Method – Concentration and Buffer Exchange of Solutions*

Fractions containing DNA were transferred to an Amicon stirred ultrafiltration cell model 8050 (Millipore, UK) with a 10000 kDA molecular weight cut off filter. DNA was concentrated under nitrogen gas pressure (~ 70 PSI). Phosphate buffer was replaced with DNA digest buffer through a series of washes under nitrogen gas pressure. DNA was collected from the cell in approximately 1 ml DNA digest buffer after the cell was stirred for 1hr with no nitrogen gas. This was necessary to allow the release of DNA from the membrane, thereby maximising DNA recovery. DNA concentration was determined by measuring OD<sub>260nm</sub> using a NanoDrop spectrophotometer as described in section 2.5.3.

## 2.9: Anion exchange chromatography

### *Principle*

Ion exchange chromatography is a technique that allows separation of molecules based on their charge and can be sub-divided into cation and anion exchange chromatography. Cation exchange chromatography relies on positively charged molecules binding to negatively charged residues on the stationary phase of a column, whereas anion exchange chromatography relies on negatively charged molecules binding to positively charged residues on the stationary phase of the column. In the ion exchange chromatography method used here the ionic strength was increased over time by mixing together two buffers of different ionic composition. Samples were introduced in a starting buffer (low chloride ion concentration) and became bound to the column. The concentration of chloride ions was increased by steadily increasing the proportion of the second buffer (high chloride ion concentration). Molecules were selectively eluted based on their different binding affinity to the column at varying ionic strengths.

### *Method*

DNA nucleotides (negatively charged) were separated using a MonoQ 5/50 GL anion exchange column (Amersham, UK) which carries  $-\text{CH}_2\text{-N}^+(\text{CH}_3)_3$  as the charged group. Chromatography was carried out using a modified "FPLC system" with two P-500 pumps (Pharmacia, Sweden) coupled to a mixer (Pharmacia, Sweden) and a Waters 2487 dual  $\lambda$  absorbance detector (Waters, UK) with an inert taper split flow cell (Waters, UK). Samples were introduced through a Rheodyne 9725i manual injector port. Fractions of eluent were collected in a Frac 100 collector (Pharmacia, Sweden). The system was controlled through Clarity<sup>®</sup> Chromatography data station software

(DataApex, UK). The pumps were controlled via a Clarity CB20 digital to frequency converter board and outputs from the UV monitor and injection valve were connected to a Clarity Int7 analogue to digital converter board.

The chromatographic method for separating Pt-DNA adducts after enzymatic digestion was based on a method published previously (Fichtinger-Schepman et al 1985). Before sample injection the column was equilibrated with  $\text{Cl}^-$  ions by performing the salt gradient program as used for elution. This gradient was formed between HPLC buffers A and B by altering the proportion of each buffer entering the column by varying the pump rates (Table 2.1). The overall flow rate was 1 ml/min, with a typical pressure of between 3-3.5 MPa. During elution 500  $\mu\text{l}$  fractions were collected every 30 seconds over a 25 minutes period. Fractions were stored at  $-20^\circ\text{C}$  prior to further analysis.

A mixture of dAMP, dCMP, TMP and dGMP (50  $\mu\text{g}/\text{ml}$  final concentration) was analysed at the beginning and end of each set of chromatographic analyses of experimental samples to serve as a control to confirm satisfactory performance of the MonoQ column.

*Table 2.1: Chromatographic gradient used for selective elution of mono- and di-nucleotides from the MonoQ column*

<b>Time (Minutes)</b>	<b>HPLC Buffer B</b>	<b>Salt Ion (M)</b>
0 – 1	Isocratic elution, 5%	0.05
1 – 4	Linear Increase, 5% to 7.5%	0.05 to 0.075
4 – 7.5	Isocratic elution, 7.5%	0.075
7.5 – 10.5	Linear Increase, 7.5% to 10%	0.075 to 0.1
10.5 – 25	Linear Increase, 10% to 25%	0.1 to 0.25
25 – 26	Linear Increase, 25% to 100%	0.25 to 1
26 – 30	Isocratic elution, 100%	1
30 – 34	Wash, 0%	0

## **2.10: Graphite furnace Atomic Absorption Spectrometry (AAS)**

### *Principle*

Atomic absorption is a process that occurs when a ground state atom, usually a vapour, absorbs energy in the form of light of a specific wavelength and becomes elevated to an excited state. The amount of light energy absorbed at this wavelength increases as the number of atoms increases. Unknown concentrations of an element in a sample can be calculated by comparison to the amounts of light absorbed by a series of known standards. Graphite furnace AAS requires 1: a primary light source, e.g. a hollow cathode lamp; 2: an atom source, which is a sample in the form of a vapour generated in an electrically heated graphite cartridge; 3: a monochromator to isolate a specific wavelength of light; 4: a detector to measure light accurately; and 5: electronics to treat the signal and process the results. Samples are injected directly into a graphite tube and heated through a series of programmed steps to remove solvent and matrix components, before then finally atomising the remaining sample for analysis.

### *Method*

Analysis was performed using a flameless Perkin Elmer AAnalyst 600 graphite furnace AAS (Perkin Elmer, UK) using a method designed for analysis of Pt. The monochromator was set to a wavelength of 265.9 nm. The furnace program steps are shown in Table 2.2.

A standard curve of known Pt concentrations ranging from 0-2000 ng/ml was prepared by diluting stock Pt standards 10-fold in 0.1 M nitric acid. These standards were used to determine Pt concentration in samples. Standards for analysis of gel filtration fractions contained 5 mM sodium phosphate to match the concentration of phosphate ions in the diluted samples. Samples were diluted 10-fold in 0.1 M nitric acid. Analysis of each sample was carried out in duplicate. 20  $\mu$ l aliquots were injected into the graphite tube by an autosampler.

*Table 2.2: Furnace program used for determination of Pt concentration*

<b>Step</b>	<b>Temperature (°C)</b>	<b>Ramp Time (secs)</b>	<b>Hold Time (secs)</b>
1	110	1	60
2	130	15	30
3	1300	10	20
4	2200	1	5
5	2450	1	10

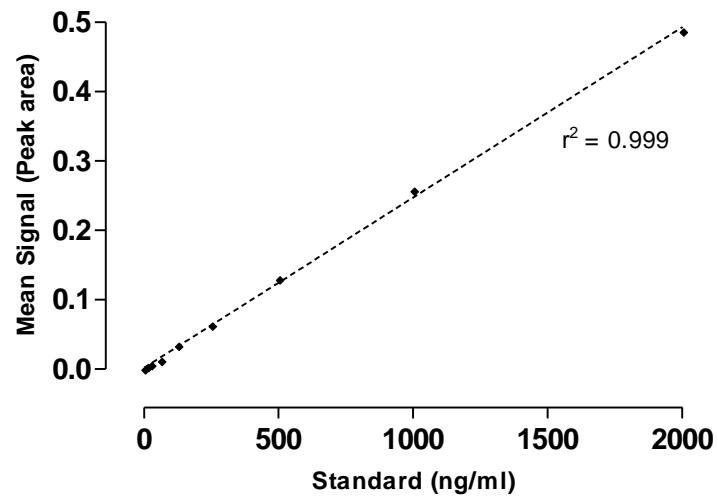


*Figure 2.2: Typical standard curve used for determination of unknown Pt concentrations in samples by atomic absorption spectrometry*

## 2.11: Inductively-Coupled Plasma Mass Spectrometry (ICP-MS)

### *Principle*

ICP-MS is an analytical technique used to determine the isotopic composition and concentration of elements present in samples. Samples are converted to atoms by high temperature and become ionised whereby they can be analysed by mass spectrometry. Sensitivity of detection varies between elements as a result of differences in: 1, ease of ionisation; 2, background levels of elements in the environment; 3, matrix effect and 4, interferences from combinations of atoms that form ions with the same mass/charge ratio as the element being detected.

High temperature and ionisation is achieved by passing a volume of sample through an atomiser. This generates a fine mist which is then sprayed into an inductively coupled plasma (ICP) torch. Argon gas flows inside the ICP torch, connected to a radio-frequency (RF) generator connected to an RF load coil. As power is supplied to the load coil from the RF generator, oscillating electric and magnetic fields are generated at the tip of the ICP torch. When a spark is applied to argon flowing through the torch, electrons are stripped from the argon atom to form argon ions. These ions collide with other argon ions in the oscillating fields to form the argon plasma torch, maintained at approximately 10'000°K by an induction coil supplied with an electric current. The Atomic Spectroscopy detection limit for Pt by ICP-MS is 0.002 µg/L. Samples are typically introduced in liquid state and nebulised before entry into the plasma torch, where in the high temperature of the plasma metals become ionised through electron loss and are extracted into the mass spectrometer. ICP-MS is a method suitable for

detecting low levels of Pt as sensitivity of detection is less than 0.1 parts per trillion (PPT).

Two instruments were used in this thesis – A Sciex Elan 6000 Quadrupole ICP-MS (Perkin Elmer, UK) and a Finnigan Element2 Magnetic Sector Field ICP-MS (Thermo Electron, Germany). All ICP-MS analysis was carried out at the Northern Centre for Isotopic and Elemental Tracing at the Department of Earth Sciences, Durham University, Durham, UK.

### **2.11.1: Sciex Elan 6000 Quadrupole ICP-MS**

#### *Detection Principle*

Metals ions are extracted through a series of cones with decreasing sample holes (1 mm ‘sampler’ cone and 0.4 mm ‘skimmer’ cone) into the quadrupole mass spectrometer. The quadrupole consists of four parallel metal rods. Opposing rods are connected electrically, and a radio frequency applied between paired-rods. A direct current voltage is superimposed over the radio frequency voltage and ions are separated based on the stability of their trajectories in the oscillating electric fields that are applied to the quadrupole rods. Only ions of a certain mass/charge ratio can pass through the quadrupole to the detector. Pt ions hitting the detector were counted and the count rate was proportional to the concentration of Pt in the sample. The actual concentrations were calculated using a standard curve of known Pt concentrations.

### *Sample Preparation*

All samples were prepared in ultrapure nitric acid (UpA) (Romil, UK) with a Pt contamination of < 1 PPT diluted to 3.5% w/v in high purity water. For analysis of total Pt-DNA adducts on DNA, 20 µl samples were diluted in 980 µl UpA, then acid hydrolysed at 70°C overnight. For analysis of chromatographically separated individual adducts, 100 µl samples were diluted in 900 µl UpA. Maximum salt concentration in samples after dilution was 25 mM.

### *Sample Analysis*

Samples were introduced by a peristaltic pump into a standard cross-flow nebuliser fitted to a Scott type double pass spray chamber. This ensured a fine mist entered the plasma torch, and removed large droplets of liquid that would hamper ionisation. Nebuliser gas flow rate was between 0.8-1.0 L/min, and this was optimised to maintain the production of cerium (Ce) oxide ( $\text{CeO}^+$ ) at less than 3% of the total  $\text{Ce}^+$  signal. Ce is prone to formation of oxides and is used as a measure of oxide formation for monitoring elemental interference. Maintaining low levels of interference ensures the detected signal originates from the element of interest. This is especially important for low level elemental analysis. RF power was generally 1150 W.

Three isotopes of Pt were monitored:  $^{194}\text{Pt}$  (32.97% abundance),  $^{195}\text{Pt}$  (33.83% abundance) and  $^{196}\text{Pt}$  (25.24% abundance) allowing for evaluation of isotopic differences as a check for errors or interferences in the analysis. Concentrations calculated using each Pt isotope agreed within analytical error, indicating that other potential interferences are negligible. Hafnium (Hf) oxide species ( $^{178}\text{Hf}^{16}\text{O}$  and  $^{179}\text{Hf}^{16}\text{O}$ ) are the commonest potential isobaric interference when detecting Pt. The

very low levels of Hf in the DNA solutions meant that such interferences were insignificant to the analyses in this thesis and therefore no oxide corrections were required. Pt concentrations in samples were calculated from average values produced by the three isotopes. Previous studies at Newcastle had determined that procedural blanks of approximately 1 PPT, give limits of quantitation of close to 1.1 PPT in the final solution (Azim-Araghi 2001). Therefore, no blank corrections were made to the data.

The samples analysed were low in dissolved solids and therefore could be analysed using instrument calibration based on standard Pt solutions. Pt standards of 0, 100, 500, 1000 and 2000 PPT were made from a 1000 PPM Pt stock (Romil, UK). Most samples in the study gave signals within this range. The standard solutions were analysed at the beginning of the analytical session, and again at the end. The 500 PPT standard was checked routinely during each analysis. It was critical to monitor the standards before, during and after analysis for two reasons: 1, instrumental drift can occur as the number of analyses increases and 2, the mass spectrometer was set to detect Pt using a detection process called peak hopping. During peak hopping the spectrometer moves between pre-set peaks (values entered as integers) causing the mass spectrometer to detect the tops of the mass peaks. This requires knowledge of the composition of the element being analysed to ensure the tops of the mass peaks are correctly identified. The calibration was monitored routinely to ensure this. An alternative to peak hopping is mass focusing (see section 2.11.2).

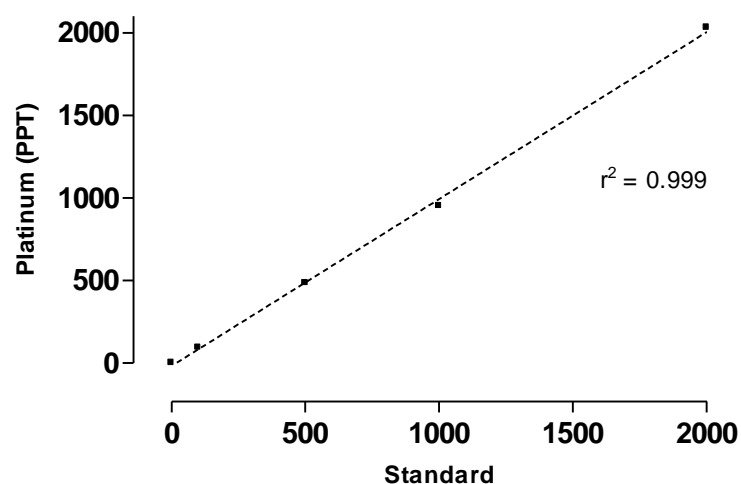


*Figure 2.3: Typical standard curve used for determination of unknown Pt concentrations in samples on the Sciex Elan*

### **2.11.2: Finnigan Element2 Magnetic Sector Field ICP-MS**

#### *Detection Principle*

Magnetic sector field ICP-MS relies on a magnetic field to disperse metal ions according to their mass and energy, determining the trajectory by which they pass through the mass analyser. Faster moving (lighter) ions are deflected more than slower moving (heavier) ions and the mass analyser can be adjusted to deflect and thus detect a narrow range of ion masses, or to scan through a range of known ion mass/charge ratios to analyse specific ions.

#### *Sample Preparation*

All samples were prepared in UpA nitric acid (Romil, UK). This was diluted to 7% w/v in high purity water. The 7% UpA was spiked with a small volume of 3% UpA spiked with 50 PPB thallium (Tl) for analysis of instrumental drift and Pt sample correction

(see data analysis section below). This acid had a final composition of 7% UpA with 2 PPB Tl. DNA samples (100 µg/ml) were prepared in ultra pure water and diluted with equal volumes of 7% UpA with 2 PPB Tl to achieve a final concentration of 50 µg/ml DNA in 3.5% UpA, 1PPB Tl. Samples were acid hydrolysed at 70°C overnight. 500 µl of sample was sufficient for analysis.

A series of Pt standards were prepared for calibration of the ICP-MS. These standards were made fresh for each analysis. 7% UpA was diluted to 3.5% UpA with high purity water. The 3.5% UpA was spiked with a small volume of 3% UpA spiked with 50 PPB Tl to ensure the acid used in the standards was of the same final composition as the samples. This acid had a final composition of 3.5% UpA with 2 PPB Tl. A stock of 1000 PPM Pt (Johnson Matthey, USA) was prepared in 3.5% UpA, 2PPB Tl was used to prepare standards. This was diluted to 1000 PPT Pt in 3.5% UpA, 2PPB Tl, and mixed at varying volumes with 3.5% UpA to achieve the desired final concentrations as shown in Table 2.3.

*Table 2.3: Standards used for calibration of the Element2 ICP-MS. The 1000 PPT Pt stock was prepared in 3.5% UpA/2 PPB Tl*

<b>Standard (PPT)</b>	<b>Vol. 3.5% UpA (<math>\mu</math>l)</b>	<b>Vol. 1000 PPT Stock (<math>\mu</math>l)</b>
0	10000	0
1	9990	10
2	9980	20
5	9950	50
10	9900	100
50	9500	500
100	9000	1000
250	7500	2500
500	5000	5000

### *Sample Analysis*

Unlike the Sciex Elan which uses a peristaltic pump, samples are introduced into the Element2 by capillary action. This is a much slower method of sample introduction. Samples entered into a 100  $\mu$ l/min microflow nebuliser fitted to a cyclone scott double pass spray chamber. This set up was similar to the Sciex Elan but sample flow was greatly reduced. Nebuliser gas flow rate was varied to maintain a CeO/Ce of less than 3%. Typically, nebuliser gas flow was in the region of 0.95 L/min. RF power was 1300 W. Plasma cool gas (Argon) flow rate was 16 L/min. Auxillary gas flow rate (Argon) was 1 L/min. Individual sample analysis time was 26 seconds.

Very low levels of Pt were expected to be detected in the samples analysed on the Element2 ICP-MS, so an increased number of elements were detected. As with the Sciex Elan, three isotopes of Pt were monitored:  $^{194}\text{Pt}$  (32.967% abundance),  $^{195}\text{Pt}$  (33.832% abundance) and  $^{196}\text{Pt}$  (25.242% abundance). As mentioned above, samples were spiked with Tl, and two isotopes of Tl were measured:  $^{203}\text{Tl}$  (29.524% abundance) and  $^{205}\text{Tl}$  (70.476% abundance). At the expected low levels of Pt, isotopic interference has a greater effect on accurately determining the actual element levels, so a number of elements were detected by the Element2 ICP-MS to confirm the detected Pt levels were correct. These are shown in Table 2.4.

*Table 2.4: Isotopes detected by the Element2 ICP-MS. Natural abundance values were obtained from Rosman and Taylor 1998*

Element	Isotope Measured	Natural Abundance
Neodymium	$^{143}\text{Nd}$	12.18%
Dysprosium	$^{161}\text{Dy}$	18.91%
Hafnium	$^{178}\text{Hf}$	27.28%
	$^{179}\text{Hf}$	13.62%
Platinum	$^{194}\text{Pt}$	32.967%
	$^{195}\text{Pt}$	33.832%
	$^{196}\text{Pt}$	25.242%
Mercury	$^{200}\text{Hg}$	23.10%
Thallium	$^{203}\text{Tl}$	29.524%
	$^{205}\text{Tl}$	70.476%

The standard solutions (Table 2.3) were analysed at the beginning of the analytical session, and again at the end. The 5 PPT standard was checked routinely during each analysis. The Element2 mass spectrometer detector uses a process of mass focusing to determine the levels of each isotope analysed. In this process a mass is programmed for each isotope, and around this a mass window is determined. In this mass window the mass spectrometer is focused to finding the nominal peak for each isotope through a number of scans inside the window, allowing a more accurate determination of the levels of each element. For this analysis a mass window of 60 was used ( $\pm 30$ ). Three passes were made per isotope, and an average value per isotope calculated per run. Five runs were made in total, meaning the final value produced for elemental concentration was a result of 5 distinct averages.

#### *Data Analysis*

The measured levels of neodymium, dysprosium and hafnium were determined to be at satisfactorily low levels that they were having no interference on the levels of Pt being detected. As a result, they were excluded from further analysis of the data. Mercury is commonly detected in nitric acid (Dr Chris Ottley, personal communication) but does not interfere with the elements being detected and such was excluded also.

Throughout analysis of samples, a blank UpA sample and the 5 PPT standard were analysed. An average value of all the blank UpA samples analysed for each of the three Pt and two Tl isotopes was calculated, and subtracted from all samples to subtract background element levels. The 5 PPT values were compared after the wash value had been subtracted to monitor instrument drift. No significant drift was detected in any analyses, and therefore no correction was applied.

To confirm all ICP-MS readings were reliable, the ratio of  $^{203}\text{Tl}$ : $^{205}\text{Tl}$  was calculated. The natural abundances are 29.524%  $^{203}\text{Tl}$  and 70.476%  $^{205}\text{Tl}$  so a ratio of 1:2.3 was expected. An average ratio of 1:2.95 (+/- 0.1) was achieved, though this was constant throughout all analyses. To normalise the detected Pt values throughout, the individual counts per second (CPS) was divided by the CPS for the  $^{205}\text{Tl}$  isotope. This was applied to all standards to produce a standard curve of Pt (PPT) against CPS Pt/CPS  $^{205}\text{Tl}$ . A typical standard curve is shown in Figure 2.4. The concentration of Pt (PPT) in each sample was calculated in Prism4 (GraphPad Software). This value was converted to moles/ml by multiplying the value (PPT) by  $5.13\text{e}^{-15}$ . An average value for the three Pt isotopes was determined, and subsequently divided by the concentration of DNA in the sample ( $5.0\text{e}^{-5}$  g/ml) to determine an overall Pt-DNA adduct level in  $\text{nmol Pt g}^{-1}$  DNA.

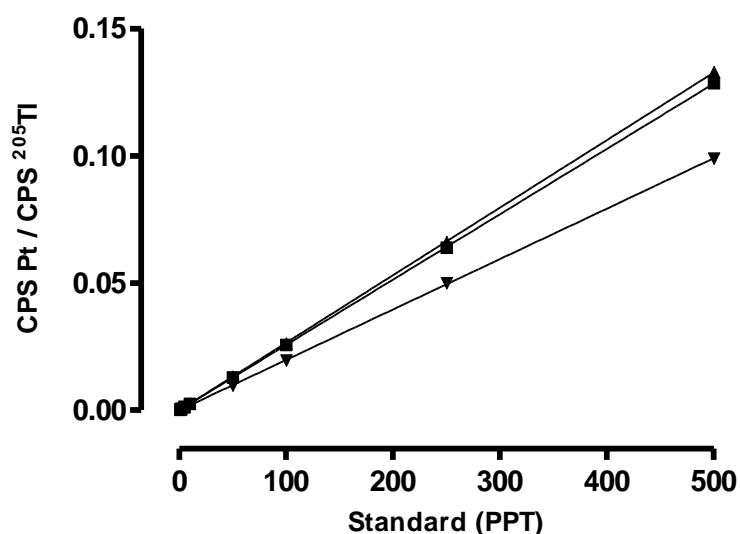
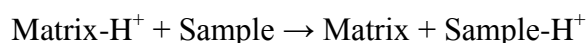


Figure 2.4: Typical standard curve used for determination of unknown Pt concentrations in samples analysed on the Element2 ICP-MS. ( $\blacksquare$ )  $^{194}\text{Pt}$ , ( $\blacktriangle$ )  $^{195}\text{Pt}$  and ( $\blacktriangledown$ )  $^{196}\text{Pt}$

## 2.12: Matrix-Assisted Laser Desorption/Ionisation Time-of-Flight Mass Spectrometry (MALDI-TOF)

MALDI-TOF mass spectrometry is a widely used technique for biomolecule analysis. Samples are mixed with a molar excess of ultraviolet absorbing matrix and dried on MALDI plates. MALDI is a “soft” ionisation technique in which samples become ionized by laser pulses through proton transfer:



Ions of varying sizes are formed in pulses and extracted through a drift tube to a detector, with smaller ions reaching the detector more rapidly. The “Time-of-Flight” (TOF) mass analyser measures the time taken for ions to reach the detector (drift time). The mass/charge ratio of the ions is proportional to the square of the drift time, and is calculated using the following equation:

$$m/z = 2t^2 \times K / L^2$$

m      mass

z      number of charges on ion

t      drift time

K      kinetic energy of ion

L      drift length

MALDI-TOF mass spectrometry was performed at the Institute for Cell and Molecular Biosciences Pinnacle laboratory for Proteomics and Biological Mass Spectrometry, Newcastle University by Dr Joe Gray and Mr Robert Liddell. MALDI-TOF mass spectrometry was carried out using a Voyager-DE STR Biospectrometry workstation (Applied Biosystems, UK).

### 2.13: Nuclear Magnetic Resonance Spectrometry (NMR)

NMR is a powerful spectroscopic method based on absorption of energy in the radiofrequency region of the electromagnetic spectrum by nuclei (hydrogen) of elements that have spin angular momentum and a magnetic moment. Elements whose nuclei possess spin angular momentum and a magnetic moment are assigned half-integral or integral numbers, which determine the number of orientations in space that can be adopted by the spinning nuclei when an external magnetic field is applied. Electrons also possess a spin angular momentum, which generates a magnetic moment that affects the magnitude of the external field experienced by the nuclei.

Nuclei of a particular element that occur in different chemical environments generally experience slightly different magnetic field strengths due to shielding and deshielding by nearby electrons, and thus their resonant frequencies differ in a way that is defined as a chemical shift value. The spin states of one nucleus can affect the magnetic field experienced by nearby elements and groups through intervening bonds causing the absorption peaks to split into multiple components. This effect provides information that permits interpretation of spectra to determine specific locations of nuclei in compounds. NMR spectrometers comprise a superconducting solenoid or electromagnet to generate a stable magnetic field, a transmitter to generate the required radiofrequencies, and a receiver coil to monitor the detector signal.

Two NMR methods were applied in this thesis – proton NMR ( $^1\text{H}$ -NMR) and two-dimensional correlation NMR (COSY-NMR). NMR spectra are often too complex to interpret due to signal overlap. Two dimensional NMR (such as COSY-NMR) allows

determination of molecular connectivity based on spin-spin interactions. In two-dimensional NMR both the X and Y axes plot chemical shifts and 2D spectra can be plotted like a grid.

Samples for NMR were prepared in ultrapure water. dGMP and GSH were dissolved at 10 mM, and cisplatin at 5 mM. For NMR analyses of dGMP and GSH alone, samples were freeze dried then re-dissolved in D<sub>2</sub>O. This was done twice. For NMR analyses of platinated dGMP and GSH, samples were incubated with cisplatin (2:1 molar ratio) for 72hr, then freeze-dried and re-dissolved in D<sub>2</sub>O. This was done once. All samples for NMR were dissolved in 0.7 ml D<sub>2</sub>O.

NMR was performed at the School of Chemistry by Professor William McFarlane using a Jeol Eclipse 11.7 Tesla (<sup>1</sup>H at 500 MHz) spectrophotometer with Delta software.

## 2.14: Statistical analysis

Statistical analyses were carried out using GraphPad prism software version 4.0. Unless otherwise indicated, unpaired t-tests were used for analysing significance.

For the curve fitting to data (SRB data) the following logistic equation was used:

$$Y = M \cdot X^S / (X^S + K^S)$$

Where

M = Maximum value of Y

S = Slope

K = Value of X at which  $Y = 0.5 \cdot M$

So:

Y = OD as % of control and M is fixed at 100%, X = drug concentration

K therefore is the drug concentration at which  $Y = 50\%$  ( $GI_{50}$  value)

## Chapter 3

### ***In vitro* characterisation of potential new Pt-DNA adducts formed in the presence of glutathione**

#### **3.1: Introduction**

The early works of Roberts et al (1972) and Fichtinger-Schepman et al (1985) described in detail in chapter one provided the foundation for the understanding of the cytotoxic properties mechanisms of Pt-based anticancer drugs (Roberts and Pascoe 1972, Fichtinger-Schepman et al 1985). Their findings provided evidence that formation of lesions across DNA was a major part of the mechanism attributed to such drugs, and although the exact mechanisms of cytotoxicity are still unclear, it is accepted that DNA is the major target.

A major limitation in many early studies however was the lack of sensitivity in detection. AAS was often used to determine the levels of Pt in DNA hydrolysates or chromatographically separated DNA which had been enzymatically digested to mono- and dinucleotides. AAS was used with pure DNA that had been reacted with high concentrations of cisplatin, but unfortunately it was not possible to extend such techniques to the study of DNA from drug-treated cells. The development of sensitive immunochemical methods (Tilby et al 1991, Meczes et al 2005, Liedert et al 2006) and <sup>32</sup>P post-labelling assays (Blommaert and Saris 1995, Welters et al 1997, Pluim et al 1999) as described in chapter 1, enabled investigation of more clinically relevant levels

of Pt and investigation of DNA from drug treated cells. However, there are inherent limitations with both approaches. Immunochemical studies involve antibodies raised against specific lesions, and thus are limited to detection of those specific adducts. Postlabelling assays are highly sensitive for the 1,2-intrastrand *cis*-Pt(NH<sub>3</sub>)<sub>2</sub>d(GpG) adduct, and to a lesser extent the *cis*-Pt(NH<sub>3</sub>)<sub>2</sub>d(ApG) adduct. Indeed, neither method is appropriate for the study of all types of adducts that might be present in DNA in cells.

The limitation of AAS for detecting Pt in DNA from drug-treated cells has more recently been overcome through the development of assays involving the highly sensitive method of ICP-MS. Although originally a geochemical technique developed for studying low level elements, ICP-MS has been used in studying the interactions of Pt with cytoplasmic molecules (Esteban-Fernandez et al 2007, Esteban-Fernandez et al 2008) and Pt-DNA adducts (Sar et al 2008, Harrington et al 2010). In more recent years, through the application of ICP-MS, evidence has been obtained suggesting that an additional class of novel Pt-DNA adducts is formed in drug-treated cells, accounting for up to 25% of the total Pt-DNA products (Azim-Araghi 2003). These data arose from the novel combination of anion exchange chromatographic separation of enzymatically digested DNA from drug treated cells as described previously (Fichtinger-Schepman et al 1985, Azim-Araghi 2003) with ICP-MS to detect Pt in chromatographic fractions. In this work, DNA from two lung carcinoma cell lines (H69/p and Mor/p) incubated with cisplatin was enzymatically digested and separated as described above. Analysis by ICP-MS revealed the presence of additional products not detected when purified DNA was incubated with cisplatin. From these data it was hypothesised that the newly detected product was a result of a Pt-mediated cross-link to a non-DNA molecule with this molecule proposed to be glutathione (GSH).

The first evidence that GSH is able to cross-link to DNA via Pt was published over twenty years ago (Eastman 1987). Eastman provided evidence that GSH was able to form lesions with monofunctionally bound Pt and proposed that this form of binding stopped the conversion of monofunctional to bifunctional cross-links, believed to be responsible for cytotoxicity. These data fitted with previous findings that GSH could quench monofunctional adducts (Micetich et al 1983). No indication was presented however to support the role that such adducts could contribute to the cytotoxic mechanism of Pt-based drugs.

Previous work at Newcastle (Azim-Araghi 2003) has indicated that GSH is able to cross-link to DNA via cisplatin, forming a novel adduct in cells. However, there is limited information on the chromatographic properties of such a product. The experiments presented in this chapter investigated the *in vitro* formation of putative *cis*-Pt(NH<sub>3</sub>)<sub>2</sub>(DNA)(GSH) adducts. The aim of the experiments was to synthesise putative products using 5'-deoxyguanosine monophosphate (dGMP) as a surrogate for DNA products. This would allow characterisation of the chromatographic properties of GSH-containing adducts, thereby facilitating their identification in DNA hydrolysates. The use of dGMP permitted investigations at high concentrations of cisplatin so that Pt-containing products formed in the reactions with cisplatin in the presence and absence of GSH could be readily detected by AAS.

Following characterisation of the chromatographic system to be used, initial experiments were aimed at generating dGMP-Pt-Cl, whereby dGMP is bound to one of the arms of cisplatin, mimicking the formation of monofunctional Pt-DNA adducts. These products would then be further reacted with GSH with the aim of generating *cis*-

Pt(NH<sub>3</sub>)<sub>2</sub>(dGMP)(GSH) products. It was anticipated that this approach would also provide sufficient quantities of product to allow for structural analysis. The findings in this chapter would therefore provide important information for investigating novel Pt-DNA adducts formed in cells incubated with Pt drugs.

### 3.2: Chromatographic system

Experiments in this study investigating the formation of Pt-DNA adducts used an anion exchange chromatographic system with a MonoQ column (section 2.9) to detect potential products by UV absorbance, and either AAS (dGMP) or ICP-MS (DNA) to detect Pt in collected fractions. Anion exchange was chosen for the separation procedure for three reasons: (1) a similar setup had previously been used for the identification of Pt-DNA adducts formed in pure DNA (Fichtinger-Schepman et al 1985); (2) the combination of the MonoQ system with ICP-MS had provided the initial evidence of additional types of DNA adducts formed in cells to those characterised in purified DNA (Azim-Araghi 2003) and (3) anion exchange analysis allowed for the study of nucleotides. Eastman had previously used a reverse-phase chromatographic system to study nucleosides (Eastman 1983), but this involved additional enzymatic digestion of DNA incubation with alkaline phosphatase. As the nature and stability of the putative *cis*-Pt(NH<sub>3</sub>)<sub>2</sub>(DNA)(GSH) products was unclear, limiting the processing steps prior to analysis was favourable. The actual MonoQ chromatographic setup and method is described in section 2.9.

### **3.3: Results**

#### **3.3.1: Characterisation of the chromatographic system using mononucleotides**

Four mononucleotides of dAMP, dCMP, dGMP and TMP were analysed individually using the MonoQ system to determine their retention times for future reference. Mixtures containing the four mononucleotides were analysed to assess the effectiveness of the MonoQ column in separating multiple components. Solutions (100  $\mu$ l at 50  $\mu$ g/ml) were injected onto the column and the optical densities of the eluents were measured at 254nm and 230nm. Typical results are shown in order of increasing retention time for dCMP, dAMP, TMP and dGMP (Figure 3.1), with elution patterns for a mixture containing 50  $\mu$ g/ml or 100  $\mu$ g/ml of the four mononucleotides shown in Figure 3.2. Typical retention times compared to previous analyses (Fichtinger-Schepman et al 1985, Azim-Araghi 2003) are shown in Table 3.1.

Absorbance at 254 nm was higher for dAMP, dGMP and TMP than at 230 nm. Conversely, absorbance was higher at 230 nm for dCMP. This is in agreement with data obtained for each solution (50  $\mu$ g/ml) analysed for absorbance in the UV wavelength region of 210-320 nm, using the scanning function of the Lambda 2 UV/Vis spectrophotometer (typically used for measuring DNA concentration (section 2.5.3)) (Figure 3.3) and data published previously (Cavaluzzi and Borer 2004).

Separation of the four nucleotides confirmed that the MonoQ system gave reproducible results and the separations were consistent with previous work (Fichtinger-Schepman et al 1985, Azim-Araghi 2003).

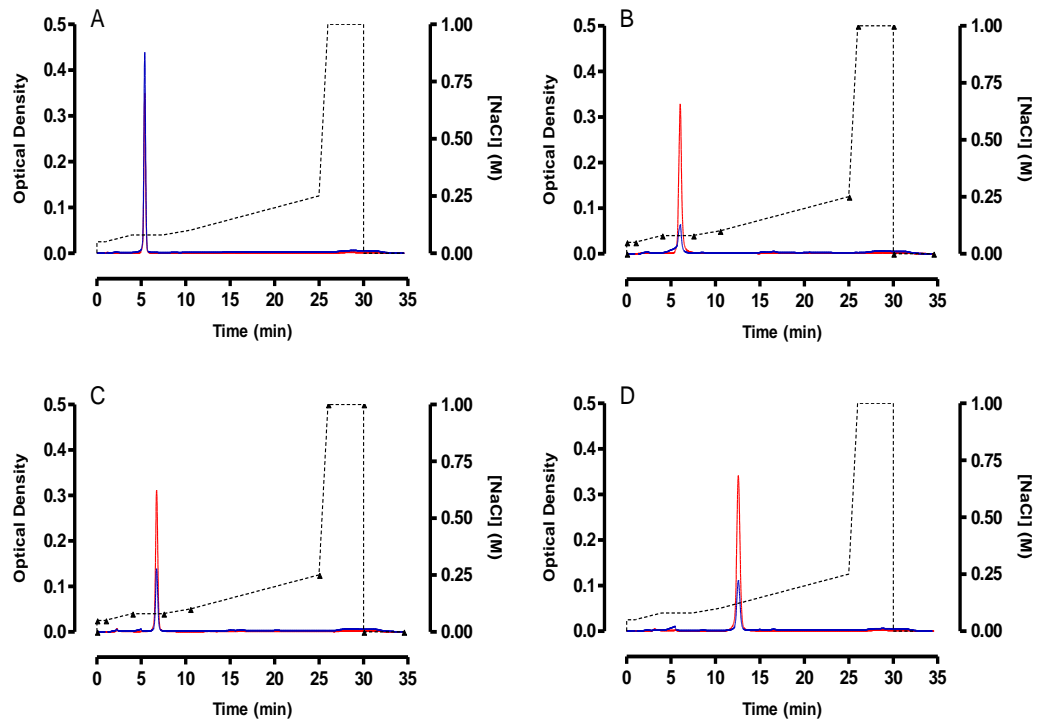


Figure 3.1: Typical MonoQ elution profiles for individual mononucleotides. Solutions (100  $\mu$ l at 50  $\mu$ g/ml) of dCMP (A), dAMP (B), TMP (C) and dGMP (D) were injected onto the MonoQ column and eluted at 1 ml/min with increasing NaCl concentrations. ( $\blacktriangle$ , dotted black line): NaCl concentration gradient; solid red line: OD 254 nm; solid blue line: OD 230 nm

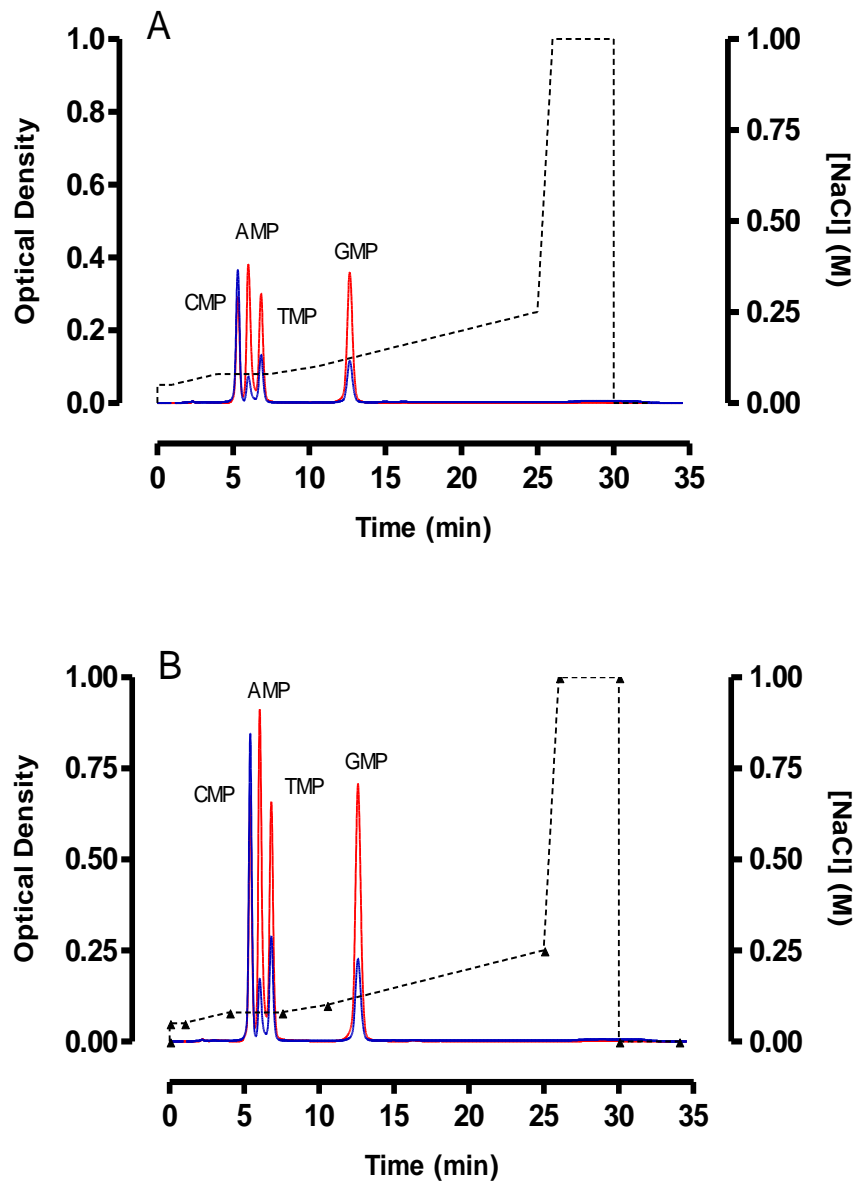
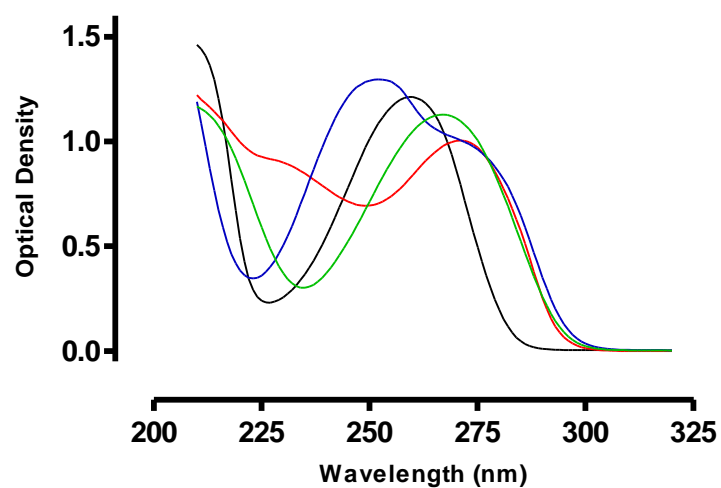


Figure 3.2: Typical MonoQ elution profile for a mixture of the four mononucleotides. Solutions (100  $\mu$ l at 50  $\mu$ g/ml (A) or 100  $\mu$ g/ml (B)) of the mononucleotide mixture were injected onto the MonoQ column and eluted at 1 ml/min with increasing NaCl concentrations. ( $\blacktriangle$ , dotted black line): NaCl concentration gradient; solid red line: OD 254 nm; solid blue line: OD 230 nm



*Figure 3.3: Analysis of absorbance of dAMP (black), dCMP (red), dGMP (blue) and TMP(green) in the UV region 210-320 nm using scanning function of the Lambda 2 UV/Vis spectrophotometer. Solutions (50  $\mu\text{g/ml}$ ) were placed inside a 10 mm path length cuvette and UV absorbance measured.*

*Table 3.1: Average retention times on MonoQ column for the four mononucleotides compared with previous observations by Azim-Araghi (2003) and Fichtinger-Schepman et al (1985). Standard deviation for this study is shown in brackets.*

	<b>Retention Time (min)</b>	<b>Retention Time (min)</b>	<b>Retention Time (min)</b>
	<b>Current Study</b>	<b>Azim-Araghi</b>	<b>Fichtinger-Schepman</b>
<b>dCMP</b>	5.2 (0.1)	4.6	5.0
<b>dAMP</b>	6.0 (0.2)	5.6	5.8
<b>TMP</b>	6.7 (0.2)	6.1	6.4
<b>dGMP</b>	12.5 (0.1)	11.8	12.0

### 3.3.2: Anion exchange separation of enzymatically digested calf thymus DNA

Before analysing Pt-DNA adducts in DNA from drug-treated cells, it was important to confirm that the MonoQ chromatographic system used here yielded the same pattern of Pt-DNA adducts previously identified on purified DNA (Fichtinger-Schepman et al 1985).

Calf thymus DNA (500 µg/ml) was incubated with or without cisplatin (15 µM) for 2 hours at 37°C, then DNA was separated from unreacted drug by gel filtration on a G-75 Sephadex column (section 2.8). DNA (0.25 mg/ml) was enzymatically digested to mono and dinucleotides (section 2.6), then nucleotides were separated using the MonoQ anion exchange column (section 2.9). Pt species in collected fractions were detected using ICP-MS (section 2.11).

A typical MonoQ elution profile for enzymatically digested calf thymus DNA not exposed to cisplatin is shown in Figure 3.4 (graph A). The four mononucleotides eluted in a similar manner to that seen with a mixture of deoxynucleotides (Figure 3.2). As expected Pt levels were at instrument background, showing no major Pt contamination during sample preparation.

Calf thymus DNA incubated with 15 µM cisplatin (Figure 3.4, graph B) showed the presence of four Pt-containing products with similar retention times to previous studies (Fichtinger-Schepman et al 1985, Azim-Araghi 2003). Retention times for these products and the percentage of total Pt eluted in each adduct is shown in Table 3.2. A comparison of these data with the above mentioned studies is also given in Table 3.2.

The similarity between the present data and those of Fichtinger-Schepman et al (1985) and Azim-Araghi (2003), regarding retention times and distribution of Pt across the four peaks, suggests that the nature of the four detected products in this study is the same as the products characterised by DEAE-Sephacel and NMR previously (Fichtinger-Schepman et al 1985). The four peaks therefore were attributed to: A:  $\text{Pt}(\text{NH}_3)_2(\text{R})(\text{dGMP})$ ; B: *cis*- $\text{Pt}(\text{NH}_3)_2\text{d}(\text{ApG})$ ; C: *cis*- $\text{Pt}(\text{NH}_3)_2\text{d}(\text{GpG})$  and D: *cis*- $\text{Pt}(\text{NH}_3)_2(\text{dGMP})_2$  (Figure 3.4).

The percentage of Pt eluted for each individual product is similar between this study and previous studies, although a difference was seen in the total percentage of eluted Pt in the *cis*- $\text{Pt}(\text{NH}_3)_2\text{d}(\text{GpG})$  between this study (64.4%) and Azim-Araghi 2003 (66.6%), when compared to the percentage reported by Fichtinger-Schepman et al 1985 (47%). The quantity of the four eluted adducts expressed as a percentage of total eluted Pt was similar in this study (94.7%) to that of Azim-Araghi (95.2%). Total Pt recovery was always greater than 90% of the total amount of Pt injected.

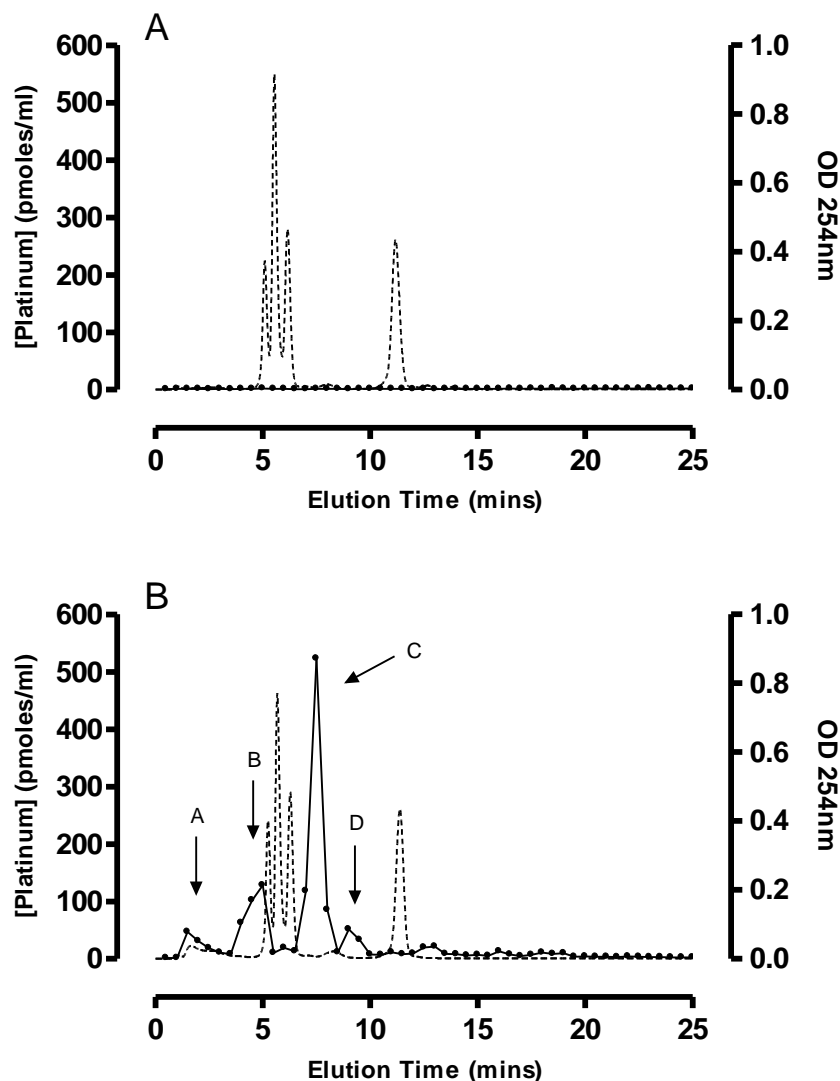


Figure 3.4: Typical MonoQ elution profile for enzymatically digested calf thymus DNA (A) and calf thymus DNA incubated with 15  $\mu\text{M}$  cisplatin (B). Solutions (100  $\mu\text{l}$ ) were injected onto the MonoQ column and eluted at 1 ml/min with increasing NaCl concentrations. Pt concentration in collected fractions was determined by ICP-MS. (●) Pt concentration; dotted line: OD 254 nm. Peaks A:  $\text{Pt}(\text{NH}_3)_2(\text{R})(\text{dGMP})$ ; B:  $\text{cis-Pt}(\text{NH}_3)_2\text{d}(\text{ApG})$ ; C:  $\text{cis-Pt}(\text{NH}_3)_2\text{d}(\text{GpG})$  and D:  $\text{cis-Pt}(\text{NH}_3)_2(\text{dGMP})_2$

Table 3.2: Chromatographic separation of enzymatically digested pure DNA reacted with cisplatin. Retention times (RT) of 8 substances eluted from the MonoQ column and quantity of adducts expressed as a percentage of the total Pt recovered. Data from three separate digestions in this current study, compared to Azim-Araghi 2003 and Fichtinger-Schepman 1985. SD is shown in brackets

Peak	Substance	This Study		Azim-Araghi 2003		Fichtinger-Schepman 1985	
		RT (min)	% Pt Eluted	RT (min)	% Pt Eluted	RT (min)	% Pt Eluted
	<b>dCMP</b>	5.2 (0.1)		4.6		5.0	
	<b>dAMP</b>	6.0 (0.2)		5.6		5.8	
	<b>TMP</b>	6.7 (0.2)		6.1		6.4	
	<b>dGMP</b>	12.5 (0.1)		11.8		12.0	
<b>A</b>	<b>Pt(NH<sub>3</sub>)<sub>2</sub>(R)(dGMP)</b>	1.5 (1.0)	2.9 (0.8)	1.0	1.4	1.7	3
<b>B</b>	<b>cis-Pt(NH<sub>3</sub>)<sub>2</sub>d(ApG)</b>	4.0 (1.0)	20.5 (3.5)	2.5	20.7	3.5	23
<b>C</b>	<b>cis-Pt(NH<sub>3</sub>)<sub>2</sub>d(GpG)</b>	7.5 (1.5)	64.4 (3.1)	8.0	66.6	7.8	47
<b>D</b>	<b>cis-Pt(NH<sub>3</sub>)<sub>2</sub>(dGMP)<sub>2</sub></b>	9.5 (2.0)	6.9 (1.8)	11.5	6.5	9.7	8
<b>TOTAL (% of Pt in adducts)</b>			<b>94.7 (3.7)</b>		<b>95.2</b>		<b>81</b>

### **3.3.3: Identification of products formed in the reaction of cisplatin with deoxyguanosine monophosphate**

The key aim of this particular section of the study was to determine appropriate incubation conditions for the reaction between cisplatin and dGMP to maximise formation of the monofunctionally bound cisplatin-dGMP species. Three incubation conditions were considered: cisplatin and dGMP in an equimolar ratio, cisplatin in excess of dGMP in a 2:1 molar ratio or dGMP in excess of cisplatin in a 2:1 molar ratio. Cisplatin in excess of dGMP would be advantageous as it would favour the formation of monofunctionally bound dGMP products, although this condition was eliminated due to concerns of excess cisplatin interacting with other molecules during further reactions. An excess of dGMP was also excluded as this condition would favour the formation of bifunctionally bound species, which are considered to be non-reactive. An equimolar ratio was chosen for the reaction conditions to maximise the formation of monofunctionally bound products, accepting that there would be some bifunctional products also formed.

### 3.3.3.1: Preliminary Identification of products formed between cisplatin and dGMP

Reaction of equimolar cisplatin and dGMP was predicted to yield four products. Three of these products were predicted to be monofunctionally bound cisplatin-dGMP with the chemical composition  $cis\text{-Pt}(\text{NH}_3)_2(\text{R})(\text{dGMP})$ , where R could be either an aqua ( $\text{OH}_2$ ), hydroxy (OH) or chlorine (Cl) ligand. The fourth product was predicted to have dGMP bifunctionally bound to cisplatin ( $cis\text{-Pt}(\text{NH}_3)_2(\text{dGMP})_2$ ). The retention time for the four products was unknown, but  $cis\text{-Pt}(\text{NH}_3)_2(\text{OH}_2)(\text{dGMP})$  was predicted to elute first due to a net electropositive charge across the molecule.

As the equimolar incubation of cisplatin with dGMP was predicted to leave residual unreacted cisplatin in the reaction mixture, it was necessary to initially identify the chromatographic nature of cisplatin alone. A typical MonoQ elution profile for 1 mM cisplatin is shown in Figure 3.5. Analysis of Pt content in collected fractions (by AAS) showed that cisplatin typically eluted very rapidly from the column (less than 2 minutes retention).

Equimolar cisplatin and dGMP were incubated for 24 hours, with aliquots removed at 2hr, 4hr, 8hr and 24hr and analysed by MonoQ anion exchange chromatography (Figure 3.6). Incubation times of 2hr and 4hr were insufficient for the reaction, with detectable levels of unreacted dGMP observed in the UV traces (Figure 3.6, graphs A and B). When incubated for 8hr (Figure 3.6, graph C) and 24hr (Figure 3.6, graph D) there was no detectable unreacted dGMP. AAS analysis of collected fractions eluted from the MonoQ column indicated five Pt-containing species (Figure 3.7). The first

eluting species (approximately 1.5 minutes, label cis) had previously been determined to be unreacted cisplatin in the reaction mixture. The remaining four species were believed to represent the predicted three monofunctionally bound *cis*-Pt(NH<sub>3</sub>)<sub>2</sub>(R)(dGMP) species and one bifunctionally bound *cis*-Pt(NH<sub>3</sub>)<sub>2</sub>(dGMP)<sub>2</sub> species, although at this stage the order of elution was unknown.

The average retention time for peak 4 (later identified as the *cis*-Pt(NH<sub>3</sub>)<sub>2</sub>(GMP)<sub>2</sub> species) was 10 minutes, although the range of retention varied between 9-12 minutes in different experiments. As the analyses were performed on different days it is most likely that this difference arose from subtle variations in the salt concentration and overall pH of buffer B (12.5 mM tris, 1 M NaCl, pH 8.8). The elution of products is based on varying concentrations of ions, so it is most probable that when the product eluted at later times, it was a result of slightly lower salt concentrations. However, as the overall effect of this would be reflected in the elution of all products (larger variations seen as the salt concentrations increases) this was not deemed to be detrimental to the analyses.

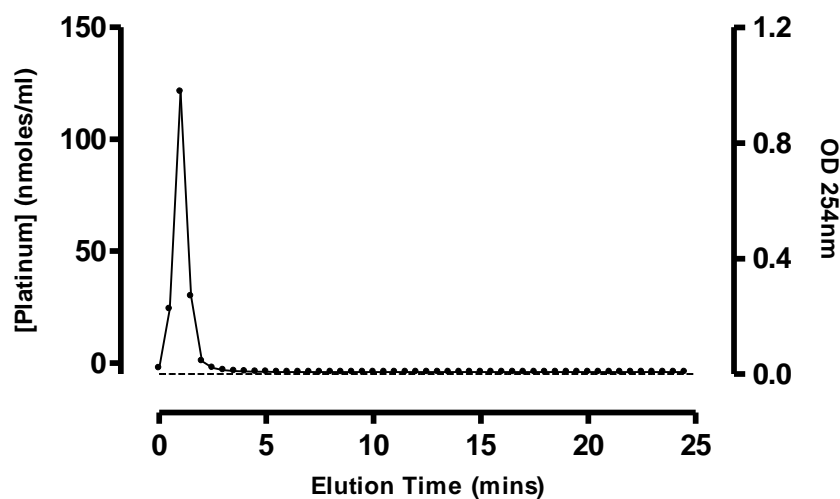


Figure 3.5: Typical MonoQ elution profile for 1mM cisplatin. Solutions (100  $\mu$ l) were injected onto the MonoQ column and eluted at 1 ml/min with increasing NaCl concentrations. Pt concentration in collected fractions was determined by AAS. (●) Pt concentration; dotted line: OD 254 nm. Pt recovery was always greater than 90% of the total Pt loaded.

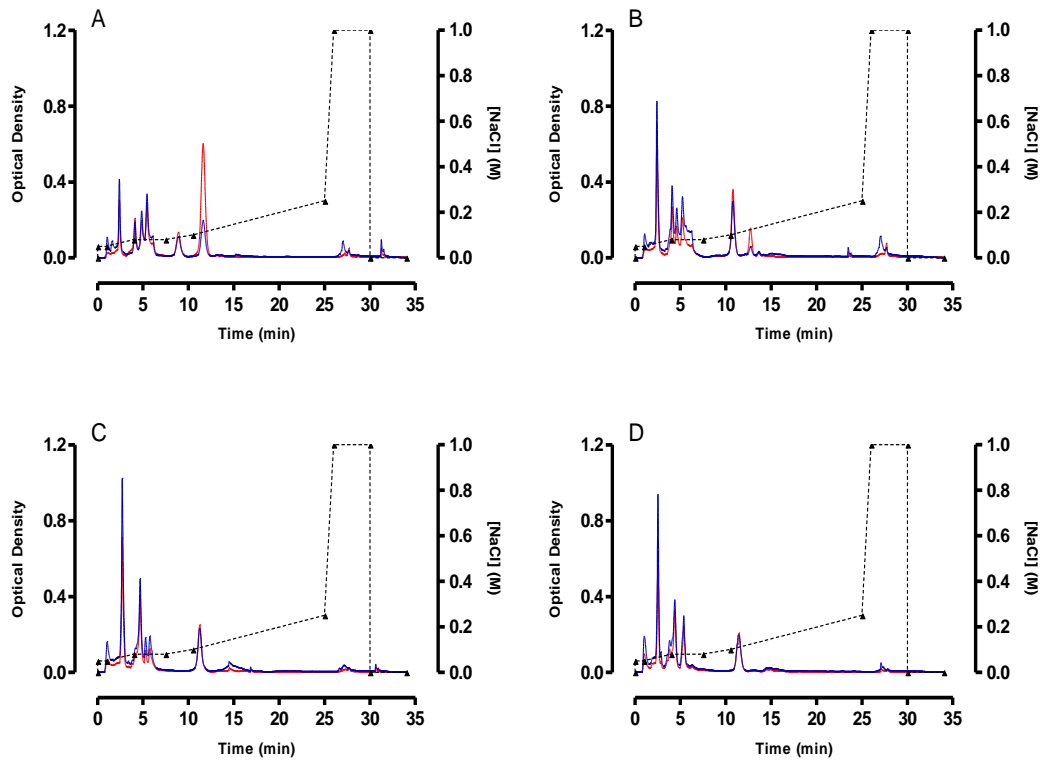


Figure 3.6: Typical MonoQ elution profile for 1mM cisplatin incubated with 1 mM dGMP. Solutions (100  $\mu$ l) of cisplatin and dGMP incubated for 2 hours (A), 4 hours (B), 8 hours (C) and 24 hours (D) were injected onto the MonoQ column and eluted at 1 ml/min with increasing NaCl concentrations. ( $\blacktriangle$ , dotted black line): NaCl concentration gradient; solid red line: OD 254 nm; solid blue line: OD 230 nm

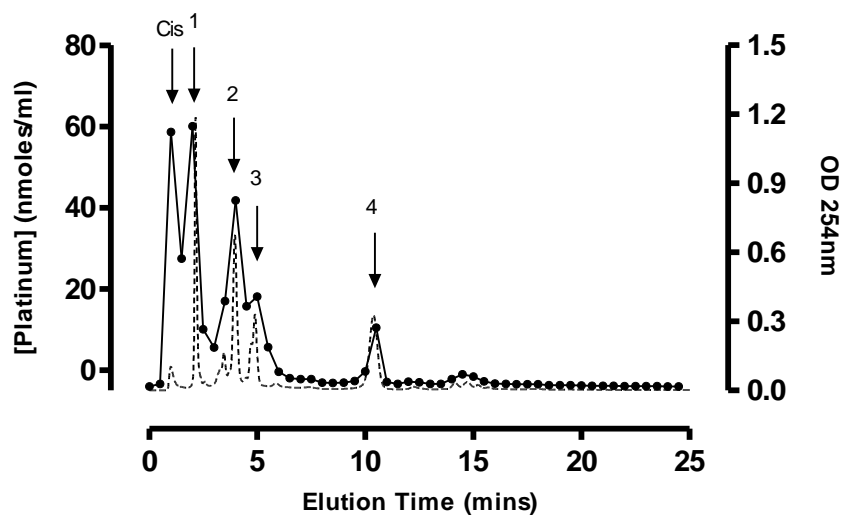


Figure 3.7: Typical MonoQ elution profile for 1mM cisplatin incubated with 1 mM dGMP for 24hr. Solutions (100  $\mu$ l) were injected onto the MonoQ column and eluted at 1 ml/min with increasing NaCl concentrations. Pt concentration in collected fractions was determined by AAS. (●) Pt concentration; dotted line: OD 254 nm. Peak cis represents unreacted cisplatin as identified previously. Peaks 1-4 are unknown species. Total Pt recovery was always greater than 90% of total Pt loaded.

### 3.3.3.2: Determination of the chemical nature of the products formed between cisplatin and dGMP

Four cisplatin-dGMP products were identified by MonoQ anion exchange chromatography coupled with Pt species detection by AAS (Figure 3.7). These were predicted to be three monofunctionally bound  $cis\text{-Pt}(\text{NH}_3)_2(\text{R})(\text{dGMP})$  and one bifunctionally bound  $cis\text{-Pt}(\text{NH}_3)_2(\text{dGMP})_2$  species. A series of experiments were conducted to determine the identities of the four Pt-containing species, in which cisplatin and dGMP were incubated initially for 24 hours, followed by a further 24 hours in the presence of 1 mM and 2.5 mM dGMP, NaCl and NaOH. The rationale for incubating further with dGMP was to favour the conversion of monofunctionally bound to the bifunctionally bound  $cis\text{-Pt}(\text{NH}_3)_2(\text{dGMP})_2$  species. Further incubation with NaCl and NaOH was designed to favour the formation and/or conversion to the monofunctionally bound  $cis\text{-Pt}(\text{NH}_3)_2(\text{Cl})(\text{dGMP})$  and  $cis\text{-Pt}(\text{NH}_3)_2(\text{OH})(\text{dGMP})$  species respectively. The remaining Pt-containing species was predicted therefore to be the  $cis\text{-Pt}(\text{NH}_3)_2(\text{OH}_2)(\text{dGMP})$  species, expected to elute first of the four based on its net electropositive charge.

Further incubation with 1 mM and 2.5 mM dGMP favoured the formation of peak 4 (Figure 3.7), with increases in ratio of peak area of 1:1.6 and 1:2.3 for 1 mM (Figure 3.8, graph A) and 2.5 mM (Figure 3.8, graph B) respectively, when compared to the initial identified peak (Figure 3.7). Incubation with 1 mM and 2.5 mM NaCl favoured the formation of peak 3 (Figure 3.7), with increases in ratio of peak area of 1:1.3 and 1:1.8 for 1 mM (Figure 3.9, graph A) and 2.5 mM (Figure 3.9, graph B) respectively, when compared to the initial identified peak (Figure 3.7). Incubation with 1 mM and

2.5 mM NaOH favoured the formation of peak 2 (Figure 3.7), with increases in ratio of peak area of 1:1.1 and 1:2.1 for 1 mM (Figure 3.10, graph A) and 2.5 mM (Figure 3.10, graph B) respectively, when compared to the initial identified peak (Figure 3.7). The remaining unidentified peak (Figure 3.7, peak 1) therefore was assigned to be the *cis*-Pt(NH<sub>3</sub>)<sub>2</sub>(OH<sub>2</sub>)(dGMP) species, eluting first of the four species as predicted. The order of elution for the four species was *cis*-Pt(NH<sub>3</sub>)<sub>2</sub>(OH<sub>2</sub>)(dGMP), *cis*-Pt(NH<sub>3</sub>)<sub>2</sub>(OH)(dGMP), *cis*-Pt(NH<sub>3</sub>)<sub>2</sub>(Cl)(dGMP) and finally *cis*-Pt(NH<sub>3</sub>)<sub>2</sub>(dGMP)<sub>2</sub>.

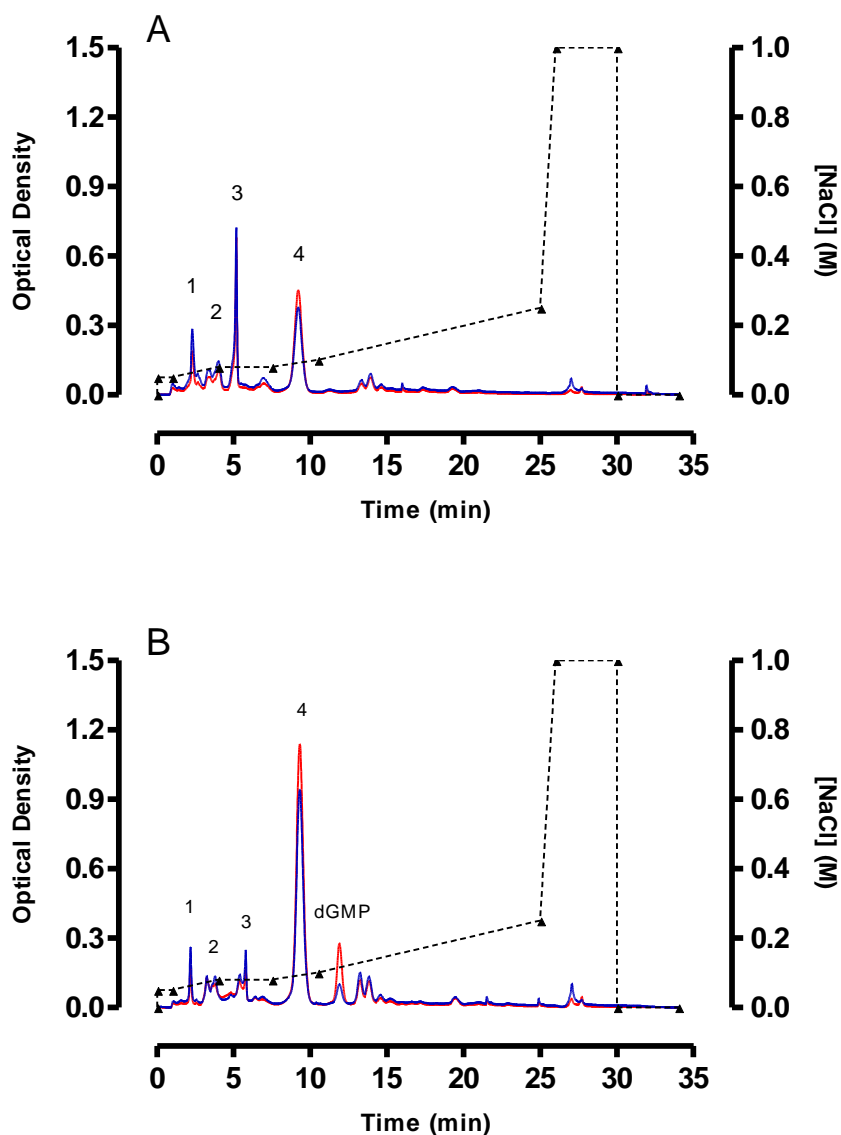


Figure 3.8: Typical MonoQ elution profile for cisplatin-dGMP incubated with dGMP. Solutions (100  $\mu$ l) of cisplatin-GMP reacted with 1 mM dGMP (A) and 2.5 mM dGMP (B) were injected onto the MonoQ column and eluted at 1 ml/min with increasing NaCl concentrations. ( $\blacktriangle$ , dotted black line): NaCl concentration gradient; solid red line: OD 254 nm; solid blue line: OD 230 nm. Proposed nature of the peaks is 1:  $\text{cis-Pt}(\text{NH}_3)_2(\text{OH}_2)(\text{dGMP})$ , 2:  $\text{cis-Pt}(\text{NH}_3)_2(\text{OH})(\text{dGMP})$ , 3:  $\text{cis-Pt}(\text{NH}_3)_2(\text{Cl})(\text{dGMP})$ , and 4:  $\text{cis-Pt}(\text{NH}_3)_2(\text{dGMP})_2$ .

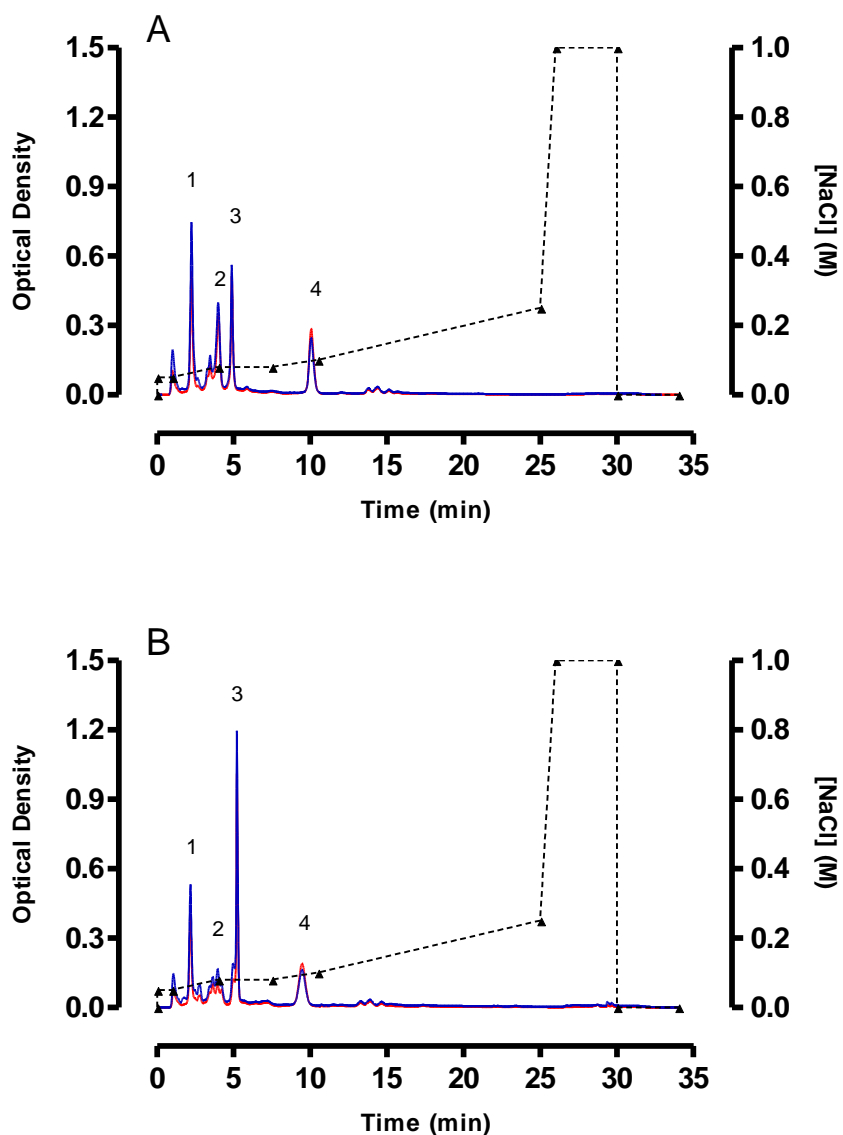


Figure 3.9: Typical MonoQ elution profile for cisplatin-dGMP incubated with NaCl. Solutions (100  $\mu$ l) of cisplatin-dGMP reacted with 1 mM NaCl (A) and 2.5mM NaCl (B) were injected onto the MonoQ column and eluted with increasing NaCl concentrations. ( $\blacktriangle$ , dotted black line): NaCl concentration gradient; solid red line: OD 254 nm; solid blue line: OD 230 nm. Proposed nature of the peaks is 1: cis-Pt(NH<sub>3</sub>)<sub>2</sub>(OH)<sub>2</sub>(dGMP), 2: cis-Pt(NH<sub>3</sub>)<sub>2</sub>(OH)(dGMP), 3: cis-Pt(NH<sub>3</sub>)<sub>2</sub>(Cl)(dGMP), and 4: cis-Pt(NH<sub>3</sub>)<sub>2</sub>(dGMP)<sub>2</sub>.

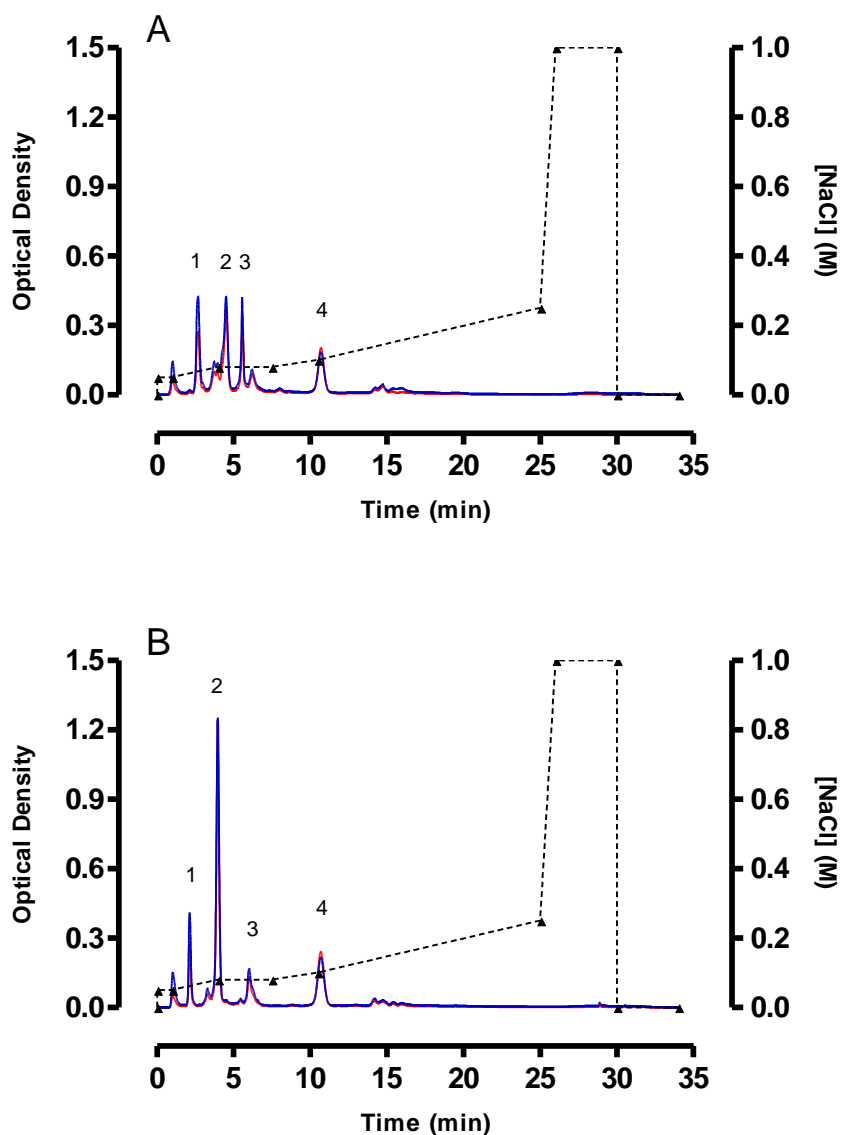


Figure 3.10: Typical MonoQ elution profile for cisplatin-dGMP incubated with NaOH. Solutions (100  $\mu$ l) of cisplatin-dGMP reacted with 1 mM NaOH (A) and 2.5mM NaOH (B) were injected onto the MonoQ column and eluted with increasing NaCl concentrations. ( $\blacktriangle$ , dotted black line): NaCl concentration gradient; solid red line: OD 254 nm; solid blue line: OD 230 nm. Proposed nature of the peaks is 1:  $\text{cis-Pt}(\text{NH}_3)_2(\text{OH}_2)(\text{dGMP})$ , 2:  $\text{cis-Pt}(\text{NH}_3)_2(\text{OH})(\text{dGMP})$ , 3:  $\text{cis-Pt}(\text{NH}_3)_2(\text{Cl})(\text{dGMP})$ , and 4:  $\text{cis-Pt}(\text{NH}_3)_2(\text{dGMP})_2$ .

### 3.3.3.3: Timecourse of the formation of products between cisplatin and dGMP

The reaction of cisplatin with dGMP was performed on three separate occasions. Aliquots were taken at 2, 4, 8 and 24hr (Figure 3.6) and analysed using the MonoQ system. Using Clarity 4.0 software (DataApex, UK), peak area for the detected peaks as a percentage of total peak area was determined. Analysis of the loss of free dGMP over time is shown in Figure 3.11. Analysis of the formation of the four products is shown in Figure 3.12.

Using Prism 4 software (GraphPad), a one-phase exponential decay was fitted to the data for the loss of the free dGMP in the reaction with cisplatin (Figure 3.11). From this a half-life of 1.5hr was determined. After 8 and 24hr reactions, the total amount of free GMP accounted for less than 1% of the total products detected.

Peaks 2 and 4, attributed to *cis*-Pt(NH<sub>3</sub>)<sub>2</sub>(OH)(dGMP) and *cis*-Pt(NH<sub>3</sub>)<sub>2</sub>(dGMP)<sub>2</sub> respectively, increased over the 24hr incubation period (Figure 3.12). Peak 1, attributed to *cis*-Pt(NH<sub>3</sub>)<sub>2</sub>(OH)<sub>2</sub> reached its maximum amount after 8hr, then decreased at 24hr. Peak 3, attributed to *cis*-Pt(NH<sub>3</sub>)<sub>2</sub>(Cl)(dGMP), reached its maximum amount after 2hr, and then levels decreased up to 8hr and remained constant through 24hr.

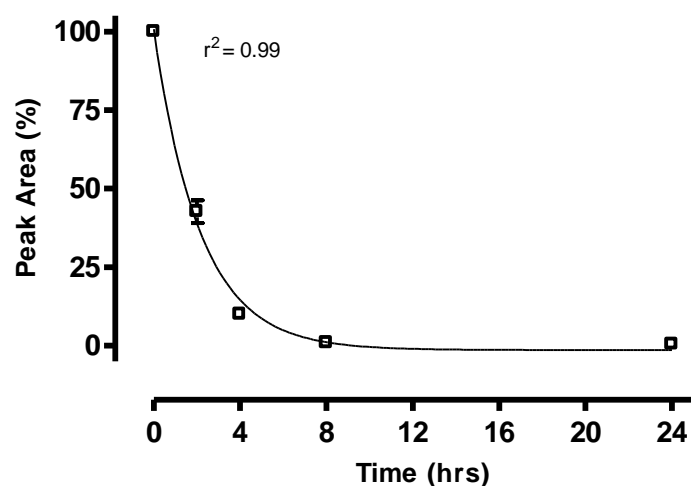


*Figure 3.11: Timecourse of the decrease in free dGMP in the reaction of equimolar (1 mM) cisplatin and dGMP. Peak area was determined using Clarity 4.0 software and is expressed as a percentage of total area. A one-phase exponential decay line was fitted in Prism 4 software. Each point represents the mean of 3 different experiments and error bars reflect standard deviation. Where not shown, error bars lie within the points.*

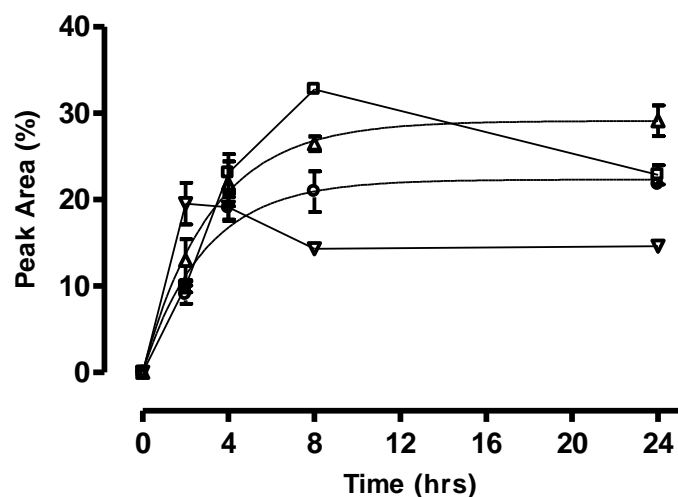


Figure 3.12: Timecourse of the formation of four products during the reaction of equimolar (1 mM) cisplatin and dGMP. Peak area was determined using Clarity 4.0 software and is expressed as a percentage of total area. ( $\square$ ): Peak 1, ( $\triangle$ ): Peak 2, ( $\nabla$ ): peak 3, and ( $\circ$ ): Peak 4. One-phase exponential association line fitted in Prism 4 software for peaks 2 and 4 ( $r^2$  of 0.98 and 0.97 respectively). Peak identities are proposed to be 1:  $\text{cis-Pt}(\text{NH}_3)_2(\text{OH}_2)(\text{dGMP})$ , 2:  $\text{cis-Pt}(\text{NH}_3)_2(\text{OH})(\text{dGMP})$ , 3:  $\text{cis-Pt}(\text{NH}_3)_2(\text{Cl})(\text{dGMP})$  and 4:  $\text{cis-Pt}(\text{NH}_3)_2(\text{dGMP})_2$ .

### 3.3.3.4: MALDI-TOF mass spectrometric analysis of products formed in the reaction of cisplatin and dGMP

Equimolar (1 mM) cisplatin and dGMP were incubated at 37°C for 24hr, and then stored at -20°C. Prior to storage, aliquots of the reaction mixture were removed and analysed by MALDI-TOF mass spectrometry. Mass spectrometry of reaction mixtures was either performed by Mr Robert Liddell or Dr Joe Gray in the Pinnacle Lab in the Institute for Cell and Molecular Biosciences at Newcastle University.

Monofunctionally bound cisplatin-dGMP could be in the form of 3 individual products of the species *cis*-Pt(NH<sub>3</sub>)<sub>2</sub>(R)(dGMP) where R was either OH<sub>2</sub>, OH or Cl. Based on computer analysis of such species using ChemOffice software, products with masses of 594.38, 593.37 and 611.81 were predicted to be detected by mass spectrometry, based on the <sup>195</sup>Pt isotope. The *cis*-Pt(NH<sub>3</sub>)<sub>2</sub>(dGMP)<sub>2</sub> species was predicted to have a mass of 923.58. Typical MALDI-TOF mass spectrometric analyses are shown in Figure 3.13 and Figure 3.14.

Three major peaks with masses of 921.1, 922.1 and 923.1 were detected, and these were attributed to the *cis*-Pt(NH<sub>3</sub>)<sub>2</sub>(dGMP)<sub>2</sub> species, with the three masses representing the <sup>194</sup>Pt, <sup>195</sup>Pt and <sup>196</sup>Pt isotopes of cisplatin (Figure 3.13). Masses in the region of 904-906 m/z were also detected, and these were attributed to the loss of one NH<sub>3</sub> ligand to form the species [*cis*-Pt(NH<sub>3</sub>)(dGMP)<sub>2</sub>]<sup>+</sup>. Further species with masses in the region of 887-889 were also detected, and these were attributed to the loss of the both NH<sub>3</sub> ligands, possibly during ionisation, forming [*cis*-Pt(dGMP)<sub>2</sub>]<sup>2+</sup>.

Three major peaks of 610.0 m/z, 611.0 m/z and 612.0 m/z were detected, and these were attributed to the  $^{194}\text{Pt}$ ,  $^{195}\text{Pt}$  and  $^{196}\text{Pt}$  isotopes of cisplatin in the species *cis*-Pt(NH<sub>3</sub>)<sub>2</sub>(Cl)(dGMP) (Figure 3.14).

A series of peaks were detected in the region of 592-597 m/z, and in these peaks were the two remaining monofunctional species (*cis*-Pt(NH<sub>3</sub>)<sub>2</sub>(OH<sub>2</sub>)(dGMP) and *cis*-Pt(NH<sub>3</sub>)<sub>2</sub>(OH)(dGMP)) (Figure 3.14). The group of products detected with masses in the region 574-576 m/z were predicted to be isotopic variants of the [*cis*-Pt(NH<sub>3</sub>)<sub>2</sub>(dGMP)]<sup>+</sup> species (Figure 3.14).

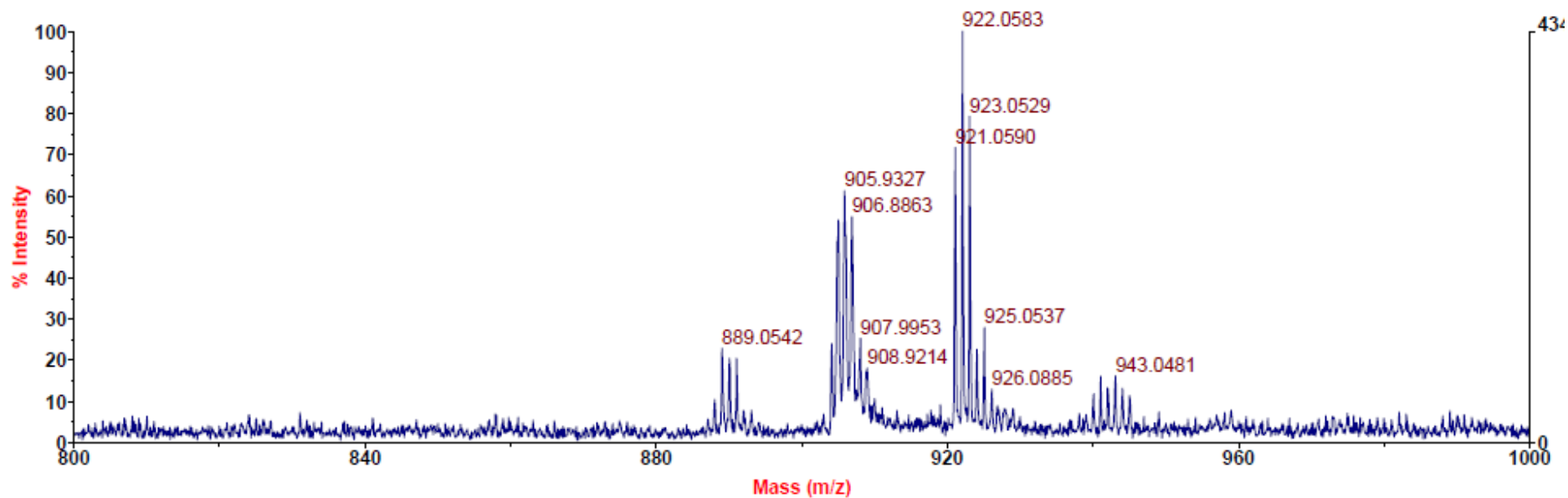


Figure 3.13: Typical MALDI-TOF mass spectrometry analysis of products formed in the reaction of equimolar (1mM) cisplatin and dGMP after a 24hr incubation. Products with masses in the range of 250-1500 m/z were scanned, and a typical 800-1000 m/z region is shown. MALDI-TOF mass spectrometry data were acquired by either Mr Robert Liddell or Dr Joe Gray (Newcastle University)

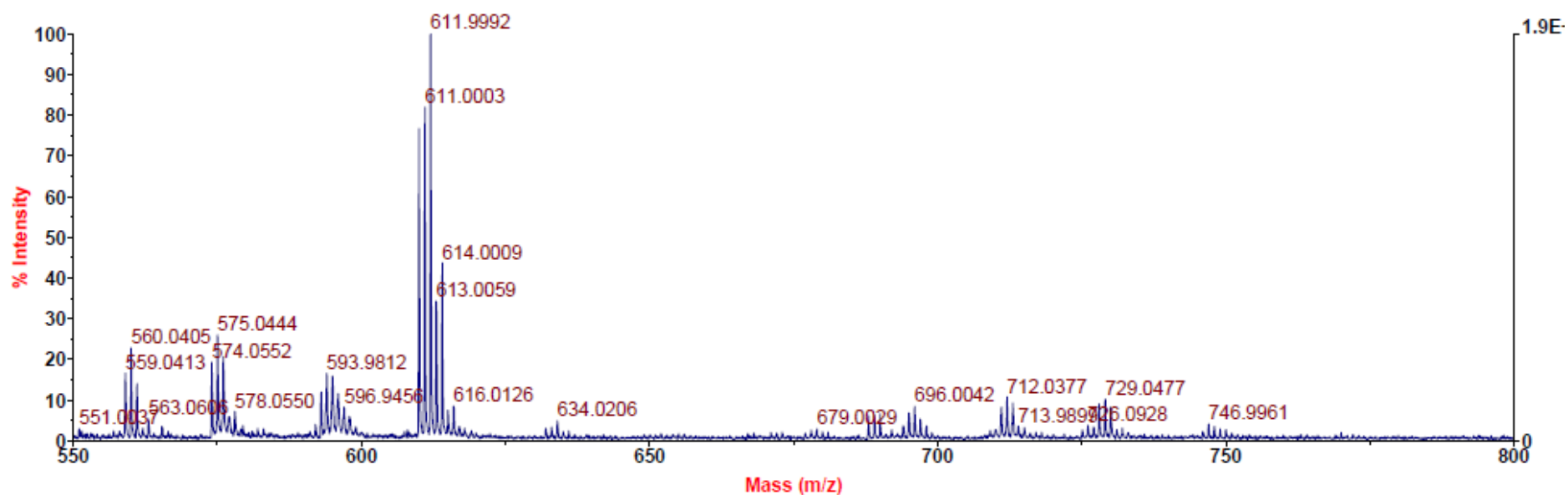


Figure 3.14: Typical MALDI-TOF mass spectrometry analysis of products formed in the reaction of equimolar (1mM) cisplatin and dGMP after a 24hr incubation. Products with masses in the range of 250-1500 m/z were scanned, and a typical 550-800 m/z region is shown. MALDI-TOF mass spectrometry data were acquired by either Mr Robert Liddell or Dr Joe Gray (Newcastle University)

**Summary of the evidence presented to support the proposed peak identities**

Peak	Identification	Evidence
<b>Peak 1</b> <b>Retention Time ~ 2.5mins</b>  <b>Mono-Aqua</b>	<p style="text-align: center;"> <math display="block">  \begin{array}{c}  \text{H}_3\text{N}^{(+)} \quad \text{OH}_2 \\  \diagdown \quad \diagup \\  \text{Pt} \\  \diagup \quad \diagdown \\  \text{H}_3\text{N} \quad \text{GMP}  \end{array}  </math> </p>	<ul style="list-style-type: none"> <li>• Decreases after further incubation with dGMP</li> <li>• Decreases when NaCl added - Not mono-chloro</li> <li>• Decreases when NaOH added - Not mono-hydroxy</li> <li>• Net positive charge - should interact least with the MonoQ column</li> <li>• MALDI-TOF data showing product with correct mass</li> </ul>
<b>Peak 2</b> <b>Retention Time ~ 4.5mins</b>  <b>Mono-Hydroxy</b>	<p style="text-align: center;"> <math display="block">  \begin{array}{c}  \text{H}_3\text{N} \quad \text{OH} \\  \diagdown \quad \diagup \\  \text{Pt} \\  \diagup \quad \diagdown \\  \text{H}_3\text{N} \quad \text{GMP}  \end{array}  </math> </p>	<ul style="list-style-type: none"> <li>• Decreases after further incubation with dGMP</li> <li>• Decreases when NaCl added - Not mono-chloro</li> <li>• Increases when NaOH added - Favours mono-hydroxy</li> <li>• MALDI-TOF data showing product with correct mass</li> </ul>
<b>Peak 3</b> <b>Retention Time ~ 5.5mins</b>  <b>Mono-Chloro</b>	<p style="text-align: center;"> <math display="block">  \begin{array}{c}  \text{H}_3\text{N} \quad \text{Cl} \\  \diagdown \quad \diagup \\  \text{Pt} \\  \diagup \quad \diagdown \\  \text{H}_3\text{N} \quad \text{GMP}  \end{array}  </math> </p>	<ul style="list-style-type: none"> <li>• Decreases after further incubation with dGMP</li> <li>• Increases when NaCl added - Favours mono-chloro</li> <li>• Decreases when NaOH added - Not mono-hydroxy</li> <li>• MALDI-TOF data showing product with correct mass</li> </ul>
<b>Peak 4</b> <b>Retention Time ~ 9.5mins</b>  <b>di-GMP</b>	<p style="text-align: center;"> <math display="block">  \begin{array}{c}  \text{H}_3\text{N} \quad \text{GMP} \\  \diagdown \quad \diagup \\  \text{Pt} \\  \diagup \quad \diagdown \\  \text{H}_3\text{N} \quad \text{GMP}  \end{array}  </math> </p>	<ul style="list-style-type: none"> <li>• Increases after addition of dGMP</li> <li>• Peaks 1-3 all decrease after addition of dGMP, whereas peak 4 increases</li> <li>• MALDI-TOF data showing product with correct mass</li> </ul>

### **3.3.4: Identification of products formed in the reaction of platinated dGMP with GSH**

Having identified three monofunctional products with reactive potential, the next step was to incubate further with various concentrations of GSH. As carried out the reactions described earlier, equimolar (1 mM) cisplatin and dGMP were initially incubated for 24hr. At 24hr, varying concentrations of GSH were added and further incubated for 24hr. GSH was added after the initial incubation of cisplatin and dGMP because cisplatin rapidly reacts with glutathione and under such incubation conditions the amounts of product formed are markedly lower. As described earlier, the reaction conditions chosen meant that there was unreacted cisplatin remaining in the mixture. It was therefore also important to investigate the reaction of cisplatin and GSH alone.

### 3.3.4.1: Incubation of cisplatin with GSH

Immediately before incubation with cisplatin, GSH was dissolved in water (4 mM) and pH adjusted to 7.0. It was important to dissolve GSH before each reaction to limit the amount of the oxidised GSSG product in the mixture. Cisplatin was incubated with GSH in a 1:2 molar ratio to ensure that no unreacted drug would be present in the mixture. Immediately after addition of cisplatin, reaction mixtures were gassed with nitrogen to limit the oxidation of GSH to GSSG. Reaction mixtures were analysed using the MonoQ system. Pt content in collected fractions was measured by AAS. A typical MonoQ elution for the reaction of cisplatin with GSH is shown in Figure 3.15.

Cisplatin had been identified as having a very short elution time on the MonoQ column (Figure 3.5). However; it was unclear where cisplatin-GSH conjugates would elute. Two peaks were detected by UV with elution times of approximately 7 minutes and 27 minutes (Figure 3.15). The latter peak was the only detected species associated with Pt, and this was therefore determined to be Pt-GSH conjugate (Figure 3.15). The Pt-GSH conjugate eluted during the phase of the chromatographic program in which the salt concentration was at 1 M. The earlier peak was unreacted GSH in the mixture. This had previously been determined by injecting GSH alone into the chromatographic system.

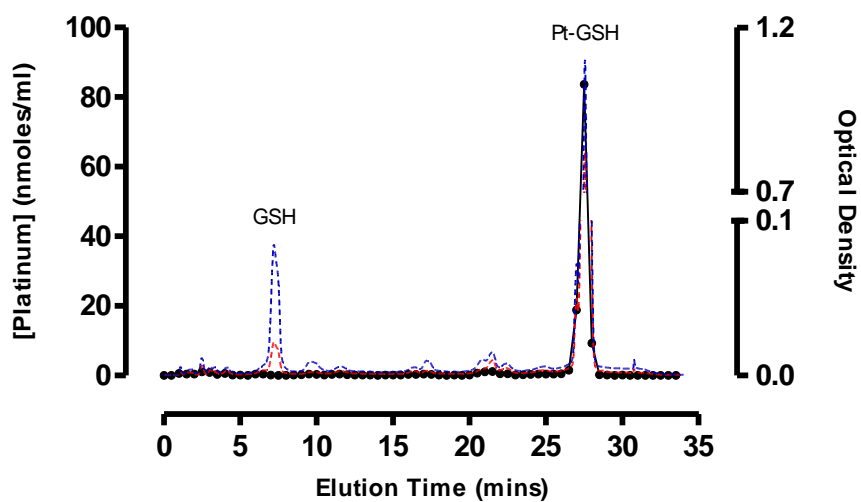


Figure 3.15: Typical MonoQ elution profile for 1 mM cisplatin incubated with 2 mM GSH for 24hr. Solutions (100  $\mu$ l) were injected onto the MonoQ column and eluted at 1ml/min with increasing NaCl concentrations. Pt concentration in collected fractions was determined by AAS. (●) Pt concentration; dotted red line: OD 254 nm; dotted blue line: OD 230 nm. Total Pt recovery was always greater than 90% of total Pt loaded.

### **3.3.4.2: Identification of products formed in the reaction of cisplatin-dGMP with GSH**

Equimolar (1 mM) cisplatin and dGMP were incubated at 37°C for 24hr. Aliquots were removed and analysed using the standard MonoQ system. The remaining mixture was split and further incubated with GSH (1 mM, 2.5 mM and 5 mM) for 24hr. These reaction mixtures were again analysed using the standard MonoQ system, with Pt content in collected fractions determined by AAS. Typical MonoQ elution profiles are shown in Figure 3.16.

Analysis of the aliquots removed prior to addition of GSH showed similar elution profiles and UV absorbing peaks with similar chromatographic properties as those observed previously (Figure 3.16, graph A). Following further incubation with GSH, a number of additional UV absorbing peaks were detected (Figure 3.16, graph B-D). These products typically eluted at 14, 17 and 21 minutes. AAS analysis of fractions eluted from the MonoQ column confirmed that all three species contained Pt (Figure 3.17). An additional product was also seen in the incubations with 2.5 mM and 5 mM GSH that eluted at approximately 25.5mins (Figure 3.16, graphs C and D), but no Pt was associated with this species.

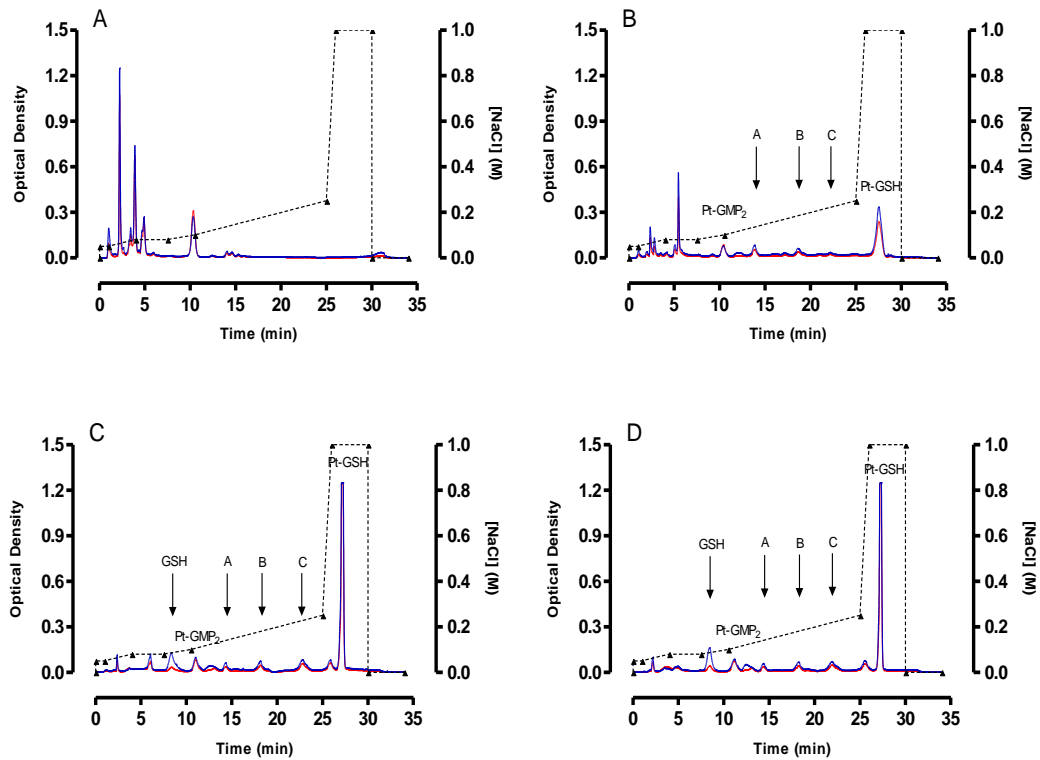


Figure 3.16: Typical MonoQ elution profile for 1mM cisplatin incubated for 24hr with 1 mM dGMP (A), then incubated for a further 24hr with 1 mM GSH (B), 2.5 mM GSH (C) and 5 mM GSH (D). Solutions (100  $\mu$ l) were injected onto the MonoQ column and eluted at 1 ml/min with increasing NaCl concentrations. ( $\blacktriangle$ , dotted black line): NaCl concentration gradient; solid red line: OD 254 nm; solid blue line: OD 230 nm. The identities of peaks A-C are unknown

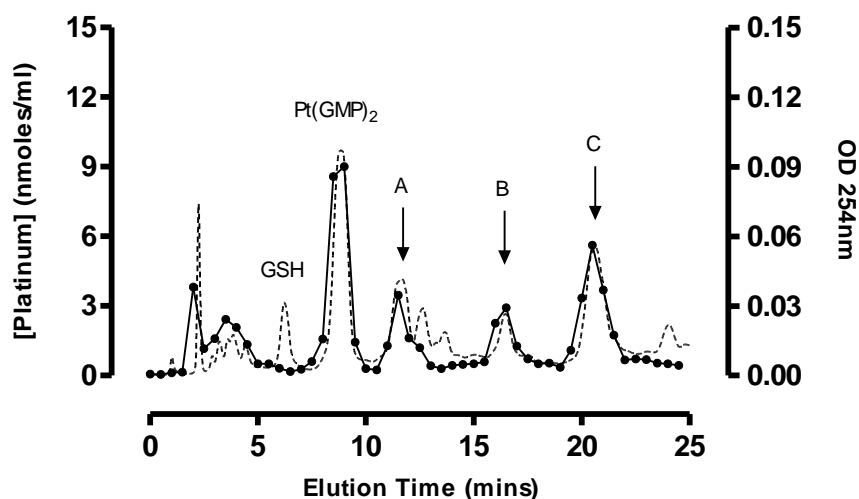


Figure 3.17: Typical MonoQ elution profile for cisplatin-dGMP incubated with 2.5 mM GSH for 24hr. Solutions (100  $\mu$ l) were injected onto the MonoQ column and eluted at 1 ml/min with increasing NaCl concentrations. Pt concentration in collected fractions was determined by AAS. (●) Pt concentration; dotted line: OD 254 nm. The identities of peaks A-C are unknown. Total Pt recovery was always greater than 90% of total Pt loaded.

### 3.3.4.3: Analysis of the three peaks identified in the reaction of GSH with platinumated dGMP

Three new Pt-containing products were identified in the reaction of cisplatin-dGMP with GSH. It was unclear at this point which, if any, were the proposed *cis*-Pt(NH<sub>3</sub>)<sub>2</sub>(dGMP)(GSH) cross-links. Total peak areas for each of the three peaks with varying concentrations of GSH were therefore calculated to provide further evidence. Total peak areas were calculated using Clarity software. To ensure only the peaks of interest were analysed, integrations were applied between two timepoints: 0-7 minutes and 10-25 minutes. By applying such limitations the peak areas of unreacted GSH and of Pt-GSH were excluded from the calculations, as the increase of these peaks could in theory affect changes in the amount of each product. Analysis of the three monofunctional and *cis*-Pt(NH<sub>3</sub>)<sub>2</sub>d(GMP<sub>2</sub>) products is shown in Figure 3.18. Analysis of the three products identified following further incubation with GSH is shown in Figure 3.19.

As would be expected, the net pattern is a loss of detection of the three monofunctional products as the concentration of GSH in the reaction mixture increases, with the exception of *cis*-Pt(NH<sub>3</sub>)<sub>2</sub>(Cl)(dGMP) in the incubation with 1 mM GSH which appeared to increase (Figure 3.18). This rise however is most probably due to the loss of the other peaks and the overall effect of this on total peak area, as opposed to an increase in the amount of this product. When the specific peak areas were calculated in Clarity, total areas of 5168 mV/min (+/- 847 SD) and 4497 mV/min (+/- 983 SD) were calculated at 0 mM GSH and 1 mM GSH respectively for the *cis*-Pt(NH<sub>3</sub>)<sub>2</sub>(Cl)(dGMP)

product, showing the increase in peak area wasn't reflective of increases in product amount. Levels of the *cis*-Pt(NH<sub>3</sub>)<sub>2</sub>(dGMP)<sub>2</sub> product remained constant.

Three potential *cis*-Pt(NH<sub>3</sub>)<sub>2</sub>(dGMP)(GSH) candidates were identified by UV absorbance and AAS after the reaction of cisplatin-dGMP with GSH. Of the three peaks identified, only levels of peak C, which typically eluted at 21 minutes, increased as the concentration of GSH in the reaction mixture increased. Although it is not possible to exclude peaks A and B from being potential GSH containing cross-links, the most probable candidate of the three newly identified products is peak C.

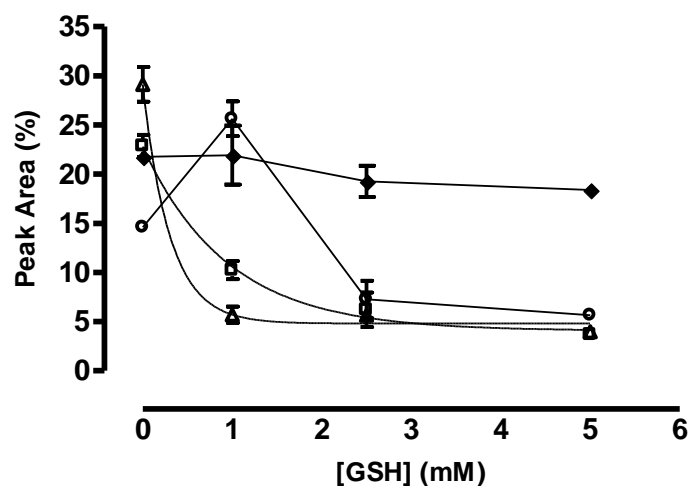


Figure 3.18: Analysis of the changes in peak area for the four products identified in the reaction of equimolar (1 mM) cisplatin with dGMP (24hr) prior to further incubation with GSH. Peak areas were determined using Clarity 4.0 software and are expressed as a percentage of total area. ( $\square$ ):  $\text{cis-Pt}(\text{NH}_3)_2(\text{OH}_2)(\text{dGMP})$ , ( $\Delta$ ):  $\text{cis-Pt}(\text{NH}_3)_2(\text{OH})(\text{dGMP})$ , ( $\circ$ ):  $\text{cis-Pt}(\text{NH}_3)_2(\text{Cl})(\text{dGMP})$ , and ( $\blacklozenge$ ):  $\text{cis-Pt}(\text{NH}_3)_2\text{d}(\text{GMP}_2)$ . One-phase exponential decay line fitted to data for  $\text{cis-Pt}(\text{NH}_3)_2(\text{OH}_2)(\text{dGMP})$  and  $\text{cis-Pt}(\text{NH}_3)_2(\text{OH})(\text{dGMP})$  peak in Prism 4 software. Each point represents the mean of 3 different experiments and error bars reflect standard deviation. Where not shown, error bars lie within the points.

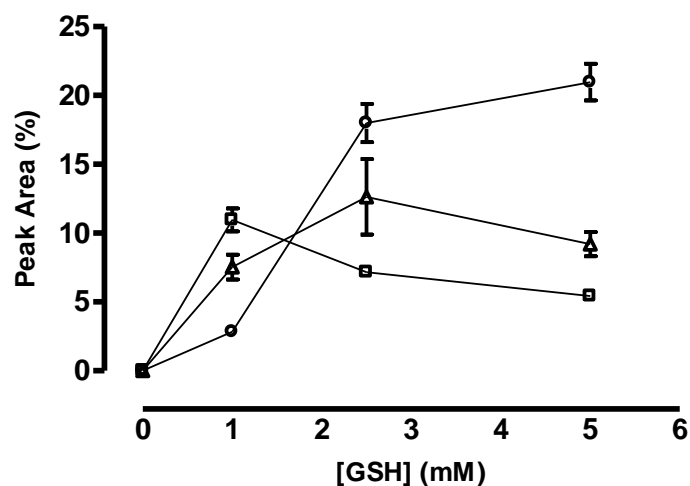


Figure 3.19: Analysis of the changes in peak area for the three products identified in the reaction of equimolar (1 mM) cisplatin with dGMP (24hr) followed by further incubation with GSH. Peak area was determined using Clarity 4.0 software and is expressed as a percentage of total area. ( $\square$ ): Peak 1, ( $\triangle$ ): Peak 2 ( $\circ$ ): Peak 3. Each point represents the mean of 3 different experiments and error bars reflect standard deviation. Where not shown, error bars lie within the points.

### **3.3.5: Structural analysis of products formed in the reaction of platinated dGMP with GSH**

Seven regions of dGMP were predicted to be detected by NMR. These include the C(8)-H proton of guanine, five C-H protons on the deoxyribose sugar ring, and the C-H<sub>2</sub> protons between the sugar ring and phosphate. The locations of these protons are shown in the appendix. NMR analyses of dGMP alone showed the presence of seven protons. Analyses of platinated dGMP showed seven detectable protons, comparable to those of dGMP alone.

Six regions of GSH were predicted to be detected by NMR. These included a C-H and two C-H<sub>2</sub> protons on the glutamate chain, C-H and C-H<sub>2</sub> protons on the cysteine chain, and C-H<sub>2</sub> protons on the glycine chain. The locations of these protons are shown in the appendix. NMR analyses of GSH alone showed the presence of six protons. NMR analysis of platinated GSH failed to give interpretable data.

Analyses of the putative *cis*-Pt(NH<sub>3</sub>)<sub>2</sub>(dGMP)(GSH) products described in chapter 3 failed to give interpretable data. Possible reasons for this are discussed in chapter 7. Typical NMR data are presented in the appendix of this thesis.

### 3.4: Discussion

The main aim of the experiments described in this chapter was to produce and characterise *cis*-Pt(NH<sub>3</sub>)<sub>2</sub>(dGMP)(GSH) cross-links that would help in the analysis of putative *cis*-Pt(NH<sub>3</sub>)<sub>2</sub>(DNA)(GSH) cross-links formed in DNA from drug-treated cells. Azim-Araghi (2003) had provided evidence for the formation of such adducts, but very little information on their chromatographic behaviour was available. A secondary aim of this chapter was to attempt to confirm the structural nature of such products.

Initial experiments were carried out to re-establish the MonoQ chromatographic system Azim-Araghi had used in the analyses of DNA from drug-treated cells. Having re-established the MonoQ setup, analyses were carried out on calf thymus DNA incubated in the presence and absence of cisplatin. Calf thymus DNA incubated with 15 μM cisplatin showed the presence of four Pt-containing products. The similarity between the present data and that of Fichtinger-Schepman et al (1985) and Azim-Araghi (2003) regarding retention times and distribution of Pt across the four peaks suggests that the four products detected in this study are the same as the products characterised by DEAE-Sephacel and NMR previously (Fichtinger-Schepman et al 1985).

Determining the chromatographic nature of putative *cis*-Pt(NH<sub>3</sub>)<sub>2</sub>(dGMP)(GSH) cross-links was the main aim for this chapter. This was approached using a two-step methodology. In the initial step, cisplatin and dGMP were reacted at equimolar (1 mM) concentrations. The second step in the approach was then to add GSH and carry out additional incubations, with the products of these reactions analysed during each step using the MonoQ system re-established as described above.

In the reaction of equimolar cisplatin and dGMP, four products were detected by UV absorbance. Confirmation that these products contained Pt was achieved using AAS. Further experiments showed that three of the products involved dGMP bound to one arm of cisplatin forming the species *cis*-Pt(NH<sub>3</sub>)<sub>2</sub>(R)(dGMP) in which R could be either a Cl, OH or OH<sub>2</sub> ligand. MALDI-TOF mass spectrometry of the reaction mixture confirmed products of the expected masses were produced. The fourth product identified was *cis*-Pt(NH<sub>3</sub>)<sub>2</sub>(dGMP)<sub>2</sub>. Again, MALDI-TOF mass spectrometry of the reaction mixture confirmed this product was of the expected mass.

The second step in the approach was to incubate GSH with the products of the cisplatin-dGMP reaction. The production of monofunctionally bound dGMP products in the first step was key to this reaction, to allow further formation of the species *cis*-Pt(NH<sub>3</sub>)<sub>2</sub>(dGMP)(GSH). The chromatographic nature of this species would be important in analysing the Pt-DNA adducts formed in drug-treated cells. After reacting GSH with platinated dGMP, three products were detected by UV, all containing Pt (determined by AAS). Of these, the extent of formation of a product with an elution times of 21 minutes, increased as the concentration of GSH in the reaction mixture was increased. However, the other two products couldn't be eliminated as *cis*-Pt(NH<sub>3</sub>)<sub>2</sub>(dGMP)(GSH) cross-links. Attempts were made to purify these products for structural analysis but these were unsuccessful.

## Chapter 4

### Analysis of Pt-DNA adducts formed in cells

#### 4.1: Introduction

Whilst investigating Pt-DNA adducts formed in human lung cancer cell lines (H69/p and Mor/p) (Azim-Araghi 2003), a novel Pt-containing product was detected that had different chromatographic properties to the known Pt-DNA adducts previously characterised (Fichtinger-Schepman et al 1985). As described in chapter 3, this product was proposed to be the result of GSH becoming cross-linked to DNA via Pt.

Prior to the work by Azim-Araghi, evidence had been published suggesting that GSH can cross-link to monofunctionally bound Pt-DNA (Eastman 1987). Binding of radioactively labelled GSH to DNA in the presence of cisplatin had also been observed (Tilby, unpublished data). The novel Pt-DNA product observed in DNA extracted from drug-treated cells by Azim-Araghi was detected using a combination of MonoQ anion exchange chromatography with ICP-MS. When this setup was applied by Azim-Araghi to studying pure calf thymus DNA incubated with GSH in the presence of cisplatin, the same novel product seen in cellular DNA hydrolysates was detected. It is therefore hypothesised that the novel product detected previously is *cis*-Pt(NH<sub>3</sub>)<sub>2</sub>(DNA)(GSH). The implications of such a product for the cellular pharmacology of Pt-drugs are unknown. These observations need to be confirmed and extended to other Pt-containing drugs and other cell lines.

Four human tumour cell lines were chosen for investigation. 833K, A2780 and LoVo cells were derived from testicular, ovarian and colorectal cancer respectively, and were chosen as these types of cancers are often treated with the platinum-based drugs used in this study. The cisplatin-resistant Mor/CPR cells were chosen for two reasons: firstly, the parental line Mor/P was used by Ali Azim-Araghi (Azim-Araghi 2003). Unfortunately the parental line wasn't available for this study. Secondly, in order to include a drug-resistant cell line in the investigation.

Initially the sensitivity of the four chosen cell lines to the growth inhibitory effects of the drugs was defined in order to ensure that the drug concentration/DNA adducts levels being studied were biologically relevant. Also, as a body of data was to be accumulated this sensitivity data would permit comparisons between adducts levels and growth inhibitory effects.

By analysing the products of reactions with cisplatin with dGMP and GSH (see chapter 3), a putative *cis*-Pt(NH<sub>3</sub>)<sub>2</sub>(dGMP)(GSH) species has been synthesised and purified by anion exchange chromatography. The aim of the work described in this chapter was to investigate the potential formation of GSH-containing Pt-DNA adducts in the DNA of human tumour cells incubated with cisplatin. This was approached as follows:

1. Analyse the chromatographic behaviour of all adducts formed in cells by cisplatin to compare with adducts formed on pure DNA and, hopefully, identify the additional products observed previously.
2. Extension of these analyses to the other clinically used platinum-based drugs carboplatin and oxaliplatin

## **4.2: Results**

### **4.2.1: Sensitivity of human tumour cells to Pt-drugs**

#### **4.2.1.1: Determination of optimal seeding density**

The optimal incubation period of cell cultures before and after drug treatments varies between individual cell lines. Therefore, initial experiments were carried out to determine the optimal growth conditions for each of the four cell lines. Appropriate inoculation densities could then be chosen that would ensure cells remained in active phase throughout the whole period of incubation with Pt-drugs. Cells were seeded at a number of increasing densities into 96 well plates, and incubated at 37°C for 24hr initially to allow cells to settle and attach. Cells were then fixed at 0hr, 24hr, 48hr and 72hr. Cell density was determined using the SRB assay.

Typical growth curves are shown in Figure 4.1. The four cell lines were subsequently inoculated at 8000 cells/well.

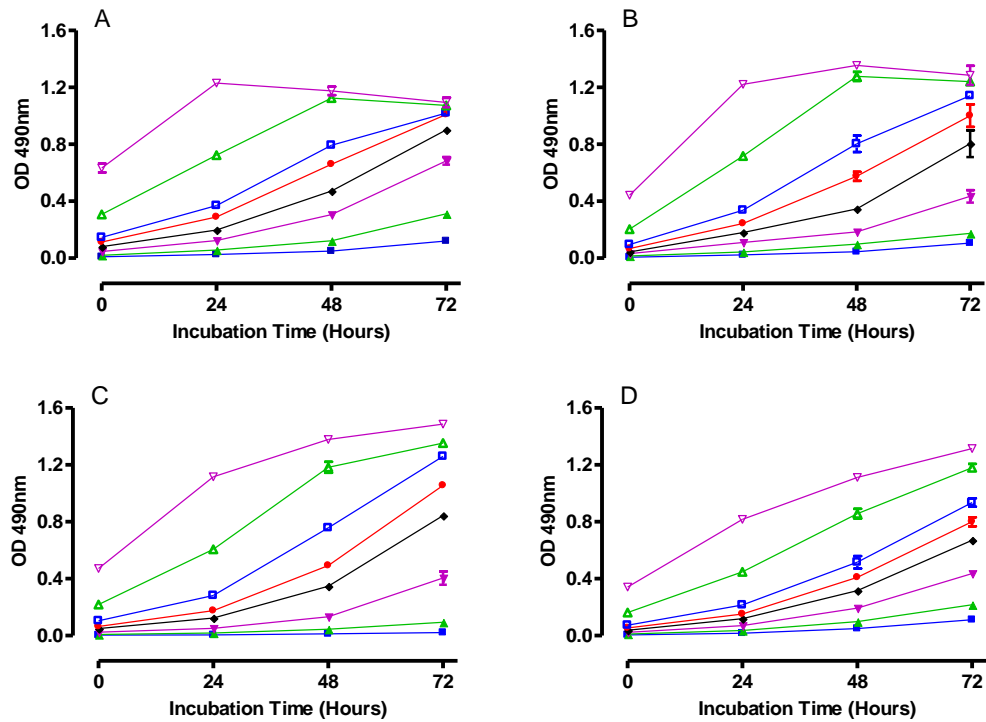


Figure 4.1: Typical analysis of growth of 833K (A), A2780 (B), LoVo (C) and MorCPR (D) cells. Cells from each cell line were seeded in 96 well plates at (■): 1000 cells/well, (▲): 2000 cells/well, (▼): 4000 cells/well, (◆): 6000 cells/well, (●): 8000 cells/well, (□): 10000 cells/well, (△): 20000 cells/well and (▽): 40000 cells/well. Cell density was measured by the SRB assay at 24, 48 and 72 hours. Absorbance was measured at 490nm. Error bars represent the mean  $\pm$  standard deviation. Where not shown, error bars lie within the data point.

#### **4.2.1.2: Determination of sensitivity to Pt drugs**

Cells were inoculated at the chosen density (8000 cells/well) and after 24hr; cisplatin, carboplatin or oxaliplatin was added at a range of concentrations. Medium in the wells was replaced with drug-free medium after 2, 6 or 24hr and cells were fixed at 72hr after addition of drugs.

Initial experiments to establish appropriate ranges of drug concentrations were performed in triplicate. From these experiments, the final ranges of drug concentrations for each of the three drugs for the four cell lines were chosen. Results for triplicate experiments in the chosen drug concentrations are shown in Figure 4.2 - Figure 4.4. Calculated  $GI_{50}$  values are presented in Table 4.1.

##### *Comparison of $GI_{50}$ values in each cell line with time*

$GI_{50}$  values following exposure times of 2hr and 6hr were compared to  $GI_{50}$  values after 24hr exposure. Data is shown in Table 4. 2. 24hr incubation gave the lowest  $GI_{50}$  values as expected, whereas for cisplatin shorter incubations gave  $GI_{50}$  values up to 9-fold higher. For carboplatin and oxaliplatin, the length of incubation time generally had a larger effect on survival with  $GI_{50}$  values up to 23-fold higher

##### *Analysis of sensitivity to carboplatin and oxaliplatin compared to cisplatin*

$GI_{50}$  values for carboplatin and oxaliplatin were compared to cisplatin. Data is shown in Table 4. 3. Carboplatin was 7-52-times less toxic than cisplatin, depending on cell line and exposure time. Oxaliplatin showed comparable  $GI_{50}$  values to cisplatin, except in Mor/CPR cells where it was about 10-fold less toxic.

*Analysis of variation in cell line sensitivity*

GI<sub>50</sub> values for A2780, LoVo and Mor/CPR cells were compared to 833K cells. Data is presented in Table 4. 4. A2780 cells were 1.4-2.2 times less sensitive to cisplatin and 1.9-2.6 times less sensitive to carboplatin. A2780 cells were however more sensitive to oxaliplatin than cisplatin. LoVo cells were 1.8-2.3, 2.7-5.5 and 1.3-1.5 times less sensitive to cisplatin, carboplatin and oxaliplatin respectively. Mor/CPR cells were markedly the least sensitive of all the cell lines.

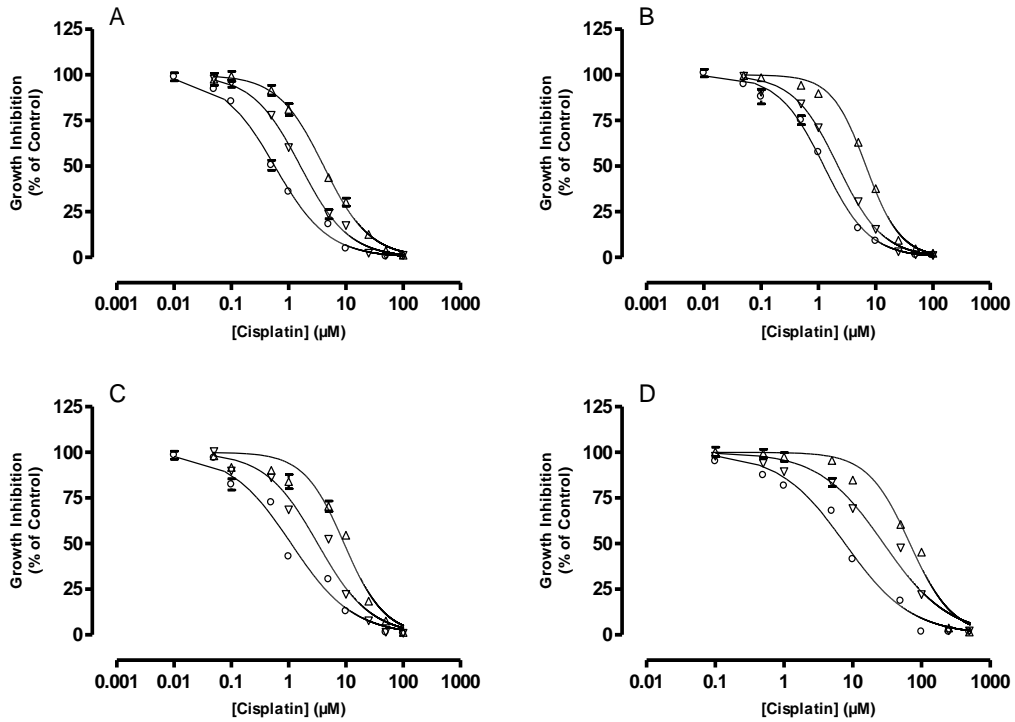


Figure 4.2: The effect of cisplatin on growth inhibition in human tumour 833K (A), A2780 (B), LoVo (C) and Mor/CPR (D) cells. Cells were incubated with various concentrations of drug for 2hr ( $\Delta$ ), 6hr ( $\nabla$ ) and 24 hr ( $\circ$ ). Growth inhibition was measured using the SRB assay. Each data point represents the mean of three individual experiments  $\pm$  standard deviation. Where not shown, error bars lie within the data point.

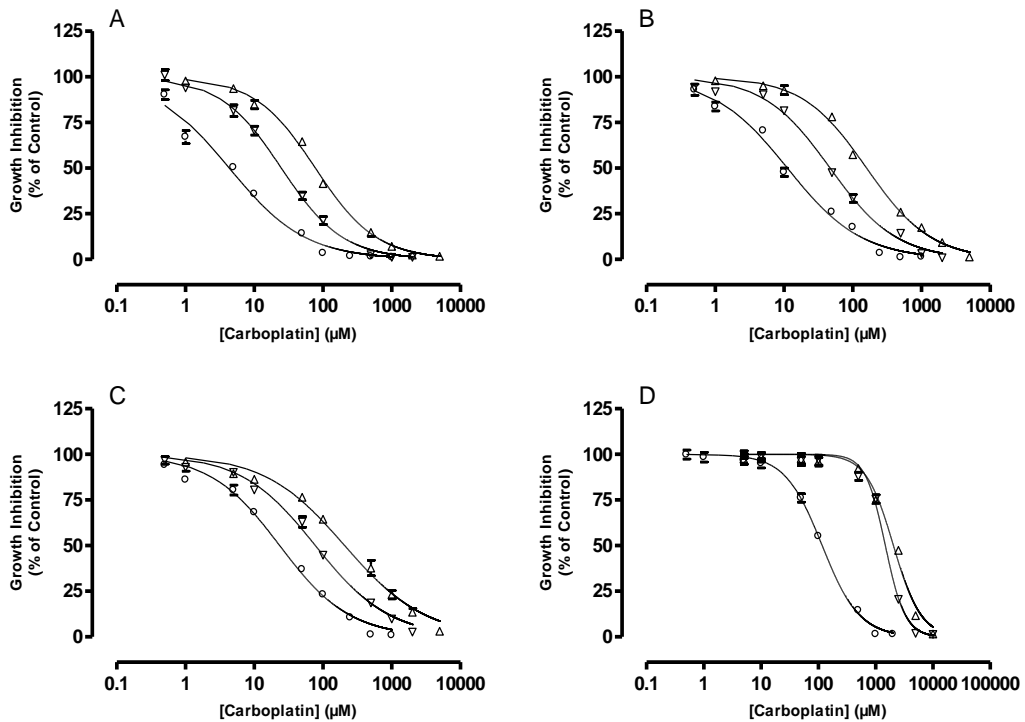


Figure 4.3: The effect of carboplatin on growth inhibition in human tumour 833K (A), A2780 (B), LoVo (C) and Mor/CPR (D) cells. Cells were incubated with various concentrations of drug for 2hr ( $\Delta$ ), 6hr ( $\nabla$ ) and 24 hr ( $O$ ). Growth inhibition was measured using the SRB assay. Each data point represents the mean of three individual experiments  $\pm$  standard deviation. Where not shown, error bars lie within the data point.

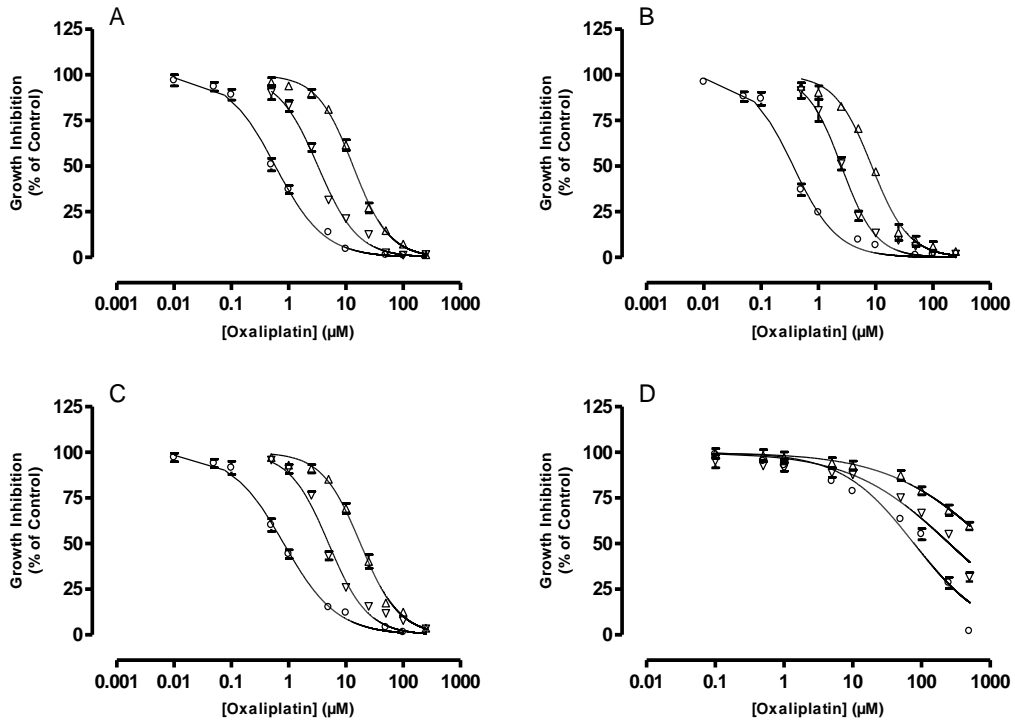


Figure 4.4: The effect of oxaliplatin on growth inhibition in human tumour 833K (A), A2780 (B), LoVo (C) and Mor/CPR (D) cells. Cell were incubated with various concentrations of drug for 2hr ( $\Delta$ ), 6hr ( $\nabla$ ) and 24 hr ( $O$ ). Growth inhibition was measured using the SRB assay. Each data point represents the mean of three individual experiments  $\pm$  standard deviation. Where not shown, error bars lie within the data point.

Table 4.1:  $GI_{50}$  values for 833K, A2780, LoVo and Mor/CPR human tumour cells exposed to cisplatin, carboplatin and oxaliplatin for 2hr, 6hr and 24hr at 37°C. Growth Inhibition was measured at 72hr by the SRB assay. Each value represents the mean readings from 3 individual experiments. Standard deviation is shown in brackets.

Cell Line	Incubation Time	$GI_{50}$ : Cisplatin ( $\mu\text{M}$ )	$GI_{50}$ : Carboplatin ( $\mu\text{M}$ )	$GI_{50}$ : Oxaliplatin ( $\mu\text{M}$ )
833K	2hr	4.1 (0.1)	77.6 (1.2)	13.4 (0.2)
	6hr	1.6 (0.02)	24.9 (0.4)	3.3 (0.1)
	24hr	0.6 (0.01)	4.3 (0.1)	0.6 (0.01)
A2780	2hr	6.8 (0.1)	159.5 (2.6)	8.6 (0.2)
	6hr	2.2 (0.04)	47.0 (1.0)	2.5 (0.1)
	24hr	1.3 (0.02)	11.2 (0.3)	0.4 (0.01)
LoVo	2hr	9.3 (0.3)	207.2 (5.7)	18.0 (0.3)
	6hr	3.2 (0.1)	77.6 (1.7)	5.0 (0.1)
	24hr	1.1 (0.04)	23.5 (0.6)	0.8 (0.02)
Mor/CPR	2hr	68.0 (1.9)	2049 (33)	986.2 (52.5)
	6hr	28.2 (1.1)	1479 (18.2)	251.5 (11.4)
	24hr	7.7 (0.2)	116.8 (1.6)	77.8 (3.7)

*Table 4. 2: GI<sub>50</sub> ratios for 833K, A2780, LoVo and Mor/CPR cells incubated with cisplatin, carboplatin or oxaliplatin. Each ratio is calculated compared to the 24hr incubation value (2hr/24hr or 6hr/24hr).*

<b>Cell Line</b>	<b>Inc. Time</b>	<b>Cisplatin</b>	<b>Carboplatin</b>	<b>Oxaliplatin</b>
833K	2hr	6.8	18.0	22.3
	6hr	2.7	5.8	5.5
	24hr	1	1	1
A2780	2hr	5.2	14.2	21.5
	6hr	1.7	4.2	6.3
	24hr	1	1	1
LoVo	2hr	8.5	8.8	22.5
	6hr	2.9	3.3	6.3
	24hr	1	1	1
Mor/CPR	2hr	8.8	17.5	12.7
	6hr	3.7	12.7	3.2
	24hr	1	1	1

Table 4. 3:  $GI_{50}$  ratios for 833K, A2780, LoVo and Mor/CPR cells incubated with carboplatin or oxaliplatin compared to cisplatin. Each ratio is calculated compared to cisplatin.

Cell Line	Inc. Time	Cisplatin	Carboplatin	Oxaliplatin
833K	2hr	1	18.9	3.3
	6hr	1	15.6	2.1
	24hr	1	7.2	1
A2780	2hr	1	23.5	1.3
	6hr	1	21.4	1.1
	24hr	1	8.6	0.3
LoVo	2hr	1	22.3	1.9
	6hr	1	24.3	1.6
	24hr	1	21.4	0.7
Mor/CPR	2hr	1	30.1	14.5
	6hr	1	52.4	8.9
	24hr	1	15.2	10.1

*Table 4. 4: Ratio of  $GI_{50}$  values for A2780, LoVo and Mor/CPR cells to 833K  $GI_{50}$  values. All 833K values are considered to be 1 (not shown in table).*

<b>Cell Line</b>	<b>Inc. Time</b>	<b>Cisplatin</b>	<b>Carboplatin</b>	<b>Oxaliplatin</b>
A2780	2hr	1.7	2.1	0.6
	6hr	1.4	1.9	0.8
	24hr	2.2	2.6	0.7
LoVo	2hr	2.3	2.7	1.3
	6hr	2.0	3.1	1.5
	24hr	1.8	5.5	1.3
Mor/CPR	2hr	16.6	26.4	73.6
	6hr	17.6	59.4	76.2
	24hr	12.8	27.2	129.7

#### **4.2.1.3: Total Pt-DNA adducts formed in cells**

833K, A2780, LoVo and Mor/CPR cells were incubated in medium containing cisplatin, carboplatin or oxaliplatin at a range of concentrations for 2hr and 24hr. The concentration ranges were chosen from previous preliminary experiments. Cells were harvested immediately after drug exposure and cell pellets were stored at -20°C prior to DNA extraction. Pt levels in DNA hydrolysates were determined by ICP-MS.

Mean levels of Pt-DNA adducts determined from triplicate experiments are shown in Figure 4.5 - Figure 4.7. Values for total Pt-DNA adducts (+/- SD) for all four cell lines and all three drugs are given in Table 4.5 - Table 4.7.

There were clear linear relationships between drug concentration and Pt-DNA adducts levels at both incubation times. For both incubation schedules the total amount of Pt-DNA adducts was highest in the A2780 cells, followed by LoVo and 833K cells, except after 2hr incubation with carboplatin, where the total Pt-DNA adducts level was highest in the 833K cells. For both incubation schedules, the total Pt-DNA adducts levels were lowest in the Mor/CPR cells.

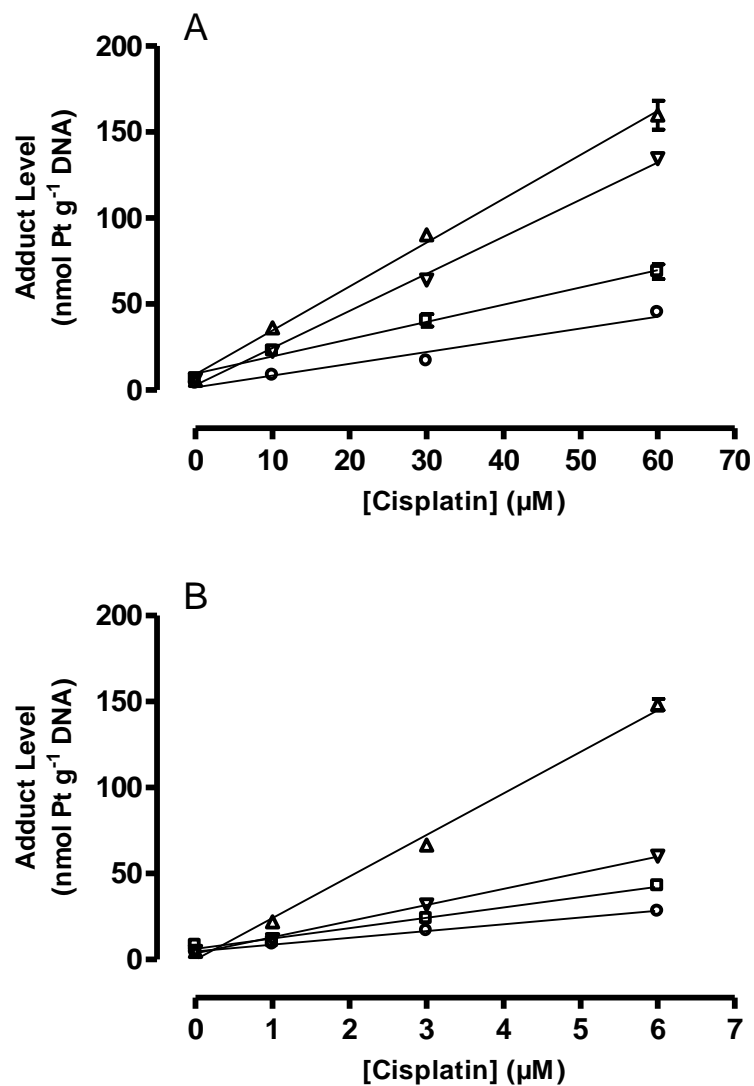


Figure 4.5: Total Pt-DNA adducts levels formed in human tumour 833K (□), A2780 (Δ), LoVo (▽) and Mor/CPR (○) cells following incubation with various concentrations of cisplatin for 2hr (A) and 24hr (B). Pt levels were measured by ICP-MS. Linear regression lines fitted by Prism 4 software. Each data point represents the mean of three individual experiments +/- standard deviation. Where not shown, error bars lie within the data point.

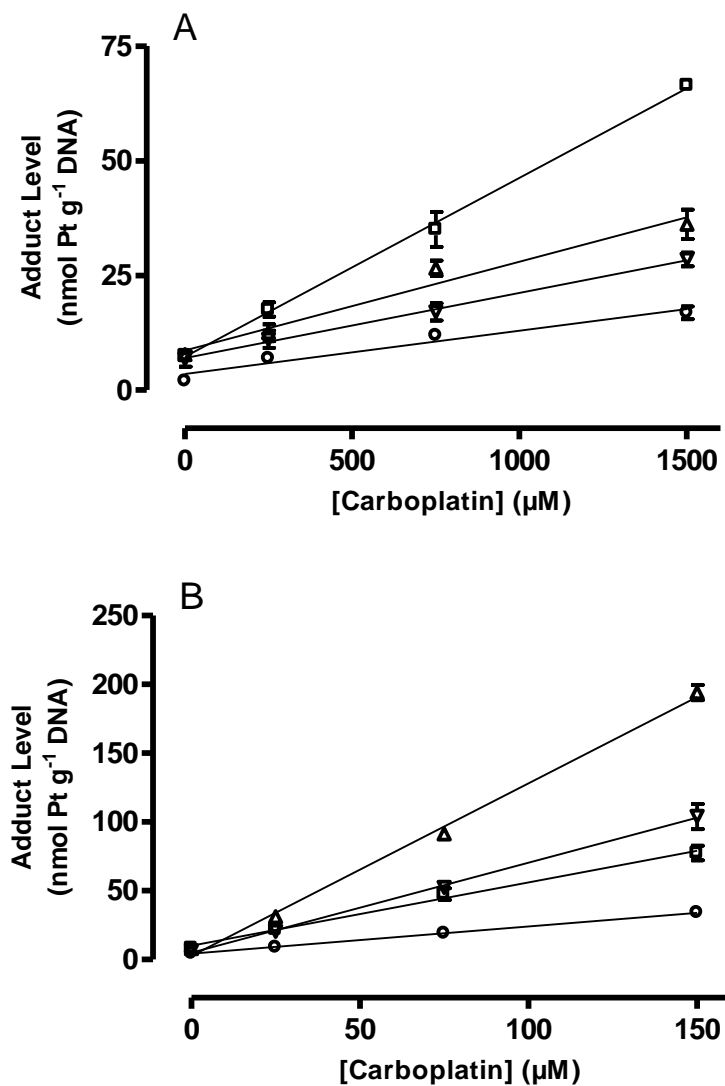


Figure 4.6: Total Pt-DNA adducts levels formed in human tumour 833K ( $\square$ ), A2780 ( $\Delta$ ), LoVo ( $\nabla$ ) and Mor/CPR ( $\circ$ ) cells following incubation with various concentrations of carboplatin for 2hr (A) and 24hr (B). Pt levels were measured by ICP-MS. Linear regression lines fitted by Prism 4 software. Each data point represents the mean of three individual experiments  $\pm$  standard deviation. Where not shown, error bars lie within the data point.

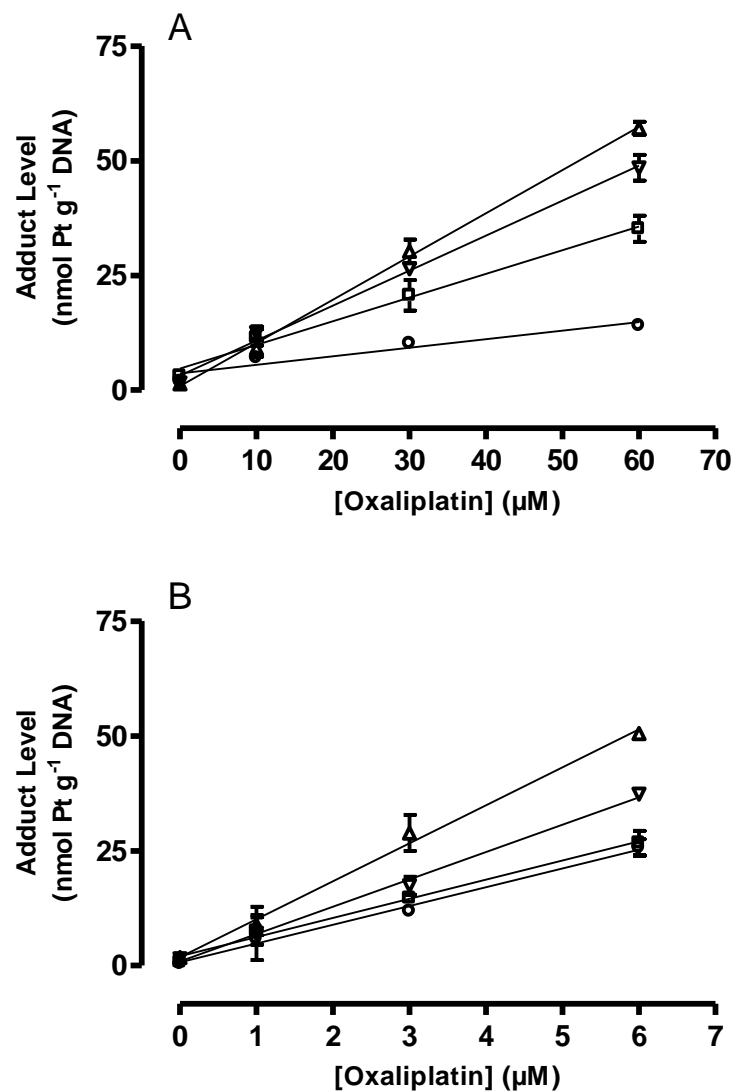


Figure 4.7: Total Pt-DNA adducts levels formed in human tumour 833K ( $\square$ ), A2780 ( $\Delta$ ), LoVo ( $\nabla$ ) and Mor/CPR ( $\circ$ ) cells following incubation with various concentrations of oxaliplatin for 2hr (A) and 24hr (B). Pt levels were measured by ICP-MS. Linear regression lines fitted by Prism 4 software. Each data point represents the mean of three individual experiments  $\pm$  standard deviation. Where not shown, error bars lie within the data point.

Table 4.5: Pt-DNA adduct levels in human tumour 833K, A2780, LoVo and Mor/CPR cells following incubation with various concentrations of cisplatin for 2hr and 24hr. Standard deviation is shown in brackets.

		Total Pt-DNA Adduct Level (nmol Pt g <sup>-1</sup> DNA)							
	Cisplatin (μM)	0	10	30	60	0	1	3	6
833K	2hr	6.5 (0.7)	22.7 (1.45)	40.5 (3.6)	68.8 (4.2)				
	24hr					8.2 (1.6)	10.3 (0.7)	23.8 (0.5)	42.9 (0.7)
A2780	2hr	5.6 (1.2)	36.2 (1.4)	90.3 (2.7)	159.8 (9.3)				
	24hr					4.7 (0.1)	21.9 (2.2)	66.6 (2.0)	148.2 (3.3)
LoVo	2hr	6.4 (1.3)	22.5 (1.7)	63.9 (0.5)	134.5 (3.1)				
	24hr					4.6 (2.0)	11.6 (0.7)	31.7 (1.6)	60.1 (1.0)
Mor/CPR	2hr	4.0 (0.8)	8.6 (0.1)	17.0 (1.4)	45.1 (1.5)				
	24hr					4.3 (0.8)	9.0 (0.4)	16.8 (1.5)	28.1 (2.4)

Table 4.6: Pt-DNA adduct levels in human tumour 833K, A2780, LoVo and Mor/CPR cells following incubation with various concentrations of carboplatin for 2hr and 24hr. Standard deviation is shown in brackets.

		Total Pt-DNA Adduct Level (nmol Pt g <sup>-1</sup> DNA)							
Cell Line	Carboplatin (μM)	0	250	750	1500	0	25	75	150
833K	2hr	7.6 (0.2)	17.6 (1.6)	35.0 (3.8)	66.4 (0.7)				
	24hr					8.2 (1.0)	21.9 (2.2)	47.6 (4.2)	77.4 (5.3)
A2780	2hr	7.8 (0.7)	12.5 (1.8)	26.6 (1.7)	36.1 (3.2)				
	24hr					8.0 (1.1)	31.0 (2.1)	91.3 (1.2)	194.1 (5.7)
LoVo	2hr	6.8 (1.7)	11.1 (1.9)	17.1 (1.9)	28.5 (1.5)				
	24hr					6.3 (1.2)	20.5 (1.2)	52.5 (1.2)	104.0 (9.0)
Mor/CPR	2hr	2.0 (0.3)	6.9 (0.2)	11.9 (0.3)	16.9 (1.4)				
	24hr					4.6 (0.7)	8.8 (0.4)	19.2 (1.2)	34.1 (0.6)

Table 4.7: Pt-DNA adduct levels in human tumour 833K, A2780, LoVo and Mor/CPR cells following incubation with various concentrations of oxaliplatin for 2hr and 24hr. Standard deviation is shown in brackets.

		Total Pt-DNA Adduct Level (nmol Pt g <sup>-1</sup> DNA)							
Oxaliplatin (μM)		0	10	30	60	0	1	3	6
833K	2hr	3.1 (1.1)	11.5 (1.8)	20.7 (3.3)	35.2 (2.9)				
	24hr					0.8 (0.2)	7.5 (3.0)	14.7 (0.9)	26.7 (2.7)
A2780	2hr	1.4 (0.5)	9.1 (1.8)	30.2 (2.6)	57.1 (1.4)				
	24hr					1.7 (0.7)	8.8 (2.2)	28.9 (3.9)	50.5 (1.0)
LoVo	2hr	1.6 (0.8)	12.5 (1.3)	26.4 (1.2)	48.5 (2.8)				
	24hr					1.5 (0.3)	7.0 (5.8)	17.4 (2.0)	37.3 (1.0)
Mor/CPR	2hr	1.9 (0.4)	7.0 (0.4)	10.2 (0.7)	14.1 (0.7)				
	24hr					0.4 (0.1)	5.8 (0.5)	11.8 (0.7)	25.7 (1.9)

#### **4.2.2: Chromatographic Analysis of Pt-DNA adducts formed in cells**

As discussed in detail previously (see chapters 1 and 3) the combination of ICP-MS with chromatographic separation of Pt-DNA adducts permits the detection of all the types of adducts even at low levels. This permits the direct analysis of adducts formed in cells without relying on their ability to be detected by a suitable antibody or a specialised post-labelling assay. It was of particular interest to survey adducts formed in a number of cell lines because of previous results which indicated the formation, in cells, of a new type of adduct, hypothesised to involve GSH.

Cells were incubated for 24hr with either 6  $\mu$ M cisplatin or oxaliplatin, or 150  $\mu$ M carboplatin. 24hr incubation was initially chosen for all four cell lines as previous work had shown monofunctional platinum products to form quickly, but closure to bifunctional products and/or binding of GSH to take many hours (Eastman 1987). DNA was extracted from cells and enzymatically digested as described in section 2.6. Previous work by Azim-Araghi (Azim-Araghi 2003) had confirmed that the levels of enzymes used in the initial digest were more than sufficient to achieve total digestion of the DNA. DNA ultrafiltrates were collected by centrifugation at 13000 x g, 4°C for 60 minutes using a Microcon YM-10 ultrafiltration unit (Millipore, UK) to remove proteins that would increase contamination of the MonoQ column. Solutions (100  $\mu$ l) of the digested mixture were injected into the MonoQ system and eluted at 1 ml/min in increasing NaCl concentrations. UV absorbance was monitored at 254 nm and fractions collected as described in section 2.9. Pt levels were then measured by ICP-MS.

#### 4.2.2.1: DNA adducts formed in cells exposed to cisplatin for 24hr

Measurements before and after ultrafiltration of enzymatic hydrolysates of DNA confirmed that less than 5% of the total Pt was retained by the ultrafilter. Typical MonoQ elution profiles for hydrolysates of DNA from 833K, A2780, LoVo and Mor/CPR cells incubated for 24hr with 6  $\mu\text{M}$  cisplatin are shown in Figure 4.8 (graphs A-D respectively). Mean retention times of the four mononucleotides (detected by UV) and four Pt-containing species are shown in Table 4.8. This also shows that the recovery of Pt from the column exceeded 92%.

Analyses of Pt content in collected chromatographic fractions showed the presence of four Pt-containing products. These products had similar retention times and relative Pt levels of adducts formed by the reaction of cisplatin with pure DNA analysed using a similar method (Meczes et al 2005). Therefore, these products are suggested to be of the same nature as the major Pt-DNA products characterised previously (Fichtinger-Schepman et al 1985). The chemical nature of the four peaks in order of elution therefore was designated as: 1:  $\text{Pt}(\text{NH}_3)_2(\text{R})(\text{dGMP})$ , 2: *cis*- $\text{Pt}(\text{NH}_3)_2\text{d}(\text{ApG})$ , 3: *cis*- $\text{Pt}(\text{NH}_3)_2\text{d}(\text{GpG})$  and 4: *cis*- $\text{Pt}(\text{NH}_3)_2(\text{dGMP})_2$ . Four products that were detected by UV eluted at similar times to the previously characterised mononucleotides described in chapter 3, and therefore were assigned in order of elution as dCMP, dAMP, TMP and dGMP.

The mean yields of each adduct type as a percent of total Pt recovered was calculated from three analyses of separate DNA preparations. The results (Table 4.11) show that peak 3, attributed to *cis*- $\text{Pt}(\text{NH}_3)_2\text{d}(\text{GpG})$  was the major Pt-containing product detected,

contributing approximately 60% of the total Pt detected. Peak 2, attribute to *cis*-Pt(NH<sub>3</sub>)<sub>2</sub>d(ApG) was the second major Pt-containing product detected, contributing approximately 20% of the total Pt detected. An approximate ratio of 1: 2.5 was observed for the ApG: GpG adducts which is similar to previous analyses (Azim-Araghi 2003). Levels of peak 1 (attributed to Pt(NH<sub>3</sub>)<sub>2</sub>(R)(dGMP)) ranged from 2.6-7.3%, and levels of peak 4 (attributed to *cis*-Pt(NH<sub>3</sub>)<sub>2</sub>(dGMP)<sub>2</sub>) ranged from 7.1-13.3%.

However, no additional Pt-containing products were detected in any of the four cell lines investigated and no evidence for the putative *cis*-Pt(NH<sub>3</sub>)<sub>2</sub>(DNA)(GSH) cross-link was observed.

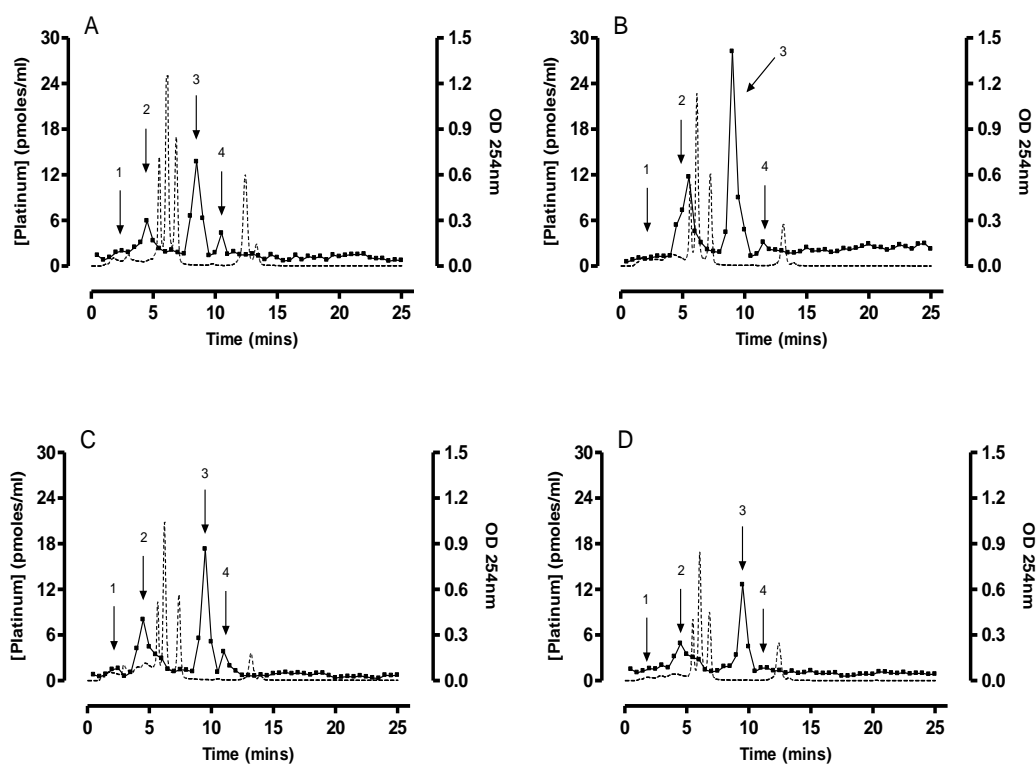


Figure 4.8: Typical MonoQ elution pattern for 833K (A), A2780 (B), LoVo (C) and Mor/CPR (D) cells incubated with 6  $\mu\text{M}$  cisplatin for 24hr. Solutions (100  $\mu\text{l}$ ) of DNA were injected into the MonoQ column and eluted at 1 ml/min. Fractions were collected with increasing NaCl concentration and Pt levels in each fraction measured by ICP-MS. (■), Pt concentration; dotted line: OD 254 nm. Peaks 1:  $\text{Pt}(\text{NH}_3)_2(\text{R})(\text{dGMP})$ ; 2:  $\text{cis-Pt}(\text{NH}_3)_2(\text{ApG})$ ; 3:  $\text{cis-Pt}(\text{NH}_3)_2(\text{GpG})$  and 4:  $\text{cis-Pt}(\text{NH}_3)_2(\text{dGMP})_2$

Table 4.8: Mean retention times for the products detected by UV absorbance and ICP-MS in DNA extracted from cisplatin-treated cells. Mean values from three individual analyses are shown. Ranges in retention time are shown in brackets except for total Pt recovered in which SD is shown.

Peak	Identity	833K	A2780	LoVo	Mor/CPR
	dCMP	5.3 (0.1)	5.4 (0.1)	5.6 (0.2)	5.4 (0.1)
	dAMP	5.8 (0.1)	6.1 (0.2)	6.2 (0.2)	5.9 (0.2)
	TMP	6.7 (0.2)	7.1 (0.2)	7.3 (0.1)	6.9 (0.1)
	dGMP	12.5 (0.2)	13.0 (0.3)	13.2 (0.2)	12.4 (0.1)
1	Pt(NH <sub>3</sub> ) <sub>2</sub> (R)(dGMP)	2.5 (0.5)	3.0 (0.5)	2.5 (0.5)	2.0 (0.5)
2	cis-Pt(NH <sub>3</sub> ) <sub>2</sub> d(ApG)	4.5 (0.5)	5.5 (1.0)	4.5 (0.5)	4.5 (0.5)
3	cis-Pt(NH <sub>3</sub> ) <sub>2</sub> d(GpG)	8.5 (1.0)	9.0 (1.0)	9.0 (1.0)	9.5 (1.0)
4	cis-Pt(NH <sub>3</sub> ) <sub>2</sub> (dGMP) <sub>2</sub>	10.5 (1.0)	11.5 (1.0)	11.0 (0.5)	10.5 (0.5)
<b>Total Pt Recovery (%)</b>		<b>103.5 (6.7)</b>	<b>92.3 (4.4)</b>	<b>91.7 (5.6)</b>	<b>98.3 (3.3)</b>

#### **4.2.2.2: DNA adducts formed in cells exposed to carboplatin for 24hr**

Typical MonoQ elution profiles for hydrolysates of DNA from 833K, A2780 and LoVo cells incubated for 24hr with 150  $\mu$ M carboplatin are shown in Figure 4.9 (graphs A-C respectively). Mean retention times of the four mononucleotides (detected by UV) and four Pt-containing species are shown in Table 4.9. This also confirms that recovery of Pt from the column exceeded 92%.

Analyses of Pt content in collected chromatographic fractions showed the presence of four Pt-containing products. These products had similar retention times and relative Pt levels of adducts to those seen in the incubation with cisplatin and therefore are suggested to be of the same nature.

The mean yields of each adduct type as a percent of total Pt recovered was calculated from three analyses of separate DNA preparations. The results (Table 4.11) show that the relative proportions of the peaks were very similar to those values for cisplatin and, like cisplatin, did not vary markedly between cell lines.

Similarly to cisplatin, no additional Pt-containing products were detected in any of the three cell lines. No evidence has previously been presented for potential carboplatin-DNA cross-links with GSH although, as adducts formed are believed to be the same as those for cisplatin, their formation was plausible. However, the data in this section provides no evidence to support their formation.

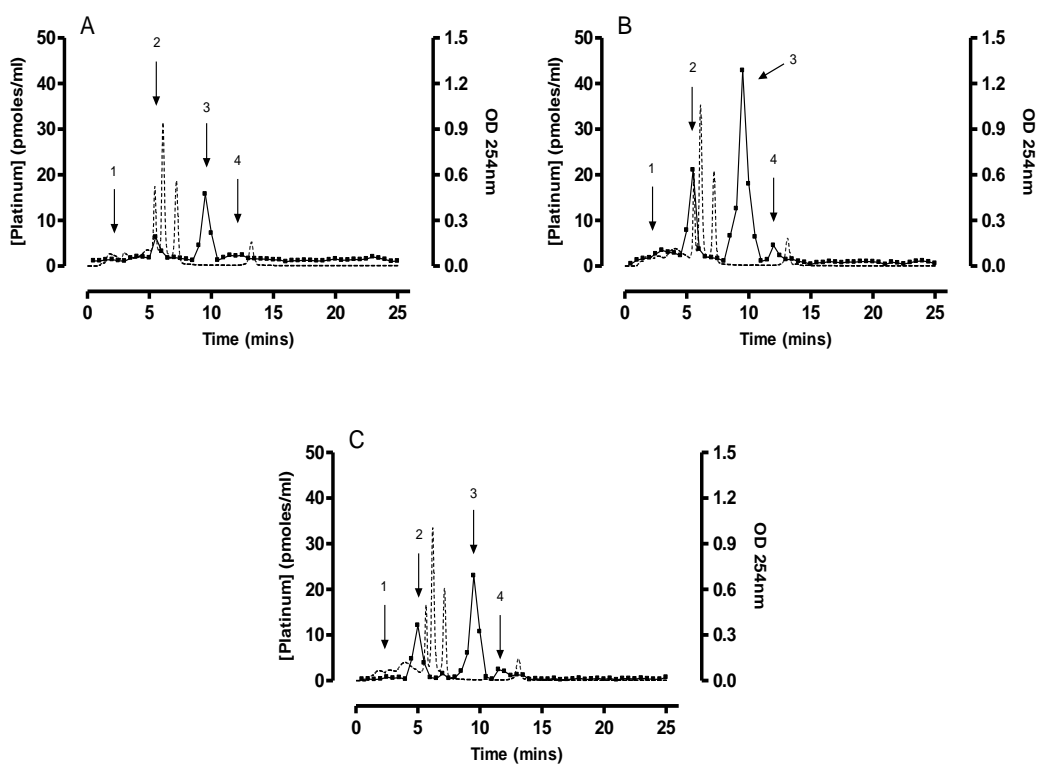


Figure 4.9: Typical MonoQ elution pattern for 833K (A), A2780 (B) and LoVo (C) cells incubated with 150  $\mu\text{M}$  carboplatin for 24hr. Solutions (100  $\mu\text{l}$ ) of DNA were injected into the MonoQ column and eluted at 1 ml/min. Fractions were collected with increasing NaCl concentration and Pt levels in each fraction measured by ICP-MS. (■), Pt concentration; dotted line: OD 254 nm. Peaks 1:  $\text{Pt}(\text{NH}_3)_2(\text{R})(\text{dGMP})$ ; 2: *cis*- $\text{Pt}(\text{NH}_3)_2\text{d}(\text{ApG})$ ; 3: *cis*- $\text{Pt}(\text{NH}_3)_2\text{d}(\text{GpG})$  and 4: *cis*- $\text{Pt}(\text{NH}_3)_2(\text{dGMP})_2$

Table 4.9: Mean retention times for the products detected by UV absorbance and ICP-MS in DNA extracted from carboplatin-treated cells. Mean values from three individual analyses are shown. Ranges in retention time are shown in brackets except for total Pt recovered in which SD is shown.

Peak	Identity	833K	A2780	LoVo
	dCMP	5.4 (0.1)	5.5 (0.1)	5.6 (0.1)
	dAMP	6.0 (0.1)	6.0 (0.1)	6.1 (0.1)
	TMP	7.0 (0.2)	7.1 (0.1)	7.0 (0.1)
	dGMP	13.1 (0.1)	13.1 (0.2)	13.1 (0.2)
1	Pt(NH <sub>3</sub> ) <sub>2</sub> (R)(dGMP)	2.0 (0.5)	3.0 (1.0)	2.5 (0.5)
2	cis-Pt(NH <sub>3</sub> ) <sub>2</sub> d(ApG)	5.5 (1.0)	5.5 (0.5)	5.0 (0.5)
3	cis-Pt(NH <sub>3</sub> ) <sub>2</sub> d(GpG)	9.5 (1.0)	9.5 (1.0)	9.5 (1.0)
4	cis-Pt(NH <sub>3</sub> ) <sub>2</sub> (dGMP) <sub>2</sub>	12.0 (1.0)	12.0 (1.0)	11.5 (1.0)
<b>Total Pt Recovery (%)</b>		<b>92.3 (6.7)</b>	<b>104.5 (7.8)</b>	<b>101.3 (8.6)</b>

#### **4.2.2.3: DNA adducts formed in cells exposed to oxaliplatin for 24hr**

Typical MonoQ elution profiles for hydrolysates of DNA from 833K, A2780 and LoVo cells incubated for 24hr with 6  $\mu$ M oxaliplatin are shown in Figure 4.10 (graphs A-C respectively). Mean retention times of the four mononucleotides (detected by UV) and four Pt-containing species are shown in Table 4.10. Recovery of Pt from the column exceeded 95%.

Oxaliplatin is believed to form similar Pt-DNA cross-links as cisplatin (Jennerwein et al 1989, Saris et al 1996) with the major difference being the DACH ligand in place of the two  $\text{NH}_3$  ligands of cisplatin. Analyses of Pt content in collected chromatographic fractions showed the presence of four Pt-containing products. These products had similar retention times and relative Pt levels of adducts to those seen in the incubation with cisplatin and therefore are suggested to be of a similar nature.

The mean yields of each adduct type as a percent of total Pt recovered was calculated from three analyses of separate DNA preparations. The results (Table 4.11) show that the relative proportions of the peaks were very similar to those values for cisplatin and, like cisplatin, did not vary markedly between cell lines.

Similarly to cisplatin, no additional Pt-containing products were detected in any of the three cell lines. No evidence has previously been presented for potential oxaliplatin-DNA cross-links with GSH although, as adducts formed are believed to be similar to those for cisplatin, their formation was plausible. However, the data in this section provides no evidence to support their formation.

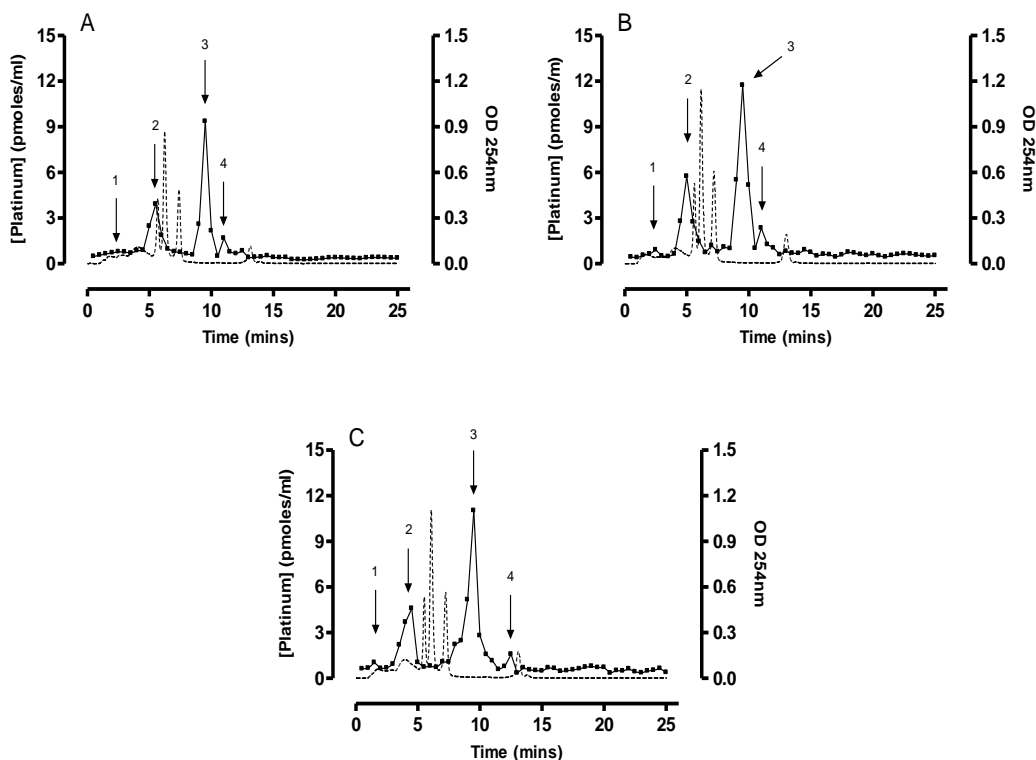


Figure 4.10: Typical MonoQ elution pattern for 833K (A), A2780 (B) and LoVo (C) cells incubated with 6  $\mu\text{M}$  oxaliplatin for 24hr. Solutions (100  $\mu\text{l}$ ) of DNA were injected into the MonoQ column and eluted at 1 ml/min. Fractions were collected with increasing NaCl concentration and Pt levels in each fraction measured by ICP-MS. (■), Pt concentration; dotted line: OD 254 nm. Peaks are proposed to be 1: Pt(DACH)(R)(dGMP); 2: cis-Pt(DACH)d(ApG); 3: cis-Pt(DACH)d(GpG) and 4: cis-Pt(DACH)(dGMP)<sub>2</sub>

Table 4.10: Mean retention times for the products detected by UV absorbance and ICP-MS in DNA extracted from oxaliplatin-treated cells. Mean values from three individual analyses are shown. Ranges in retention time are shown in brackets except for total Pt recovered in which SD is shown.

Peak	Identity	833K	A2780	LoVo
	dCMP	5.6 (0.1)	5.6 (0.1)	5.4 (0.1)
	dAMP	6.1 (0.1)	6.1 (0.1)	6.0 (0.1)
	TMP	7.4 (0.2)	7.1 (0.2)	7.2 (0.2)
	dGMP	13.0 (0.1)	12.9 (0.2)	13.0 (0.2)
1	Pt(DACH)(R)dGMP)	2.5 (0.5)	2.5 (0.5)	2.0 (1.0)
2	cis-Pt(DACH)d(ApG)	5.5 (0.5)	5.0 (0.5)	4.5 (0.5)
3	cis-Pt(DACH)d(GpG)	9.5 (1.0)	9.5 (0.5)	9.5 (1.0)
4	cis-Pt(DACH)(dGMP) <sub>2</sub>	11.0 (0.5)	11.0 (1.0)	12.5 (1.5)
<b>Total Pt Recovery (%)</b>		<b>95.3 (3.3)</b>	<b>103.2 (4.7)</b>	<b>101.2 (5.5)</b>

Table 4.11: Pt content of each of the four main peaks of Pt-containing material recovered from anion exchange chromatographic analysis of enzymatic hydrolysates of DNA extracted from drug-treated cells. Pt content is expressed as a percentage of Pt contained in the four identified peaks in relation to the total Pt recovered. Each value represents the mean of three individual analyses. Standard deviation is shown in brackets.

Drug (conc. used)	Peak Identity	833K	A2780	LoVo	MorCPR
<b>Cisplatin</b> (60 $\mu$ M)	1	7.1 (0.5)	2.6 (0.2)	5.2 (0.2)	7.3 (0.1)
	2	21.2 (1.5)	26.5 (1.9)	26.1 (1.2)	23.6 (0.4)
	3	58.3 (0.8)	63.8 (4.6)	56.3 (2.5)	61.0 (1.0)
	4	13.3 (0.7)	7.1 (0.5)	12.4 (0.5)	8.1 (0.1)
<b>Carboplatin</b> (150 $\mu$ M)	1	4.7 (0.4)	3.7 (0.1)	1.9 (0.2)	
	2	24.7 (1.9)	29.6 (0.7)	31.7 (2.4)	
	3	61.5 (4.8)	60.3 (1.3)	60.1 (4.5)	
	4	9.2 (0.7)	6.3 (0.1)	6.3 (0.5)	
<b>Oxaliplatin</b> 60 ( $\mu$ M)	1	5.0 (0.2)	4.6 (0.2)	3.7 (0.1)	
	2	24.9 (1.2)	29.3 (1.2)	25.8 (1.0)	
	3	59.5 (2.8)	59.7 (2.4)	61.7 (2.4)	
	4	10.7 (0.5)	6.4 (0.3)	8.8 (0.3)	

#### 4.2.2.4: DNA adducts formed in LoVo cells exposed to drugs for 2hr

Since the previous described experiments failed to provide evidence for the formation of additional DNA adducts in cells, the possibility was considered that the hypothesised adducts were short-lived because either 1, the putative *cis*-Pt(NH<sub>3</sub>)<sub>2</sub>(DNA)(GSH) cross-links were unstable and/or 2, the putative cross-links were more readily repaired by cells than the established classes of adducts. To investigate such possibilities, LoVo cells were incubated for 2hr with either 60 μM cisplatin or oxaliplatin or 1500 μM carboplatin. Typical MonoQ elution results for DNA hydrolysates analysed using the standard MonoQ system are shown in Figure 4.11.

Table 4.12 shows results for three separate experiments for each drug where the quantity of Pt in each peak is expressed as a percentage of the total recovered platinum. For the LoVo cells incubated with cisplatin and carboplatin, similar proportions of the peaks 2 and 3 (proposed to be *cis*-Pt(NH<sub>3</sub>)<sub>2</sub>d(ApG) and *cis*-Pt(NH<sub>3</sub>)<sub>2</sub>d(GpG) respectively) were detected between the two incubation times. As would be expected with these incubation periods, proportions of the peak 1 (proposed to be Pt(NH<sub>3</sub>)<sub>2</sub>(R)(dGMP)) decreased between 2hr and 24hr incubations, and proportions of peak 4 (proposed to be *cis*-Pt(NH<sub>3</sub>)<sub>2</sub>(dGMP)<sub>2</sub>) increased. These changes in yield were of comparable proportions (- 3.7 and + 5.1 for cisplatin and - 4.2 and + 3.3 for carboplatin).

Similarly to cisplatin and carboplatin, for oxaliplatin the proportion of Pt in peak 1 (proposed to be Pt(DACH)(R)(dGMP)) decreased between 2hr and 24hr. However,

unlike cisplatin and carboplatin, this was accompanied with a more marked increase in peak 3 (proposed to be *cis*-Pt(DACH)d(GpG).

Overall, no additional Pt-containing products were detected following the 2hr incubations with cisplatin, carboplatin or oxaliplatin. This indicates a lack of any evidence for formation of the proposed *cis*-Pt(NH<sub>3</sub>)<sub>2</sub>(DNA)(GSH) cross-links, as was the case for the samples from cells exposed to drugs for 24hr.

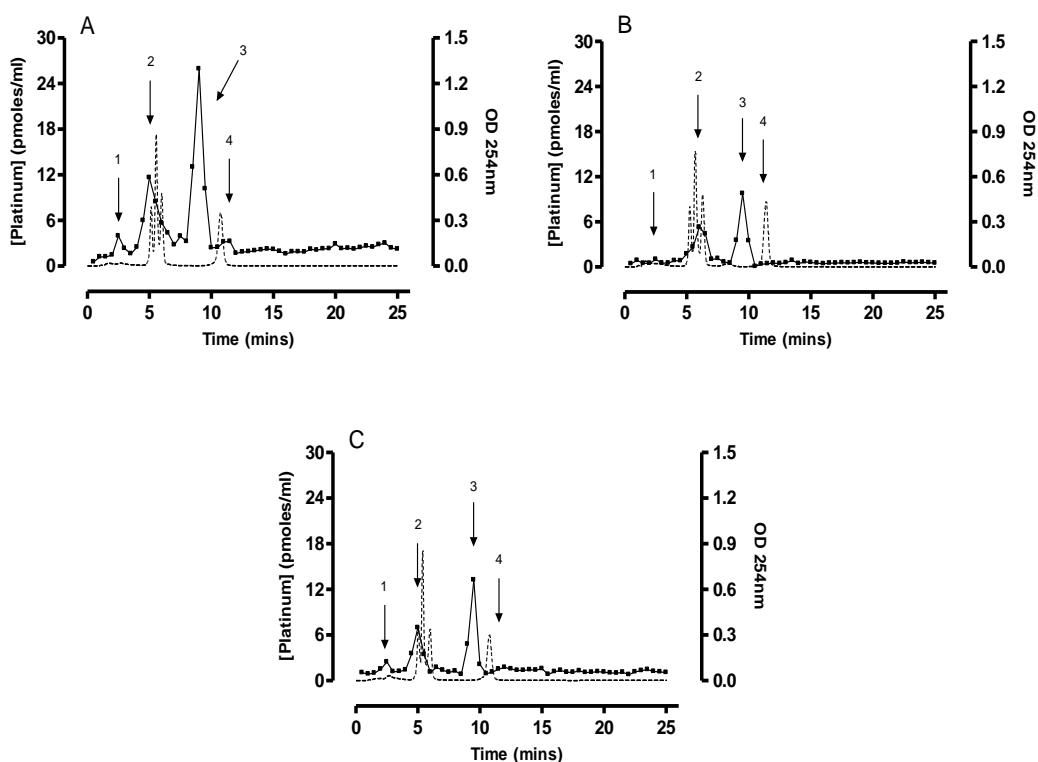


Figure 4.11: Typical MonoQ elution pattern for LoVo cells incubated with 60  $\mu\text{M}$  cisplatin (A), 1500  $\mu\text{M}$  carboplatin (B) and 60  $\mu\text{M}$  oxaliplatin (C) for 2hr. 100  $\mu\text{g/ml}$  DNA was applied to the column. Fractions were collected with increasing NaCl concentration and Pt levels in each fraction measured by ICP-MS. (■), Pt concentration; dotted line: OD 254 nm. Peaks for cisplatin and carboplatin are 1:  $\text{Pt}(\text{NH}_3)_2(\text{R})(\text{dGMP})$ ; 2:  $\text{cis-Pt}(\text{NH}_3)_2\text{d}(\text{ApG})$ ; 3:  $\text{cis-Pt}(\text{NH}_3)_2\text{d}(\text{GpG})$  and 4:  $\text{cis-Pt}(\text{NH}_3)_2(\text{dGMP})_2$ . Peaks for oxaliplatin are proposed to be 1:  $\text{Pt}(\text{DACH})(\text{R})(\text{dGMP})$ ; 2:  $\text{cis-Pt}(\text{DACH})\text{d}(\text{ApG})$ ; 3:  $\text{cis-Pt}(\text{DACH})\text{d}(\text{GpG})$  and 4:  $\text{cis-Pt}(\text{DACH})(\text{dGMP})_2$ .

Table 4.12: Pt content of each of the four main peaks of Pt-containing material recovered from anion exchange chromatographic analysis of enzymatic hydrolysates of DNA extracted from drug-treated LoVo cells. Pt content is expressed as a percentage of Pt contained in the four identified peaks in relation to the total Pt recovered. Each value represents the mean of three individual analyses. Standard deviation is shown in brackets.

	Peak Identity	% Pt (2hr)	% Pt (24hr)	Difference (2hr-24hr)
<b>Cisplatin</b>	1	8.9 (0.2)	5.2 (0.2)	- 3.7
	2	25.9 (0.7)	26.1 (1.2)	+ 0.2
	3	57.9 (1.5)	56.3 (2.5)	- 1.6
	4	7.3 (0.2)	12.4 (0.5)	+ 5.1
<b>Carboplatin</b>	1	6.1 (0.3)	1.9 (0.2)	- 4.2
	2	31.9 (1.4)	31.7 (2.4)	- 0.2
	3	59.0 (2.6)	60.1 (4.5)	+ 1.1
	4	3.0 (0.1)	6.3 (0.5)	+ 3.3
<b>Oxaliplatin</b>	1	10.1 (0.5)	3.7 (0.1)	- 6.4
	2	28.6 (1.5)	25.8 (1.0)	- 2.8
	3	54.2 (2.9)	61.7 (2.4)	+ 7.5
	4	7.1 (0.4)	8.8 (0.3)	+ 1.7

#### 4.2.3: Pt-DNA adducts formed on purified DNA in the presence of GSH

The main aim of studying adducts formed in cells by cisplatin was to confirm the previous findings that an additional major class of Pt-containing DNA adducts could be detected when DNA extracted from cisplatin-treated cells was analysed by anion exchange chromatography and ICP-MS. As discussed in chapter 1, such adducts had been detected previously (Azim-Araghi 2003) and were thought to contain GSH cross-linked to DNA. However, the data described in this section so far for four cell lines incubated with cisplatin has shown no evidence to support this hypothesis.

In the previous work (Azim-Araghi 2003) a novel Pt-containing product with similar chromatographic properties to the product seen in cells had been identified in pure DNA incubated with cisplatin. As discussed in chapter 1, this finding was consistent with a number of other preliminary observations and, if correct, could have significant implications for the cellular pharmacology of Pt-based drugs. Therefore, attempts were made to reproduce the putative formation of *cis*-Pt(NH<sub>3</sub>)<sub>2</sub>(DNA)(GSH) cross-links of purified DNA to determine the plausibility of such products occurring in cells.

Initial experiments were aimed at defining the conditions for reacting cisplatin with DNA in the presence of GSH so as to generate suitable quantities of adducts for subsequent analysis. Then, the main aim was to test the hypothesis that the additional adducts could be detected on such DNA when analysed by anion exchange chromatography/ICP-MS compared to adducts formed in the absence of GSH.

Pure calf thymus DNA (500 µg/ml) was mixed with 0, 10, 25, 50 and 100 mM GSH before addition of 15 µM cisplatin. The mixtures were incubated for 2hr and 24hr at 37°C under anoxic conditions (see section 2.7.1) and then stored at -80°C. DNA was then separated from low molecular weight products such as unreacted drug and products of the reaction of cisplatin with GSH by gel filtration on a G-75 Sephadex column as described in section 2.8. Collected fractions were analysed for DNA concentration by measuring O.D. at 254nm. All fractions containing DNA were pooled together and concentrated by ultrafiltration. Pt-DNA adduct levels were determined by ICP-MS.

#### **4.2.3.1: Gel Filtration separation of platinated DNA**

Typical gel filtration chromatographic separations for reaction mixtures in the absence (A) and presence (B) of GSH are shown in Figure 4.12. These results showed that DNA passed through the column rapidly; typically eluting between 40 and 60 minutes post injection (Figure 4.12, peak 1). This is consistent with its exclusion from the G-75 Sephadex beads because of its high molecular weight. Unbound Pt eluted typically between 110 and 150 minutes (Figure 4.12, peak 2). Following 2hr incubation, 32% of the total Pt eluted was associated with the DNA (Figure 4.12, graph A peak 1).

The presence of 10 mM GSH in the incubation caused a decrease from 32% to 9% of the total Pt associated with DNA (Figure 4.12, graph B peak 1). An additional optical density peaked was observed between 110 and 140 minutes that eluted slightly earlier than unbound platinum (Figure 4.12– Graph B peak 3). This product is likely to be a conjugate between cisplatin and GSH. Typical Pt recovery was greater than 90% of the total Pt loaded for all separations.

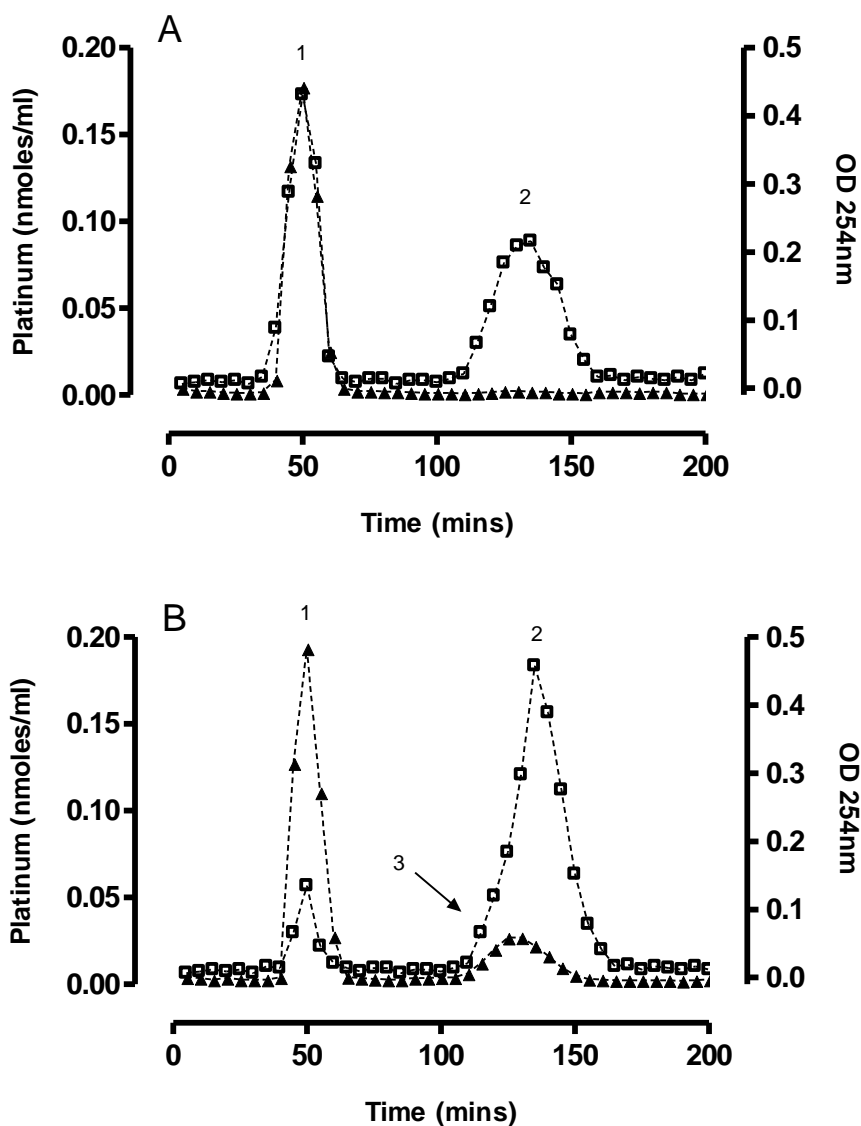


Figure 4.12: Typical Sephadex G-75 gel elution profiles of calf thymus DNA (500 µg/ml) incubated for 2hr with cisplatin (15 µM) alone (A) and with 10 mM GSH (B). (□), Optical density was measured at OD 254 nm. (▲), Platinum concentrations determined by AAS. Peaks are: 1, DNA; 2, low molecular weight products such as unreacted cisplatin or GSH; 3, possible cisplatin-GSH conjugate

#### 4.2.3.2: Effect of GSH on total Pt-DNA adduct level

Pt-DNA adducts levels for calf thymus DNA (500 µg/ml) reacted with cisplatin (15 µM) in the presence of increasing concentrations of GSH for 2hr and 24hr are shown in Table 4.13. Total adduct levels expressed as a percentage of control for 2hr (A) and 24hr (B) are shown in Figure 4.13.

When no GSH was added, a total adduct level of 3.9 (+/- 0.1 SD) µmol Pt g<sup>-1</sup> DNA was observed after a 2hr incubation with cisplatin. This increased to 13.5 (+/- 0.4 SD) µmol Pt g<sup>-1</sup> DNA when incubated for 24 hours. Incubation with 10 mM GSH decreased the total adduct level to 0.7 (+/- 0.03 SD) and 1.2 (+/- 0.1 SD) µmol Pt g<sup>-1</sup> DNA (18.7% and 8.5% of control) for the 2hr and 24hr incubations respectively. Data interpolated from the graph (first order exponential decay line fitted in Prism) suggests concentrations of values of 3.9 mM and 2.7 mM GSH are required to achieve a 50% decrease in total Pt-DNA adducts levels for 2hr and 24hr respectively.

*Table 4.13: Pt-DNA adduct levels expressed as  $\mu\text{moles Pt/g DNA}$  and as a percentage of the control for calf thymus DNA mixed with increasing concentration of GSH, then incubated with  $15 \mu\text{M}$  cisplatin for 2 and 24 hours. Each value represents the mean of 3 individual experiments. Standard deviation is shown in brackets.*

		Concentration of GSH (mM)				
		Control (0)	10	25	50	100
<b>2 hours</b>	$\mu\text{mol Pt g}^{-1}$ DNA	3.9 (0.1)	0.7 (0.03)	0.3 (0.01)	0.1 (0.01)	0.02 (0.01)
	% Control		18.5 (0.7)	6.4 (0.3)	2.0 (0.1)	0.5 (0.1)
<b>24 hours</b>	$\mu\text{mol Pt g}^{-1}$ DNA	13.5 (0.4)	1.2 (0.1)	0.3 (0.01)	0.1 (0.01)	0.03 (0.01)
	% Control		8.7 (0.1)	2.2 (0.01)	0.7 (0.03)	0.2 (0.02)

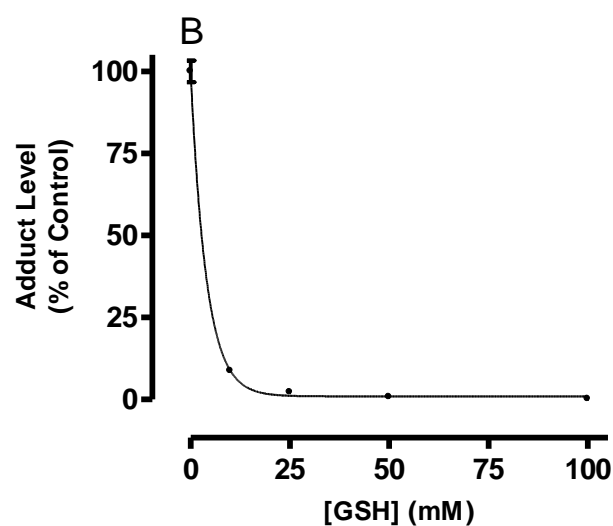
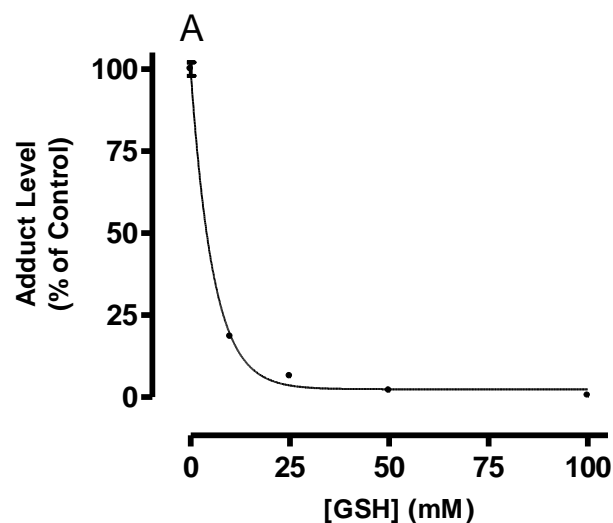


Figure 4.13: Effect of increasing GSH concentration on total adducts formation of cisplatin-DNA adducts. Calf thymus DNA (500  $\mu\text{g/ml}$ ) was reacted with 15  $\mu\text{M}$  cisplatin for 2 hours (A) and 24 hours (B) with increasing concentrations of GSH. (•) Total platinum levels determined by ICP-MS. Solid line indicates one phase exponential decay curve fitted by Prism software. Each point represents the mean of 3 different experiments and error bars reflect standard deviation. Where not shown, error bars lie within the points.

#### **4.2.3.3: Effect of GSH on the formation of specific types of Pt-DNA adducts**

Typical MonoQ elution profiles for calf thymus DNA (500 µg/ml) incubated with 15 µM cisplatin for 2hr is shown in Figure 4.14 and with 10 mM GSH and 15 µM cisplatin for 2hr and 24hr in Figure 4.15. Analyses of Pt content in collected chromatographic fractions showed that there were four major Pt-containing products detected with similar retention times seen in the previous analyses with cisplatin (section 4.2.2.1). The four peaks were therefore assigned the same chemical nature as those observed in the cisplatin analyses.

Mean retention times of the four mononucleotides (detected by UV) and four Pt-containing species are shown in Table 4.14. The percentage of Pt contained in the products detected by ICP-MS is shown in Table 4.15. No difference in retention times or relative Pt contained in the peaks was observed in the presence of absence of GSH. Levels of Pt were lower in the reactions containing GSH but were still readily detectable.

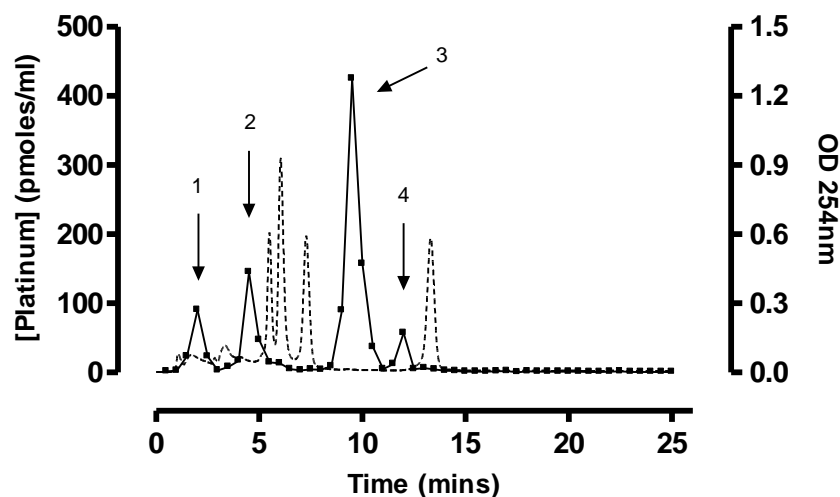


Figure 4.14: Typical MonoQ elution pattern for calf thymus DNA (500 µg/ml) incubated with 15 µM cisplatin for 2hr. Solutions (100 µl) of DNA were applied to the column and eluted at 1 ml/min. Fractions were collected with increasing NaCl concentration and Pt levels in each fraction measured by ICP-MS. (■), Pt concentration; dotted line: OD 254 nm. Peaks 1:  $Pt(NH_3)_2(R)(dGMP)$ ; 2:  $cis-Pt(NH_3)_2d(ApG)$ ; 3:  $cis-Pt(NH_3)_2d(GpG)$  and 4:  $cis-Pt(NH_3)_2(dGMP)_2$

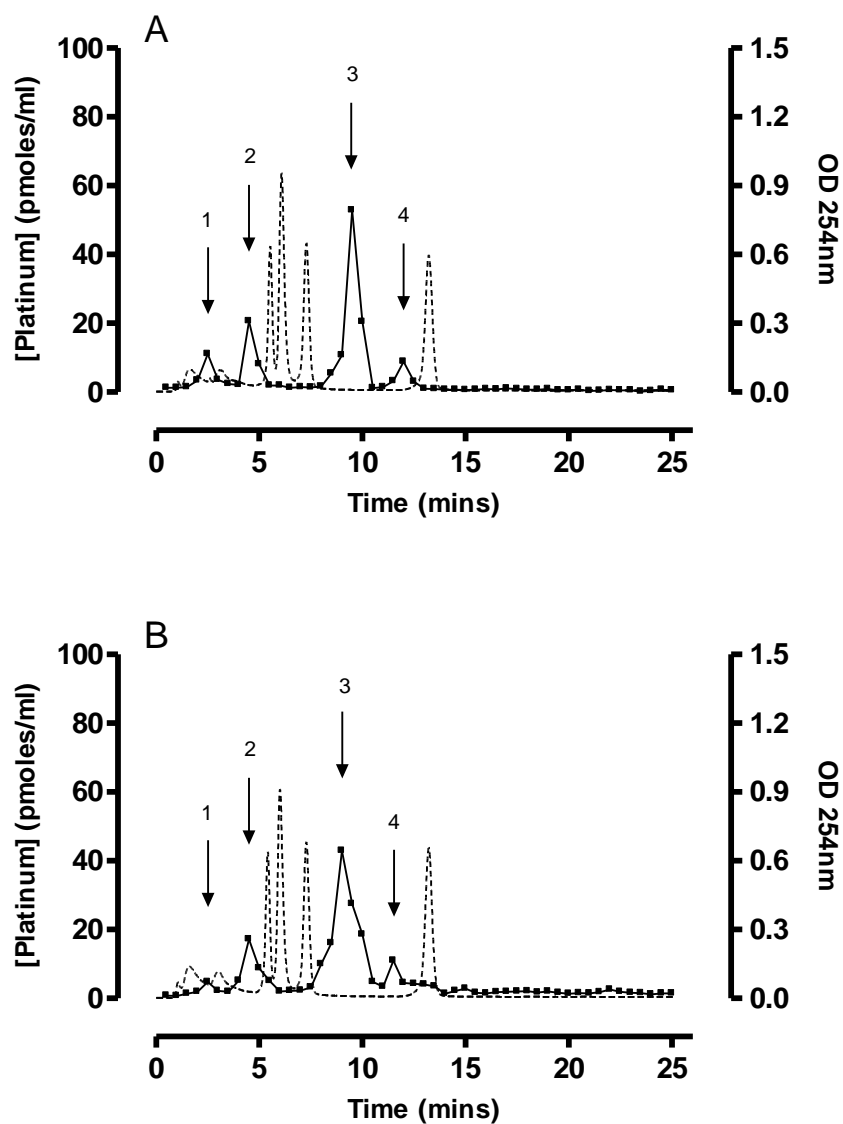


Figure 4.15: Typical MonoQ elution pattern for calf thymus DNA (500  $\mu\text{g/ml}$ ) incubated with 15  $\mu\text{M}$  cisplatin and 10 mM GSH for 2hr (A) and 24hr (B). Solutions (100  $\mu\text{l}$ ) of DNA were applied to the column and eluted at 1 ml/min. Fractions were collected with increasing NaCl concentration and Pt levels in each fraction measured by ICP-MS. (■), Pt concentration; dotted line: OD 254 nm. Peaks 1:  $\text{Pt}(\text{NH}_3)_2(\text{R})(\text{DGMP})$ ; 2:  $\text{cis-Pt}(\text{NH}_3)_2\text{d}(\text{ApG})$ ; 3:  $\text{cis-Pt}(\text{NH}_3)_2\text{d}(\text{GpG})$  and 4:  $\text{cis-Pt}(\text{NH}_3)_2(\text{dGMP})_2$

Table 4.14: Mean retention times for the products detected by UV absorbance and ICP-MS in purified DNA exposed to 15  $\mu$ M cisplatin in the presence and absence of 10 mM GSH. Mean values from individual analyses of three separate DNA preparation are shown. Ranges in retention time are shown in brackets except for total Pt recovered in which SD is shown.

Peak	Identity	Cisplatin Alone	10 mM GSH 2hr	10 mM GSH 24hr
	dCMP	5.4 (0.1)	5.4 (0.1)	5.3 (0.2)
	dAMP	5.9 (0.1)	6.0 (0.1)	6.0 (0.1)
	TMP	7.2 (0.1)	7.2 (0.1)	7.2 (0.1)
	dGMP	13.1 (0.2)	13.0 (0.1)	13.1 (0.2)
1	Pt(NH <sub>3</sub> ) <sub>2</sub> (R)(dGMP)	2.0 (0.5)	2.0 (0.5)	2.5 (0.5)
2	cis-Pt(NH <sub>3</sub> ) <sub>2</sub> d(ApG)	4.5 (0.5)	4.5 (0.5)	4.5 (0.5)
3	cis-Pt(NH <sub>3</sub> ) <sub>2</sub> d(GpG)	9.5 (0.5)	9.5 (1.0)	9.0 (1.0)
4	cis-Pt(NH <sub>3</sub> ) <sub>2</sub> (dGMP) <sub>2</sub>	12.0 (1.0)	12.0 (0.5)	11.5 (0.5)
<b>Total Pt Recovery (%)</b>		<b>97.3 (2.1)</b>	<b>103.4 (4.2)</b>	<b>106.5 (7.2)</b>

*Table 4.15: Percentage of the Pt in peaks formed in calf thymus DNA (500 µg/ml) incubated with 15 µM cisplatin +/- 10 mM GSH for 2hr and 24hr. The percentage of total Pt is expressed as a percentage of Pt contained in the four identified peaks in relation to the total Pt in the four peaks combined. Each value represents the mean of three individual analyses. Standard deviation is shown in brackets.*

<b>Peak</b>	<b>CT-DNA</b>	<b>10 mM GSH 2hr</b>	<b>10 mM GSH 24hr</b>
1	12.6 (0.4)	11.8 (0.2)	6.3 (0.1)
2	20.2 (0.6)	22.1 (0.4)	22.7 (0.4)
3	59.3 (1.7)	56.6 (0.9)	56.6 (1.1)
4	7.9 (0.2)	9.4 (0.2)	14.5 (0.3)

It seemed possible that the formation of the *cis*-Pt(NH<sub>3</sub>)<sub>2</sub>(DNA)(GSH) cross-links was not detected because of factors such as steric hindrance resulting in a very low probability that GSH would react with Pt monofunctionally bound to DNA before the latter had undergone second arm reaction with DNA. When cisplatin was initially reacted with dGMP, and then further incubated with GSH (see chapter 3), there was evidence of GSH cross-linking to Pt-dGMP. Therefore an attempt was made to detect the proposed adduct in samples in which DNA was allowed to react with cisplatin before addition of GSH. This approach was not physiologically relevant, but previous published data had shown the initial reaction of cisplatin with DNA to form monofunctional Pt-DNA products was rapid (Eastman 1987). The strategy for these experiments therefore was to initially incubate with cisplatin for 1hr, and then add GSH to the incubation mixture and incubate further.

Pure calf thymus DNA (500 µg/ml) was incubated with 15 µM cisplatin for 1hr, followed by addition of 10 mM GSH and further incubation for 2hr or 24hr at 37°C under anoxic conditions (see section 2.7.1) and then stored at -80°C. DNA was then separated from low molecular weight products such as unreacted drug and products of the reaction of cisplatin with GSH by gel filtration on a G-75 Sephadex column as described in section 2.8. Collected fractions were analysed for DNA concentration by measuring O.D. at 254nm. All fractions containing DNA were pooled together and concentrated by ultrafiltration. Pt-DNA adduct levels were determined by ICP-MS.

A Typical MonoQ elution profile for calf thymus DNA (500 µg/ml) incubated with 15 µM cisplatin for 1hr is shown in Figure 4.16. Mean retention times of the four mononucleotides (detected by UV) and four Pt-containing species are shown in Table

4.16. The percentage of Pt contained in the products detected by ICP-MS is shown in Table 4.17.

The data confirms the expected pattern of Pt containing products similar to the data for purified DNA incubated with cisplatin for 2hr. The main difference was the increase in peak 1 (attributed to *cis*-Pt(NH<sub>3</sub>)<sub>2</sub>(R)(dGMP)) which was expected be higher in this incubation due to the rapid formation of monofunctional products and slower closure to bifunctional. Levels of the monofunctional product would most likely have been higher at the time of GSH addition to the data presented here because second-arm reactions would have continued during the gel filtration procedure (200 minutes). Similar to previous analyses however, no evidence was found of the putative *cis*-Pt(NH<sub>3</sub>)<sub>2</sub>(DNA)(GSH) cross-link after further incubation in the presence of 10 mM GSH (Figure 4.17)

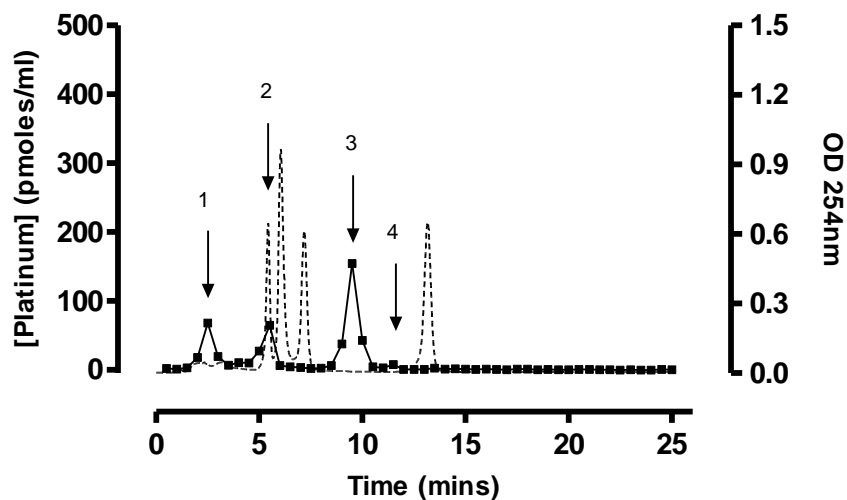


Figure 4.16: Typical MonoQ elution pattern for calf thymus DNA (500 µg/ml) incubated with 15 µM cisplatin for 1hr. Solutions (100 µl) of DNA were applied to the column and eluted at 1 ml/min. Fractions were collected with increasing NaCl concentration and Pt levels in each fraction measured by ICP-MS. (■), Pt concentration; dotted line: OD 254 nm. Peaks 1:  $\text{Pt}(\text{NH}_3)_2(\text{R})(\text{dGMP})$ ; 2:  $\text{cis-Pt}(\text{NH}_3)_2\text{d}(\text{ApG})$ ; 3:  $\text{cis-Pt}(\text{NH}_3)_2\text{d}(\text{GpG})$  and 4:  $\text{cis-Pt}(\text{NH}_3)_2(\text{dGMP})_2$

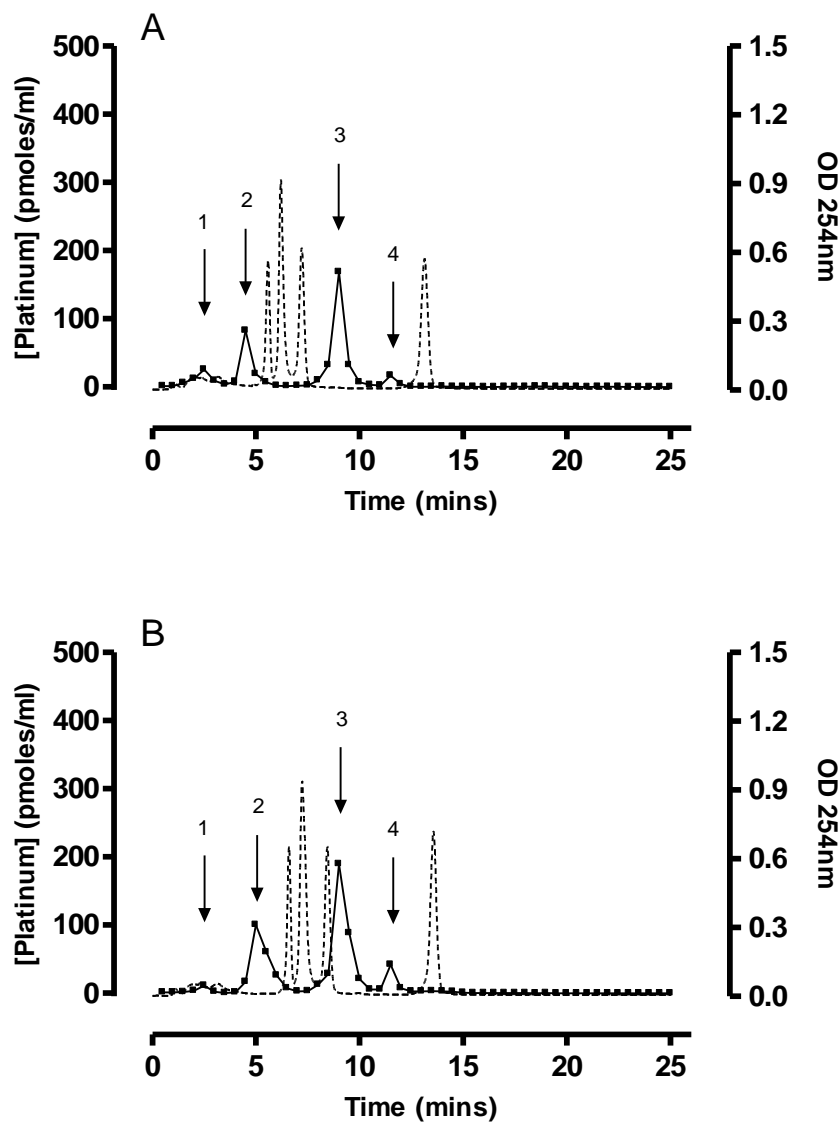


Figure 4.17: Typical MonoQ elution pattern for calf thymus DNA (500  $\mu\text{g/ml}$ ) incubated with 15  $\mu\text{M}$  cisplatin for 1hr, followed by further incubation with 10 mM GSH for 2hr (A) and 24hr (B). Solutions (100  $\mu\text{l}$ ) of DNA were applied to the column and eluted at 1 ml/min. Fractions were collected with increasing NaCl concentration and Pt levels in each fraction measured by ICP-MS. (■), Pt concentration; dotted line: OD 254 nm. Peaks 1:  $\text{Pt}(\text{NH}_3)_2(\text{R})(\text{dGMP})$ ; 2:  $\text{cis-Pt}(\text{NH}_3)_2\text{d}(\text{ApG})$ ; 3:  $\text{cis-Pt}(\text{NH}_3)_2\text{d}(\text{GpG})$  and 4:  $\text{cis-Pt}(\text{NH}_3)_2(\text{dGMP})_2$

Table 4.16: Mean retention times for the products detected by UV absorbance and ICP-MS in purified DNA exposed to 15  $\mu$ M cisplatin in the delayed presence and absence of 10 mM GSH. Mean values from individual analyses of three separate DNA preparation are shown. Ranges in retention time are shown in brackets except for total Pt recovered in which SD is shown.

Peak	Identity	Cisplatin Alone	10 mM GSH 2hr	10 mM GSH 24hr
	dCMP	5.4 (0.1)	5.5 (0.1)	5.4 (0.1)
	dAMP	5.9 (0.1)	6.2 (0.1)	6.1 (0.1)
	TMP	7.1 (0.1)	7.1 (0.1)	7.1 (0.2)
	dGMP	13.1 (0.1)	13.1 (0.2)	12.9 (0.2)
1	Pt(NH <sub>3</sub> ) <sub>2</sub> (R)(dGMP)	2.5 (0.5)	2.5 (0.5)	2.5 (0.5)
2	cis-Pt(NH <sub>3</sub> ) <sub>2</sub> d(ApG)	5.5 (1.0)	4.5 (0.5)	5.0 (1.0)
3	cis-Pt(NH <sub>3</sub> ) <sub>2</sub> d(GpG)	9.5 (0.5)	9.0 (1.0)	9.0 (1.0)
4	cis-Pt(NH <sub>3</sub> ) <sub>2</sub> (dGMP) <sub>2</sub>	11.5 (0.5)	11.5 (1.0)	11.5 (1.0)
<b>Total Pt Recovery (%)</b>		<b>92.4 (2.3)</b>	<b>94.3 (1.7)</b>	<b>91.3 (3.4)</b>

*Table 4.17: Percentage of the Pt in peaks formed in calf thymus DNA (500 µg/ml) incubated with 15 µM cisplatin for 1hr, followed by further incubation with 10 mM GSH for 2hr and 24hr. The percentage of total Pt is expressed as a percentage of Pt contained in the four identified peaks in relation to the total Pt in the four peaks combined. Each value represents the mean of three individual analyses. Standard deviation is shown in brackets.*

<b>Peak</b>	<b>CT-DNA</b>	<b>10 mM GSH 2hr</b>	<b>10 mM GSH 24hr</b>
1	23.0 (0.4)	8.7 (0.3)	3.2 (0.1)
2	21.9 (0.2)	28.1 (0.9)	29.2 (1.4)
3	52.6 (0.9)	57.5 (1.9)	55.4 (2.6)
4	2.5 (0.1)	5.6 (0.2)	12.2 (0.6)

### 4.3: Discussion

#### Analysis of Pt-DNA adducts formed in cells by cisplatin

Previous analyses of Pt-DNA adducts had described the nature of four major Pt-containing products formed in purified DNA. However, these studies had been limited to using purified DNA due to the need to work with large quantities of cisplatin-DNA adducts because of the limitations of using AAS to detect Pt. Advances in studying Pt-DNA adducts were made with the development of highly sensitive immunoassays and  $^{32}\text{P}$  post-labelling assays which allowed the study of adducts at clinically relevant drug concentrations and analyses of Pt-DNA adducts formed in cells. These methods however were inherently limited to the study of specific Pt-DNA adducts, specifically the 1,2-intrastrand *cis*-Pt(NH<sub>3</sub>)<sub>2</sub>d(ApG) and *cis*-Pt(NH<sub>3</sub>)<sub>2</sub>d(GpG) adducts.

Azim-Araghi (2003) applied ICP-MS to the previously described method of separating enzymatically digested DNA by anion exchange chromatography (Fichtinger-Schepman et al 1985), and provided evidence for the formation of novel Pt-DNA adducts in cells incubated with cisplatin. Further analysis with purified calf thymus DNA provided evidence that such adducts potentially contained GSH.

Evidence that GSH is able to cross-link to monofunctionally bound Pt-DNA adducts was published over twenty years ago (Micetich et al 1983, Eastman 1987). More recently a number of strands of unpublished evidence had accumulated in studies at Newcastle which supported the possibility that such adducts can form. Furthermore, it seemed possible that they could have interesting biologically relevant properties.

In the present work, similar methodology to that used by Azim-Araghi was applied to study, in greater depth, the adducts formed by cisplatin using four human tumour cell lines (833K, A2780, LoVo and Mor/CPR) following incubations with cisplatin. The results confirmed the presence of the four major previously identified Pt-DNA adducts. The percentage contribution of the two major Pt-DNA products is similar to previous studies (Fichtinger-Schepman et al 1985, Eastman 1986). These products were also identified in purified calf thymus DNA incubated with cisplatin at a similar ratio.

The additional Pt-containing peak identified in the analyses of Azim-Araghi however was not observed in any of the four cell lines investigated in this study. Azim-Araghi used H69/p and Mor/p cell lines. Although the H69/p cell line was not used in this study, both investigations used the Mor cell line. Azim-Araghi used the parental Mor/p cell line, whereas this study used the cisplatin-resistant Mor/CPR sub-line because the original cells had become contaminated and could not be procured from elsewhere. The Mor/CPR cell line had been derived from the Mor/P line by selection for drug resistance (Twentyman et al 1991). It is possible that the resistance mechanisms resulted in altered types of DNA adducts being formed in the Mor/CPR line compared to the cells used by Azim-Araghi, but it seems unlikely that a major class of adducts would be completely lost, especially since the extra peak could not be detected in analyses of DNA from three other cell lines.

The evidence for the putative *cis*-Pt(NH<sub>3</sub>)<sub>2</sub>(DNA)(GSH) cross-link observed by Azim-Araghi in cellular DNA was previously supported by data from incubations of cisplatin with calf thymus DNA in the presence of GSH. In these analyses, a product with the same chromatographic properties was observed to the product identified in cellular

DNA. No evidence for such products in purified DNA was observed in this study using the same incubation conditions or when GSH addition was delayed to allow initial binding of cisplatin to DNA. Possible reasons for the discrepancy between the previous results and the present data will be discussed in chapter 7.

### **Analysis of Pt-DNA adducts formed in cells by carboplatin and oxaliplatin**

Although the main aim was to confirm the presence of additional adducts formed by cisplatin in cells, the study has also investigated adducts formed by carboplatin and oxaliplatin using the same methods, which, as described above, permit, for the first time, the analysis of essentially all of the Pt-containing adducts present in DNA from drug-treated cells. This type of analysis has never been reported before for carboplatin or oxaliplatin.

ICP-MS analysis of Pt content in collected fractions of DNA hydrolysates from drug treated cells separated using the standard MonoQ system showed the presence of four Pt-containing products for both carboplatin and oxaliplatin. In both cases, these products had similar retention times and relative Pt levels of adducts to those seen in the incubation with cisplatin and therefore are suggested to be of a similar nature (except for the non-leaving groups of  $\text{NH}_3$  for carboplatin and the DACH ligand for oxaliplatin). The relative proportions of the four products were very similar to those values for cisplatin and, like cisplatin, did not vary markedly between cell lines.

No additional Pt-containing products were detected following either 2hr or 24hr incubations with carboplatin or oxaliplatin. This indicates a lack of any evidence for formation of additional adducts species such as *cis*-Pt(NH<sub>3</sub>)<sub>2</sub>(DNA)(GSH) cross-links.

However, the formation of such adducts cannot be excluded. It is possible that they are being formed, but at levels which fall below the limit of detection of MonoQ/ICP-MS detection method. The lack of detection in this work does fit with the general belief that the effect of GSH is to inactivate intracellular cisplatin.

### **Relationship between adduct levels and sensitivity to growth inhibition**

Factors that affect the sensitivity of cells to Pt drugs can be grouped into three classes: 1, factors that affect access of drug to DNA, such as differences in uptake or intracellular thiols; 2, the properties of the adducts formed; and 3, factors that affect how the cell responds to the damage, such as repair or replication by-pass mechanisms. The latter factors are very dependent upon the nature of adducts formed.

All of these factors contribute towards the  $GI_{50}$  values. However, if the level of adducts required to achieve a 50% growth inhibition ( $AL_{50}$ ) is determined, this data is independent of the first set of factors and so reflects the nature of adducts and how cells respond to them. Since the relationship between adduct levels and drug concentrations were linear, these values were straightforward to calculate by combining  $GI_{50}$  values and adduct dose responses. These values are shown in Table 4.18.

The  $GI_{50}$  values for all cell lines and drugs showed a marked decrease when the exposure time was increased from 2hr to 24hr, as would be expected. The ratio of  $GI_{50}$  for 2hr exposure was 5-22 times larger than the equivalent 24hr values (mean ratio = 14). A similar analysis of the  $AL_{50}$  values shows that exposure time affected these to a much smaller degree, with ratios of  $AL_{50}$  (2hr) to  $AL_{50}$  (24hr) showing an average of 1.3 across all the cell lines and drugs investigated. These data are shown in Table 4.19.

These findings are consistent with the decrease in  $GI_{50}$  with increased exposure being due to increased access of drug to intracellular targets.

If two drugs form the same types of adducts then they should exhibit similar  $AL_{50}$  values in the same cell lines. It is not clear from the literature if DNA adducts formed by cisplatin and carboplatin differ and, if so, to what extent and in what manner. Chemically they are expected to form the same adducts because the non-leaving groups on Pt are the same. However, data from Fichtinger-Schepman et al (1995 a) indicated that carboplatin forms a larger proportion of the 1,2-intrastrand *cis*-Pt(NH<sub>3</sub>)<sub>2</sub>d(ApG) adducts. Analysis of the  $AL_{50}$  data in Table 4.18 shows that for the 833K cells the  $AL_{50}$  values of cisplatin and carboplatin are similar. However for the other cells the values for carboplatin are about half of the values for cisplatin, except for LoVo cells exposed for 24hr. This suggests that adducts formed by carboplatin can be slightly more toxic than those formed by cisplatin. However, the chromatographic analysis of DNA adducts formed in cells by cisplatin and carboplatin (Table 4.11) showed no detectable differences.

$AL_{50}$  values for oxaliplatin are generally similar to those of cisplatin and carboplatin after 2hr exposure and lower after 24hr, except for Mor/CPR cells where the  $AL_{50}$  values are markedly higher. These data suggest that Mor/CPR cells are able to tolerate much larger amounts of oxaliplatin-DNA adducts than the other cell lines investigated in this study. This contrasts with previous findings that showed that oxaliplatin forms fewer Pt-DNA adducts at equitoxic concentrations. However, these were in other cell lines and using less sensitive or less direct methods to measure Pt-DNA adduct levels (Saris et al 1996, Woynarowski et al 1998, Woynarowski et al 2000).

Table 4.18: Units of adduct levels ( $AL_{50}$ ) values for 833K, A2780, LoVo and Mor/CPR cells exposed to cisplatin, carboplatin or oxaliplatin. Values were calculated in Prism 4.0 and are expressed in  $\mu\text{M}$ .

<b>Drug</b>	<b>Inc. Time</b>	<b>833K</b>	<b>A2780</b>	<b>LoVo</b>	<b>Mor/CPR</b>
<b>Cisplatin</b>	<b>2hr</b>	13.7	26.5	23.0	48.1
	<b>24hr</b>	9.8	31.4	13.9	35.0
<b>Carboplatin</b>	<b>2hr</b>	10.3	11.7	9.9	22.9
	<b>24hr</b>	12.0	16.8	20.3	27.4
<b>Oxaliplatin</b>	<b>2hr</b>	11.6	9.0	17.0	187.3
	<b>24hr</b>	4.5	5.1	5.7	319.0

*Table 4.19: Ratios of 2hr and 24hr GI<sub>50</sub> and AL<sub>50</sub> values for 833K, A2780, LoVo and Mor/CPR cells exposed to cisplatin, carboplatin or oxaliplatin.*

Cell Line	Cisplatin		Carboplatin		Oxaliplatin	
	GI <sub>50</sub>	AL <sub>50</sub>	GI <sub>50</sub>	AL <sub>50</sub>	GI <sub>50</sub>	AL <sub>50</sub>
833K	6.8	1.4	18.0	0.9	22.3	2.6
A2780	5.2	0.8	14.2	0.7	21.5	1.8
LoVo	8.5	1.7	8.8	0.5	22.5	3.0
Mor/CPR	8.8	1.4	17.5	0.8	12.7	0.6

## Chapter 5

# Characterisation of cisplatin-DNA adducts formed in the presence of sodium thiosulfate

### 5.1: Introduction

Platinum-based anticancer complexes are often associated with severe toxicities that can limit their clinical usage. Endogenous sulfur-containing compounds such as glutathione and thiourea have been shown to bind to and inactivate platinum complexes (Burchenal et al 1978, Filipski et al 1979, Micetich et al 1983, Eastman 1987). As described in chapter 1, exogenous sulfur-containing compounds have been proposed as potential protective agents to limit normal tissue toxicity, and have shown promising protection against chemotherapy drugs both in experimental studies and clinical trials. These have been recently reviewed (Wang et al 2007).

Sodium thiosulfate (STS) is an exogenous compound that has been proposed as a protective agent for patients receiving cisplatin or carboplatin-based chemotherapy. As described in chapter 1, STS has been recently used in oncology to reduce nephrotoxicity associated with cisplatin treatment. The mechanism through which this occurs is unclear, but is proposed to be a result of STS reducing delivery of cisplatin, and by reducing cisplatin accumulation (Weiner and Jacobs 1983, Shea and Howell 1984, Elferink et al 1986). Based on the positive data accumulated for STS in protection against nephrotoxicity, it was proposed that STS may have a protective role

against cisplatin-induced ototoxicity. Neuwelt et al investigated the effects of STS *in vitro* and *in vivo* in protecting against carboplatin-induced ototoxicity (Neuwelt et al 1996). They showed that STS protected against carboplatin toxicity *in vitro* when incubated for up to 8 hours after carboplatin was added, but no protection was seen when STS was added 24hr post-carboplatin (Neuwelt et al 1996). Further *in vitro* studies and investigations in animals and patients have confirmed the findings that delayed administration of STS can reduce ototoxicity and also have indicated that this occurs without compromising the anti-tumour effects of either cisplatin or carboplatin (Neuwelt et al 1998, Muldoon et al 2000, Doolittle et al 2001, Harned 2008).

STS is currently in a phase III clinical trial (SIOPEL 6) to investigate its potential application as a protective against ototoxicity in paediatric patients receiving cisplatin for standard risk hepatoblastoma. This trial is built on positive data from experiments in animals that led to the hypothesis that delayed administration of STS in patients can protect against ototoxicity without reducing antitumour efficacy. This is based on the assumption that STS will inactivate any unreacted drug present in patients.

It is widely believed that, like endogenous sulfur-containing compounds found inside cells, exogenous compounds have the potential to bind and inactivate platinum complexes. STS is known to rapidly react with cisplatin, therefore it may have a greater potential than endogenous compounds such as glutathione in blocking second arm reactions. However, there is very limited data available on whether STS is able to enter cells, and whether STS has the potential to alter cisplatin-DNA adducts. There is evidence suggesting STS remains extracellular, however this conclusion was drawn from indirect evidence from studies in dogs (Gilman et al 1946), and more recently the

SLC13 family of sulfate transporters has been shown to have an involvement in thiosulfate transport into cells (Pajor 2006).

The aim of this section was to test the hypothesis that, like endogenous sulfur-containing compounds, STS has the potential to affect the formation of cisplatin-DNA adducts. This was investigated as follows:

1. The hypothesis that STS has the ability to interact with platinated DNA to form novel cross-links was tested in two ways:
  - a. Calf thymus DNA was incubated with cisplatin in the presence and absence of STS. Enzymatically digested platinum-DNA cross-links were separated by anion exchange chromatography and Pt-containing species detected by ICP-MS
  - b. STS was incubated with monofunctionally bound cisplatin-dGMP (as described in chapter 3). Products were separated by anion-exchange chromatography and Pt-containing species were detected by AAS.
  
2. The effects of concurrent/delayed administration of STS on the formation of platinum-DNA adducts in four human tumour cell lines was investigated in two ways:
  - a. The effects of concurrent/delayed administration of STS on growth inhibition of cisplatin was measured by SRB assay
  - b. The effects of concurrent/delayed administration of STS on total cisplatin-DNA adduct formation was measured by ICP-MS.

## 5.2: Results

Pure calf thymus DNA (500  $\mu\text{g/ml}$ ) was mixed with 0, 0.1, 0.3, 1, 3 and 10 mM STS before addition of 15  $\mu\text{M}$  cisplatin. The mixtures were incubated for 2hr and 24hr at 37°C under anoxic conditions, and then stored at -80°C. DNA was then separated from low molecular weight products such as unreacted drug and products of the reaction of cisplatin with STS by gel filtration on a G-75 Sephadex column as described in section 2.8 (and as used in chapter 4 to separate glutathione reaction mixtures). Collected fractions were analysed for DNA concentration by measuring OD at 254nm and Pt concentration by AAS (section 2.10). All fractions containing DNA were pooled together and concentrated by ultrafiltration as described in section 2.8. Pt-DNA adduct levels were determined by ICP-MS (section 2.11).

### **5.2.1: Gel filtration separation of platinated DNA**

Typical gel filtration chromatographic separations for reaction mixtures in the absence (A) and presence (B) of STS are shown in Figure 5.1. These results showed that DNA passed through the column rapidly typically eluting between 40 and 60 minutes post-injection (Figure 5.1, peak 1). This is consistent with its exclusion from the G-75 Sephadex beads because of its high molecular weight. Unbound platinum eluted typically between 115 and 155 minutes (Figure 5.1 – Graph A peak 2). Following 2 hour incubation, 37.2% of the total platinum eluted was associated with the DNA (Figure 5.1 – Graph A peak 1). These findings are consistent with similar separations in this thesis for glutathione reactions (see chapter 4).

The presence of 0.1 mM STS in the incubation caused a decrease from 37% to 17% of the total platinum associated with DNA (Figure 5.1 – Graph B peak 1). An additional optical density peak was observed between 110 and 140 minutes that eluted slightly earlier than unbound platinum (Figure 5.1 – Graph B peak 2), a phenomenon also seen with glutathione (see chapter 4). This product is likely to be a conjugate between cisplatin and STS. Typical Pt recovery was greater than 90% of the total Pt loaded for all separations.

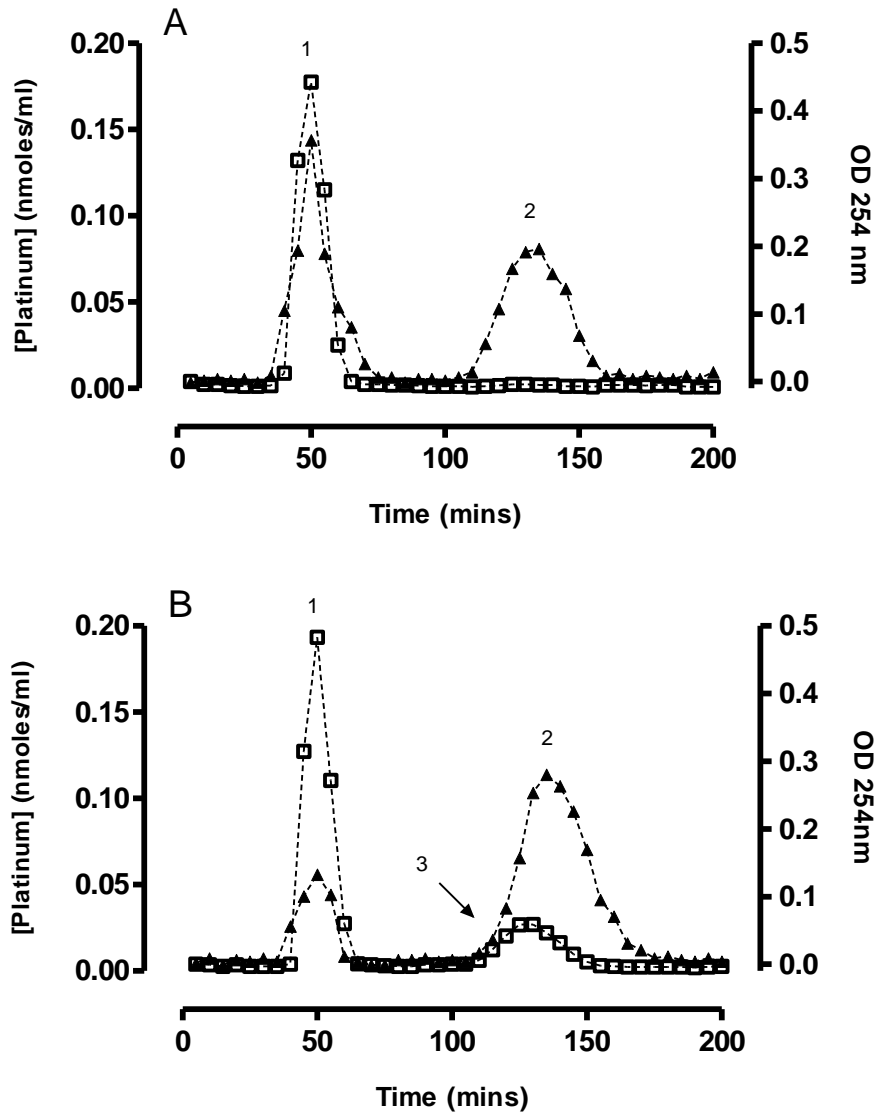


Figure 5.1: Typical Sephadex G-75 gel elution profiles of calf thymus DNA (500  $\mu\text{g/ml}$ ) incubated for 2hr at 37°C with cisplatin (15  $\mu\text{M}$ ) alone (A) and with 0.1 mM STS (B). ( $\square$ ), Optical density was measured at OD 254 nm. ( $\blacktriangle$ ), Platinum concentrations determined by AAS. Peaks are: 1, DNA; 2, low molecular weight products such as unreacted cisplatin or STS; 3, possible cisplatin-STs conjugate

### 5.2.1.1: Effect of STS on total Pt-DNA adduct level

Pt-DNA adducts levels for calf thymus DNA mixed with increasing concentrations of STS and incubated with 15  $\mu\text{M}$  cisplatin for 2hr or 24hr are shown in Table 5.1. Total adduct levels as a percentage of control for 2 hours (A) and 24 hours (B) incubation are plotted in Figure 5.2.

When no STS was added, a total adduct level of 10.5 ( $\pm$  0.7 SD)  $\mu\text{mol Pt g}^{-1}$  DNA was observed after a 2hr incubation with cisplatin. This increased to 20.8 ( $\pm$  0.4 SD)  $\mu\text{mol Pt g}^{-1}$  DNA when incubated for 24 hours. Incubation with 0.1 mM STS decreased the total adduct level to 4.1 ( $\pm$  0.2 SD) and 5.8 ( $\pm$  0.5 SD)  $\mu\text{mol Pt g}^{-1}$  DNA (39% and 28% of control) for the 2hr and 24hr incubations respectively. Incubation with 1 mM STS caused a decrease to less than 5% of the control value. Data interpolated from the graph (first order exponential decay line fitted in Prism) suggests concentrations of values of 0.07 and 0.05 mM STS are required to achieve a 50% decrease in total Pt-DNA adducts levels for 2hr and 24hr respectively.

*Table 5.1: Overall Pt-DNA adducts levels formed by the reaction of cisplatin with pure DNA in the presence of varied concentrations of STS. DNA was reacted with 15  $\mu\text{M}$  cisplatin for 2hr and 24hr. Each value represents the mean of 3 individual experiments. Standard deviation is shown in brackets.*

		Concentration of STS (mM)					
		Control (0)	0.1	0.3	1	3	10
<b>2 hours</b>	$\mu\text{mol Pt g}^{-1}$ DNA	10.5 (0.7)	4.1 (0.2)	1.6 (0.1)	0.5 (0.01)	0.2 (0.01)	0.03 (0.01)
	% Control		39.2 (1.6)	14.9 (0.5)	4.3 (0.1)	1.5 (0.1)	0.3 (0.01)
<b>24 hours</b>	$\mu\text{mol Pt g}^{-1}$ DNA	20.8 (0.4)	5.8 (0.5)	2.6 (0.1)	0.8 (0.1)	0.2 (0.01)	0.06 (0.01)
	% Control		28.0 (2.4)	12.4 (0.5)	3.6 (0.3)	0.8 (0.02)	0.3 (0.03)

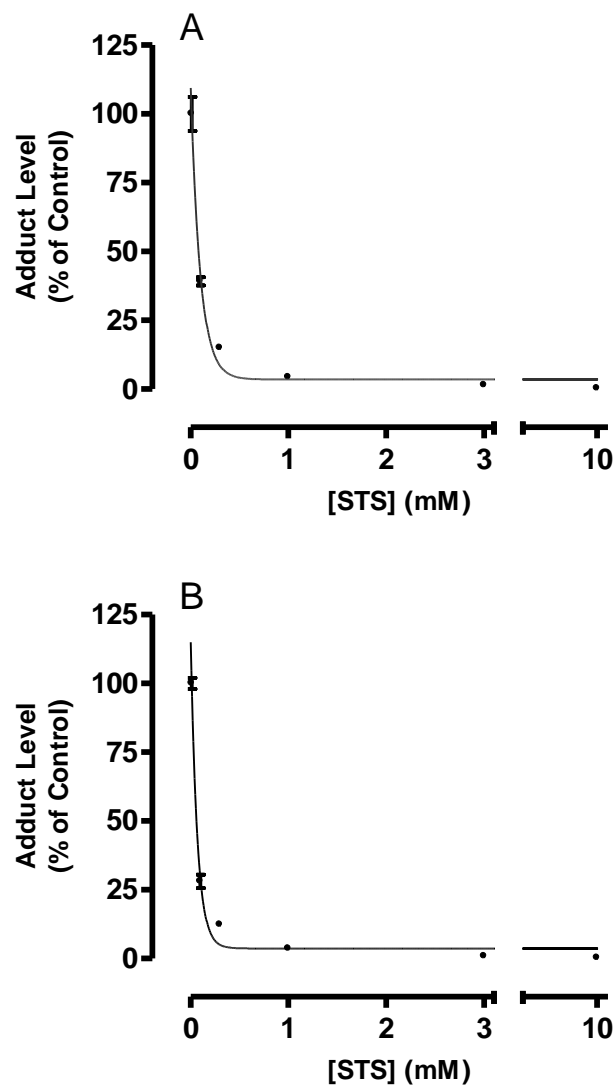


Figure 5.2: Effect of increasing STS concentration on the level of total adducts formed on DNA by cisplatin. 500  $\mu\text{g/ml}$  calf thymus DNA was reacted with 15  $\mu\text{M}$  cisplatin for 2 hours (A) and 24 hours (B) with increasing concentrations of STS. (•) Total platinum levels determined by ICP-MS. Solid line indicates one phase exponential decay curve fitted by Prism software. Each point represents the mean of 3 different experiments and error bars reflect standard deviation. Where not shown, error bars lie within the points.

### 5.2.1.2: Reaction of cisplatin with STS

Cisplatin was initially reacted alone with STS to determine the chromatographic properties of cisplatin-TS. This was important to ensure any novel chromatographic products formed in reactions involving dGMP, cisplatin and STS were not cisplatin-TS conjugates. Cisplatin was dissolved in water to a concentration of 2 mM. STS was dissolved in water to a concentration of 4 mM, and pH adjusted to 7.0. Cisplatin and GSH were incubated for 24hr in a 1:2 molar ratio (1:2 mM). Products of the reaction were analysed using the standard MonoQ system (section 2.9). The concentration of Pt in each fraction was determined by AAS. A typical MonoQ elution profile is shown in Figure 5.3.

Cisplatin had previously been shown to elute very rapidly from the MonoQ column (see chapter 3). However, it was unclear where cisplatin-TS conjugates would elute. Three peaks were detected by UV absorbance eluting at approximately 21 minutes, and 28-29 minutes (Figure 5.3). The latter peaks were the only detected species associated with Pt, and these were therefore attributed to be Pt-TS conjugates. The earlier peak eluting at approximately 21 minutes was unreacted STS in the mixture and not an impurity. This had previously been determined by injecting STS alone into the chromatographic system. UV absorbance for STS (injected alone) was higher at 230 nm than at 254 nm, and this fits in with data published showing TS has a UV absorbance, maximum at 212 nm (Krull and LaCourse 1987).

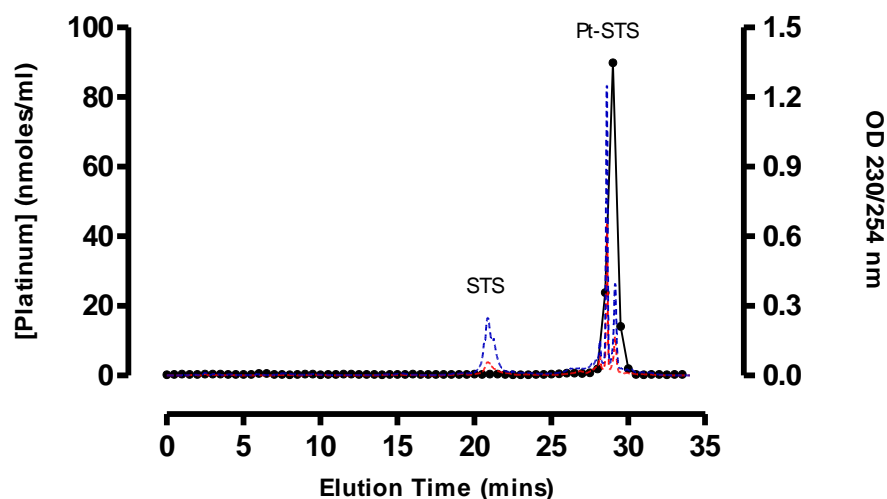


Figure 5.3: Typical MonoQ elution profile for 1 mM cisplatin incubated with 2 mM STS for 24hr: 100  $\mu$ l was applied to the MonoQ column and eluted with increasing NaCl concentrations. Pt concentration in collected fractions was determined by AAS. (●) Pt concentration; dotted red line: OD 254 nm; dotted blue line: OD 230 nm. Overall Pt recovery was always with 10% of total Pt loaded.

### 5.2.2: Effect of STS on the formation of Pt-DNA adducts in pure DNA

Calf thymus DNA was incubated with 15  $\mu\text{M}$  cisplatin in the presence and absence of 2 mM STS as described earlier, and separated from low molecular weight material by gel filtration and concentrated by ultrafiltration. This DNA was enzymatically digested and the products by MonoQ anion exchange chromatography. Platinum eluted in collected fractions was measured by ICP-MS.

Chromatographic separation and analysis of platinum in collected fractions of calf thymus DNA incubated with 15  $\mu\text{M}$  cisplatin for 2 hours (Figure 5.4) confirmed the formation of the four known major adducts as described in chapters 3 and 4. In order of elution these were:  $\text{Pt}(\text{NH}_3)_2(\text{R})(\text{dGMP})$ , *cis*- $\text{Pt}(\text{NH}_3)_2\text{d}(\text{ApG})$ , *cis*- $\text{Pt}(\text{NH}_3)_2\text{d}(\text{GpG})$  and *cis*- $\text{Pt}(\text{NH}_3)_2(\text{dGMP})_2$ .

Analysis of Pt-DNA adducts present on the first preparation of DNA that had been reacted with cisplatin in the presence of STS revealed a clear additional Pt-containing peak which eluted at approximately 16 minutes (Figure 5.5, graph A). This was confirmed by further hydrolysis and chromatographic analysis of the same DNA preparation and was thought to potentially represent a cross-link between DNA and thiosulfate (TS). However, when further preparations of DNA were made (3 individual preparations) in subsequent reactions of DNA with cisplatin and STS under exactly the same conditions, these failed to confirm the presence of the additional peak (Figure 5.5, graph B).

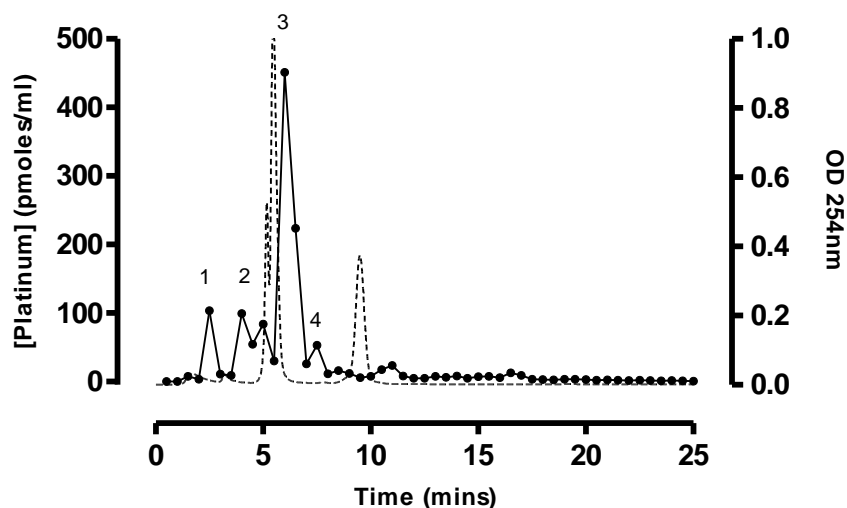


Figure 5.4: Typical MonoQ elution profile for enzymatically digested calf thymus DNA (500  $\mu\text{g/ml}$ ) digested after reaction with 15  $\mu\text{M}$  cisplatin. Solutions (100  $\mu\text{l}$ ) of DNA were injected onto the MonoQ column and eluted at 1 ml/min with increasing NaCl concentrations. Platinum levels in collected fractions was determined by ICP-MS. (●) Platinum concentration; dotted line: OD 254 nm. Peaks are 1: *cis*-Pt(NH<sub>3</sub>)<sub>2</sub>(R)(dGMP); 2: *cis*-Pt(NH<sub>3</sub>)<sub>2</sub>d(ApG); 3: *cis*-Pt(NH<sub>3</sub>)<sub>2</sub>d(GpG) and 4: *cis*-Pt(NH<sub>3</sub>)<sub>2</sub>(dGMP)<sub>2</sub>. Overall Pt recovery was greater than 90% of total Pt loaded.

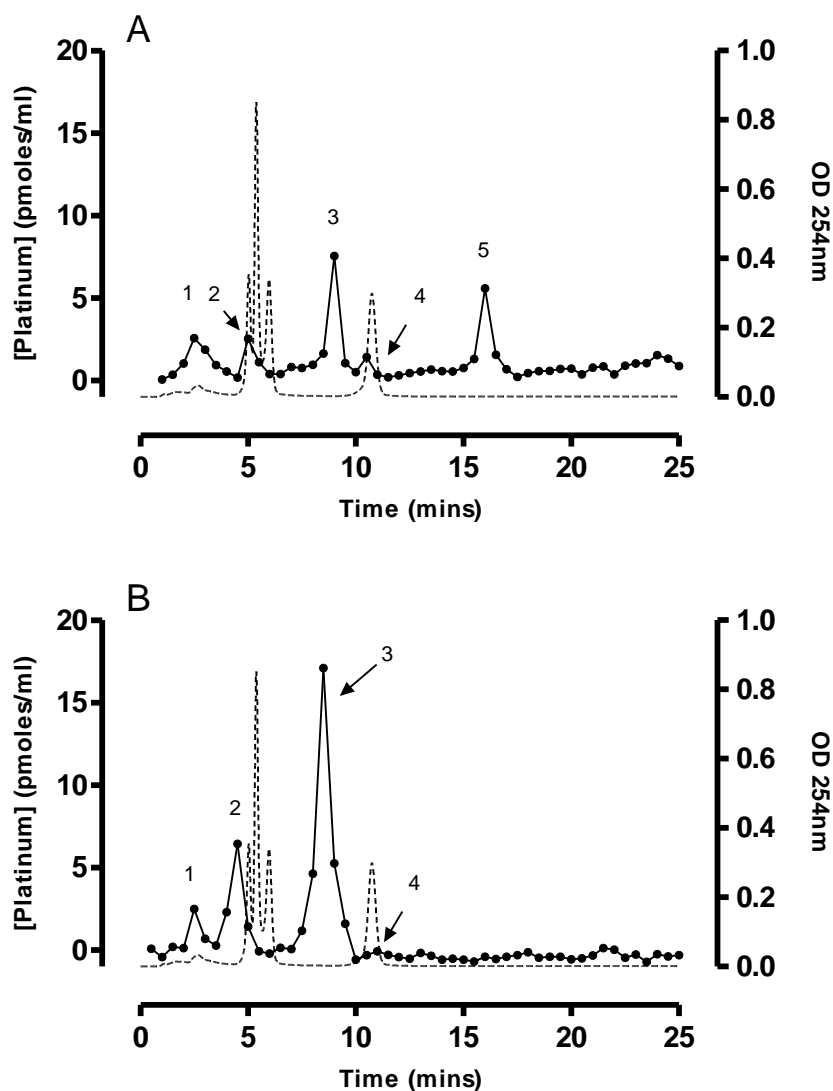


Figure 5.5: Typical MonoQ elution profiles for enzymatically digested calf thymus DNA (500  $\mu\text{g/ml}$ ) digested after reaction with 15  $\mu\text{M}$  cisplatin and 2 mM STS for 2hr. Figures A and B are individual analyses of separate DNA preparations. Solutions (100  $\mu\text{l}$ ) of DNA were injected onto the MonoQ column and eluted at 1 ml/min with increasing NaCl concentrations. Platinum levels in collected fractions was determined by ICP-MS. (●) Platinum concentration; dotted line: OD 254 nm. Peaks are 1: cis-Pt(NH<sub>3</sub>)<sub>2</sub>(R)(dGMP); 2: cis-Pt(NH<sub>3</sub>)<sub>2</sub>d(ApG); 3: cis-Pt(NH<sub>3</sub>)<sub>2</sub>d(GpG) and 4: cis-Pt(NH<sub>3</sub>)<sub>2</sub>(dGMP)<sub>2</sub>. The putative identity of 5 is cis-Pt(NH<sub>3</sub>)<sub>2</sub>(dGMP)(TS). Overall Pt recovery was greater than 90% of total Pt loaded.

### 5.2.3: Effect of STS on the reaction of cisplatin with dGMP

The initial experiment with calf thymus DNA showed evidence of a potential *cis*-Pt(NH<sub>3</sub>)<sub>2</sub>(DNA)(STS) cross-link. As the evidence for such a product was very limited, experiments similar to those described in chapter 3 with dGMP were carried out to determine if it was plausible that STS-nucleotide cross-links could form and, if so, to determine their chromatographic behaviour.

Incubation of equimolar (1 mM) cisplatin with dGMP led to the formation of three monofunctional products and one bifunctional platinum product. The identification of these products is described in detail in section 3.3. Figure 5.6 (graph A) shows a typical MonoQ elution profile for the products formed by reaction of cisplatin with dGMP for 24hr in the present series of experiments. The identities of the peaks are *cis*: unreacted cisplatin; 1: *cis*-Pt(NH<sub>3</sub>)<sub>2</sub>(OH<sub>2</sub>)(dGMP); 2: *cis*-Pt(NH<sub>3</sub>)<sub>2</sub>(OH)(dGMP); 3: *cis*-Pt(NH<sub>3</sub>)<sub>2</sub>(Cl)(dGMP) and 4: *cis*-Pt(NH<sub>3</sub>)<sub>2</sub>(dGMP)<sub>2</sub>. Interestingly, peak 5 appeared to elute quicker in the reaction with STS, although this is probably reflective of subtle variations in chromatographic buffer conditions as discussed in chapter 3.

After the initial incubations of cisplatin with dGMP for 24hr to generate the products shown in Figure 5.6 (graph A), STS (1 mM) was added to the reaction mixture and further incubated at 37°C for 24hr. The products present at that time were analysed by chromatography using the MonoQ column Figure 5.6 (graph B). Trace levels of the *cis*-Pt(NH<sub>3</sub>)<sub>2</sub>(OH<sub>2</sub>)(dGMP) species of cisplatin (peak 1) were still detectable, as was the bifunctional *cis*-Pt(NH<sub>3</sub>)<sub>2</sub>(dGMP)<sub>2</sub> species (peak 4). There was no evidence of any unreacted cisplatin. An additional platinum-containing species was detected that eluted

at approximately 16 minutes (Figure 5.6 – Graph B). This product was observed in 3 MonoQ analyses each of an individual reaction. It is proposed that this product is a *cis*-Pt(NH<sub>3</sub>)<sub>2</sub>(dGMP)(STS) cross-link.

Interestingly, the levels of the bifunctional *cis*-Pt(NH<sub>3</sub>)<sub>2</sub>(dGMP)<sub>2</sub> peak were lower (10 nmoles/ml (Figure 5.6 – Graph A peak 4) to 4 nmoles/ml (Figure 5.6 – Graph B peak 4)). This is further complicated by the appearance of detectable levels of dGMP (Figure 5.6 – Graph B, peak dGMP). The reason for this phenomenon is unknown, but it suggests a possibility that STS may have the capacity to displace dGMP bound to platinum. The work in this thesis does not address that possibility.

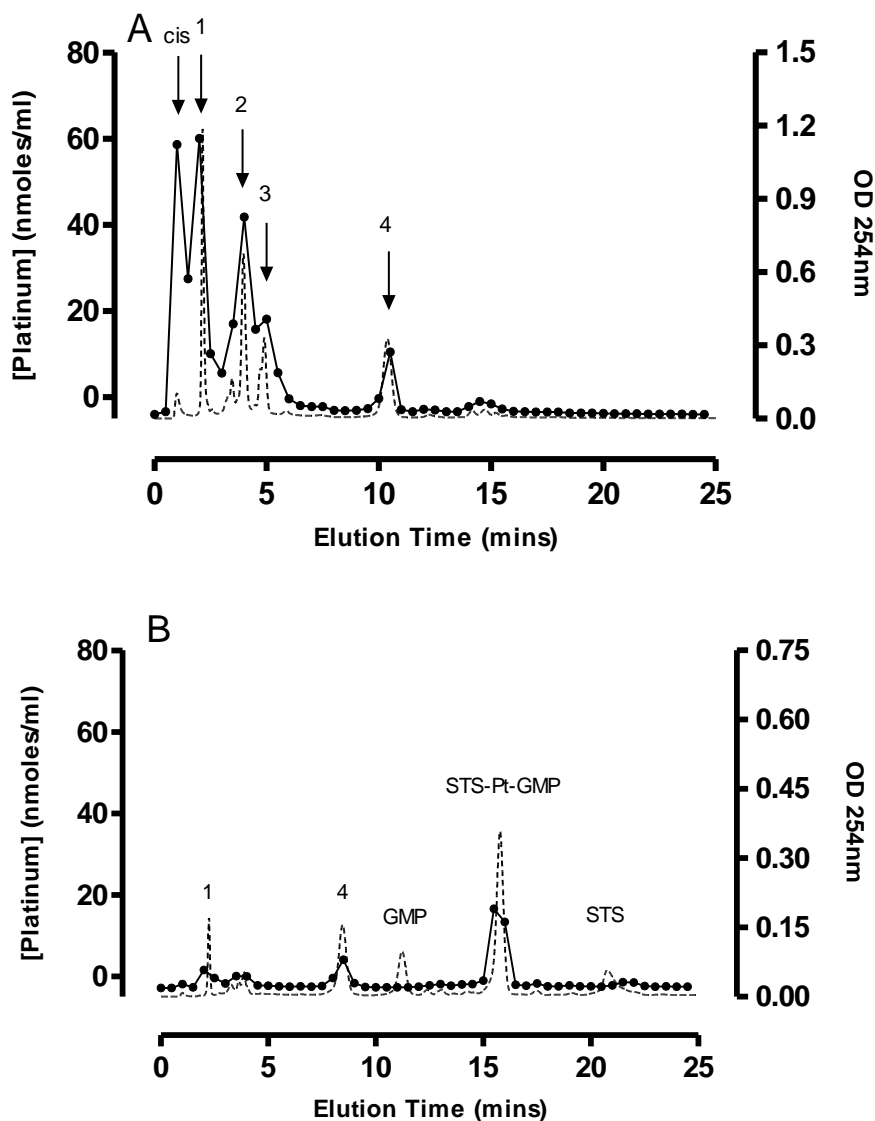
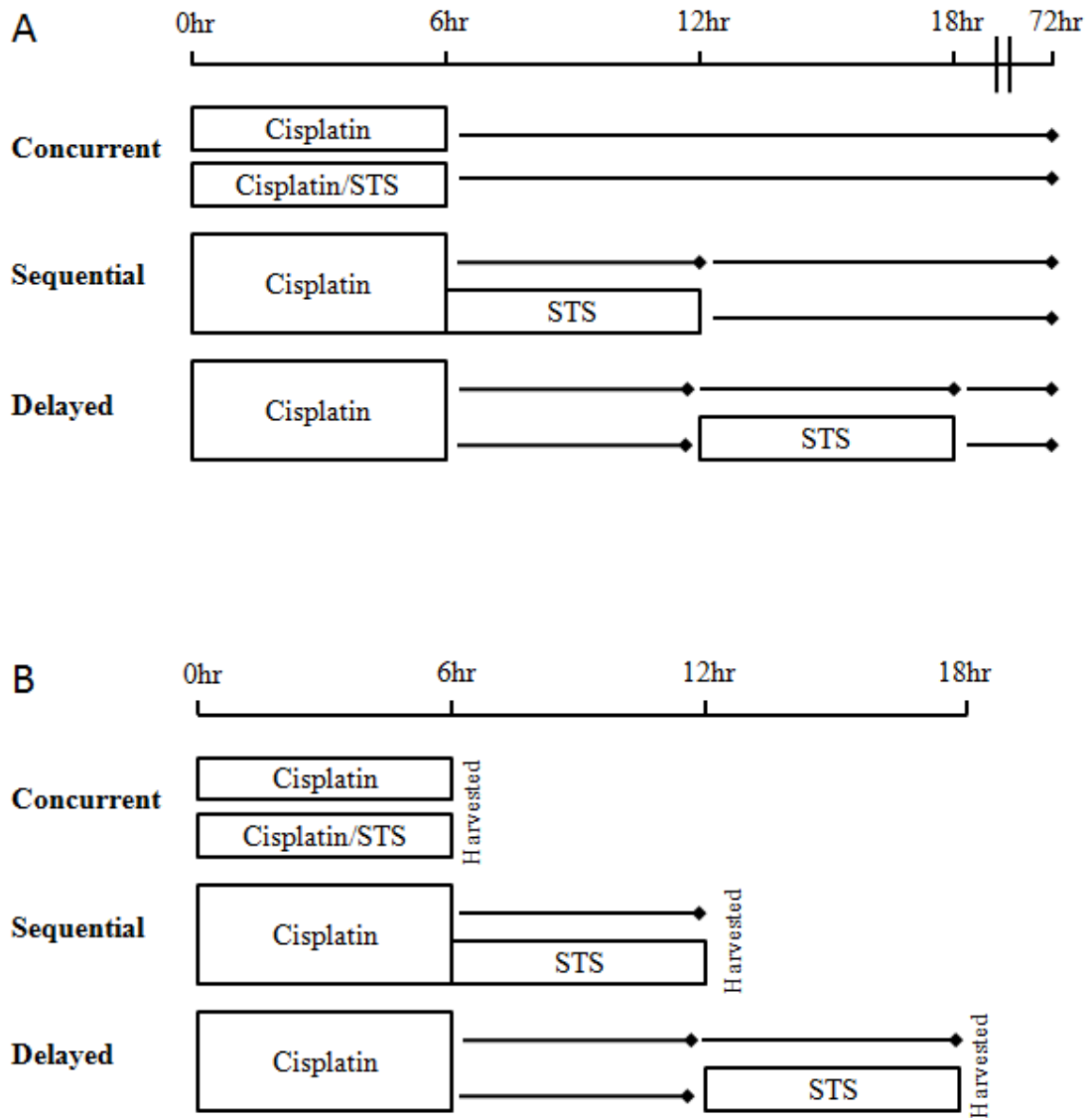


Figure 5.6: MonoQ elution profile for 1mM cisplatin and dGMP 24hr (A) and with STS (1 mM) for a further 24hr (B): Solutions (100  $\mu$ l) were applied to the MonoQ column and eluted with increasing NaCl concentrations. Platinum concentration in collected fractions was determined by AAS. (●) Platinum concentration; dotted line: OD 254 nm. Peaks are 1: unreacted cisplatin; 2:  $cis\text{-Pt}(\text{NH}_3)_2(\text{OH}_2)(\text{dGMP})$ ; 3:  $cis\text{-Pt}(\text{NH}_3)_2(\text{OH})(\text{dGMP})$ ; 4:  $cis\text{-Pt}(\text{NH}_3)_2(\text{Cl})(\text{dGMP})$  and 5:  $cis\text{-Pt}[(\text{NH}_3)_2(\text{dGMP})_2]$ . Overall Pt recovery was greater than 90% of total Pt loaded.

#### **5.2.4: Effect of STS on the antiproliferative activity of cisplatin in human tumour cell lines**

As discussed in section 5.1, an aim of the work described in this chapter was to investigate the effects of STS on cisplatin-induced DNA adduct formation in cells. Initially the effects of STS on cisplatin sensitivity of the cells to be used for adduct studies was confirmed.

Three incubation schedules were chosen for measuring the effects of STS on human tumour cells exposed to cisplatin. The individual schedules are described in Figure 5.7. In the SIOPEL 6 clinical trial, cisplatin is infused i.v. over a 6hr period with accompanying hydration, followed by a further 6hr hydration period. At this 12hr point, STS infusion begins over a 6hr period, although the actual infusion is 125 mg/ml STS i.v. for 15 minutes. In patients with normal renal function, STS has a half-life in serum of 15 minutes (Schulz 1984, Araya et al 2006). The delayed schedule used in this study most clearly mimics this setup. A lower concentration of STS (12.6 mM) was chosen for these incubations to that used in the clinical trial. This equates to 2 mg/ml STS, which is the concentration of STS used in earlier experiments (Neuwelt et al 1996). The concurrent schedule is expected to demonstrate the greatest effect but this could result from extracellular as well as intracellular interactions of STS and cisplatin. The sequential schedule should eliminate the effects resulting from extracellular reactions of STS with cisplatin and any effects should result from inactivation of intracellular cisplatin or its reactive derivatives.



*Figure 5.7: Incubation schedule for exposure of human tumour cell lines to cisplatin in the presence and absence of STS. Incubation schedule for growth inhibition experiments is shown in panel A and for determination of total Pt-DNA adducts in panel B.*

### **5.2.5: Effect of STS on growth inhibition by cisplatin**

Human tumour cells 833K, A2780, LoVo and Mor/CPR were seeded into 96 well plates at 8000 cells/well and incubated with various concentrations of cisplatin. STS concentration was constant at 12.6 mM. Cisplatin and STS were added at various times as described in Figure 5.7 (panel A). Growth inhibition experiments were terminated at 72hr post-cisplatin addition. This is the same endpoint used in growth inhibition experiments with cisplatin alone in chapter 4. Growth inhibition was assessed using the SRB assay as described in section 2.4. The effects of concurrent, sequential and delayed administration of STS are shown in Figure 5.8 - Figure 5.10. GI<sub>50</sub> values for the four cell lines are given in Table 5.2.

Co-incubation of cisplatin and STS led to 35, 21, 22 and >17-fold increases in GI<sub>50</sub> values for 833K, A2780, LoVo and Mor/CPR cells respectively. Sequential and delayed exposure to STS had no significant effect on growth inhibition in any of the four cell lines tested.

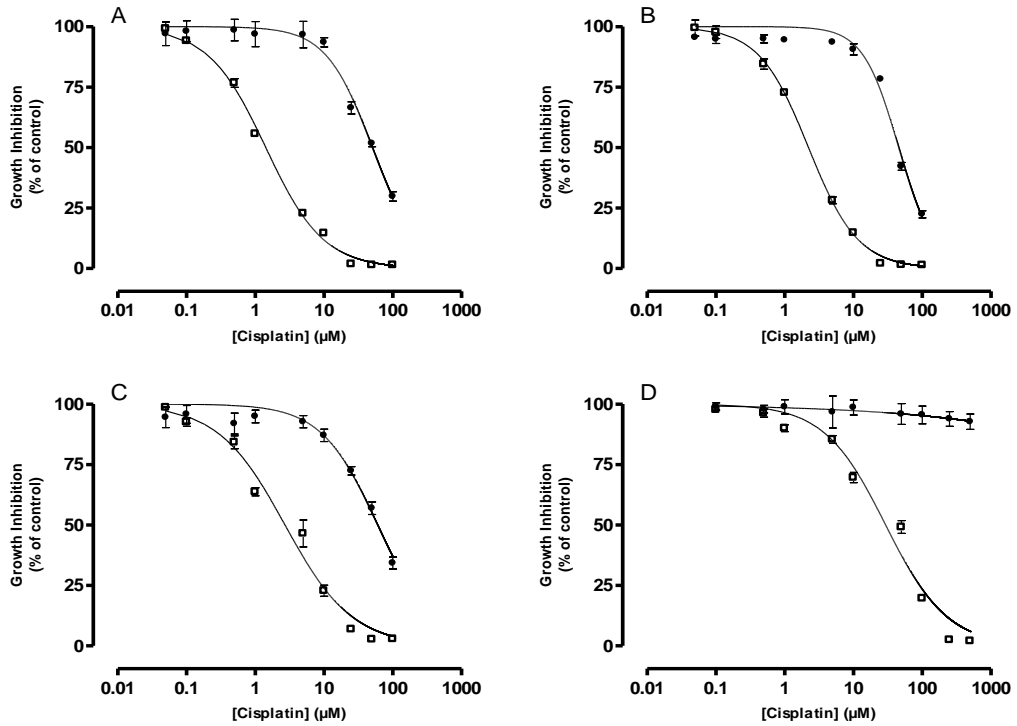


Figure 5.8: The effect of concurrent administration of STS on growth inhibition by cisplatin in 833K (A), A2780 (B), LoVo (C) and Mor/CPR (D) cells. Cells were incubated with cisplatin alone (□) or cisplatin and 12.6 mM STS (●). Each point represents the mean of 3 different experiments and error bars reflect standard deviation. Where not shown, error bars lie within the points.

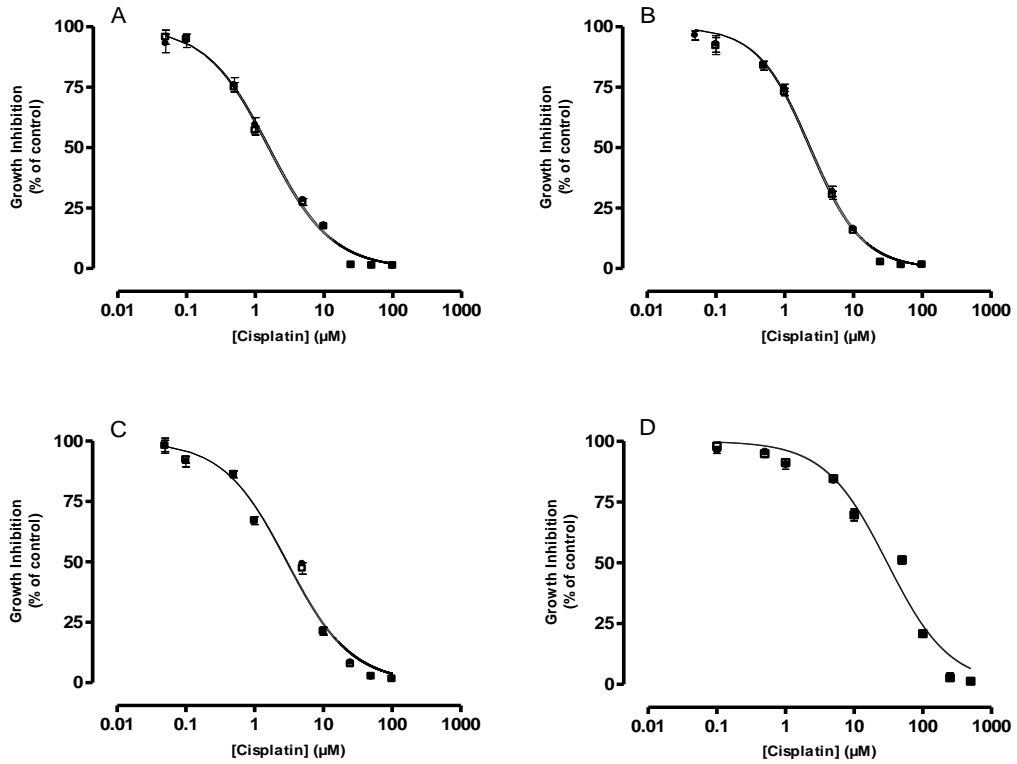


Figure 5.9: The effect of sequential administration of STS on growth inhibition by cisplatin in 833K (A), A2780 (B), LoVo (C) and Mor/CPR (D) cells. Cells were incubated with cisplatin alone ( $\square$ ) or cisplatin and 12.6 mM STS ( $\bullet$ ). Each point represents the mean of 3 different experiments and error bars reflect standard deviation. Where not shown, error bars lie within the points.

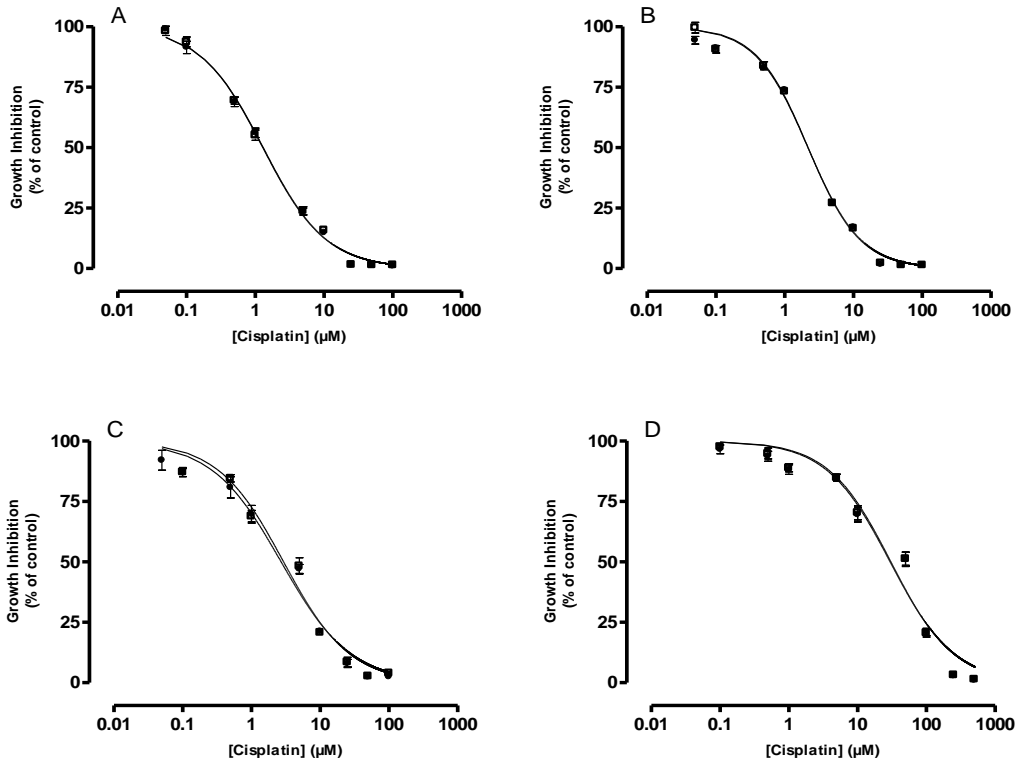


Figure 5.10: The effect of delayed administration of STS on growth inhibition by cisplatin in 833K (A), A2780 (B), LoVo (C) and Mor/CPR (D) cells. Cells were incubated with cisplatin alone ( $\square$ ) or cisplatin and 12.6 mM STS ( $\bullet$ ). Each point represents the mean of 3 different experiments and error bars reflect standard deviation. Where not shown, error bars lie within the points.

Table 5.2:  $GI_{50}$  values for 833K, A2780, LoVo and Mor/CPR cells incubated with cisplatin +/- STS and respective ratio's. Ratios are calculated as :  $GI_{50}$  cisplatin + STS/  $GI_{50}$  cisplatin.

Cell Line	Incubation	Concurrent	Sequential	Delayed
<b>833K</b>	Cisplatin	1.4 $\mu$ M	1.5 $\mu$ M	1.3 $\mu$ M
	Cisplatin + STS	50.3 $\mu$ M	1.6 $\mu$ M	1.3 $\mu$ M
	<b>Ratio</b>	<b>35</b>	<b>1</b>	<b>1</b>
<b>A2780</b>	Cisplatin	2.2 $\mu$ M	2.3 $\mu$ M	2.2 $\mu$ M
	Cisplatin + STS	45.5 $\mu$ M	2.4 $\mu$ M	2.2 $\mu$ M
	<b>Ratio</b>	<b>21</b>	<b>1</b>	<b>1</b>
<b>LoVo</b>	Cisplatin	2.7 $\mu$ M	2.9 $\mu$ M	2.9 $\mu$ M
	Cisplatin + STS	59.9 $\mu$ M	3.0 $\mu$ M	2.7 $\mu$ M
	<b>Ratio</b>	<b>22</b>	<b>1</b>	<b>1</b>
<b>Mor/CPR</b>	Cisplatin	29.4 $\mu$ M	30.5 $\mu$ M	30.5 $\mu$ M
	Cisplatin + STS	> 500 $\mu$ M	30.3 $\mu$ M	29.7 $\mu$ M
	<b>Ratio</b>	<b>&gt; 17</b>	<b>1</b>	<b>1</b>

### 5.2.6: Effect of STS on total Pt-DNA adduct formation

Human tumour cells 833K, A2780 and LoVo cells were incubated with 3  $\mu$ M cisplatin in the presence and absence of 12.6 mM STS. Mor/CPR cells were incubated with 30  $\mu$ M cisplatin +/- STS. The choice of concentrations was based on  $GI_{50}$  concentrations determined in chapter 4. Incubation times are shown in Figure 5.7 (panel B). Immediately after the endpoint, cells were harvested and tubes containing pellets were frozen at  $-80^{\circ}\text{C}$ . DNA was extracted using the hydroxyapatite method as described in section 2.5. DNA extracted from cells was hydrolysed overnight at  $70^{\circ}\text{C}$  in 3.5% nitric acid. Total Pt-DNA adducts levels were determined by ICP-MS as described in 2.11.

For the incubation schedules described earlier (Figure 5.7) the three treatment schedules resulted in sets of samples where cells were all exposed to cisplatin for 6hr but were harvested at three different time points. The data (Figure 5.11) shows a general decline in total adduct level with time, although there appears to be a transient rise in adduct levels at the 12hr time point for 833K cells. This will be discussed further at the end of this chapter.

Concurrent incubation of human tumour cells with cisplatin and STS led to 2.4, 3.6, 3.1 and 10.1 fold reductions in adduct level for 833K, A2780, LoVo and Mor/CPR cells respectively (Figure 5.12, Table 5.3). These values were significant ( $p = < 0.0001, 0.02, 0.0002$  and  $0.0034$  for 833K, A2780, LoVo and Mor/CPR cells respectively). No significant decreases in Pt-DNA adducts levels were observed in any of the four cell lines when STS was added in the sequential or delayed regimes (Figure 5.12, Table 5.3).

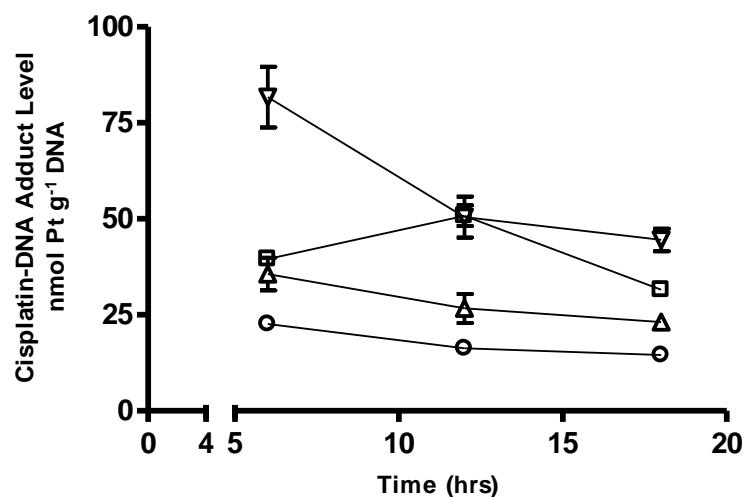


Figure 5.11: Changes in total Pt-DNA adducts formed in 833K (□), A2780 (△), LoVo (○) and Mor/CPR (▽) cells following incubation with cisplatin at 3, 3, 3 and 30  $\mu\text{M}$  respectively. Cells were incubated with cisplatin and harvested at varying timepoints. Total Pt-DNA adducts levels were determined by ICP-MS. Each point represents the mean of 3 different experiments and error bars reflect standard deviation. Where not shown, error bars lie within the points.

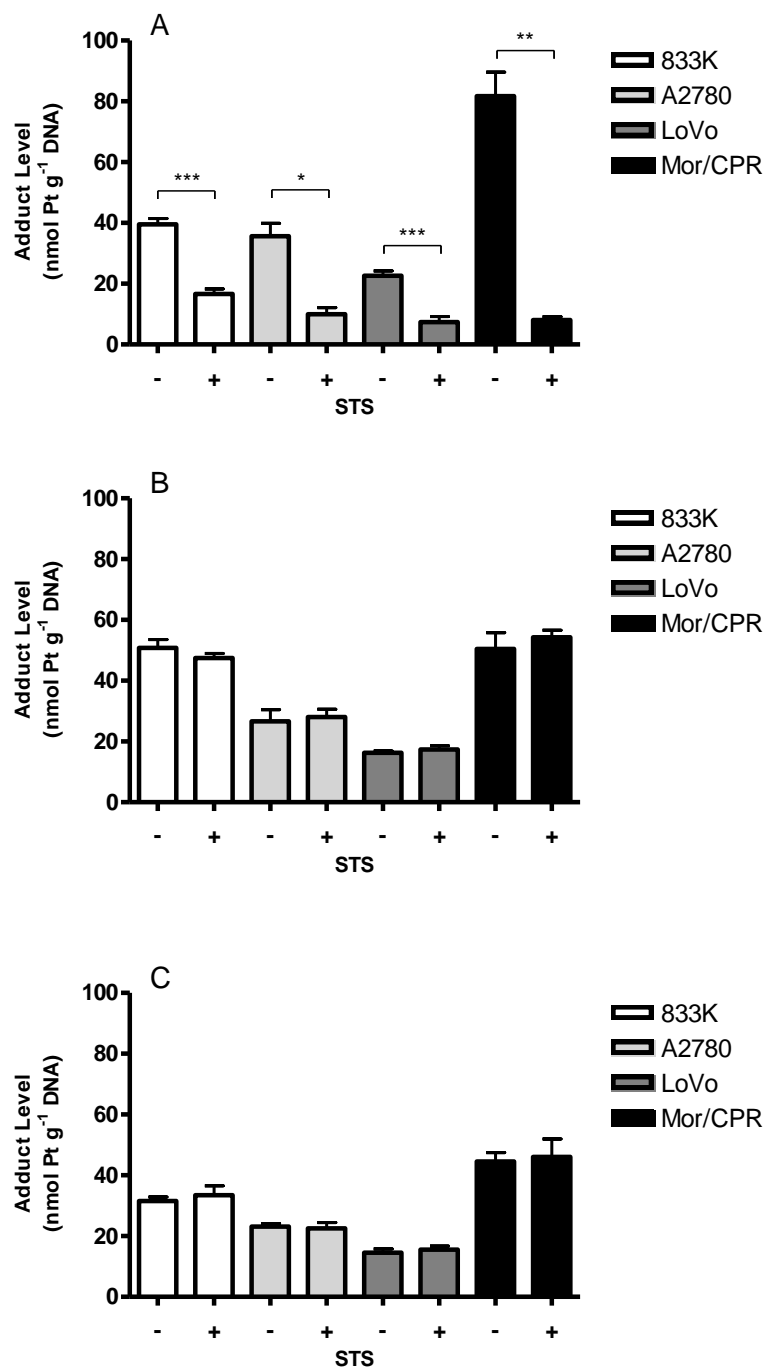


Figure 5.12: Analysis of total cisplatin-DNA adduct level in 833K, A2780, LoVo and Mor/CPR cells following concurrent (A), sequential (B) and delayed (C) incubation with cisplatin +/- STS. Each bar represents the mean of 3 different experiments and error bars reflect standard deviation. Where not shown, error bars lie within the points. \*,  $p = <0.05$ , \*\*,  $p = < 0.01$ , \*\*\*,  $p = < 0.001$

Table 5.3: Effect of STS of cisplatin-DNA adducts formation in four cell lines exposed to cisplatin using three different schedules. 833K, A2780, LoVo and Mor/CPR cells were incubated (6hr) with (3, 3, 3 and 30  $\mu\text{M}$  cisplatin respectively. STS (12.6 mM, 6hr) was present concurrently, immediately after of or after a 6hr delay relative to the exposure of cisplatin. Each value represents the mean of 3 individual experiments. Standard deviation is shown in brackets.

		Concurrent		Sequential		Delayed	
		Cisplatin	Cisplatin + STS	Cisplatin	Cisplatin + STS	Cisplatin	Cisplatin + STS
<b>833K</b>	nmol Pt g <sup>-1</sup> DNA	39.6 (1.9)	16.6 (1.7)	50.8 (2.7)	47.5 (1.5)	31.5 (1.4)	33.5 (3.1)
	% Cisplatin Alone		<b>41.9 (4.2)</b>		<b>93.3 (3.8)</b>		<b>106.1 (7.9)</b>
<b>A2780</b>	nmol Pt g <sup>-1</sup> DNA	35.6 (4.3)	10.0 (2.2)	26.7 (3.8)	28.0 (2.6)	23.1 (1.0)	22.5 (2.0)
	% Cisplatin Alone		<b>28.0 (6.1)</b>		<b>105.2 (7.2)</b>		<b>97.4 (5.6)</b>
<b>LoVo</b>	nmol Pt g <sup>-1</sup> DNA	22.6 (1.6)	7.4 (1.8)	16.3 (0.6)	17.3 (1.3)	14.6 (1.2)	15.6 (1.2)
	% Cisplatin Alone		<b>32.5 (8.2)</b>		<b>106.4 (6.0)</b>		<b>106.9 (5.2)</b>
<b>Mor/CPR</b>	nmol Pt g <sup>-1</sup> DNA	81.7 (7.9)	8.0 (1.0)	50.4 (5.4)	54.4 (2.3)	44.5 (2.9)	46.0 (5.9)
	% Cisplatin Alone		<b>9.8 (1.2)</b>		<b>107.8 (2.8)</b>		<b>103.5 (7.3)</b>

### 5.3: Discussion

STS is currently in a phase III clinical trial (SIOPEL 6) to investigate its ability to reduce ototoxicity in patients receiving cisplatin for standard risk hepatoblastoma. It is hypothesised that STS binds to unreacted platinum compounds in extracellular compartments, inactivating the drug before it interacts with DNA. Although there is recent evidence suggesting that thiosulfate ions are transported into cells by the SLC13 family of sulfate transporters (Pajor 2006), it is generally assumed that STS does not enter cells and this view is based on pharmacokinetic data from dogs (Gilman et al 1946). In the clinical trial, STS is administered 6 hours after cessation of cisplatin infusion. This was based on data showing that delayed administration of STS can significantly reduce toxicity without affecting platinum drug antitumour efficacy (Howell and Taetle 1980, Neuwelt et al 1996, Muldoon et al 2000).

There is however no conclusive data to eliminate the possibility of STS entering cells. Also, it is not clear whether or not, if STS did accumulate intracellularly, it might affect the quantity or quality of the DNA adducts that were formed by cisplatin. Other sulfur-containing compounds such as glutathione and thiourea have previously been shown to bind DNA via Pt (Burchenal et al 1978, Filipski et al 1979, Micetich et al 1983, Eastman 1987). It was therefore hypothesised that STS could potentially alter the types of Pt-DNA adducts formed in cells if it were able to enter cells.

The data presented in this chapter showed that STS is able to inhibit the binding of cisplatin to purified DNA (Table 5.1). The extent of this inhibition is concentration dependent. For 2hr incubations it was estimated that 0.07 mM STS would cause a 50%

decrease in DNA adduct formation. In contrast, data in chapter 4 shows that 3.9 mM GSH was needed to cause a similar effect under exactly the same conditions of DNA and cisplatin concentration. For 24hr incubations, the equivalent concentrations were estimated to be 0.05 mM STS and 2.7 mM GSH. Thus, to achieve similar effects of adduct formation STS needed to be present at concentrations of approximately 55-fold lower than GSH. This implies that if a small quantity of STS entered cells it could, in principle, exert a strong effect on the intracellular pharmacology of cisplatin.

Chromatographic separation and analysis of individual platinum adducts on calf thymus DNA by ICP-MS failed to give consistent evidence for the formation of cross-links involving STS. Although there was evidence for a novel platinum-containing product in some analyses (Figure 5.5), the majority of experiments failed to show the presence of detectable quantities of this product. A platinum-containing product with the same chromatographic properties as the novel Pt-containing product detected in hydrolysates of one of the DNA preparations was observed when dGMP was incubated with cisplatin, followed by incubation with STS (Figure 5.6). It is therefore concluded that although such novel products could not be reproducibly induced, the possibility that STS is able to form novel products with DNA can be excluded.

Growth inhibition experiments confirmed that in four cell lines, concurrent incubation with cisplatin and STS is detrimental to the anti-tumour efficacy of cisplatin, with 35-, 21- and 22-fold increases in  $GI_{50}$  concentrations observed for 833K, A2780 and LoVo cells. This data is consistent with previous experiments which showed that STS has an antagonistic effect on platinum drugs when exposed simultaneously or within a short period of time after (Howell and Taetle 1980, Neuwelt et al 1996, Muldoon et al 2000).

Neither sequential nor delayed administration of STS had any effect in this study on the antiproliferative effects of cisplatin as reported previously (Neuwelt et al 1996, Muldoon et al 2000).

The incubation schedules described above for the study of total Pt-DNA adducts resulted in a consistent 6hr exposure to cisplatin, but varying time points at which cells were harvested. The data for all cell lines showed a decrease in overall adduct level with increase in time after the end of cisplatin incubation (Figure 5.11). This could reflect the effects of DNA repair processes. It is however possible that this could be a result of dilution of DNA adducts levels due to increases in the amount of total DNA in the culture as a result of continued DNA replication. Although DNA damage can halt DNA replication (e.g. via p53 mediated G1 arrest) or stalling at replication sites, this does not always occur. The p53 pathway is likely to be inactivated in cancer cell lines and DNA replication can by-pass Pt-DNA adducts.

A general decline is seen in total adduct level over although there appears to be a transient rise in adduct levels at the 12hr time point for the 833K cells. This phenomenon is seen in both the cells incubated with cisplatin alone and the cells incubated with cisplatin followed by STS. Adduct levels decrease at the 18hr timepoint. It is possible therefore that in the 833K cells Pt-DNA adduct levels continue to increase during the time between the 6hr and 12hr timepoints. As the 833K cells are the most sensitive to cisplatin of the four cell lines studied it is possible that they were more strongly inhibited during the first few hours after drug exposure hence the lower values in the 6hr incubation.

The data presented in this chapter support the hypothesis that STS is unable to enter cells, and is effective in the extracellular compartment. The data also support the previous findings that delaying administration of STS has no effect on the antitumour effects of STS. Neither sequential nor delayed administration of STS had any significant effect on GI<sub>50</sub> values in any of the four human cell lines analysed (Table 5.2). However, concurrent incubation of human tumour cells with cisplatin and STS caused significant increases in GI<sub>50</sub> values (Table 5.2). A similar trend was seen when total Pt-DNA adducts levels were measured, with significant decreases in total Pt-DNA adducts levels observed when human tumour cells were incubated with cisplatin and STS concurrently, and no significant effect observed when administration of STS was delayed (Table 5.3).

What is not apparent however is the discrepancy between the fold changes observed for GI<sub>50</sub> values and those found for total Pt-DNA adducts? Adduct levels are normally linearly related to drug dose, and higher levels of adducts observed at higher drug doses. In this study, 2.4-, 3.6-, 3.1- and 10.1-fold decreases in total Pt-DNA adducts levels were observed for 833K, A2780, LoVo and Mor/CPR cells respectively when cisplatin and STS were incubated with cells concurrently. However, GI<sub>50</sub> values increased by 35-, 21- and 22-fold for 833K, A2780 and LoVo cells respectively. One potential explanation for this phenomenon is that Pt-DNA adducts formed in cells in the presence of STS are of a different nature to those formed when exposed to cisplatin alone. This is discussed further in chapter 7.

## Chapter 6

# Investigation of adducts formed in biopsies from ovarian cancer patients following treatment with carboplatin

### 6.1: Introduction

Understanding of Pt drug pharmacology *in vitro* has provided substantial information on the formation of Pt-DNA adducts. Suitable techniques have been developed and optimised that have shed light on the nature of adducts formed, although their individual contribution to the cytotoxic mechanism of Pt-containing anticancer drugs remains unclear. However, there has been very little investigation into the formation of Pt-DNA adducts in patients receiving Pt-based chemotherapy clinically. Such studies are limited by the difficulties in obtaining tumour samples, especially from patients immediately after chemotherapy, which is critical to allow accurate reporting of drug levels in tumours at times that are clinically relevant to drug administration. The inability to repeatedly remove such biopsies is an additional constraint resulting in studies limited to small sample sizes and numbers. Investigating intra-tumoural Pt levels is also limited by the inherently low levels of Pt-DNA adducts. For this reason analysis of clinical samples has required the development of highly sensitive assays for studying Pt-DNA adducts.

Early investigations indicated associations between adducts formed in PBLs and clinical response and toxicity (Reed et al 1988, Reed et al 1990) and showed

correlations between adducts formed in PBLs in patients receiving cisplatin chemotherapy and PBLs incubated with cisplatin *in vitro* (Fichtinger-Schepman et al 1995, Oshita et al 1995). However, contradictory evidence has been published (Bonetti et al 1996). Unfortunately these earlier studies did not investigate the pharmacokinetics of Pt drugs. When pharmacokinetics was studied along with Pt-DNA adduct formation in PBLs poor correlation was found between *in vivo* adduct levels and unbound or total cisplatin plasma concentrations, leading to the conclusion that variations in Pt-DNA adduct formation is not predominantly determined by free drug concentration in the circulation (Peng et al 1997, Veal et al 2001, Veal et al 2007).

It is important to note however that the studies mentioned above investigated Pt-DNA adduct formation in normal blood cells. Studies on tumour tissue are much less common. Drug exposure in tissues is intrinsically more complex than in the blood stream and factors such as differences in vasculature access, blood flow, capillary permeability, interstitial pressure and lymphatic drainage may vary in tumours (Jain 1996). Drug access is also limited by the surrounding tissues (Hobbs et al 1998).

One of the first reported *in vivo* studies on solid tumour Pt levels was published by Fichtinger-Schepman et al (Fichtinger-Schepman et al 1989). This study involved administration of cisplatin to female LOU/M rats bearing either a cisplatin-resistant or sensitive IgM immunocytoma, with animals sacrificed at 1hr or 24hr after administration. Total levels of Pt were determined for the kidneys, liver, spleen, tumour and blood by ELISA and/or AAS. After a 1hr exposure, total tissue levels of Pt were in the order of kidney > liver > tumour > spleen. After 24hr, Pt levels were in the order of kidney > liver > spleen > tumour. The greatest decrease in Pt levels was observed in the

resistant tumours. Cisplatin-DNA adduct levels determined by competitive ELISA showed the same ranking as Pt levels. Except for the kidneys, all samples showed a decrease in Pt-DNA adduct level between 1hr and 24hr. It was concluded from the data that the difference in susceptibility to cisplatin between sensitive and resistant tumours was not a result of decreased Pt content or lower levels of Pt-DNA adduct formation. In another study, Zamboni et al implanted human non-small cell lung cancer H23 cells into SCID mice and investigated Pt disposition in cells (Zamboni et al 2004). Total Pt in plasma ultrafiltrate and tissue homogenates (tumour, liver, kidney and spleen) was determined by AAS. Tumour extracellular fluid (ECF) was collected by microdialysis for determination of unbound Pt concentration. After microdialysis, tumour samples were collected (at the site of probe insertion). Total Pt in tumour samples was determined by AAS and levels of 1,2-intrastrand *cis*-Pt(NH<sub>3</sub>)<sub>2</sub>d(GpG) and *cis*-Pt(NH<sub>3</sub>)<sub>2</sub>d(ApG) adducts determined using a <sup>32</sup>P post-labelling assay. Zamboni et al found that the AUC of free cisplatin in the plasma increased with dose, but this was not consistent with the AUC<sub>ECF</sub>. They also showed a considerable variability in total unbound Pt in both ECF and tumour homogenates, and no relationship between AUC<sub>ECF</sub> and total Pt or Pt-DNA adduct formation.

More recently, studies have been published investigating formation of Pt-DNA adducts in biopsies of head and neck squamous cell carcinoma (HNSCC) removed from patients (Hoebbers et al 2006, Hoebbers et al 2008). These studies investigated Pt-DNA adduct formation following two types of infusion – selective intra-arterial (IA) high dose cisplatin with systemic STS rescue and intravenous (IV) standard dose cisplatin. The hypothesis behind this approach was that adduct formation in the primary tumour would be significantly greater with the higher dose IA administration. However, no

significant difference was observed in primary tumours. Also, Pt-DNA adducts levels were found to be higher in white blood cells (WBC) following standard dose IV administration. No correlation was observed between Pt-DNA adducts levels in WBC and in tumour tissue. These findings further confirm data obtained from previous studies (Peng et al 1997, Veal et al 2001, Veal et al 2007), indicating that variation in Pt-DNA adducts formation cannot be attributed simply to drug dose or AUC of drug in the plasma, and suggest that WBC adducts levels may not be predictive markers for patient response to Pt drug chemotherapy.

The aim of the work presented in this chapter was to determine Pt-DNA adduct levels in human ovarian tumour biopsies and compare these levels with Pt-DNA adduct levels in peripheral blood cells, and to compare adduct levels with plasma pharmacokinetics following carboplatin treatment. The techniques used here have not been previously applied to measuring Pt-DNA adducts levels in solid human tumour tissue and no data at all for adduct levels in clinical solid ovarian tumour has previously been reported.

## **6.2: Study Methods**

### **6.2.1: Ovarian Cancer Overview and Patient Details**

Ovarian cancer is a term used to describe over 30 different types of malignancies, each with its own unique characteristics and responses. Ovarian tumours are divided into three major categories based on the cell types they originated within: epithelial tumours, germ-cell tumours and sex-cord stromal tumours. Epithelial tumours arise in the cells that cover the ovaries. All four patients in this study presented with epithelial tumours.

Epithelial ovarian tumours are further classified by the cells from which they originate. The most common are serous tumours, accounting for 40% of the total epithelial tumours. Serous tumours typically occur in patients between the ages of 40 and 60. Endometrioid tumours account for 20% of total epithelial tumours and typically occur in patients between the ages of 50-70. Clear cell (6%) and mucinous (1%) tumours occur to a lesser extent and typically occur between the ages of 30-50 and 40-80 respectively. The remaining 30% of epithelial tumours is comprised of Brenner tumours, undifferentiated tumours (cannot be classified by microscopy) and borderline ovarian tumours (occur on the surface of the ovary, not inside).

Two of the most important details about a tumour are the stage and the grade of the cancer. Doctors use the FIGO system for determining the stage of ovarian tumours and assign a value of 1-4 based on how far the tumour has spread, and use this information to determine suitable treatment regimes (specifics of the FIGO staging system for

ovarian cancer are summarised in the appendix of this thesis). Lower stage tumours are generally considered to have a more favourable outcome.

Ovarian tumours are also graded, measuring how normal/malignant the cells look under the microscope. Grade 0 tumours are undifferentiated/borderline ovarian tumours. Grade 1 tumours have well differentiated cells (similar to normal, healthy epithelial cells), Grade 2 tumours consist of moderately differentiated cells and Grade 3 tumour cells are poorly differentiated. Grade 3 tumours have the worse prognosis.

Patient 1 was initially diagnosed in 2001 at the age of 47 and presented with serous cell ovarian cancer (stage 1C, grade 1). Patient 1 was treated with carboplatin and therapeutic outcome was classified as complete. Patient 1 subsequently relapsed in 2007 at the age of 52 and was treated with carboplatin/taxol as per the adduct study treatment schedule. Patient 1 is still alive with disease (last recorded status 13<sup>th</sup> November 2008).

Patient 2 was initially diagnosed in 2005 at the age of 74 and presented with endometrioid cell ovarian cancer (stage 1C, grade 3). Patient 2 was treated with carboplatin and therapeutic outcome was classified as complete. Patient 2 subsequently relapsed in 2007 at the age of 76 and was treated with carboplatin/taxol as per the adduct study treatment schedule. The subsequent status of Patient 2 is unknown.

Patient 3 was initially diagnosed in 2004 at the age of 65 and presented with clear cell ovarian cancer (stage 3C, grade 3). Patient 3 was treated with carboplatin and taxol, therapeutic outcome was classified as optimal. Patient 3 subsequently relapsed in 2007

at the age of 68 and was treated with carboplatin/taxol as per the adduct study treatment schedule. The therapeutic outcome was classified as complete. Patient 3 subsequently died of the disease.

Patient 4 was initially diagnosed in 2002 at the age of 62 and presented with clear cell ovarian cancer (stage 1C, grade 3). Patient 4 was treated with carboplatin and taxol, therapeutic outcome was classified as optimal. Patient 4 subsequently relapsed in 2007 at the age of 68 and was treated with carboplatin/taxol as per the adduct study treatment schedule. The therapeutic outcome was classified as complete. Patient 4 is still alive with disease (last recorded status 6<sup>th</sup> July 2010).

### **6.2.2: Treatment Schedule and Sampling Time**

All samples were collected according to a protocol and using a patient information sheet and consent that had been approved by the Local Regional Ethics Committee. All samples were stored in accordance with the Human Tissue Act in a secure freezer in the NICR.

Patients initially received a 3 hour taxol infusion i.v. followed by a 45 minute rest period. During this rest period a pretreatment blood sample (20 ml) was taken as a control for determining background levels of Pt bound to DNA in peripheral blood mononuclear cells (PB-MNC) and for measuring pharmacokinetics at defined timepoints following administration. Carboplatin was infused i.v. over a 30 minute period. The dosing in this time was calculated taking into account renal function to achieve a target AUC of 5.5 mg/ml.min. Blood samples (2 ml) for pharmacokinetic

analysis were taken pre-infusion, 15 minutes after the start of infusion and at 30 minutes at the end of infusion. Further blood samples (2 ml) for pharmacokinetics were taken at 30, 60, 120 and 180 minutes after the end of infusion. At 180 minutes an additional blood sample (20 ml) was collected to determine Pt-DNA adducts levels in PB-MNC. At the same time biopsies were removed from accessible ovarian tumour for determining intra-tumoural Pt-DNA adduct levels and for histological analysis. Biopsies for adduct measurement were placed in 2 ml vials and maintained on dry ice pending transfer to the NICR and storage at -80°C.

### **6.2.3: Preparation of blood samples at the Queen Elizabeth Hospital**

#### *Determination of pharmacokinetic parameters*

Blood samples were collected into lithium heparinised tubes and were immediately centrifuged at 1200 x g for 10 minutes at room temperature to separate plasma. A 1 ml aliquot of plasma was transferred to an Amicon Centrifree micropartition unit with a MW cut-off of 30 kDa (Millipore, UK). The remaining plasma was transferred to a screw-capped 1.5 ml microfuge tube and stored on dry ice. The micropartition unit containing the plasma sample was centrifuged at 1900 x g for 15 minutes at 4°C, and the cup containing the plasma ultrafiltrate was removed, capped, and stored on dry ice. Samples were transferred to the NICR and stored at -80°C. Pt levels were determined by AAS by Dr Gareth Veal as described in section 2.10.

#### *Measurement of Pt-DNA adducts levels*

Blood samples (20 ml) were collected into lithium heparinised tubes which were maintained at room temperature. Samples were immediately transferred to Leucosep

tubes (Greiner Bio-One) containing 15 ml sterile Lymphoprep solution, centrifuged (1000 x g, 15 minutes at room temperature) and then plasma removed. The plasma/cells/lymphoprep layer was transferred into a clean 50 ml tube, diluted with a 2-fold excess of cold PBS, and centrifuged (1000 x g, 5mins at room temperature). PB-MNCs were washed twice with cold PBS and mononuclear cells collected as pellets by further centrifugation (1000 x g, 5 minutes at room temperature). Tubes containing the pellets were placed in dry ice. Samples were transferred to the NICR and maintained at -80°C prior to DNA extraction.

#### **6.2.4: Sample Handling in the NICR**

Pt levels in the patient samples were predicted to be very low, and therefore precautions were taken to ensure that external Pt was not introduced into the sample preparations at any time. All sample handling was carried out in a dedicated Pt-free laminar flow cabinet in a designated Pt-free room. All equipment used in sample preparation was unique to this analysis to prevent contamination from external sources, and was stored in a locked Pt-free cabinet when not in use.

Dedicated reagents were prepared for this analysis and stored in a locked Pt-free cabinet when not in use. Ultrapure nitric acid (Romil, UK) was used for all preparations with a certified Pt content of less than 0.1 PPT. Ultrapure water (Elga, UK) was used throughout. All reagents (including QIAGEN kit reagents) were analysed by ICP-MS to confirm no external Pt content was present.

DNA concentration was determined using the NanoDrop spectrophotometer as described in section 2.5.3. An additional quality control DNA sample (50 µg/ml) was analysed with every sample batch to ensure accuracy. The concentration of DNA measured in this sample was always within 5%.

#### **6.2.5: Samples for checking the techniques and reagents to be used**

Control samples not treated with carboplatin were used to confirm both the techniques and reagents used in this study did not introduce external Pt into the analysis which could affect the results. These samples were also used to determine the background levels of Pt as an indicator of the significance of the results obtained from the clinical samples. Four kidneys obtained from (individual) female CD-1 nude mice that had not been treated with any drugs were used. Pre-carboplatin blood samples obtained from three of the four study patients, and blood from healthy volunteers incubated with saline were also included. An additional set of mouse kidneys which had been treated with 25 mg/kg carboplatin for either 30 or 60 minutes were pooled together and aliquots of the tissue homogenate used as a quality control with each batch of samples for DNA extraction and analysis. DNA was extracted from all samples using the QIAGEN method described in section 2.5.2. DNA was hydrolysed overnight in nitric acid (3.5%) at 70°C, and total Pt levels determined by ICP-MS (section 2.11 and below).

#### **6.2.6: ICP-MS analysis**

All samples in this chapter were analysed using a Finnigan Element2 Magnetic Sector Field ICP-MS (section 2.11.2). Three isotopes of Pt ( $^{194}\text{Pt}$ ,  $^{195}\text{Pt}$  and  $^{196}\text{Pt}$ ) were measured. Thallium (Tl) was added (1 PPB final concentration) to all samples and

standards to act as an internal reference to enable monitoring of instrumental performance and correction for variations due to matrix effects and instrumental variation, particularly variation in the rate of sample entry into the plasma torch. Two isotopes of thallium ( $^{203}\text{Tl}$  and  $^{205}\text{Tl}$ ) were measured on the ICP-MS.

Isotopes of neodymium ( $^{143}\text{Nd}$ ), dysprosium ( $^{161}\text{Dy}$ ) and hafnium ( $^{178}\text{Hf}$  and  $^{179}\text{Hf}$ ) were also measured. These isotopes were chosen because they are known to have the potential to cause interferences if present in samples being analysed for Pt. In this study no correction for interference was required on any samples analysed as the measured concentrations of each isotope in the samples were significantly lower than measured values for Pt, and oxide interference readings therefore contributed significantly less than 1% of the detected Pt signal.

At the beginning of each analysis, ultrapure water and ultrapure nitric acid samples were analysed to ensure Pt levels were low. These samples were always followed by the standards (0-500 PPT Pt), followed by a series of wash samples. During analysis of tumour/blood samples, routine analysis of the 5 PPT standard and blank nitric acid samples were incorporated to monitor instrument drift.

### **6.2.7: Data Analysis**

During all analyses, the ratio of  $^{203}\text{Tl}$ : $^{205}\text{Tl}$  was calculated to monitor instrument sensitivity. An average ratio of 1:2.95 (range +/- 0.1) was observed confirming no drift in instrument performance. The natural abundances are 29.524%  $^{203}\text{Tl}$  and 70.476%  $^{205}\text{Tl}$  so a ratio of 1:2.3 was expected. Counts-per-second (CPS) values for  $^{205}\text{Tl}$  were

chosen to correct the Pt data. CPS values for  $^{205}\text{Tl}$  varied by less than 10% across all analyses.

CPS values for the ultrapure nitric acid wash samples often drifted down slightly during the analyses. This was most probably a result of continued flushing of residual Pt out of the instrument during analysis of a series of blanks and samples with low levels of Pt.

Therefore where necessary drifts in instrumental background was corrected by subtracting the drift in CPS from the CPS values for the standards used to generate the standard curve. The ratio of  $^{194}\text{Pt}:$  $^{205}\text{Tl}$ ,  $^{195}\text{Pt}:$  $^{205}\text{Tl}$  and  $^{196}\text{Pt}:$  $^{205}\text{Tl}$  were calculated for all blanks and standards, and this was plotted against Pt standard concentration to generate a standard curve for each Pt isotope and for each analysis batch (section 2.11.2, Figure 2.4).

The concentration of Pt (PPT) in each sample was calculated in Prism4 (GraphPad Software) using the appropriate standard curve. This value was converted to moles/ml by multiplying the value (PPT) by  $5.13\text{e}^{-15}$ . An average value for the three Pt isotopes was determined, and subsequently divided by the concentration of DNA in the sample ( $5.0\text{e}^{-5}$  g/ml) to determine an overall Pt-DNA adduct level in  $\text{nmol Pt g}^{-1}$  DNA.

## **6.3: Results**

### **6.3.1: Patient Pharmacokinetics**

The antitumour effects of carboplatin have previously been related to its pharmacokinetics, which vary markedly between patients, mainly as a result of variation in kidney function (Newell et al 1987, Harland et al 1991, Horwich et al 1991). Doses of carboplatin are therefore typically adjusted to each individual patient taking into account a measurement of renal function, using a dosing formula (Calvert et al 1989, Newell et al 1993) to target the desired area under the plasma drug concentration time curve (AUC). Individualised dosing results in a more consistent exposure to carboplatin than dosing based on surface area alone, as is typically applied for cisplatin. Typically a range of 4-7 mg/ml.min AUC is targeted for conventional carboplatin dosing (Veal et al 2007). In this study, the target AUC was 5.5 mg/ml.min.

Concentrations of Pt in plasma ultrafiltrates were determined by AAS by Dr Gareth Veal. Unbound (ultrafilterable) plasma Pt concentrations for the four patients are plotted in Figure 6.1. The maximum observed unbound plasma carboplatin for all four patients was at 30 minutes, with concentrations of 43.72 µg/ml, 33.70 µg/ml, 34.72 µg/ml and 23.56 µg/ml reported for patients 1-4 respectively. There was an approximate two fold difference in peak plasma levels, which is common for patients receiving carboplatin following renal-function based dosing (Veal et al 1997).

AUC values for each patient were calculated using the trapezoid rule. Patients 1, 2 and 3 achieved AUC values of 5.1, 6.2 and 4.9 mg/ml.min. Patient 4 achieved a lower AUC

value of 3.0 mg/ml.min. The AUC values for patients 1-3 fell within -10 to +15% of the target AUC whereas; the AUC for patient 4 was 44% below the target value.

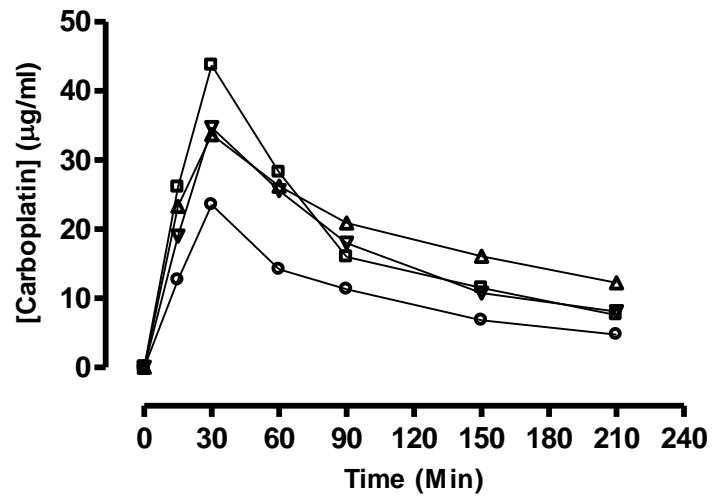


Figure 6.1: Concentrations of unbound Pt in the plasma of four patients after a 30 minute infusion of carboplatin. ( $\square$ ), patient 1; ( $\triangle$ ), patient 2; ( $\nabla$ ), patient 3; ( $\circ$ ), patient 4. AUC values were 5.1 mg/ml.min for patient 1, 6.2 mg/ml.min for patient 2, 4.9 mg/ml.min for patient 3 and 3.0 mg/ml.min for patient 4.

### **6.3.2: Determination of background Pt levels in control samples**

Initial test samples (not treated with carboplatin) were analysed to ensure that the methods and the batch of reagents to be used for the clinical tumour and blood samples gave low background levels of Pt associated with DNA. Confirmation that no platinum contamination was introduced was critical to maintain accuracy in evaluating the clinical samples, which were predicted to have very low Pt levels. Furthermore, the data from these samples helped form a basis to assess the statistics of the background readings against which the post-carboplatin samples could be compared. This was particularly important because the patient number was small, and therefore only a small number of pre-treatment blood samples were available and it was not possible to collect pre-treatment samples of tumour. Mouse kidney tissue was used as a blank to assess the methods for purification of DNA from solid tissue and blood samples (additional to the pre-treatment samples from the four patients) were used to assess methods for purification of DNA from blood cells.

Pt concentrations were calculated for each sample from the values for each Pt isotope using the appropriate standard curve. Pt concentrations in DNA hydrolysates for the mouse tissues (Table 6.1) and volunteer blood samples (Table 6.2) were all low, close to the limit of detection typically seen with this instrument, with a mean of 1.4 PPT (+/- 0.8 SD) for the mouse tissues and 0.5 PPT (+/- 0.5 SD) for the volunteer blood samples. This indicated that the methods and reagents used to process the biological samples were not introducing appreciable levels of Pt into the samples and therefore samples from the patients were analysed using the same batch of reagents.

The pre-treatment blood samples from patients 2-4 gave similarly low levels of Pt seen in the volunteer blood (Table 6.2) with a mean of 0.7 PPT (+/- 0.7 SD).

The overall mean Pt concentration in the solutions analysed by ICP-MS was 0.8 PPT (+/- 0.5 SD), which equates to 4.4 fmoles/ml (+/- 2.4 SD). The overall background Pt-DNA adducts level was 0.08 nmol Pt g<sup>-1</sup> DNA (+/- 0.05 SD).

Table 6.1: Pt concentration and total adduct level in control mouse kidney tissues. Standard deviation is shown in brackets

	DNA Conc. ( $\mu\text{g/ml}$ )	Pt Isotope	Pt Concentration		Adduct Level ( $\text{nmol Pt g}^{-1}$ DNA)
			PPT	Fmoles/ml	
Mouse Kidney 1	418.4	$^{194}\text{Pt}$	1.2	5.9	0.15
		$^{195}\text{Pt}$	1.2	5.9	
		$^{196}\text{Pt}$	1.2	6.2	
		<b>Average</b>	<b>1.2 (0.03)</b>	<b>6.0 (0.1)</b>	
Mouse Kidney 2	348.3	$^{194}\text{Pt}$	0.5	2.6	0.14
		$^{195}\text{Pt}$	0.4	2.3	
		$^{196}\text{Pt}$	0.7	3.6	
		<b>Average</b>	<b>0.6 (0.1)</b>	<b>2.8 (0.7)</b>	
Mouse Kidney 3	430.2	$^{194}\text{Pt}$	2.8	14.4	0.15
		$^{195}\text{Pt}$	2.4	12.3	
		$^{196}\text{Pt}$	2.5	12.6	
		<b>Average</b>	<b>2.7 (0.2)</b>	<b>13.1 (1.1)</b>	
Mouse Kidney 4	322.2	$^{194}\text{Pt}$	1.1	5.5	0.13
		$^{195}\text{Pt}$	1.4	7.1	
		$^{196}\text{Pt}$	1.3	6.6	
		<b>Average</b>	<b>1.3 (0.2)</b>	<b>6.4 (0.9)</b>	
<b>Overall Average</b>			<b>1.4 (0.8)</b>	<b>7.1 (4.3)</b>	<b>0.14 (0.01)</b>

Table 6.2: Pt concentration and total adduct level in control human blood. Hydrolysates from the same DNA preparation were prepared and analysed on three individual occasions for the patient samples or twice for the volunteer sample and average values presented. Standard deviation is shown in brackets

	DNA Conc. ( $\mu\text{g/ml}$ )		Pt Concentration		Adduct Level ( $\text{nmol Pt g}^{-1}$ DNA)
			PPT	Fmoles Pt/ml	
Patient 2	147.74	A	1.8 (0.3)	9.3	<b>0.16 (0.03)</b>
		B	1.5 (0.5)	7.8	
		C	1.3 (0.3)	6.5	
		<b>Average</b>	<b>1.5 (0.3)</b>	<b>7.8 (1.4)</b>	
Patient 3	230.60	A	1.2 (0.1)	6.0	<b>0.05 (0.06)</b>
		B	0.2 (0.3)	1.1	
		C	0.1 (0.2)	0.5	
		<b>Average</b>	<b>0.5 (0.6)</b>	<b>2.5 (3.0)</b>	
Patient 4	281.75	A	0.3 (0.1)	1.4	<b>0.01 (0.02)</b>
		B	0.1 (0.2)	0.6	
		C	0.2 (0.3)	1.0	
		<b>Average</b>	<b>0.2 (0.1)</b>	<b>1.0 (0.4)</b>	
		<b>Average</b>	<b>0.7 (0.7)</b>	<b>3.7 (3.7)</b>	<b>0.07 (0.08)</b>
Volunteer A	144.25	A	0.9 (0.4)	4.4	0.09
		B	0.0 (0.0)	0.0	0.00
Volunteer B	304.76	A	0.5 (0.4)	2.7	0.05
		B	0.0 (0.0)	0.0	0.00
Volunteer C	162.7	A	0.9 (0.1)	4.8	0.09
		<b>Average</b>	<b>0.5 (0.5)</b>	<b>2.4 (2.3)</b>	<b>0.05 (0.05)</b>

### **6.3.3: Analysis of Pt-DNA adducts levels in patient blood samples**

PB-MNCs isolated from blood samples 15 minutes prior to carboplatin infusion (Pre) and 180 minutes after carboplatin infusion (Post) were analysed for determination of therapy-induced Pt-DNA adduct levels. Data for pre- and post-carboplatin blood samples are presented in Table 6.3 and Table 6.4 respectively.

Pt concentrations in patient pre-treatment blood samples all fell within 2 SD of the overall mean background Pt concentration (Table 6.3). Pt concentrations in patient post-carboplatin blood samples ranged from 2.8-68.4 SD above overall mean background Pt concentration (Table 6.4).

All patient post-carboplatin blood Pt-DNA adducts levels were significantly higher than overall mean background Pt-DNA adducts levels ( $p = 0.0008$ ,  $<0.0001$ ,  $<0.0001$  and  $0.0029$  for patients 1-4 respectively). Patients 2-4 had significantly higher Pt-DNA adducts levels in their post-carboplatin sample compared to their pre-carboplatin samples ( $p = <0.0001$ ,  $0.009$  and  $0.001$  for patients 2-4 respectively).

Table 6.3: Pt concentration and adduct level in patient pre-carboplatin blood samples (repeat data from Table 6.2). Hydrolysates from the same DNA preparation were prepared and analysed on three individual occasions and average values presented. Number of SD above background is calculated as: ((Average patient Pt conc. (PPT) – Mean background Pt conc. (0.8 PPT)/ SD of background data (0.5)) SD is shown in brackets.

	DNA Conc. ( $\mu\text{g/ml}$ )		Average Pt Concentration		Number of SD above background	Adduct Level ( $\text{nmol Pt g}^{-1}$ DNA)
			PPT	Fmoles Pt/ml		
Patient 2	147.7	A	1.8 (0.3)	9.3	<b>1.4</b>	<b>0.16 (0.03)</b>
		B	1.5 (0.5)	7.8		
		C	1.3 (0.3)	6.5		
		<b>Average</b>	<b>1.5 (0.3)</b>	<b>7.9 (1.4)</b>		
Patient 3	230.6	A	1.2 (0.1)	6.0	<b>0</b>	<b>0.05 (0.06)</b>
		B	0.2 (0.3)	1.1		
		C	0.1 (0.2)	0.5		
		<b>Average</b>	<b>0.5 (0.6)</b>	<b>2.5 (3.0)</b>		
Patient 4	281.8	A	0.3 (0.1)	1.4	<b>0</b>	<b>0.01 (0.02)</b>
		B	0.1 (0.2)	0.6		
		C	0.2 (0.3)	1.0		
		<b>Average</b>	<b>0.2 (0.1)</b>	<b>1.0 (0.4)</b>		

Table 6.4: Pt concentration and adduct level in patient post-carboplatin blood samples. Hydrolysates from the same DNA preparation were prepared and analysed on three individual occasions and average values presented. Number of SD above background is calculated as:  $((\text{Average patient Pt conc. (PPT)} - \text{Mean background Pt conc. (0.8 PPT)}) / \text{SD of background data (0.5)})$  SD is shown in brackets. ND = no data available for sample.

	DNA Conc. ( $\mu\text{g/ml}$ )	Average Pt Concentration		Number of SD above background	Adduct Level ( $\text{nmol Pt g}^{-1}$ DNA)
		PPT	Fmoles Pt/ml		
Patient 1	66.21	A	3.7 (0.6)	6.4	0.8 (0.1)
		B	4.4 (0.2)		
		C	ND		
		<b>Average</b>	<b>4.0 (0.5)</b>		
Patient 2	171.98	A	31.3 (0.04)	68	3.6 (0.3)
		B	36.1 (0.4)		
		C	37.2 (0.1)		
		<b>Average</b>	<b>35.0 (3.2)</b>		
Patient 3	319.14	A	2.2 (0.2)	2.8	0.2 (0.01)
		B	2.2 (0.5)		
		C	2.1 (0.5)		
		<b>Average</b>	<b>2.2 (0.1)</b>		
Patient 4	311.51	A	2.7 (0.1)	2.8	0.2 (0.04)
		B	1.8 (0.8)		
		C	2.1 (0.7)		
		<b>Average</b>	<b>2.2 (0.4)</b>		

#### **6.3.4: Analysis of Pt-DNA adducts in patient tumour biopsies**

Tumour biopsies, obtained from patients 180 minutes after carboplatin infusion, were analysed for determination of therapy-induced Pt-DNA adduct levels. Biopsies that were sufficiently large were subdivided to give 13 pieces of tissue that were processed and analysed separately. These are summarised in Figure 6.2. Only one sample was available for patient 4, due to the tumour being less surgically accessible than patients 1-3. Histology of additional biopsy samples confirmed the obtained material was from the tumour (Dr Richard Edmondson, personal communication). Data is summarised in Table 6.5.

Pt concentrations in the DNA preparations extracted from the 13 biopsy pieces ranged from 18.6 to 37.1 PPT Pt (Table 6.5). These Pt concentrations were between 36 and 62 SD above the overall mean background Pt concentration (Table 6.5)

All seven biopsy pieces analysed (by ICP-MS) on three separate occasions had significantly higher Pt-DNA adducts levels compared to overall mean background Pt-DNA adducts levels: P1-A,  $p = 0.0002$ ; P1-B,  $p = 0.0021$ ; P2-A1,  $p = 0.0002$ ; P2-B2,  $p = 0.0001$ ; P3-B,  $p = 0.0006$ , P3-C,  $p = <0.0001$  and P4-A,  $p = <0.0001$ .

Only patient 3 demonstrated any significance between pieces of biopsy from the same tumour (P3-B and P3-C,  $p = 0.0242$ ). No significant difference in Pt-DNA adduct level was observed between patients 1-3. Patient 4 had significantly higher Pt-DNA adducts levels than patients 1-3 ( $p = 0.0002$ ,  $<0.0001$  and  $0.0096$  respectively).

Figure 6.2: Summary of the source of the 13 biopsy pieces used in this study for measuring Pt-DNA adducts in patient tumours following carboplatin administration.

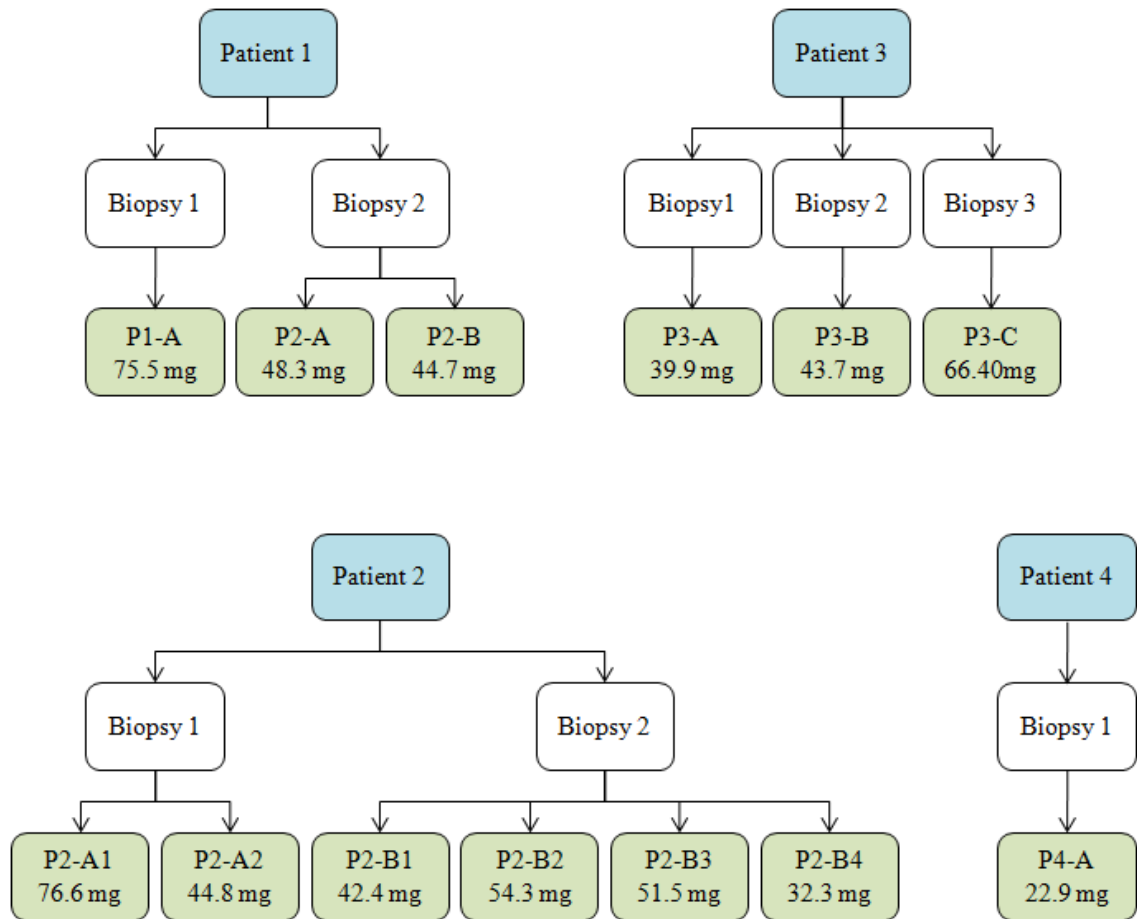


Table 6.5: Pt concentration and adduct level in patient biopsies. Individual hydrolysates were analysed either on one occasion, or hydrolysates from the same DNA preparation were prepared and analysed on three individual occasions and average values (+/- SD) presented. Number of SD above background is calculated as: ((Average patient Pt conc. (PPT) – Mean background Pt conc. (0.8 PPT)/ SD of background data (0.5)).

	Biopsy Piece	Pt Concentration		Number of SD above background	Adduct Level (nmol Pt g <sup>-1</sup> DNA)
		PPT	Fmoles/ml		
Patient 1	P1-A	24.1 (0.4)	123.4 (15.8)	47	2.5 (0.3)
	P1-B	22.7 (0.1)	116.4 (26.4)	44	2.3 (0.5)
	P1-B2	18.6	95.2	36	1.9
Patient 2	P2-A1	21.6 (0.3)	110.7 (15.1)	54	2.2 (0.3)
	P2-A2	27.2	139.3	53	2.8
	P2-B1	23.7	121.4	46	2.4
	P2-B2	19.0 (0.4)	97.6 (10.8)	36	2.0 (0.2)
	P2-B3	20.1	103.0	39	2.1
	P2-B4	24.8	127.1	48	2.5
Patient 3	P3-A	31.7	162.7	62	3.3
	P3-B	31.7 (0.3)	162.4 (26.1)	62	3.2 (0.5)
	P3-C	19.9 (0.4)	102.3 (9.4)	38	2.0 (0.2)
Patient 4	P4-A	20.6 (0.3)	105.8 (3.8)	40	4.2 (0.2)

#### **6.4: Comparison of patient pharmacokinetic parameters with adduct levels**

##### *AUC vs. PB-MNCs*

A very weak relationship was observed between plasma carboplatin AUC and post-treatment Pt-DNA adducts levels in the PB-MNC. A weak correlation was observed between plasma carboplatin AUC and post-treatment Pt-DNA adducts levels in PB-MNCs. ( $r^2 = 0.5772$ , slope 0.9166) (Figure 6. 3A). This correlation was not significant ( $p = 0.2402$ ).

##### *AUC vs. Tumour Biopsies*

A weak correlation was apparent between plasma carboplatin AUC and Pt-DNA adduct levels detected in the tumour biopsies ( $r^2 = 0.7845$ , slope -0.5738) (Figure 6. 3B). This correlation was not significant ( $p = 0.1143$ ). Furthermore, it was a negative trend which is opposite to what would be expected.

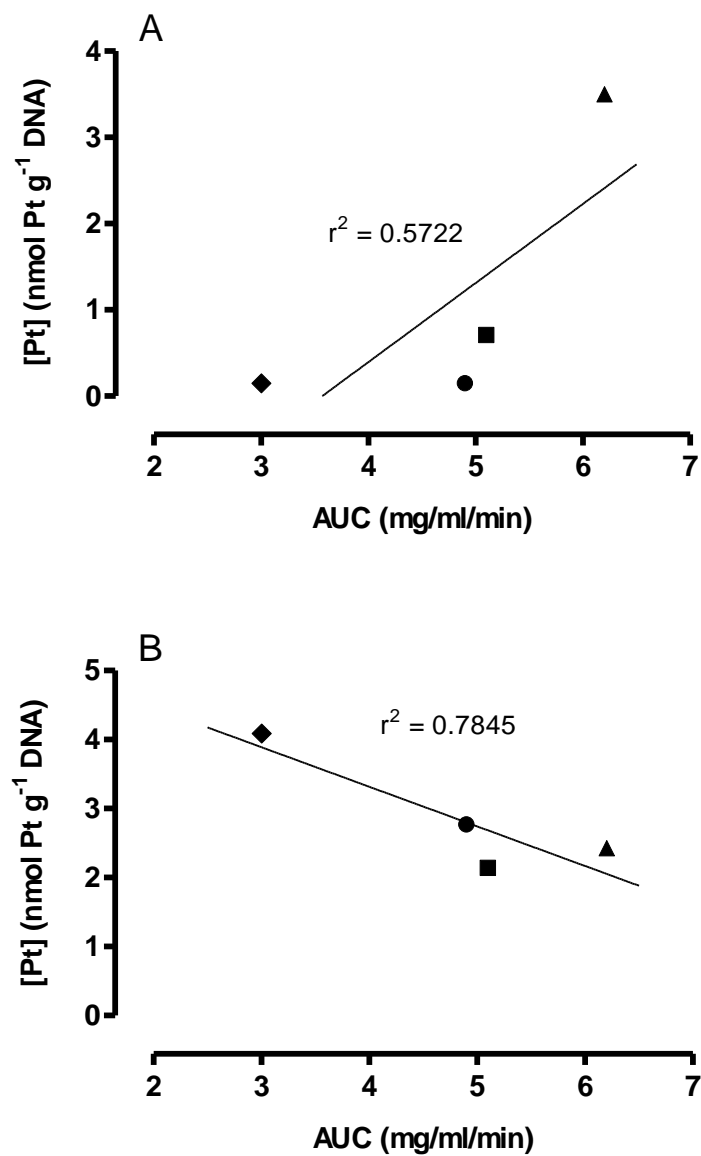


Figure 6. 3: Relationship between patient AUC and Pt-DNA adduct levels in PB-MNCs (A) and human tumour biopsies (B). (■), patient 1; (▲), patient 2; (●), patient 3; (◆), patient 4. No significant correlation was observed (graph A,  $p = 0.2402$ ; graph B,  $p = 0.1143$ ).

### **6.5: Comparison of adduct levels in blood cells and tumour**

No correlation was observed between Pt-DNA adducts levels in PB-MNCs and in tumour biopsies ( $r^2 = 0.1960$ , slope  $-0.2377$ ) (Figure 6. 4). Furthermore, it was a negative trend which is opposite to what would be expected. These findings suggest that Pt-DNA adduct levels in patient blood are not a good marker for Pt-DNA adduct levels in patient biopsies.

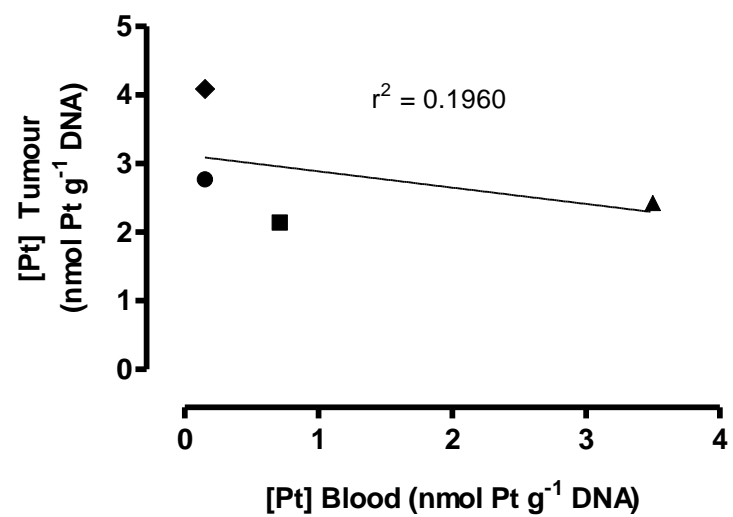


Figure 6. 4: Relationship between in vivo Pt-DNA adducts levels in PBLs and human tumour biopsies. (■), patient 1; (▲), patient 2; (●), patient 3; (◆), patient 4

## 6.6: Discussion

There is currently limited data available on levels of Pt-DNA adducts in tumours of patients receiving Pt-based chemotherapy. Several factors have probably contributed to this, as described in section 6.1. A sensitive  $^{32}\text{P}$  post-labelling assay has recently been applied to investigations of intra-tumoural Pt-DNA adducts levels in patients receiving cisplatin-based chemotherapy for HNSCC (Hoebers et al 2006, Hoebers et al 2008). The results described in this chapter are the first application of ICP-MS to the analysis of therapy-induced Pt-DNA adducts levels in solid clinical tumours.

Initially, an absolute background level of Pt was calculated using control human blood and mouse tissues. This was important to ensure the methods involved did not introduce external Pt to the clinical samples ensuring reliability in the measurements, and also to provide a value for background levels of Pt present resulting from the control samples and from the reagents and apparatus used, including the ICP-MS instrument itself. A background level of Pt of 0.8 PPT ( $\pm$  0.5 SD) was measured in this study (4.1 fmoles/ml). The corresponding background Pt-DNA adducts level was 0.08 nmol Pt  $\text{g}^{-1}$  DNA (0.05 SD).

An AUC of 5.5 mg/ml.min carboplatin was targeted for the four patients studied, with dosing based on renal function. The range of AUC values for free Pt in plasma was within the range of values expected which, for a targeted AUC value in conjunction with renal-based dosing typically covers a 2-fold range (Dr Gareth Veal, personal communication).

Pt-DNA adducts levels in PB-MNCs obtained from patients post-carboplatin therapy ranged from 0.2-3.6 nmol Pt g<sup>-1</sup> DNA and are comparable to previous studies (Peng et al 1997, Veal et al 2001). Peng et al had previously published Pt-DNA adduct levels in PBLs of patients receiving carboplatin therapy of 1-3.2 nmol Pt g<sup>-1</sup> DNA 6hr after the end of infusion, and 1-5.9 nmol Pt g<sup>-1</sup> DNA 24hr after the end of infusion (Peng et al 1997). These values had been determined by ELISA. More recently Veal et al have published data on Pt-DNA adduct levels in children receiving high dose carboplatin for solid tumours using ICP-MS to measure Pt (Veal et al 2007). They found Pt-DNA adduct levels of 0.24-2.29 nmol Pt g<sup>-1</sup> DNA in patients 24hr after the end of infusion.

Hoebbers et al had previously measured Pt-DNA adduct formation in patients receiving cisplatin-based chemotherapy using a <sup>32</sup>P-post-labelling assay (Hoebbers et al 2006, Hoebbers et al 2008). Normal tissue (WBC) Pt-DNA adduct levels in all the regimes investigated ranged from 0.34-1.05 nmol Pt g<sup>-1</sup>DNA and 0.05-0.12 nmol Pt g<sup>-1</sup> DNA for the intrastrand 1,2-d(GpG) and 1,2-d(ApG) adducts respectively. The background Pt-DNA adduct level observed in the present work was 0.08 nmol Pt g<sup>-1</sup> DNA (range 0.0-0.19 nmol Pt g<sup>-1</sup> DNA). Hoebbers et al reported Pt-DNA adduct levels in tumour tissue ranging from 0.66-4.55 nmol Pt g<sup>-1</sup> DNA and 0.1-0.43 nmol Pt g<sup>-1</sup> DNA for the intrastrand 1,2-d(GpG) and 1,2-d(ApG) adducts respectively. Pt-DNA adducts levels in patient tumour biopsies in the present study ranged from 1.9-4.2 nmol Pt g<sup>-1</sup> DNA. Comparable levels of Pt-DNA adducts were observed between this study and the studies of Hoebbers et al.

Pt-DNA adducts level in blood cells had previously been suggested as a marker for adduct levels in tumours (Reed et al 1988, Reed et al 1990). More recent published data

however has found no correlation was seen between Pt-DNA adduct levels in blood cells and tumour biopsies (Hoebbers et al 2006, Hoebbers et al 2008). The data obtained from the present investigation are in agreement with those recent findings.

No significant differences in Pt-DNA adduct level in tumour biopsies was observed between patients 1-3. Patient 4 had significantly higher Pt-DNA adducts levels than patients 1-3 ( $p = 0.0002$ ,  $<0.0001$  and  $0.0096$  respectively). For patients 1 and 2, no significant differences in Pt-DNA adduct levels was observed in different biopsies obtained from the same tumour. Three pieces of biopsy were obtained from patient 3, and although two pieces (P3-A and P3-B) had comparable Pt-DNA adduct levels ( $3.17 \text{ nmol Pt g}^{-1} \text{ DNA}$ ), a third piece had significantly lower Pt-DNA adduct levels ( $1.97 \text{ nmol Pt g}^{-1} \text{ DNA}$ ,  $p = 0.0242$ ). These data suggest that intratumour platinumation levels may vary depending on other factors than carboplatin dose, such as tumour location and vasculature access. When Pt-DNA adduct levels were compared with calculated AUC values for each patient, no correlation was observed. This suggests that patient AUC is not a reliable indicator of adduct levels in tumours.

The application of ICP-MS in this study for measuring Pt-DNA adducts levels in solid tissues is novel, and has demonstrated that although material is hard to obtain, analyses of Pt adducts in clinical samples is possible.

The very low levels of Pt detected in the DNA samples suggests that the application of ICP-MS to detect specific types of adducts will be challenging. However, recently a method has been published that does allow for detection of the low levels of the 1,2-intrastrand *cis*-Pt(NH<sub>3</sub>)<sub>2</sub>d(GpG) adducts in DNA from PBLs obtained from patients

after cisplatin-based chemotherapy (Harrington et al 2010). In this study, PBLs were isolated from 8 patients each receiving cisplatin chemotherapy ( $60 \text{ mg m}^{-2}$ ) and DNA extracted. Levels of the *cis*-Pt(NH<sub>3</sub>)<sub>2</sub>d(GpG) adduct ranged from 0.58-6.4 nmol Pt g<sup>-1</sup> DNA, in the same range of values as reported in this chapter. The application of such a method for studying specific Pt-DNA adducts other than the *cis*-Pt(NH<sub>3</sub>)<sub>2</sub>d(GpG) or for studying Pt-DNA adducts in patient tumour biopsies is unknown.

## Chapter 7

### Final Discussion

#### 7.1: Introduction

Platinum-based anticancer drugs are believed to exert their action through chemical reactions with genomic DNA, forming adducts with DNA bases. Although the pharmacology of such adducts has been widely studied, many aspects of the cytotoxic mechanisms remain unclear. The possibility that non-DNA molecules have the potential to alter the types of adducts formed has received very little attention, and limited information is available on the levels of adducts formed in clinical tumours. Further understanding of platinum-DNA adduct formation may be important in explaining the efficacy of platinum-based drugs in different tumour types, providing insights into the cytotoxic mechanism, the development of clinical resistance and how to modulate response to therapy using additional drugs.

The aims of the work described in this thesis were: a) to analyse the nature of DNA adducts formed in cells by three clinically used platinum-based anticancer drugs and to investigate the potential intracellular formation of additional types of adducts to those previously characterised on pure DNA; b) to determine platinum-DNA adduct levels formed in solid ovarian cancer tissue following treatment of patients with carboplatin and test the hypothesis that these levels are comparable to levels of DNA adducts formed in blood cells; and c) to determine whether STS impacts on DNA adduct formation.

## **7.2: Effects of GSH and STS on total Pt-DNA adduct formation in pure DNA**

Sulfur-containing molecules are known to react rapidly with Pt-containing compounds, due to the strong affinity of the metal for sulfur (Reedijk 1999, Reedijk 2003, Deubel 2004). The effects of GSH, an endogenous sulfur containing compound found at millimolar concentrations in cells (Meister and Anderson 1983), and STS, an exogenous sulfur-containing compound currently in a phase III clinical trial investigating otoprotection, on the formation of cisplatin-DNA were therefore investigated.

The data presented in chapters 4 and 5 shows that both GSH and STS were able to markedly inhibit the binding of cisplatin to purified DNA in a concentration-dependent manner. For 2hr incubations it was estimated that 0.07 mM STS would cause a 50% decrease in DNA adduct formation. In contrast, 3.9 mM GSH was needed to cause a similar effect under exactly the same conditions of DNA and cisplatin concentration. For 24hr incubations, the equivalent concentrations were estimated to be 0.05 mM STS and 2.7 mM GSH. Thus, to achieve similar effects on adduct formation STS needed to be present at concentrations approximately 55-fold lower than GSH. These data are consistent with published data suggesting that the reaction of the thiosulfate ion (TS) with cisplatin in solution is much faster than the reaction of cisplatin with GSH under similar conditions (Leeuwenkamp et al 1991, Dabrowiak et al 2002).

### 7.3: Can GSH and STS be cross-linked to DNA by cisplatin?

Using a similar chromatographic separation to that of Fichtinger-Schepman et al (1985), Azim-Araghi (2003) investigated the formation of Pt-DNA adducts in lung cancer cell lines (H69/p and Mor/p), using ICP-MS to detect Pt species. Azim-Araghi provided evidence for an additional major class of Pt-DNA adducts in DNA from drug-treated cells compared to those described previously on purified DNA. Analysis of cisplatin-DNA adducts formed in purified DNA in the presence of GSH showed further evidence of additional types of Pt-DNA adducts being formed. Interestingly, the additional adducts found in purified DNA displayed the same chromatographic characteristics as those detected in cellular DNA, leading to the hypothesis that GSH is able to cross-link to DNA in cells via cisplatin. Evidence that GSH is able to cross-link to monofunctionally bound Pt-DNA adducts was published over twenty years ago (Micetich et al 1983, Eastman 1987). Limited information is available regarding the formation of such adducts involving STS, but assuming that the putative *cis*-Pt(NH<sub>3</sub>)<sub>2</sub>(DNA)(GSH) cross-link was formed via a Pt-S linkage, it seemed plausible that STS should react in a similar manner. If the existence of such Pt-S cross-links were to be proven, it would have a significant impact on our understanding of platinum drug pharmacology.

The hypothesis for the formation of such Pt-S cross-links was through binding of either GSH or STS to cisplatin-bound monofunctionally to DNA. An alternative to this approach would be initial binding of GSH or STS to cisplatin, which then reacts with DNA. The data described above suggest that initial binding of cisplatin to either GSH or STS is more likely to lead to inactivation of drug as opposed to being an

intermediate step in adduct formation. However, as Pt-DNA adducts do still form this mechanism cannot be totally excluded. Initial experiments were carried out to investigate the plausibility of DNA-Pt-S cross link formation, and to identify their chromatographic behaviour. The latter information would be an important step to identifying novel products formed in cells.

Following incubation of equimolar (1mM) cisplatin with dGMP (used as a surrogate for DNA) three monofunctional products were identified with the proposed chemical nature *cis*-Pt(NH<sub>3</sub>)<sub>2</sub>(R)(dGMP) where R could be any of Cl<sup>-</sup>, OH or OH<sub>2</sub>. Further incubations with GSH or STS provided evidence for the formation of *cis*-Pt(NH<sub>3</sub>)<sub>2</sub>(dGMP)(GSH) and *cis*-Pt(NH<sub>3</sub>)<sub>2</sub>(dGMP)(STS) products, eluting from the MonoQ system at 21 and 16 minutes respectively. These products provided important information about the chromatographic behaviour of putative DNA-Pt-S cross-links, and indicated the times and conditions the predicted products would elute. Incubations of cisplatin and DNA in the presence of either GSH or STS however failed to provide consistent evidence for the formation of DNA-Pt-S cross-links.

One possible reason for the lack of consistent evidence of putative DNA-Pt-S cross-links was the use of a more robust and efficient gel filtration system to that used by Azim-Araghi (2003). The gel filtration column used in this study was somewhat more efficient at separating Pt-GSH and Pt-TS products from DNA. If Pt-GSH products contaminated previous DNA preparations they could have contributed to observations such as the apparent cross-linking of radioactive GSH to DNA by cisplatin. MonoQ chromatographic analysis showed that both Pt-GSH and Pt-TS eluted much later to the dGMP-Pt-S products so it seems unlikely that this would explain the discrepancy

between the data in this study and the new peak seen previously by Azim-Araghi (2003).

Two factors that could influence the ability of either GSH or TS to interact with platinated DNA and might also explain the lack of consistent evidence of DNA-Pt-S products are steric hindrance and charge effects. GSH has a molar mass of 307.6 g/mol, and steric effects could inhibit the interaction of GSH with monofunctionally platinated DNA. As the thiosulfate ion is much smaller (molar mass of 112.12 g/mol) and more reactive, steric effects might be less pronounced. DNA is polyanionic in nature, and has an overall negative charge. At neutral pH, GSH has an overall -1 charge, and the thiosulfate ion -2. Since both GSH and TS possess negative charges, they should in theory be repelled from DNA. In cells DNA is complexed with positively charged proteins (such as histones) which would have effects on the ability of GSH and TS to interact with monofunctional adducts. While these factors could explain the lack of evidence in this study, they fail to address differences between the data presented here and in the work of Azim-Araghi (2003).

The formation of Pt-GSH and Pt-TS products is an important issue in understanding the availability of Pt binding to DNA. It is believed that cisplatin will react with DNA in its aquated form, but not in its dichloro form. GSH and STS however are believed to be reactive with cisplatin in both forms. Aquation of cisplatin is the rate limiting step in reaction with DNA. It is possible therefore that such competition limits the amount of Pt available to bind DNA. Therefore, it is possible that changes to the reaction conditions such as altered ionic strength of  $\text{Cl}^-$  could increase the probability of GSH

reacting with monofunctionally bound drug through changes to ionic interaction and/or the state of aquation of cisplatin.

A further possibility for a lack of evidence for DNA-Pt-S cross-link formation is that such cross-links lack stability. Attempts at analysing the putative dGMP-Pt-S products by MALDI-TOF mass spectrometry and NMR have proven unsuccessful and this might also be explained by lack of stability. However, the proposed DNA-Pt-GSH cross-link observed by Azim-Araghi was detected in purified DNA following 2hr and 24hr incubation.

Incomplete digestion of DNA in the work of Azim-Araghi (2003) may also explain the discrepancy between these data and findings from the current study. Azim-Araghi provided evidence showing that increased concentrations of enzymes used in the digestion of DNA did not affect the results. However it is still possible that the novel products identified by Azim-Araghi were artefacts of incomplete digestion. The ratio of DNA to enzymes in this study was less than was used previously (100 µg versus 250 µg DNA per 20 units DNAase1 and 200 units/ml nuclease P1). Also, a different preparation of P1 was used as the previous supplier ceased its production.

#### 7.4: Nature of Pt-DNA adducts formed in cells

Although Pt complexes can interact with many molecules in the intracellular environment, it is commonly accepted that platinum binding to DNA is responsible for the major cytotoxic effects of platinum complexes. The formation of Pt-DNA adducts in purified DNA has been widely studied for cisplatin, and to a lesser extent for carboplatin, with more limited data available relating to oxaliplatin-DNA adducts formation. However, markedly less information has been published on the formation of Pt-DNA adducts in cells exposed to any of the three drugs has been published. In this study, the formation of Pt-DNA adducts in four human tumour cell lines (833K, A2780, LoVo and Mor/CPR) exposed to cisplatin, carboplatin or oxaliplatin was investigated.

Analyses of adducts formed in cellular DNA incubated with cisplatin confirmed the presence of peaks corresponding to the four major previously identified Pt-DNA adducts. The percentage contribution of the two major Pt-DNA products was similar to previous studies (Fichtinger-Schepman et al 1985, Eastman 1986). Pt-DNA adducts formed in cells exposed to carboplatin or oxaliplatin showed very similar retention times and relative Pt levels to those seen in the incubation with cisplatin. It is possible that the use of a different chromatographic system, such as reverse-phase analysis of platinated nucleosides may have revealed differences between adducts formed by oxaliplatin compared to cisplatin.

Of particular importance, however, was the lack of evidence for additional types of adducts in the regions where *cis*-Pt(NH<sub>3</sub>)<sub>2</sub>(dGMP)(GSH) products eluted or where the additional Pt-containing peak was identified in the analyses of Azim-Araghi (2003).

The reasons for this are unclear, but two possible factors might have contributed: 1, the use of different cell lines and 2, differences in cross-link repair. Potential issues with enzyme levels and stability of the proposed adducts have been discussed above.

In the analyses by Azim-Araghi (2003), two non-small cell lung cancer cell lines (H69/p and Mor/p) were investigated, whereas in the current study three different cell lines were investigated (833K, A2780 and LoVo). Similar retention times of the identified peaks and relative proportions of Pt adducts were observed, therefore it seems unlikely that adducts formed in these cells differed to those formed in the H69/p and Mor/p cells in such a way as to explain the lack of novel products previously detected. Furthermore, one of the cell lines used in this study, Mor/CPR, is a cisplatin-resistant sub-line of the Mor/p cells used by Azim-Araghi. The Mor/CPR cell line had been derived from the Mor/P line by selection for drug resistance (Twentyman et al 1991). It is possible that the resistance mechanisms resulted in altered types of DNA adducts being formed in the Mor/CPR line compared to the cells used by Azim-Araghi, but it seems unlikely that a major class of adducts would be completely lost, especially since the extra peak could not be detected in analyses of DNA from the three other cell lines.

Another possibility is that *cis*-Pt(NH<sub>3</sub>)<sub>2</sub>(DNA)(GSH) cross-links were repaired more efficiently than their classical counterparts. Analysing Pt-DNA adducts in cells with compromised repair capacity would be a way of investigating this. However, repair-compromised cells demonstrate elevated sensitivity to cisplatin (Beck and Brubaker 1973, Drobnik and Horacek 1973, Markham and Brubaker 1980, Brouwer et al 1981, Beck et al 1985, Fram et al 1985, Popoff et al 1987) so such investigations would

require careful decisions regarding drug concentration. In addition, as 2hr drug exposures were investigated in the present work, it seems unlikely that the proposed adducts would have been removed by DNA repair processes in that time, with the loss of total Pt adducts proceeding over a much longer timescale (Fraval and Roberts 1979, Roberts and Friedlos 1987).

Overall, the failure to confirm the presence of additional Pt-DNA adducts in cells is consistent with the generally accepted model in which GSH protects cells against Pt drugs either directly by simple inactivation of the drug or indirectly by affecting the redox state of certain proteins.

## **7.5: Effect of STS on the antiproliferative activity of cisplatin in human tumour cell lines**

When STS was present concurrently with cisplatin it caused 35, 21, 22 and >17-fold increases in  $GI_{50}$  values for 833K, A2780, LoVo and Mor/CPR cells respectively (Table 5.2). Under the same conditions, 2.4, 3.6, 3.1 and 10.1 fold reductions in adduct level were observed (Table 5.3). In this study, the decreases in Pt-DNA adduct levels measured after concurrent incubation of cells with cisplatin and STS are lower than what would be expected based on the increase in  $GI_{50}$  concentrations.

One potential explanation for this phenomenon is that Pt-DNA adducts formed in cells in the presence of STS are of a different nature to those formed when exposed to cisplatin alone. There is very limited data however to support the idea that STS is able to enter cells, and so it is unclear what to what extent, if any, STS is altering the nature of the adducts. Further investigations into the ability of STS to enter cells are required to determine the plausibility of STS affecting Pt-DNA adduct structure. Further incubations of human tumour cells with STS and cisplatin might permit analysis of adducts formed by chromatography/ICP-MS, but significantly higher levels of cisplatin would be required due to the effectiveness of STS in binding to and inactivating cisplatin. However, such an analysis seems not worthwhile in view of the lack of reliable evidence for the formation of altered cisplatin adducts in purified DNA in the presence of STS.

A related possible explanation for the discrepancy between the effects of STS on  $GI_{50}$  and adduct levels is that STS had a particularly strong effect at blocking formation of a

minor adduct which is strongly cytotoxic. The clear candidate for this would be the interstrand cross-links but this would require entry of STS into cells. This could be studied by alkaline elution analysis, but seems an unlikely mechanism because of the lack of any effect of delayed addition of STS on growth inhibition.

Finally it is possible that STS was very effective at blocking the reaction of cisplatin with cell surface proteins which influence the way that cells respond to DNA damage. Such a mechanism could be relevant to the protective effects reports for STS on ototoxicity.

Sequential and delayed exposure to STS had no significant effect on growth inhibition or adducts levels in any of the four cell lines tested. This is consistent with the proposed delayed administration of STS to patients to protect against ototoxicity without compromising the anti-tumour activity of cisplatin.

## 7.6: Analysis of Pt-DNA adducts in relation to growth inhibition data

Factors known to affect the sensitivity of cells to Pt drugs can be grouped into three classes: 1, factors that affect access of drug to DNA, such as differences in uptake or intracellular thiols; 2, the properties of the adducts formed; and 3, factors that affect how the cell responds to the damage, such as repair or replication by-pass mechanisms. The latter factors are very dependent upon the nature of adducts formed. All of these factors contribute towards the  $GI_{50}$  values. However, if the level of adducts required to achieve a 50% growth inhibition ( $AL_{50}$ ) is determined, this data is independent of the first set of factors and so reflects the nature of adducts and how cells respond to them.

Cisplatin and carboplatin are believed to form the same types of Pt-DNA adducts; with similar relative yields of major adduct types. In three of the four cell lines investigated here (A2780, LoVo and Mor/CPR), after 2hr incubations with equitoxic concentrations, carboplatin formed 2-fold lower levels of Pt-DNA adducts in cells than cisplatin. As the Pt-DNA adducts formed are believed to be the same, it would be expected that the levels of adducts required to achieve equal toxicity would be comparable. The differences presented here suggest that adducts formed by carboplatin can be slightly more toxic than those for cisplatin. However, chromatographic analysis of DNA adducts showed no detectable differences.

Pt-DNA cross-links involving proteins were not analysed chromatographically. It is therefore possible that these adducts are contributing to cytotoxicity in a different manner in cells incubated with carboplatin or cisplatin. Another limitation of the

chromatographic separation is the lack of information about the distribution of adducts across the genome, and the implication of adducts forming at different sites.

An alternative explanation could be that the drugs interact with other non-DNA molecules either intracellularly or on the cell surface, and this could have effects on the response of cells. It is possible that interactions of cisplatin or carboplatin with intracellular structures or proteins might have detrimental effects of cell signalling which could lead to variations in cytotoxicity.

One unexpected finding was the large amount of oxaliplatin-DNA adducts tolerated by Mor/CPR cells. This increased tolerance might be a direct result of the cell line being resistant to cisplatin, and further understanding of the resistance mechanisms might provide evidence for this.

## **7.7: Analysis of Pt-DNA adducts formed in tumour biopsies and blood cells of ovarian cancer patients treated clinically with carboplatin**

Very few investigations of Pt-DNA adducts levels in solid tumours of patients receiving Pt-based chemotherapy have been published. Factors that may have contributed to this lack of data include difficulties in obtaining tumour samples at appropriate times after drug administration and the small size of such biopsies, combined with the inherent low levels of Pt-DNA adducts formed.

In this study, Pt-DNA adducts levels in tumour biopsies and blood cells obtained from four patients receiving carboplatin-based chemotherapy were analysed. Pt-DNA adducts levels measured in tumour biopsies ranged from 1.9-4.2 nmol Pt g<sup>-1</sup> DNA. These levels are comparable to Pt-DNA adduct levels detected in head and neck cancer patients receiving cisplatin-based chemotherapy by Hoebbers et al (2006 and 2008). Pt-DNA adducts levels in blood cells ranged from 0.15-3.5 nmol Pt g<sup>-1</sup> DNA, comparable to previously published studies (Peng et al 1997, Veal et al 2001, Veal et al 2007). No correlation was observed between Pt-DNA adduct levels in tumour biopsies and adduct levels in blood cells. The lack of correlation between tumour adduct levels and blood cell adduct levels is in agreement with previous published findings (Hoebbers et al 2006, Hoebbers et al 2008) It is important to note however the small sample numbers used in this study, with only four patients investigated due to the inherent limitations in obtaining samples.

In the most sensitive cell line studied (833K), adduct levels required to achieve 50% growth inhibition were 9.9 and 12.0 nmol Pt g<sup>-1</sup> DNA for 2hr and 24hr incubations

respectively. The highest adduct level detected in the tumour biopsies was 4.2 nmol Pt g<sup>-1</sup> DNA. These differences suggest that either the doses used clinically were ineffective, or the data obtained using cell line models or analysis by SRB assay is not directly relevant to the clinical situation. Investigations of drug sensitivity using a method such as a clonogenic assay might provide lower estimates of GI<sub>50</sub> concentrations and hence lower AL<sub>50</sub> values. The patients studied were being treated for advanced metastatic ovarian cancer and had been previously treated with carboplatin. Importantly, all four patients had shown prior response to carboplatin-based therapy as this was a pre-requisite in selection of suitable patients. It is possible therefore that resistance to carboplatin may have developed. Information on response of the patients has not yet been provided by the clinician.

There is currently major interest in personalising cancer therapy to individual patients. A rationale for studying Pt-DNA adducts levels is that they could be used as a predictive assay for patient response, with higher levels of adducts potentially resulting in a more favourable outcome. Pt-DNA adducts level in blood cells had previously been suggested as a possible biomarker for adduct levels in tumours (Reed et al 1988, Reed et al 1990, Bonetti et al 1996). These studies were based on the assumption that normal tissue could act as a surrogate for tumour tissue. However, more recently published data found no correlation between Pt-DNA adduct levels in blood cells and tumour biopsies (Hoebbers et al 2006, Hoebbers et al 2008). The results obtained from the present investigation are in agreement with those recent findings.

Welters et al (1999) investigated the formation of Pt-DNA adducts in biopsies taken from patients with head and neck or testicular cancer incubated *ex vivo* with cisplatin.

Adduct levels achieved were comparable between head and neck and testicular biopsies. These data suggest that analysis of Pt-DNA adducts achieved in patient tumour biopsies incubated *ex vivo* with Pt drugs is a feasible approach towards predicting patient response. However, this approach would require intensive laboratory work for each sample and it would need to be shown to produce clinically useful data.

This study has demonstrated a successful application of ICP-MS for analysis of total Pt-DNA adducts in solid ovarian tumour tissue. A major advantage of ICP-MS is the minimum preparation steps required from DNA extraction to analysis, improving sensitivity of detection. This is further supported by the comparable adduct levels detected in this study with those of Hoebbers et al (2006 and 2008). A weakness of this approach however is that any Pt present in samples will appear to be a Pt-DNA adduct. Combining chromatographic separation with ICP-MS is a potential mechanism to overcome this, but might decrease sensitivity.

## 7.8: Overall Conclusions

1. It was confirmed that adducts formed in cells incubated with cisplatin were of a similar nature to those described previously based on analysis of pure DNA incubated with cisplatin.
2. No evidence was found to support the observations of Azim-Araghi 2003, that in cells exposed to cisplatin, an additional major class of Pt-DNA adducts is formed.
3. The chromatographic behaviour of Pt-DNA adducts formed in cells exposed to either carboplatin or oxaliplatin are comparable to those of cisplatin, suggesting the nature of such adducts is broadly similar.
4. STS was much more effective than GSH at limiting reaction of cisplatin with purified DNA. However, since no evidence of either forming additional adducts with platinated DNA was found the direct protective effect appears to result from inactivation of free Pt drug rather than modulation of adduct formation.
5. STS protected cells against cisplatin but only when present concurrently. Effects on total adduct levels were not fully consistent with the effects on cytotoxicity.
6. Pt-DNA adduct levels in tumour biopsies and blood cells obtained from patients receiving Pt-based chemotherapy were shown to be quantifiable by ICP-MS
7. Pt-DNA adducts levels in tumour biopsies and blood cells showed no correlation indicating that blood cells have limited value as a marker of tumour response.

## References

- Aabo, K., M. Adams, et al. (1998). "Chemotherapy in advanced ovarian cancer: four systematic meta-analyses of individual patient data from 37 randomized trials. Advanced Ovarian Cancer Trialists' Group." British Journal of Cancer **78**(11): 1479-87.
- Abe, R., T. Akiyoshi, et al. (1986). "Protection of Antiproliferative Effect of Cis-Diamminedichloroplatinum(II) by Sodium Thiosulfate." Cancer Chemotherapy and Pharmacology **18**(2): 98-100.
- Aebi, S., B. KurdiHaidar, et al. (1996). "Loss of DNA Mismatch Repair in Acquired Resistance to Cisplatin." Cancer Research **56**(13): 3087-3090.
- Akaboshi, M., K. Kawai, et al. (1992). "The Number of Platinum Atoms Binding to DNA, RNA and Protein Molecules of HeLa-Cells Treated with Cisplatin at its Mean Lethal Concentration." Japanese Journal of Cancer Research **83**(5): 522-526.
- Al-Sarraf, M., W. Fletcher, et al. (1982). "Cisplatin hydration with and without mannitol diuresis in refractory disseminated malignant melanoma: a southwest oncology group study." Cancer Treatment Reports **66**(1): 31-5.
- Andrews, P. A., M. P. Murphy, et al. (1985). "Differential Potentiation of Alkylating and Platinating Agent Cyto-Toxicity in Human Ovarian-Carcinoma Cells by Glutathione Depletion." Cancer Research **45**(12): 6250-6253.
- Andrews, P. A., M. P. Murphy, et al. (1987). "Metallothionein-Mediated Cisplatin Resistance in Human Ovarian-Carcinoma Cells." Cancer Chemotherapy and Pharmacology **19**(2): 149-154.

- Anthoney, D. A., A. J. McIlwrath, et al. (1996). "Microsatellite Instability, Apoptosis, and Loss of p53 Function in Drug-Resistant Tumor Cells." Cancer Research **56**(6): 1374-1381.
- Araya, C. E., R. S. Fennell, et al. (2006). "Sodium thiosulfate treatment for calcific uremic arteriopathy in children and young adults." Clinical Journal of The American Society of Nephrology **1**(6): 1161-6.
- Arrick, B. A. and C. F. Nathan (1984). "Glutathione Metabolism as a Determinant of Therapeutic Efficacy - a Review." Cancer Research **44**(10): 4224-4232.
- Azim-Araghi, A. (2003). Formation of atypical cisplatin-DNA adducts in certain cancer cells. Newcastle, Newcastle University. **Ph. D.**
- Barnham, K. J., M. I. Djuran, et al. (1995). "L-Methionine Increases the Rate of Reaction of 5'-Guanosine Monophosphate with the Anticancer Drug Cisplatin - Mixed-Ligand Adducts and Reversible Methionine Binding." Journal of the Chemical Society - Dalton Transactions(22): 3721-3726.
- Barry, M. A., C. A. Behnke, et al. (1990). "Activation of programmed cell death (apoptosis) by cisplatin, other anticancer drugs, toxins and hyperthermia." Biochemical Pharmacology **40**(10): 2353-62.
- Baselga, J., L. Norton, et al. (1998). "Recombinant Humanized anti-HER2 Antibody (Herceptin (TM)) Enhances the Anti-Tumor Activity of Paclitaxel and Doxorubicin Against HER2/neu Overexpressing Human Breast Cancer Xenografts." Cancer Research **58**(13): 2825-2831.
- Baselga, J., D. Tripathy, et al. (1999). "Phase II Study of Weekly Intravenous Trastuzumab (Herceptin) in Patients with HER2/neu-Overexpressing Metastatic Breast Cancer." Seminars in Oncology **26**(4): 78-83.

- Bass, R., L. W. Ruddock, et al. (2004). "A Major Fraction of Endoplasmic Reticulum-  
Located Glutathione is present as Mixed Disulfides with Protein." Journal of  
Biological Chemistry **279**(7): 5257-5262.
- Beck, D. J. and R. R. Brubaker (1973). "Effect of *cis*-Platinum(II) Diamminodichloride  
on Wild-Type and Deoxyribonucleic Acid Repair-Deficient Mutants of  
*Escherichia coli*." Journal of Bacteriology **116**(3): 1247-1252.
- Beck, D. J., S. Popoff, et al. (1985). "Reactions of the UVRABC Excision Nuclease  
with DNA Damaged by Diamminedichloroplatinum(II)." Nucleic Acids  
Research **13**(20): 7395-7412
- Begleiter, A., K. Lee, et al. (1994). "Chlorambucil induced apoptosis in chronic  
lymphocytic leukemia (CLL) and its relationship to clinical efficacy." Leukemia  
**8 Suppl 1**: S103-6.
- Begleiter, A., M. Mowat, et al. (1996). "Chlorambucil in chronic lymphocytic  
leukemia: mechanism of action." Leukaemia and Lymphoma **23**(3-4): 187-201.
- Behrens, B. C., T. C. Hamilton, et al. (1987). "Characterization of a *cis*-  
Diamminedichloroplatinum(II)-Resistant Human Ovarian-Cancer Cell-Line and  
Its Use in Evaluation of Platinum Analogs." Cancer Research **47**(2): 414-418.
- Bellon, S. F. and S. J. Lippard (1990). "Bending studies of DNA site-specifically  
modified by cisplatin, trans-diamminedichloroplatinum(II) and *cis*-  
[Pt(NH<sub>3</sub>)<sub>2</sub>(N<sub>3</sub>-cytosine)Cl]<sup>+</sup>." Biophysical Chemistry **35**(2-3): 179-88.
- Bellon, S. F., J. H. Coleman, et al. (1991). "DNA Unwinding Produced by Site-Specific  
Intrastrand Cross-Links of the Antitumor Drug *cis*-  
Diamminedichloroplatinum(II)." Biochemistry **30**(32): 8026-8035.

- Bergers, G., K. Javaherian, et al. (1999). "Effects of angiogenesis inhibitors on multistage carcinogenesis in mice." Science **284**(5415): 808-12.
- Blommaert, F. A. and C. P. Saris (1995). "Detection of Platinum-DNA Adducts by <sup>32</sup>P Postlabeling." Nucleic Acids Research **23**(8): 1300-1306.
- Blommaert, F. A., H. C. M. Vandijkknijnenburg, et al. (1995). "Formation of DNA-Adducts by the Anticancer Drug Carboplatin - Different Nucleotide-Sequence Preferences *in vitro* and in Cells." Biochemistry **34**(26): 8474-8480.
- Bolderson, E., D. J. Richard, et al. (2009). "Recent advances in cancer therapy targeting proteins involved in DNA double-strand break repair." Clinical Cancer Research **15**(20): 6314-20.
- Bonetti, A., P. Apostoli, et al. (1996). "Inductively Coupled Plasma Mass Spectroscopy Quantitation of Platinum-DNA Adducts in Peripheral Blood Leukocytes of Patients Receiving Cisplatin- or Carboplatin-Based Chemotherapy." Clinical Cancer Research **2**(11): 1829-1835.
- Bose, R. N., S. Moghaddas, et al. (1995). "Reactivity of Glutathione and Cysteine toward Platinum(II) in the Presence and Absence of Guanosine 5'-Monophosphate." Inorganic Chemistry **34**(23): 5878-5883.
- Bose, R. N., S. K. Ghosh, et al. (1997). "Kinetic Analysis of the *cis*-Diamminedichloroplatinum(II)-Cysteine Reaction: Implications to the Extent of Platinum-DNA Binding." Journal of Inorganic Biochemistry **65**(3): 199-205.
- Brouwer, J., P. Vandeputte, et al. (1981). "Base-Pair Substitution Hotspots in GAG and GCG Nucleotide-Sequences in *Escherichia coli* K-12 Induced by *cis*-Diamminedichloroplatinum(II)." Proceedings of the National Academy of Sciences of the United States of America **78**(11): 7010-7014.

- Burchenal, J. H., K. Kalaher, et al. (1978). "Studies of cross-resistance, synergistic combinations and blocking of activity of platinum derivatives." Biochimie **60**(9): 961-965.
- Burchenal, J. H., K. Kalaher, et al. (1979). "Rationale for development of platinum analogs." Cancer Treatment Reports **63**(9-10): 1493-8.
- Burger, H., K. Nooter, et al. (1999). "Distinct p53-Independent Apoptotic Cell Death Signalling Pathways in Testicular Germ Cell Tumour Cell Lines." International Journal of Cancer **81**(4): 620-628.
- Busch, A. E., S. Waldegger, et al. (1994). "Electrogenic cotransport of Na<sup>+</sup> and sulfate in *Xenopus* oocytes expressing the cloned Na<sup>+</sup>SO<sub>4</sub><sup>2-</sup> transport protein NaSi-1." Journal of Biological Chemistry **269**(17): 12407-9.
- Cacciatore, F., C. Napoli, et al. (1999). "Quality of life determinants and hearing function in an elderly population: Osservatorio Geriatrico Campano Study Group." Gerontology **45**(6): 323-8.
- Calabrese, C. R., R. Almassy, et al. (2004). "Anticancer chemosensitization and radiosensitization by the novel poly(ADP-ribose) polymerase-1 inhibitor AG14361." Journal of the National Cancer Institute **96**(1): 56-67.
- Calvert, A. H., S. J. Harland, et al. (1982). "Early Clinical-Studies with Cis-Diammine-1,1-Cyclobutane Dicarboxylate Platinum-II." Cancer Chemotherapy and Pharmacology **9**(3): 140-147.
- Calvert, A. H., D. R. Newell, et al. (1989). "Carboplatin Dosage - Prospective Evaluation of a Simple Formula Based on Renal-Function." Journal of Clinical Oncology **7**(11): 1748-1756.

- Cantley, L. C. and B. G. Neel (1999). "New insights into tumor suppression: PTEN suppresses tumor formation by restraining the phosphoinositide 3-kinase/AKT pathway." Proceedings of the National Academy of Sciences of the United States of America **96**(8): 4240-5.
- Cassidy, J. and J. L. Misset (2002). "Oxaliplatin-Related Side Effects: Characteristics and Management." Seminars in Oncology **29**(5): 11-20.
- Cavaluzzi, M. J. and P. N. Borer (2004). "Revised UV Extinction Coefficients for Nucleoside-5'-Monophosphates and Unpaired DNA and RNA." Nucleic Acids Research **32**(1): e13.
- Cersosimo, R. J. (1989). "Cisplatin neurotoxicity." Cancer Treatment Reviews **16**(4): 195-211.
- Chen, H. H. W., I. S. Song, et al. (2008). "Elevated Glutathione Levels confer Cellular Sensitization to Cisplatin Toxicity by Up-Regulation of Copper Transporter hCtr1." Molecular Pharmacology **74**(3): 697-704.
- Chin, L., J. Pomerantz, et al. (1998). "The INK4a/ARF tumor suppressor: one gene--two products--two pathways." Trends in Biochemical Sciences **23**(8): 291-6.
- Chu, G. (1994). "Cellular-Responses to Cisplatin - the Roles of DNA-Binding Proteins and DNA-Repair." Journal of Biological Chemistry **269**(2): 787-790.
- Corrie, P. (2004). "Cytotoxic Chemotherapy: Clinical Aspects." Medicine **32**(3): 25-28.
- Costa, R. M. A., V. Chigancas, et al. (2003). "The eukaryotic nucleotide excision repair pathway." Biochimie **85**(11): 1083-1099.

- Curt, G. A., J. J. Grygiel, et al. (1983). "A Phase-I and Pharmacokinetic Study of Diamminecyclobutanedicarboxylatoplatinum (NSC-241240)." Cancer Research **43**(9): 4470-4473.
- Curtin, N. J. (2005). "PARP inhibitors for cancer therapy." Expert Reviews in Molecular Medicine **7**(4): 1-20.
- Cvitkovic, E., J. Spaulding, et al. (1977). "Improvement of Cis-Dichlorodiammineplatinum (NSC 119875) - Therapeutic Index in an Animal-Model." Cancer **39**(4): 1357-1361.
- Dabholkar, M., R. Parker, et al. (1992). "Determinants of Cisplatin Sensitivity in Nonmalignant Non-Drug-Selected Human T-Cell Lines." Mutation Research **274**(1): 45-56.
- Dabholkar, M., J. Vionnet, et al. (1994). "Messenger-RNA Levels of XPAC and ERCC1 in Ovarian-Cancer Tissue Correlate with Response to Platinum-Based Chemotherapy." Journal of Clinical Investigation **94**(2): 703-708.
- de Laat, W. L., N. G. J. Jaspers, et al. (1999). "Molecular mechanism of nucleotide excision repair." Genes & Development **13**(7): 768-785.
- de Silva, I. U., P. H. Clingen, et al. (1999). "The role of nucleotide excision repair in the repair of DNA damage induced by mono- and bifunctional, major and minor groove alkylating agents." British Journal of Cancer **80**: 42-42.
- de Silva, I. U., P. J. McHugh, et al. (2000). "Defining the roles of nucleotide excision repair and recombination in the repair of DNA interstrand cross-links in mammalian cells." Molecular and Cellular Biology **20**(21): 7980-7990.

- Dedon, P. C. and R. F. Borch (1987). "Characterization of the Reactions of Platinum Antitumor Agents with Biologic and Nonbiologic Sulfur-Containing Nucleophiles." Biochemical Pharmacology **36**(12): 1955-1964.
- Delaloge, S., A. Laadem, et al. (2000). "Pilot study of the paclitaxel, oxaliplatin, and cisplatin combination in patients with advanced/recurrent ovarian cancer." American Journal of Clinical Oncology-Cancer Clinical Trials **23**(6): 569-574.
- Deubel, D. V. (2004). "Factors governing the kinetic competition of nitrogen and sulfur ligands in cisplatin binding to biological targets." Journal of the American Chemical Society **126**(19): 5999-6004.
- Diamandopoulos, G. T. (1996). "Cancer: An Historical Perspective." Anticancer Research **16**(4A): 1595-1602.
- Doolittle, N. D., L. L. Muldoon, et al. (2001). "Delayed Sodium Thiosulfate as an Otoprotectant Against Carboplatin-Induced Hearing Loss in Patients with Malignant Brain Tumors." Clinical Cancer Research **7**(3): 493-500.
- Drobnik, J. and P. Horacek (1973). "Specific biological activity of platinum complexes. Contribution to the theory of molecular mechanism." Chemical Biological Interactions **7**(4): 223-9.
- Drummond, J. T., A. Anthoney, et al. (1996). "Cisplatin and Adriamycin Resistance are associated with MutL $\alpha$  and Mismatch Repair Deficiency in an Ovarian Tumor Cell Line." Journal of Biological Chemistry **271**(33): 19645-19648.
- Duckett, D. R., J. T. Drummond, et al. (1996). "Human MutS $\alpha$  recognizes damaged DNA base pairs containing O6-methylguanine, O4-methylthymine, or the cisplatin-d(GpG) adduct." Proceedings of the National Academy of Sciences of the United States of America **93**(13): 6443-7.

- Durant, S. T., M. M. Morris, et al. (1999). "Dependence on RAD52 and RAD1 for anticancer drug resistance mediated by inactivation of mismatch repair genes." Current Biology **9**(1): 51-54.
- Dyson, N., P. M. Howley, et al. (1989). "The human papilloma virus-16 E7 oncoprotein is able to bind to the retinoblastoma gene product." Science **243**(4893): 934-7.
- Eastman, A. (1983). "Characterization of the Adducts Produced in DNA by Cis-Diamminedichloroplatinum(II) and Cis-Dichloro(Ethylenediamine)Platinum(II)." Biochemistry **22**(16): 3927-3933.
- Eastman, A. (1985). "Interstrand Cross-Links and Sequence Specificity in the Reaction of *cis*-Dichloro(Ethylenediamine)Platinum(II) with DNA." Biochemistry **24**: 5027-5032.
- Eastman, A. (1986). "Reevaluation of Interaction of *cis*-Dichloro(Ethylenediamine)Platinum(II) with DNA." Biochemistry **25**(13): 3912-3915.
- Eastman, A. (1987). "Cross-Linking of Glutathione to DNA by Cancer Chemotherapeutic Platinum Coordination Complexes." Chemical Biological Interactions **61**: 241-248.
- Eastman, A. and N. Schulte (1988). "Enhanced DNA-Repair as a Mechanism of Resistance to *cis*-Diamminedichloroplatinum(II)." Biochemistry **27**(13): 4730-4734.
- Eisenberg, B. L. (2003). "Imatinib mesylate: a molecularly targeted therapy for gastrointestinal stromal tumors." Oncology **17**(11): 1615-20; discussion 1620, 1623, 1626 passim.

- Elferink, F., W. J. Van der Vijgh, et al. (1986). "Interaction of Cisplatin and Carboplatin with Sodium Thiosulfate: Reaction Rates and Protein Binding." Clinical Chemistry **32**(4): 641-645.
- el-Khateeb, M., T. G. Appleton, et al. (1999). "Reactions of cisplatin hydrolytes with methionine, cysteine, and plasma ultrafiltrate studied by a combination of HPLC and NMR techniques." Journal of Inorganic Biochemistry **77**(1-2): 13-21.
- Elmore, S. (2007). "Apoptosis: A Review of Programmed Cell Death." Toxicologic Pathology **35**(4): 495-516.
- Endo, T., M. Yoshikawa, et al. (2004). "Immunohistochemical metallothionein expression in hepatocellular carcinoma: relation to tumor progression and chemoresistance to platinum agents." Journal of Gastroenterology **39**(12): 1196-1201.
- Esteban-Fernandez, D., B. Canas, et al. (2007). "SEC-ICP-MS and ESI-MS as tools to study the Interaction between Cisplatin and Cytosolic Biomolecules." Journal of Analytical Atomic Spectrometry **22**(9): 1113-1121.
- Esteban-Fernandez, D., M. Montes-Bayon, et al. (2008). "Atomic (HPLC-ICP-MS) and Molecular Mass Spectrometry (ESI-Q-TOF) to study *cis*-Platin Interactions with Serum Proteins." Journal of Analytical Atomic Spectrometry **23**(3): 378-384.
- Extra, J. M., M. Espie, et al. (1990). "Phase-I Study of Oxaliplatin in Patients with Advanced Cancer." Cancer Chemotherapy and Pharmacology **25**(4): 299-303.
- Faivre, S., S. Kalla, et al. (1999). "Oxaliplatin and paclitaxel combination in patients with platinum-pretreated ovarian carcinoma: An investigator-originated compassionate-use experience." Annals of Oncology **10**(9): 1125-1128.

- Fajac, A., J. Da Silva, et al. (1996). "Cisplatin-induced apoptosis and p53 gene status in a cisplatin-resistant human ovarian carcinoma cell line." International Journal of Cancer **68**: 67-74.
- Fan, S., S. El-Deiry, et al. (1994). "The p53 gene mutations are associated with decreased sensitivity of human lymphoma cells to DNA-damaging agents." Cancer Research **54**: 5824-5830.
- Fedi, P., S. R. Tronick, et al. (1997). Growth Factors. Baltimore, MD, McGraw-Hill Medical.
- Feliu, J., J. L. Firvida, et al. (2009). "Combination therapy with docetaxel and low dose of cisplatin in elderly patients with advanced non-small cell lung cancer: multicenter phase II study." Cancer Chemotherapy and Pharmacology **63**(3): 403-9.
- Fichtinger-Schepman, A. M., J. L. van der Veer, et al. (1985). "Adducts of the Antitumor Drug *cis*-Diamminedichloroplatinum(II) with DNA: Formation, Identification, and Quantitation." Biochemistry **24**(3): 707-713.
- Fichtinger-Schepman, A. M. J., A. T. van Oosterom, et al. (1987). "*Cis*-Diamminedichloroplatinum(II)-Induced DNA Adducts in Peripheral Leukocytes from Seven Cancer Patients: Quantitative Immunochemical Detection of the Adduct Induction and Removal after a Single Dose of *cis*-Diamminedichloroplatinum(II)." Cancer Research **47**: 3000-3004.
- Fichtinger-Schepman, A. M., C. P. Vendrik, et al. (1989). "Platinum concentrations and DNA adduct levels in tumors and organs of cisplatin-treated LOU/M rats inoculated with cisplatin-sensitive or -resistant immunoglobulin M immunocytoma." Cancer Research **49**(11): 2862-7.

Fichtinger-Schepman, A. M., S. D. van der Velde-Visser, et al. (1990). "Kinetics of the formation and removal of cisplatin-DNA adducts in blood cells and tumor tissue of cancer patients receiving chemotherapy: comparison with in vitro adduct formation." Cancer Research **50**(24): 7887-94.

Fichtinger-Schepman, A. M. J., H. C. M. Vandijkknijnenburg, et al. (1995 (a)). "Cisplatin- and Carboplatin-DNA-Adducts - Is Pt-AG the Cytotoxic Lesion?" Carcinogenesis **16**(10): 2447-2453.

Fichtinger-Schepman, A. M. J., H. C. M. Vandijkknijnenburg, et al. (1995 (b)). "Effects of Thiourea and Ammonium Bicarbonate on the Formation and Stability of Bifunctional Cisplatin-DNA Adducts - Consequences for the Accurate Quantification of Adducts in (Cellular) DNA." Journal of Inorganic Biochemistry **58**(3): 177-191.

Filipski, J., K. W. Kohn, et al. (1979). "Thiourea Reverses Cross-Links and Restores Biological Activity in DNA treated with Dichlorodiaminoplatinum(II)." Science **204**(4389): 181-183.

Fink, D., S. Nebel, et al. (1996). "The Role of DNA Mismatch Repair in Platinum Drug Resistance." Cancer Research **56**(21): 4881-4886.

Folkman, J. (1997). "Angiogenesis and angiogenesis inhibition: an overview." EXS **79**: 1-8.

Fram, R. J., P. S. Cusick, et al. (1985). "Mismatch Repair of *cis*-Diamminedichloroplatinum(II)-Induced DNA Damage." Molecular Pharmacology **28**(1): 51-55.

Fram, R. J., B. A. Woda, et al. (1990). "Characterization of Acquired-Resistance to *cis*-Diamminedichloroplatinum(II) in BE Human-Colon Carcinoma-Cells." Cancer Research **50**(1): 72-77.

- Frankenberg-Schwager, M., D. Kirchermeier, et al. (2005). "Cisplatin-mediated DNA double-strand breaks in replicating but not in quiescent cells of the yeast *Saccharomyces cerevisiae*." Toxicology **212**(2-3): 175-84.
- Fuertes, M. A., C. Alonso, et al. (2003). "Biochemical Modulation of Cisplatin Mechanisms of Action: Enhancement of Antitumor Activity and Circumvention of Drug Resistance." Chemical Reviews **103**(3): 645-662.
- Fukuda, M., Y. Ohe, et al. (1995). "Evaluation of novel platinum complexes, inhibitors of topoisomerase I and II in non-small cell lung cancer (NSCLC) sublines resistant to cisplatin." Anticancer Research **15**(2): 393-8.
- Furuta, T., T. Ueda, et al. (2002). "Transcription-coupled nucleotide excision repair as a determinant of cisplatin sensitivity of human cells." Cancer Research **62**(17): 4899-4902.
- Fynan, T. M. and M. Reiss (1993). "Resistance to inhibition of cell growth by transforming growth factor-beta and its role in oncogenesis." Critical Reviews in Oncology **4**(5): 493-540.
- Gaffney, D. K., A. Du Bois, et al. (2007). "Practice patterns of radiotherapy in cervical cancer among member groups of the Gynecologic Cancer Intergroup (GCIIG)." International Journal of Radiation Oncology Biology Physics **68**(2): 485-90.
- Ghazal-Aswad, S., M. J. Tilby, et al. (1999). "Pharmacokinetically Guided Dose Escalation of Carboplatin in Epithelial Ovarian Cancer: Effect on Drug-Plasma AUC and Peripheral Blood Drug-DNA Adduct Levels." Annals of Oncology **10**(3): 329-334.
- Gilman, A., F. S. Philips, et al. (1946). "The Renal Clearance of Thiosulfate with observations on its Volume Distribution." American Journal of Physiology **146**(3): 348-357.

- Godwin, A. K., A. Meister, et al. (1992). "High-Resistance to Cisplatin in Human Ovarian-Cancer Cell-Lines Is Associated with Marked Increase of Glutathione Synthesis." Proceedings of the National Academy of Sciences of the United States of America **89**(7): 3070-3074.
- Gore, M. E., A. H. Calvert, et al. (1987). "High-Dose Carboplatin in the Treatment of Lung-Cancer and Mesothelioma - a Phase-I Dose Escalation Study." European Journal of Cancer & Clinical Oncology **23**(9): 1391-1397.
- Griffith, O. W. and A. Meister (1985). "Origin and Turnover of Mitochondrial Glutathione." Proceedings of the National Academy of Sciences of the United States of America **82**(14): 4668-4672.
- Hall, A. G. and M. J. Tilby (1992). "Mechanisms of Action of, and Modes of Resistance to, Alkylating-Agents Used in the Treatment of Hematological Malignancies." Blood Reviews **6**(3): 163-173.
- Hamaguchi, K., A. K. Godwin, et al. (1993). "Cross-Resistance to Diverse Drugs Is Associated with Primary Cisplatin Resistance in Ovarian-Cancer Cell-Lines." Cancer Research **53**(21): 5225-5232.
- Hambley, T. W. (1997). "The Influence Of Structure On The Activity and Toxicity of Pt anticancer Drugs." Coordination Chemistry Reviews **166**: 181-223.
- Hanahan, D. and J. Folkman (1996). "Patterns and emerging mechanisms of the angiogenic switch during tumorigenesis." Cell **86**(3): 353-64.
- Hanahan, D. and R. A. Weinberg (2000). "The Hallmarks of Cancer." Cell **100**(1): 57-70.

- Harder, H. C. and B. Rosenberg (1970). "Inhibitory effects of anti-tumor platinum compounds on DNA, RNA and protein syntheses in mammalian cells in vitro." International Journal of Cancer **6**(2): 207-16.
- Harland, S. J., L. A. Gumbrell, et al. (1991). "Carboplatin dose in combination chemotherapy for testicular cancer." European Journal of Cancer **27**(6): 691-5.
- Harley, C. B., A. B. Futcher, et al. (1990). "Telomeres shorten during ageing of human fibroblasts." Nature **345**(6274): 458-60.
- Harmers, F. P., W. H. Gispen, et al. (1991). "Neurotoxic side-effects of cisplatin." European Journal of Cancer **27**(3): 372-6.
- Harned, T. M., O. Kalous, et al. (2008). "Sodium Thiosulfate Administered Six Hours After Cisplatin Does Not Compromise Antineuroblastoma Activity." Clinical Cancer Research **14**(2): 533-540.
- Harrington, C. F., R. C. Le Pla, et al. (2010). "Determination of Cisplatin 1,2-intrastrand Guanine-Guanine DNA adducts in human leukocytes by high-performance liquid chromatography coupled to inductively coupled plasma mass spectrometry." Chemical Research in Toxicology **23**(8): 1313-21.
- Harris, C. C. (1996). "p53 tumor suppressor gene: from the basic research laboratory to the clinic--an abridged historical perspective." Carcinogenesis **17**(6): 1187-98.
- Harvey, V. J., B. D. Evans, et al. (1991). "Reduction of Carboplatin Induced Emesis by Ondansetron." British Journal of Cancer **63**(6): 942-944.
- Hastie, N. D., M. Dempster, et al. (1990). "Telomere reduction in human colorectal carcinoma and with ageing." Nature **346**(6287): 866-8.

- Hayes, D. M., E. Cvitkovic, et al. (1977). "High dose cis-platinum diammine dichloride: amelioration of renal toxicity by mannitol diuresis." Cancer **39**(4): 1372-81.
- Higashimoto, M., A. Kanzaki, et al. (2003). "Expression of copper-transporting P-type adenosine triphosphatase in human esophageal carcinoma." International Journal of Molecular Medicine **11**(3): 337-341.
- Hindley, P. (1997). "Psychiatric aspects of hearing impairments." Journal of Child Psychology and Psychiatry **38**(1): 101-17.
- Hirose, T., Y. Mizutani, et al. (2006). "The combination of cisplatin and vinorelbine with concurrent thoracic radiation therapy for locally advanced stage IIIA or IIIB non-small-cell lung cancer." Cancer Chemotherapy and Pharmacology **58**(3): 361-7.
- Hiyama, E., T. Yokoyama, et al. (1995 (a)). "Telomerase activity in gastric cancer." Cancer Research **55**(15): 3258-62.
- Hiyama, K., E. Hiyama, et al. (1995 (b)). "Telomerase activity in small-cell and non-small-cell lung cancers." Journal of the National Cancer Institute **87**(12): 895-902.
- Hiyama, E., L. Gollahon, et al. (1996). "Telomerase activity in human breast tumors." Journal of the National Cancer Institute **88**(2): 116-22.
- Hobbs, S. K., W. L. Monsky, et al. (1998). "Regulation of transport pathways in tumor vessels: role of tumor type and microenvironment." Proceedings of the National Academy of Sciences of the United States of America **95**(8): 4607-12.

- Hoebbers, F. J., D. Pluim, et al. (2006). "Prediction of treatment outcome by cisplatin-DNA adduct formation in patients with stage III/IV head and neck squamous cell carcinoma, treated by concurrent cisplatin-radiation (RADPLAT)." International Journal of Cancer **119**(4): 750-6.
- Hoebbers, F. J. P., D. Pluim, et al. (2008). "Cisplatin-DNA Adduct Formation in Patients Treated with Cisplatin-Based Chemoradiation: Lack of Correlation between Normal Tissues and Primary Tumor." Cancer Chemotherapy and Pharmacology **61**(6): 1075-1081.
- Hoeschele, J. D., H. D. Showalter, et al. (1994). "Synthesis, structural characterization, and antitumor properties of a novel class of large-ring platinum(II) chelate complexes incorporating the cis-1,4-diaminocyclohexane ligand in a unique locked boat conformation." Journal of Medicinal Chemistry **37**(17): 2630-6.
- Holzer, A. K., G. Samimi, et al. (2004 (a)). "The Copper Influx Transporter Human Copper Transport Protein 1 Regulates the Uptake of Cisplatin in Human Ovarian Carcinoma Cells." Molecular Pharmacology **66**(4): 817-823.
- Holzer, A. K., K. Katano, et al. (2004 (b)). "Cisplatin Rapidly Down-Regulates Its Own Influx Transporter hCTR1 in Cultured Human Ovarian Carcinoma Cells." Clinical Cancer Research **10**(19): 6744-6749.
- Horwich, A., D. P. Dearnaley, et al. (1991). "Effectiveness of carboplatin, etoposide, and bleomycin combination chemotherapy in good-prognosis metastatic testicular nonseminomatous germ cell tumors." Journal of Clinical Oncology **9**(1): 62-9.
- Hospers, G. A. P., N. H. Mulder, et al. (1988). "Characterization of a Human Small Cell Lung-Carcinoma Cell-Line with Acquired-Resistance to cis-Diamminedichloroplatinum(II) *In Vitro*." Cancer Research **48**(23): 6803-6807.

- Howell, S. B. and R. Taetle (1980). "Effect of Sodium Thiosulfate on Cis-Dichlorodiammineplatinum(II) Toxicity and Anti-Tumor Activity in L1210 Leukemia." Cancer Treatment Reports **64**(4-5): 611-616.
- Howell, S. B., C. L. Pfeifle, et al. (1982). "Intraperitoneal cisplatin with systemic thiosulfate protection." Annals of Internal Medicine **97**(6): 845-51.
- Howle, J. A. and G. R. Gale (1970). "Cis-dichlorodiammineplatinum (II). Persistent and selective inhibition of deoxyribonucleic acid synthesis in vivo." Biochemical Pharmacology **19**(10): 2757-62.
- Huang, J. C., D. B. Zamble, et al. (1994). "Hmg-Domain Proteins Specifically Inhibit the Repair of the Major DNA Adduct of the Anticancer Drug Cisplatin by Human Excision Nuclease." Proceedings of the National Academy of Sciences of the United States of America **91**(22): 10394-10398.
- Hussain, M. H., T. R. Glass, et al. (2001). "Combination cisplatin, 5-fluorouracil and radiation therapy for locally advanced unresectable or medically unfit bladder cancer cases: a Southwest Oncology Group Study." Journal of Urology **165**(1): 56-60; discussion 60-1.
- Hwang, C., A. J. Sinsky, et al. (1992). "Oxidized Redox State of Glutathione in the Endoplasmic-Reticulum." Science **257**(5076): 1496-1502.
- Ishida, S., J. Lee, et al. (2002). "Uptake of the Anticancer Drug Cisplatin Mediated by the Copper Transporter Ctr1 in Yeast and Mammals." Proceedings of the National Academy of Sciences of the United States of America **99**(22): 14298-14302.

- Ishikawa, T. and F. Aliosman (1993). "Glutathione-Associated *cis*-Diamminedichloroplatinum(II) Metabolism and ATP-Dependent Efflux from Leukemia-Cells - Molecular Characterization of Glutathione-Platinum Complex and its Biological Significance." Journal of Biological Chemistry **268**(27): 20116-20125.
- Iwamoto, Y., T. Kawano, et al. (1984). ""Two-route chemotherapy" using high-dose ip cisplatin and iv sodium thiosulfate, its antidote, for peritoneally disseminated cancer in mice." Cancer Treatment Reports **68**(11): 1367-73.
- Jain, R. K. (1996). "Delivery of molecular medicine to solid tumors." Science **271**(5252): 1079-80.
- Jamieson, E. R. and S. J. Lippard (1999). "Structure, Recognition, and Processing of Cisplatin-DNA Adducts." Chemistry Reviews **99**(9): 2467-2498.
- Jennerwein, M. M., A. Eastman, et al. (1989). "Characterization of Adducts produced in DNA by Isomeric 1,2-Diaminocyclohexaneplatinum(II) Complexes." Chemical Biological Interactions **70**: 39-49.
- Jennerwein, M. and P. A. Andrews (1995). "Effect of Intracellular Chloride on the Cellular Pharmacodynamics of *cis*-Diamminedichloroplatinum(II)." Drug Metabolism and Disposition **23**(2): 178-184.
- Johnson, N. P. (1982). "Preliminary Characterization of the Adducts Formed between the Anti-Tumor Compound  $Cis-Pt(NH_3)_2Cl_2$  and DNA." Biochemical and Biophysical Research Communications **104**(4): 1394-1400.
- Johnson, N. P., A. M. Mazard, et al. (1985). "Mechanism of the Reaction between  $Cis-[PtCl_2(NH_3)_2]$  and DNA In vitro." Journal of the American Chemical Society **107**(22): 6376-6380.

- Johnson, S. W., P. A. Swiggard, et al. (1994 (a)). "Relationship between Platinum-DNA Adduct Formation and Removal and Cisplatin Cytotoxicity in Cisplatin-Sensitive and Cisplatin-Resistant Human Ovarian-Cancer Cells." Cancer Research **54**(22): 5911-5916.
- Johnson, S. W., R. P. Perez, et al. (1994 (b)). "Role of Platinum-DNA Adduct Formation and Removal in Cisplatin Resistance in Human Ovarian-Cancer Cell-Lines." Biochemical Pharmacology **47**(4): 689-697.
- Johnson, S. W., P. B. Laub, et al. (1997). "Increased platinum-DNA damage tolerance is associated with cisplatin resistance and cross-resistance to various chemotherapeutic agents in unrelated human ovarian cancer cell lines." Cancer Research **57**(5): 850-856.
- Kantarjian, H. M., J. Shan, et al. (2001). "Response to therapy is independently associated with survival prolongation in chronic myelogenous leukemia in the blastic phase." Cancer **92**(10): 2501-7.
- Kantarjian, H. M. and M. Talpaz (2001). "Imatinib mesylate: clinical results in Philadelphia chromosome-positive leukemias." Seminars in Oncology **28**(5 Suppl 17): 9-18.
- Karran, P. and M. Bignami (1994). "DNA damage tolerance, mismatch repair and genome instability." Bioessays **16**(11): 833-9.
- Kartalou, M. and J. M. Essigmann (2001). "Mechanisms of Resistance to Cisplatin." Mutation Research **478**(1-2): 23-43.
- Katano, K., A. Kondo, et al. (2002). "Acquisition of Resistance to Cisplatin is Accompanied by Changes in the Cellular Pharmacology of Copper." Cancer Research **62**(22): 6559-6565.

- Katano, K., R. Safaei, et al. (2003). "The Copper Export Pump ATP7B Modulates the Cellular Pharmacology of Carboplatin in Ovarian Carcinoma Cells." Molecular Pharmacology **64**(2): 466-473.
- Keane, T. E., J. R. Gingrich, et al. (1994). "Combination versus single agent therapy in effecting complete therapeutic response in human bladder cancer: analysis of cisplatin and/or 5-fluorouracil in an in vivo survival model." Cancer Research **54**(2): 475-81.
- Kelland, L. R. (1993). "New platinum antitumor complexes." Critical Reviews in Oncology Hematology(3): 191-219.
- Kelland, L. R., P. Mistry, et al. (1992). "Establishment and Characterization of an *In Vitro* Model of Acquired-Resistance to Cisplatin in a Human Testicular Nonseminomatous Germ-Cell Line." Cancer Research **52**(7): 1710-1716.
- Kelland, L. (2007). "The Resurgence of Platinum-based Cancer Chemotherapy." Nature Reviews Cancer **7**(8): 573-584.
- Keller, B. K., J. L. Morton, et al. (1999). "The effect of visual and hearing impairments on functional status." Journal of the American Geriatric Society **47**(11): 1319-25.
- Kennedy, I. C. S., B. M. Fitzharris, et al. (1990). "Carboplatin Is Ototoxic." Cancer Chemotherapy and Pharmacology **26**(3): 232-234.
- Kerr, J. F., A. H. Wyllie, et al. (1972). "Apoptosis: a basic biological phenomenon with wide-ranging implications in tissue kinetics." British Journal of Cancer **26**(4): 239-57.

- Kidani, Y., K. Inagaki, et al. (1978). "Anti-Tumor Activity of 1,2-Diaminocyclohexane-Platinum Complexes against Sarcoma-180 Ascites Form." Journal of Medicinal Chemistry **21**(12): 1315-1318.
- Kim, N. W., M. A. Piatyszek, et al. (1994). "Specific association of human telomerase activity with immortal cells and cancer." Science **266**(5193): 2011-5.
- Klomp, A. E., B. B. Tops, et al. (2002). "Biochemical characterization and subcellular localization of human copper transporter 1 (hCTR1)." Biochemical Journal **364**(Pt 2): 497-505.
- Knox, R. J., F. Friedlos, et al. (1986). "Mechanism of Cytotoxicity of Anticancer Platinum Drugs - Evidence That *cis*-Diamminedichloroplatinum(II) and *cis*-Diammine-(1,1-Cyclobutanedicarboxylato)Platinum(II) Differ Only in the Kinetics of their Interaction with DNA." Cancer Research **46**(4): 1972-1979.
- Koberle, B., K. A. Grimaldi, et al. (1997). "DNA Repair Capacity and Cisplatin Sensitivity of Human Testis Tumour Cells." International Journal of Cancer **70**(5): 551-555.
- Koberle, B., J. R. W. Masters, et al. (1999). "Defective Repair of Cisplatin-Induced DNA Damage caused by Reduced XPA Protein in Testicular Germ Cell Tumours." Current Biology **9**(5): 273-276.
- Kopf-Maier, P. and S. K. Muhlhausen (1992). "Changes in the cytoskeleton pattern of tumor cells by cisplatin in vitro." Chemical Biological Interactions **82**(3): 295-316.
- Kozelka, J., F. Legendre, et al. (1999). "Kinetic Aspects of Interaction Between DNA and Platinum Complexes." Coordination Chemistry Reviews **190-192**: 61-82.

- Kremens, B., B. Gruhn, et al. (2002). "High-dose chemotherapy with autologous stem cell rescue in children with nephroblastoma." Bone Marrow Transplantation **30**(12): 893-898.
- Kurosaka, K., M. Takahashi, et al. (2003). "Silent cleanup of very early apoptotic cells by macrophages." Journal of Immunology **171**(9): 4672-9.
- Kusumoto, R., C. Masutani, et al. (2001). "Diversity of the damage recognition step in the global genomic nucleotide excision repair in vitro." Mutation Research **485**(3): 219-27.
- Langford, L. A., M. A. Piatyszek, et al. (1995). "Telomerase activity in human brain tumours." Lancet **346**(8985): 1267-8.
- Larson, C. A., B. G. Blair, et al. (2009). "The Role of the Mammalian Copper Transporter 1 in the Cellular Accumulation of Platinum-Based Drugs." Molecular Pharmacology **75**(2): 324-330.
- Lau, J. K. C. and D. V. Deubel (2005). "Loss of Ammine from Platinum(II) Complexes: Implications for Cisplatin Inactivation, Storage, and Resistance." Chemistry - A European Journal **11**(9): 2849-2855.
- Lee, A., L. Beck, et al. (2000). "The human renal sodium sulfate cotransporter (SLC13A1; hNaSi-1) cDNA and gene: organization, chromosomal localization, and functional characterization." Genomics **70**(3): 354-63.
- Lee, N. S., J. H. Byun, et al. (2004). "Combination of gemcitabine and cisplatin as first-line therapy in advanced non-small-cell lung cancer." Cancer Research Treatments **36**(3): 173-7.

- Levi, F., J. L. Misset, et al. (1992). "A Chronopharmacologic Phase-II Clinical-Trial with 5-Fluorouracil, Folinic Acid, and Oxaliplatin Using an Ambulatory Multichannel Programmable Pump - High Antitumor Effectiveness against Metastatic Colorectal-Cancer." Cancer **69**(4): 893-900.
- Liedert, B., D. Pluim, et al. (2006). "Adduct-Specific Monoclonal Antibodies for the Measurement of Cisplatin-Induced DNA Lesions in Individual Cell Nuclei." Nucleic Acids Research **34**(6): e47.
- Lin, X. J., T. Okuda, et al. (2002). "The Copper Transporter CTR1 Regulates Cisplatin Uptake in *Saccharomyces cerevisiae*." Molecular Pharmacology **62**(5): 1154-1159.
- Lin, A. and M. E. Ray (2006). "Targeted and systemic radiotherapy in the treatment of bone metastasis." Cancer Metastasis Reviews **25**(4): 669-75.
- Lippert, B. (1999). Cisplatin: Chemistry and Biochemistry of a Leading Anticancer Drug, Helvetica Chimica Acta.
- Loehrer, P. J. and L. H. Einhorn (1984). "Drugs 5 Years Later - Cisplatin." Annals of Internal Medicine **100**(5): 704-713.
- Lu, S. C. (1999). "Regulation of Hepatic Glutathione Synthesis: Current Concepts and Controversies." Faseb Journal **13**(10): 1169-1183.
- Luo, F. R., S. D. Wyrick, et al. (1998). "Cytotoxicity, cellular uptake, and cellular biotransformations of oxaliplatin in human colon carcinoma cells." Oncology Research **10**(11-12): 595-603.
- Lutzker, S. G. and A. J. Levine (1996). "A functionally inactive p53 protein in teratocarcinoma cells is activated by either DNA damage or cellular proliferation." Nature Medicine **2**: 804-810.

- Machover, D., E. DiazRubio, et al. (1996). "Two consecutive phase II studies of oxaliplatin (L-OHP) for treatment of patients with advanced colorectal carcinoma who were resistant to previous treatment with fluoropyrimidines." Annals of Oncology **7**(1): 95-98.
- Maeda, Y., K. Nunomura, et al. (1990). "Differential scanning calorimetric study of the effect of intercalators and other kinds of DNA-binding drugs on the stepwise melting of plasmid DNA." Journal of Molecular Biology **215**(2): 321-9.
- Mann, S. C., P. A. Andrews, et al. (1990). "Short-Term Cis-Diamminedichloroplatinum(II) Accumulation in Sensitive and Resistant Human Ovarian-Carcinoma Cells." Cancer Chemotherapy and Pharmacology **25**(4): 236-240.
- Marcelis, A. T. M., C. Erkelens, et al. (1984). "The Interaction of Aquated Platinum(II) Compounds with Purine Mononucleotides." Inorganica Chimica Acta **91**(2): 129-135.
- Markham, B. E. and R. R. Brubaker (1980). "Influence of Chromosome Integrity on *Escherichia-coli* Cell-Division." Journal of Bacteriology **143**(1): 455-462.
- Markowitz, S., J. Wang, et al. (1995). "Inactivation of the type II TGF-beta receptor in colon cancer cells with microsatellite instability." Science **268**(5215): 1336-8.
- Mason, M. D., J. Nicholls, et al. (1991). "The Effect of Carboplatin on Renal-Function in Patients with Metastatic Germ-Cell Tumors." British Journal of Cancer **63**(4): 630-633.
- Masters, J. R. W., R. Thomas, et al. (1996). "Sensitivity of testis tumour cells to chemotherapeutic drugs: Role of detoxifying pathways." European Journal of Cancer **32A**(7): 1248-1253.

- Masters, J. R. W. and B. Koberle (2003). "Curing Metastatic Cancer: Lessons from Testicular Germ-Cell Tumours." Nature Reviews Cancer **3**(7): 517-525.
- McAlpine, D. and B. M. Johnstone (1990). "The Ototoxic Mechanism of Cisplatin." Hearing Research **47**(3): 191-204.
- McGowan, G., S. Parsons, et al. (2005). "Contrasting chemistry of cis- and trans-platinum(II) diamine anticancer compounds: hydrolysis studies of picoline complexes." Inorganic Chemistry **44**(21): 7459-67.
- McHugh, P. J., W. R. Sones, et al. (2000). "Repair of intermediate structures produced at DNA interstrand cross-links in *Saccharomyces cerevisiae*." Molecular and Cellular Biology **20**(10): 3425-33.
- McKeage, M. J. (1995). "Comparative Adverse Effect Profiles of Platinum Drugs." Drug Safety **13**(4): 228-244.
- Meczes, E. L., A. D. J. Pearson, et al. (2002). "Schedule-Dependent Response of Neuroblastoma Cell Lines to Combinations of Etoposide and Cisplatin." British Journal of Cancer **86**(3): 485-489.
- Meczes, E. L., A. Azim-Araghi, et al. (2005). "Specific Adducts Recognised by a Monoclonal Antibody Against Cisplatin-Modified DNA." Biochemical Pharmacology **70**(12): 1717-1725.
- Medema, R. H. and J. L. Bos (1993). "The role of p21ras in receptor tyrosine kinase signaling." Critical Reviews in Oncology **4**(6): 615-61.
- Meister, A. (1983). "Selective Modification of Glutathione Metabolism." Science **220**(4596): 472-477.

- Meister, A. and M. E. Anderson (1983). "Glutathione." Annual Review of Biochemistry **52**: 711-760.
- Meister, A. (1988). "Glutathione Metabolism and Its Selective Modification." Journal of Biological Chemistry **263**(33): 17205-17208.
- Mello, J. A., S. Acharya, et al. (1996). "The Mismatch-Repair Protein hMSH2 Binds Selectively to DNA Adducts of the Anticancer Drug Cisplatin." Chemistry & Biology **3**(7): 579-589.
- Meredith, M. J. and D. J. Reed (1982). "Status of the Mitochondrial Pool of Glutathione in the Isolated Hepatocyte." Journal of Biological Chemistry **257**(7): 3747-3753.
- Micetich, K., L. A. Zwelling, et al. (1983). "Quenching of DNA:platinum(II) monoadducts as a possible mechanism of resistance to cis-diamminedichloroplatinum(II) in L1210 cells." Cancer Research **43**(8): 3609-13.
- Mishima, Y., E. Nagasaki, et al. (2004). "Combination chemotherapy (cyclophosphamide, doxorubicin, and vincristine with continuous-infusion cisplatin and etoposide) and radiotherapy with stem cell support can be beneficial for adolescents and adults with esthesioneuroblastoma." Cancer **101**(6): 1437-44.
- Misset, J. L., Y. Kidani, et al. (1991). "Oxalatoplatinum (I-Ohp) - Experimental and Clinical-Studies." Platinum and Other Metal Coordination Compounds in Cancer Chemotherapy: 369-375
- Moggs, J. G., D. E. Szymkowski, et al. (1997). "Differential human nucleotide excision repair of paired and mispaired cisplatin-DNA adducts." Nucleic Acids Research **25**(3): 480-91.

- Monti, E., M. Gariboldi, et al. (2005). "Cytotoxicity of cis-platinum(II) conjugate models. The effect of chelating arms and leaving groups on cytotoxicity: a quantitative structure-activity relationship approach." Journal of Medicinal Chemistry **48**(3): 857-66.
- Morris, W. J., M. Keyes, et al. (2009). "Evaluation of dosimetric parameters and disease response after 125 iodine transperineal brachytherapy for low- and intermediate-risk prostate cancer." International Journal of Radiation Oncology Biology Physics **73**(5): 1432-8.
- Mu, D., M. Tursun, et al. (1997). "Recognition and repair of compound DNA lesions (base damage and mismatch) by human mismatch repair and excision repair systems." Molecular and Cellular Biology **17**(2): 760-9.
- Muldoon, L. L., M. A. Pagel, et al. (2000). "Delayed Administration of Sodium Thiosulphate in Animal Models Reduces Platinum Ototoxicity Without Reduction of Antitumor Activity." Clinical Cancer Research **6**: 309-315.
- Nagai, N., K. Hotta, et al. (1995). "Effects of Sodium Thiosulfate on the Pharmacokinetics of Unchanged Cisplatin and on the Distribution of Platinum Species in Rat-Kidney - Protective Mechanism against Cisplatin Nephrotoxicity." Cancer Chemotherapy and Pharmacology **36**(5): 404-410.
- Neuwelt, E. A., R. E. Brummett, et al. (1996). "*In Vitro* and Animal Studies of Sodium Thiosulfate as a Potential Chemoprotectant against Carboplatin-Induced Ototoxicity." Cancer Research **56**(4): 706-9.
- Neuwelt, E. A., R. E. Brummett, et al. (1998). "First evidence of otoprotection against carboplatin-induced hearing loss with a two-compartment system in patients with central nervous system malignancy using sodium thiosulfate." Journal of Pharmacology and Experimental Therapeutics **286**(1): 77-84.

- Newell, D. R., Z. H. Siddik, et al. (1987). "Plasma-Free Platinum Pharmacokinetics in Patients Treated with High-Dose Carboplatin." European Journal of Cancer & Clinical Oncology **23**(9): 1399-1405.
- Newell, D. R., A. D. Pearson, et al. (1993). "Carboplatin pharmacokinetics in children: the development of a pediatric dosing formula. The United Kingdom Children's Cancer Study Group." Journal of Clinical Oncology **11**(12): 2314-23.
- Noguchi, S., Y. Kubota, et al. (1992). "Use of methotrexate, vinblastine, adriamycin, and cisplatin in combination with radiation and hyperthermia as neo-adjuvant therapy for bladder cancer." Cancer Chemotherapy and Pharmacology **30** **Suppl**: S63-5.
- Norbury, C. J. and I. D. Hickson (2001). "Cellular responses to DNA damage." Annual Review of Pharmacology and Toxicology **41**: 367-401.
- Oshita, F., N. Yamamoto, et al. (1995). "Correlation of therapeutic outcome in non-small cell lung cancer and DNA damage assayed by polymerase chain reaction in leukocytes damaged in vitro." Cancer Research **55**(11): 2334-7.
- Ozols, R. F., B. N. Bundy, et al. (2003). "Phase III Trial of Carboplatin and Paclitaxel compared with Cisplatin and Paclitaxel in Patients with Optimally Resected Stage III Ovarian Cancer: A Gynecologic Oncology Group Study." Journal of Clinical Oncology **21**(17): 3194-3200.
- Pajor, A. M. (2006). "Molecular properties of the SLC13 family of dicarboxylate and sulfate transporters." Pflugers Archiv-European Journal of Physiology **451**(5): 597-605.

- Parker, R. J., A. Eastman, et al. (1991 (a)). "Acquired Cisplatin Resistance in Human Ovarian-Cancer Cells Is Associated with Enhanced Repair of Cisplatin-DNA Lesions and Reduced Drug Accumulation." Journal of Clinical Investigation **87**(3): 772-777.
- Parker, R. J., I. Gill, et al. (1991 (b)). "Platinum DNA Damage in Leukocyte DNA of Patients Receiving Carboplatin and Cisplatin Chemotherapy, Measured by Atomic-Absorption Spectrometry." Carcinogenesis **12**(7): 1253-1258.
- Parsons, S. K., M. W. Neault, et al. (1998). "Severe ototoxicity following carboplatin-containing conditioning regimen for autologous marrow transplantation for neuroblastoma." Bone Marrow Transplantation **22**(7): 669-74.
- Peng, H. Q., D. Hogg, et al. (1993). "Mutations of the P53 Gene do not occur in Testis Cancer." Cancer Research **53**(15): 3574-3578.
- Peng, B., M. J. Tilby, et al. (1997). "Platinum-DNA Adduct Formation in Leucocytes of Children in relation to Pharmacokinetics after Cisplatin and Carboplatin Therapy." British Journal of Cancer **76**(11): 1466-1473.
- Perego, P., M. Giarola, et al. (1996). "Association between Cisplatin Resistance and Mutation of p53 Gene and Reduced BAX Expression in Ovarian Carcinoma Cell Systems." Cancer Research **56**(3): 556-562.
- Peyrone, M. (1845). "Ueber die Einwirkung des Ammoniaks auf Platinchlorür." Annalen der Chemie und Pharmacie **51**: 1-29.
- Pfeifle, C. E., S. B. Howell, et al. (1985). "High-dose cisplatin with sodium thiosulfate protection." Journal of Clinical Oncology **3**(2): 237-44.

- Piccart, M. J., J. A. Green, et al. (2000). "Oxaliplatin or paclitaxel in patients with platinum-pretreated advanced ovarian cancer: A randomized phase II study of the European Organization for Research and Treatment of Cancer Gynecology Group." Journal of Clinical Oncology **18**(6): 1193-1202.
- Pinto, A. L. and S. J. Lippard (1985). "Sequence-dependent termination of in vitro DNA synthesis by cis- and trans-diamminedichloroplatinum (II)." Proceedings of the National Academy of Sciences of the United States of America **82**(14): 4616-9.
- Pitti, R. M., S. A. Marsters, et al. (1998). "Genomic amplification of a decoy receptor for Fas ligand in lung and colon cancer." Nature **396**(6712): 699-703.
- Pluim, D., M. Maliepaard, et al. (1999). "<sup>32</sup>P-Postlabeling Assay for the Quantification of the Major Platinum-DNA Adducts." Analytical Biochemistry **275**(1): 30-38.
- Poklar, N., D. S. Pilch, et al. (1996). "Influence of Cisplatin Intrastrand Crosslinking on the Conformation, Thermal Stability, and Energetics of a 20-mer DNA Duplex." Proceedings of the National Academy of Sciences of the United States of America **93**(15): 7606-7611.
- Polgar, C. and T. Major (2009). "Current status and perspectives of brachytherapy for breast cancer." International Journal of Clinical Oncology **14**(1): 7-24.
- Ponti, M., S. M. Forrow, et al. (1991). "Measurement of the sequence specificity of covalent DNA modification by antineoplastic agents using Taq DNA polymerase." Nucleic Acids Research **19**(11): 2929-33.
- Popoff, S. C., D. J. Beck, et al. (1987). "Repair of plasmid DNA damaged in vitro with cis- or trans-diamminedichloroplatinum(II) in Escherichia coli." Mutation Research **183**(2): 129-37.

- Prakash, S., R. E. Johnson, et al. (2005). "Eukaryotic Translesion Synthesis DNA Polymerases: Specificity of Structure and Function." Annual Review of Biochemistry **74**: 317-353.
- Raaphorst, G. P., J. M. Leblanc, et al. (2005). "A comparison of response to cisplatin, radiation and combined treatment for cells deficient in recombination repair pathways." Anticancer Research **25**(1A): 53-58.
- Reed, E., R. F. Ozols, et al. (1988). "The Measurement of Cisplatin DNA Adduct Levels in Testicular Cancer-Patients." Carcinogenesis **9**(10): 1909-1911.
- Reed, E., Y. Ostchega, et al. (1990). "Evaluation of Platinum-DNA Adduct Levels Relative to Known Prognostic Variables in a Cohort of Ovarian Cancer Patients." Cancer Research **50**(8): 2256-2260.
- Reedijk, J. (1999). "Why Does Cisplatin Reach Guanine-N7 with Competing S-Donor Ligands Available in the Cell?" Chemistry Reviews **99**(9): 2499-2510.
- Reedijk, J. and J. M. Teuben (1999). Platinum-Sulfur Interactions Involved in Antitumor Drugs, Rescue Agents, And Biomolecules in Cisplatin. Zurich, Wiley.
- Reedijk, J. (2003). "New clues for platinum antitumor chemistry: kinetically controlled metal binding to DNA." Proc **100**(7): 3611-6.
- Reslova, S. (1971). "The induction of lysogenic strains of Escherichia coli by cis-dichloro-diammineplatinum (II)." Chemical Biological Interactions **4**(1): 66-70.
- Riley, C. M., L. A. Sternson, et al. (1983). "Monitoring the reactions of cisplatin with nucleotides and methionine by reversed-phase high-performance liquid chromatography using cationic and anionic pairing ions." Analytical Biochemistry **130**(1): 203-14.

- Rixe, O., W. Ortuzar, et al. (1996). "Oxaliplatin, Tetraplatin, Cisplatin, and Carboplatin: Spectrum of Activity in Drug-Resistant Cell Lines and in the Cell Lines of the National Cancer Institute's Anticancer Drug Screen Panel." Biochemical Pharmacology **52**(12): 1855-1865.
- Roberts, J. J. and J. M. Pascoe (1972). "Cross-Linking of Complementary Strands of DNA in Mammalian Cells by Antitumour Platinum Compounds." Nature **235**: 282-284.
- Roberts, J. J. and F. Friedlos (1981). "Quantitative aspects of the formation and loss of DNA interstrand crosslinks in Chinese hamster cells following treatment with cis-diamminedichloroplatinum(II) (cisplatin). I. Proportion of DNA-platinum reactions involved in DNA crosslinking." Biochimica et Biophysica Acta **655**(2): 146-51.
- Roberts, J. J. and F. Friedlos (1987). "Differential Toxicity of *cis*- and *trans*-Diamminedichloroplatinum(II) toward Mammalian-Cells - Lack of Influence of any Difference in the Rates of Loss of their DNA-Bound Adducts." Cancer Research **47**(1): 31-36.
- Rosenberg, B., L. Vancamp, et al. (1965). "Inhibition of Cell Division in *Escherichia coli* by Electrolysis Products from a Platinum Electrode." Nature **205**: 698-699.
- Rosenberg, B., E. Renshaw, et al. (1967 (a)). "Platinum-Induced Filamentous Growth in *Escherichia coli*." Journal of Bacteriology **93**(2): 716-721.
- Rosenberg, B., L. van camp, et al. (1967 (b)). "The Inhibition of Growth or Cell Division in *Escherichia coli* by Different Ionic Species of Platinum(IV) Complexes." Journal of Biological Chemistry **242**(6): 1347-1352.
- Rosenberg, B., L. Vancamp, et al. (1969). "Platinum Compounds: A New Class of Potent Antitumour Agents." Nature **222**: 385-386.

- Rosman, K. J. R. and P. D. P. Taylor (1998). "Isotopic compositions of the elements 1997." Journal of Physical and Chemical Reference Data **27**(6): 1275-1287.
- Rybak, L. P., C. A. Whitworth, et al. (2005). "Mechanisms of Cisplatin-Induced Ototoxicity and Prevention." Hearing Research **226**: 157-167.
- Sadowitz, P. D., B. A. Hubbard, et al. (2002). "Kinetics of Cisplatin Binding to Cellular DNA and Modulations by Thiol-Blocking Agents and Thiol Drugs." Drug Metabolism and Disposition **30**(2): 183-190.
- Safaei, R., K. Katano, et al. (2004 (a)). "Cross-Resistance to Cisplatin in Cells with Acquired Resistance to Copper." Cancer Chemotherapy and Pharmacology **53**(3): 239-246.
- Safaei, R., A. K. Holzer, et al. (2004 (b)). "The Role of Copper Transporters in the Development of Resistance to Pt Drugs." Journal of Inorganic Biochemistry **98**(10): 1607-1613.
- Safaei, R. and S. B. Howell (2005). "Copper Transporters Regulate the Cellular Pharmacology and Sensitivity to Pt Drugs." Critical Reviews in Oncology Hematology **53**(1): 13-23.
- Safaei, R., S. Otani, et al. (2008). "Transport of cisplatin by the copper efflux transporter ATP7B." Molecular Pharmacology **73**(2): 461-468.
- Sakakura, C., E. A. Sweeney, et al. (1997). "Overexpression of bax sensitizes breast cancer MCF-7 cells to cisplatin and etoposide." Surgery Today **27**: 676-679.
- Salles, B., P. Calsou, et al. (2006). "The DNA repair complex DNA-PK, a pharmacological target in cancer chemotherapy and radiotherapy." Pathologie Biologie (Paris) **54**(4): 185-93.

- Samimi, G., R. Safaei, et al. (2004 (a)). "Increased Expression of the Copper Efflux Transporter ATP7A Mediates Resistance to Cisplatin, Carboplatin, and Oxaliplatin in Ovarian Cancer Cells." Clinical Cancer Research **10**(14): 4661-4669.
- Samimi, G., K. Katano, et al. (2004 (b)). "Modulation of the Cellular Pharmacology of Cisplatin and its Analogs by the Copper Exporters ATP7A and ATP7B." Molecular Pharmacology **66**(1): 25-32.
- Sandercock, J., M. K. B. Parmar, et al. (2002). "First-line treatment for advanced ovarian cancer: paclitaxel, platinum and the evidence." British Journal of Cancer **87**(8): 815-824.
- Sar, D. G., M. Montes-Bayon, et al. (2008). "*In Vivo* Detection of DNA Adducts induced by Cisplatin using Capillary HPLC-ICP-MS and their Correlation with Genotoxic Damage in *Drosophila melanogaster*." Analytical and Bioanalytical Chemistry **390**(1): 37-44.
- Saris, C. P., P. J. M. van de Vaart, et al. (1996). "*In Vitro* Formation of DNA Adducts by Cisplatin, Lobaplatin and Oxaliplatin in Calf Thymus DNA in Solution and in Cultured Human Cells." Carcinogenesis **17**(12): 2763-2769.
- Savill, J. and V. Fadok (2000). "Corpse clearance defines the meaning of cell death." Nature **407**(6805): 784-8.
- Schellens, J. H., J. Ma, et al. (1996). "Relationship between the exposure to cisplatin, DNA-adduct formation in leucocytes and tumour response in patients with solid tumours." British Journal of Cancer **73**(12): 1569-75.
- Schulz, V. (1984). "Clinical pharmacokinetics of nitroprusside, cyanide, thiosulphate and thiocyanate." Clinical Pharmacokinetics **9**(3): 239-51.

- Schutte, M., R. H. Hruban, et al. (1996). "DPC4 gene in various tumor types." Cancer Research **56**(11): 2527-30.
- Shay, J. W. and W. E. Wright (1996). "Telomerase activity in human cancer." Current Opinions in Biology **8**(1): 66-71.
- Shea, M. and S. Howell (1984). "High-performance liquid chromatographic measurement of exogenous thiosulfate in urine and plasma." Analytical Biochemistry **140**(2): 589-94.
- Shea, T. C., M. Flaherty, et al. (1989). "A Phase-I Clinical and Pharmacokinetic Study of Carboplatin and Autologous Bone-Marrow Support." Journal of Clinical Oncology **7**(5): 651-661.
- Sherman, S. E. and S. J. Lippard (1987). "Structural Aspects of Platinum Anticancer Drug Interactions with DNA." Chemistry Reviews **87**(5): 1153-1181.
- Skehan, P., R. Storeng, et al. (1990). "New Colorimetric Cytotoxicity Assay for Anticancer-Drug Screening." Journal of the National Cancer Institute **82**(13): 1107-1112.
- Slamon, D. J., G. M. Clark, et al. (1987). "Human breast cancer: correlation of relapse and survival with amplification of the HER-2/neu oncogene." Science **235**(4785): 177-82.
- Sorenson, C. M. and A. Eastman (1988 (a)). "Mechanism of *cis*-Diamminedichloroplatinum(II)-Induced Cyto-Toxicity - Role of G2 Arrest and DNA Double-Strand Breaks." Cancer Research **48**(16): 4484-4488.

- Sorenson, C. M. and A. Eastman (1988 (b)). "Influence of *cis*-Diamminedichloroplatinum(II) on DNA-Synthesis and Cell-Cycle Progression in Excision Repair Proficient and Deficient Chinese-Hamster Ovary Cells." Cancer Research **48**(23): 6703-6707.
- Sorenson, C. M., M. A. Barry, et al. (1990). "Analysis of Events Associated with Cell-Cycle Arrest at G2 Phase and Cell-Death Induced by Cisplatin." Journal of the National Cancer Institute **82**(9): 749-755.
- Soulie, P., A. Bensmaine, et al. (1997). "Oxaliplatin/cisplatin (L-OHP/CDDP) combination in heavily pretreated ovarian cancer." European Journal of Cancer **33**(9): 1400-1406.
- Soussi, T. and K. G. Wiman (2007). "Shaping Genetic Alterations in Human Cancer: The p53 Mutation Paradigm." Cancer Cell **12**(4): 303-312.
- Speelmans, G., W. Sips, et al. (1996). "The Interaction of the Anticancer Drug Cisplatin with Phospholipids is Specific for Negatively Charged Phospholipids and Takes Place at Low Chloride Ion Concentration." Biochimica et Biophysica Acta **1283**(1): 60-66.
- Speelmans, G., R. Staffhorst, et al. (1997). "Cisplatin Complexes with Phosphatidylserine in Membranes." Biochemistry **36**(34): 10545-10550.
- Sporn, M. B. (1996). "The war on cancer." Lancet **347**(9012): 1377-81.
- Strandberg, M. C., E. Bresnick, et al. (1982 (a)). "The significance of DNA cross-linking to *cis*-diamminedichloroplatinum(II)-induced cytotoxicity in sensitive and resistant lines of murine leukemia L1210 cells." Chemical Biological Interactions **39**(2): 169-80.

- Strandberg, M. C., E. Bresnick, et al. (1982 (b)). "DNA crosslinking induced by 1,2-diaminocyclohexanedichloroplatinum(II) in murine leukemia L1210 cells and comparison with other platinum analogues." Biochimica et Biophysica Acta **698**(2): 128-33.
- Sugasawa, K., J. M. Y. Ng, et al. (1998). "Xeroderma Pigmentosum Group C Protein Complex is the Initiator of Global Genome Nucleotide Excision Repair." Molecular Cell **2**(2): 223-232.
- Suzukake, K., B. J. Petro, et al. (1982). "Reduction in glutathione content of L-PAM resistant L1210 Cells confers drug sensitivity." Biochemical Pharmacology **31**(1): 121-4.
- Suzukake, K., B. P. Vistica, et al. (1983). "Dechlorination of L-phenylalanine mustard by sensitive and resistant tumor cells and its relationship to intracellular glutathione content." Biochemical Pharmacology **32**(1): 165-7.
- Szymkowski, D. E., K. Yarema, et al. (1992). "An intrastrand d(GpG) platinum crosslink in duplex M13 DNA is refractory to repair by human cell extracts." Proceedings of the National Academy of Sciences of the United States of America **89**(22): 10772-6.
- Teicher, B. A., S. A. Holden, et al. (1987). "Characterization of a Human Squamous Carcinoma Cell-Line Resistant to *cis*-Diamminedichloroplatinum(II)." Cancer Research **47**(2): 388-393.
- Thomas, J. P., J. Lautermann, et al. (2006). "High Accumulation of Platinum-DNA Adducts in Strial Marginal Cells of the Cochlea is an Early Event in Cisplatin but not Carboplatin Ototoxicity." Molecular Pharmacology **70**(1): 23-29.

- Tilby, M., C. Johnson, et al. (1991). "Sensitive Detection of DNA Modifications induced by Cisplatin and Carboplatin *In Vitro* and *In Vivo* using Monoclonal Antibody." Cancer Research **51**: 123-129.
- Twentyman, P. R., K. A. Wright, et al. (1991). "Radiation Response of Human Lung-Cancer Cells with Inherent and Acquired-Resistance to Cisplatin." International Journal of Radiation Oncology Biology Physics **20**(2): 217-220.
- Urakami, S., M. Igawa, et al. (2002). "Combination chemotherapy with paclitaxel, estramustine and carboplatin for hormone refractory prostate cancer." Journal of Urology **168**(6): 2444-2450.
- Vaisman, A., M. Varchenko, et al. (1998). "The Role of hMLH1, hMSH3, and hMSH6 Defects in Cisplatin and Oxaliplatin Resistance: Correlation with Replicative Bypass of Platinum-DNA Adducts." Cancer Research **58**(16): 3579-3585.
- van Boom, S. S. G. E. and J. Reedijk (1993). "Unprecedented Migration of [Pt(Dien)]<sup>2+</sup> (Dien = 1,5-Diamino-3-Azapatane) from Sulfur to Guanosine-N7 in S-Guanosyl-L-Homocysteine (Sgh)." Journal of the Chemical Society - Chemical Communications(18): 1397-1398.
- Veal, G. J., C. Dias, et al. (2001). "Influence of Cellular Factors and Pharmacokinetics on the Formation of Platinum-DNA Adducts in Leukocytes of Children Receiving Cisplatin Therapy." Clinical Cancer Research **7**(8): 2205-2212.
- Veal, G. J., J. Errington, et al. (2007). "Adaptive Dosing and Platinum-DNA Adduct Formation in Children Receiving High-Dose Carboplatin for the Treatment of Solid Tumours." British Journal of Cancer **96**(5): 725-731.
- Vieitez, J. M., M. Valladares, et al. (2003). "Phase II study of carboplatin and 1-h intravenous etoposide and paclitaxel in a novel sequence as first-line treatment of patients with small-cell lung cancer." Lung Cancer **39**(1): 77-84.

- Volckova, E., L. P. Dudones, et al. (2002). "HPLC Determination of Binding of Cisplatin to DNA in the presence of Biological Thiols: Implications of Dominant Platinum-Thiol Binding to its Anticancer Action." Pharmaceutical Research **19**(2): 124-131.
- Von Hoff, D. D., R. Schilsky, et al. (1979). "Toxic effects of cis-dichlorodiammineplatinum(II) in man." Cancer Treatment Reports **63**(9-10): 1527-31.
- Wang, W., S. N. Ke, et al. (2004). "Effect of lung resistance-related protein on the resistance to cisplatin in human ovarian cancer cell lines." Oncology Reports **12**(6): 1365-1370.
- Wang, D. and S. J. Lippard (2005). "Cellular Processing of Platinum Anticancer Drugs." Nature Reviews Drug Discovery **4**(4): 307-320.
- Wang, X. and Z. Guo (2007). "The Role of Sulfur in Platinum Anticancer Chemotherapy." Anticancer Agents in Medicinal Chemistry **7**(1): 19-34.
- Waud, W. R. (1987). "Differential Uptake of *cis*-Diamminedichloroplatinum(II) by Sensitive and Resistant Murine L1210 Leukemia-Cells." Cancer Research **47**(24): 6549-6555.
- Weaver, D. A., E. L. Crawford, et al. (2005). "ABCC5, ERCC2, XPA and XRCC1 transcript abundance levels correlate with cisplatin chemoresistance in non-small cell lung cancer cell lines." Molecular Cancer **4**: -.
- Weinberg, R. A. (1995). "The retinoblastoma protein and cell cycle control." Cell **81**(3): 323-30.
- Weiner, M. W. and C. Jacobs (1983). "Mechanism of cisplatin nephrotoxicity." Federation of the American Societies for Experimental Biology **42**(13): 2974-8.

- Welsh, C., R. Day, et al. (2004). "Reduced levels of XPA, ERCC1 and XPF DNA repair proteins in testis tumor cell lines." International Journal of Cancer **110**(3): 352-361.
- Welters, M. J., M. Maliepaard, et al. (1997). "Improved <sup>32</sup>P-Postlabelling Assay for the Quantification of the Major Platinum-DNA Adducts." Carcinogenesis **18**(9): 1767-74.
- Werner, A. (1893). "Beitrag zur Konstitution Anorganische Verbindungen." Zeitschrift fur Anorganische Chemie **3**(1): 267-330.
- Witkin, E. M. (1967). "The Radiation Sensitivity of *Escherichia coli B*: A Hypothesis Relating Filament Formation and Prophage Induction." Proceedings of the National Academy of Sciences of the United States of America **57**(5): 1275-1279.
- Wolf, C. R., A. D. Lewis, et al. (1987). "The role of glutathione in determining the response of normal and tumor cells to anticancer drugs." Biochemical Society Transactions **15**(4): 728-30.
- Wong, E. and C. M. Giandomenico (1999). "Current Status of Platinum-Based Antitumor Drugs." Chemical Reviews **99**(9): 2451-2466.
- Woynarowski, J. M., W. G. Chapman, et al. (1998). "Sequence- and Region-Specificity of Oxaliplatin Adducts in Naked and Cellular DNA." Molecular Pharmacology **54**(5): 770-777.
- Woynarowski, J. M., S. Faivre, et al. (2000). "Oxaliplatin-Induced Damage of Cellular DNA." Molecular Pharmacology **58**(5): 920-927.
- Wright, W. E., M. A. Piatyszek, et al. (1996). "Telomerase activity in human germline and embryonic tissues and cells." Developmental Genetics **18**(2): 173-9.

- Wyllie, A. H., J. F. Kerr, et al. (1980). "Cell death: the significance of apoptosis." International Review of Cytology **68**: 251-306.
- Yamada, M., E. O'Regan, et al. (1997). "Selective Recognition of a Cisplatin-DNA Adduct by Human Mismatch Repair Proteins." Nucleic Acids Research **25**(3): 491-495.
- Yarden, Y. and A. Ullrich (1988). "Growth factor receptor tyrosine kinases." Annual Review of Biochemistry **57**: 443-78.
- Young, R. C., S. P. Hubbard, et al. (1974). "Chemotherapy of Ovarian Carcinoma." Cancer Treatment Reviews **1**(2): 99-110.
- Zakian, V. A. (1995). "Telomeres - Beginning to Understand the End." Science **270**(5242): 1601-1607.
- Zamble, D. B., D. Mu, et al. (1996). "Repair of cisplatin-DNA adducts by the mammalian excision nuclease." Biochemistry **35**(31): 10004-10013.
- Zamboni, W. C., A. C. Gervais, et al. (2004). "Systemic and Tumor Disposition of Platinum after Administration of Cisplatin or STEALTH Liposomal-Cisplatin Formulations (SPI-077 and SPI-077 B103) in a Preclinical Tumor Model of Melanoma." Cancer Chemotherapy and Pharmacology **53**: 329-336.
- Zhao, Y., H. D. Thomas, et al. (2006). "Preclinical evaluation of a potent novel DNA-dependent protein kinase inhibitor NU7441." Cancer Research **66**(10): 5354-62.
- Zhou, Y., M. C. Wood, et al. (1994). "A Time-of-Flight SIMS study of the Chemical Nature of Highly Dispersed Pt on Alumina." Journal of Catalysis **146**: 82-86.
- Zwelling, L. A., K. W. Kohn, et al. (1978). "Kinetics of Formation and Disappearance of a DNA Cross-Linking Effect in Mouse Leukemia L1210 Cells Treated With *cis*- and *trans*-Diamminedichloroplatinum(II)." Cancer Research **38**: 1762-1768.

## Appendix

### Section A: NMR

#### Section 1: Reaction of cisplatin with dGMP

Samples for NMR were prepared in ultrapure water. dGMP was dissolved at 10 mM, and cisplatin at 5 mM. For the NMR analyses of dGMP alone, samples were freeze dried then re-dissolved in 0.7 mL D<sub>2</sub>O. This was done twice. For the NMR analyses of platinated dGMP samples were incubated with cisplatin (2:1 molar ratio) for 72hrs, and then freeze dried and re-dissolved in D<sub>2</sub>O. This was done once.

NMR analysis of dGMP was predicted to detect 7 protons, as labelled in figure A1. <sup>1</sup>H- and COSY-NMR analysis of dGMP alone is shown in figures A2 and A3. <sup>1</sup>H- and COSY-NMR analysis of a reaction mixture of cisplatin with dGMP is shown in figures A4 and A5.

NMR analysis of dGMP alone showed 7 detectable proton peaks. These were assigned as shown in figure A1 (assignment by Professors Bernard Golding and William McFarlane). NMR analysis of a mixture of cisplatin-dGMP showed 7 peaks comparable to those seen in the analysis of dGMP alone.

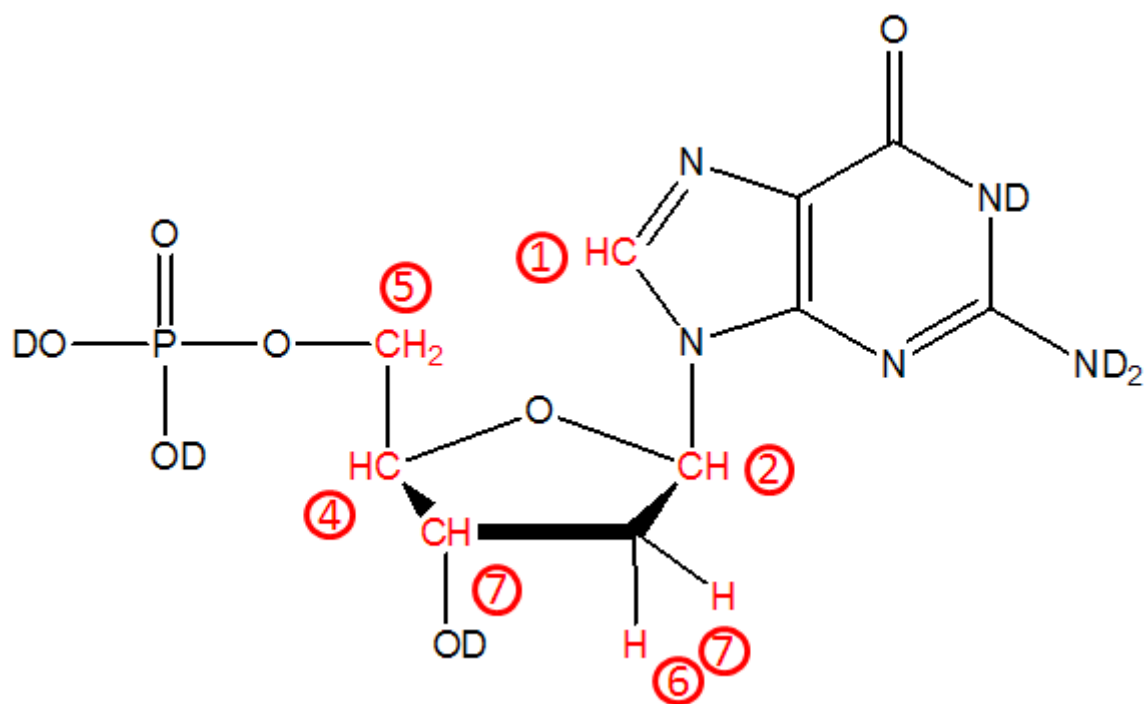


*Figure A1: Structure of dGMP and 7 protons predicted detected by NMR*

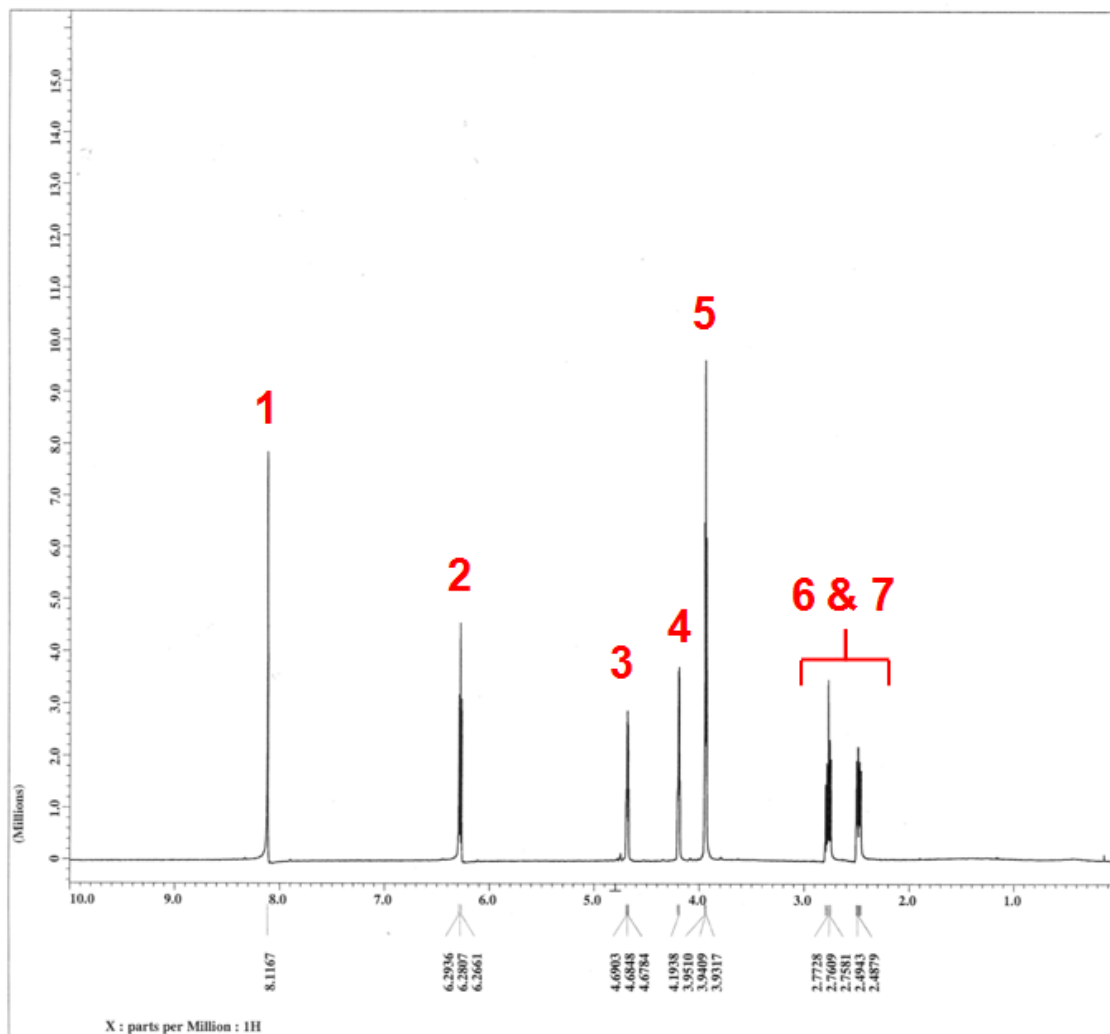


Figure A2:  $^1\text{H-NMR}$  analysis of 10 mM dGMP dissolved in water



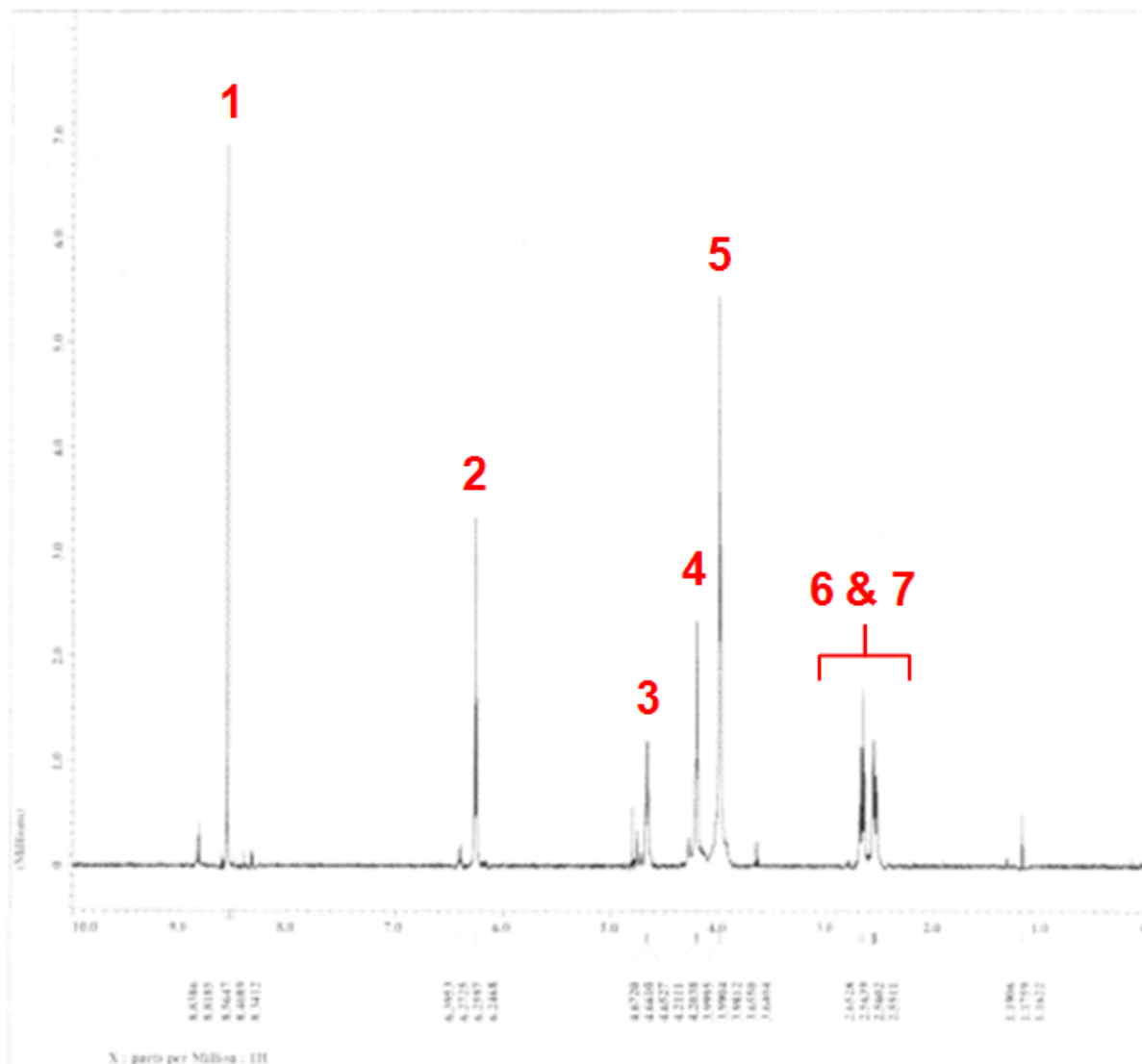


Figure A4:  $^1\text{H-NMR}$  analysis of a reaction mixture of 5mM cisplatin and 10 mM dGMP dissolved in water

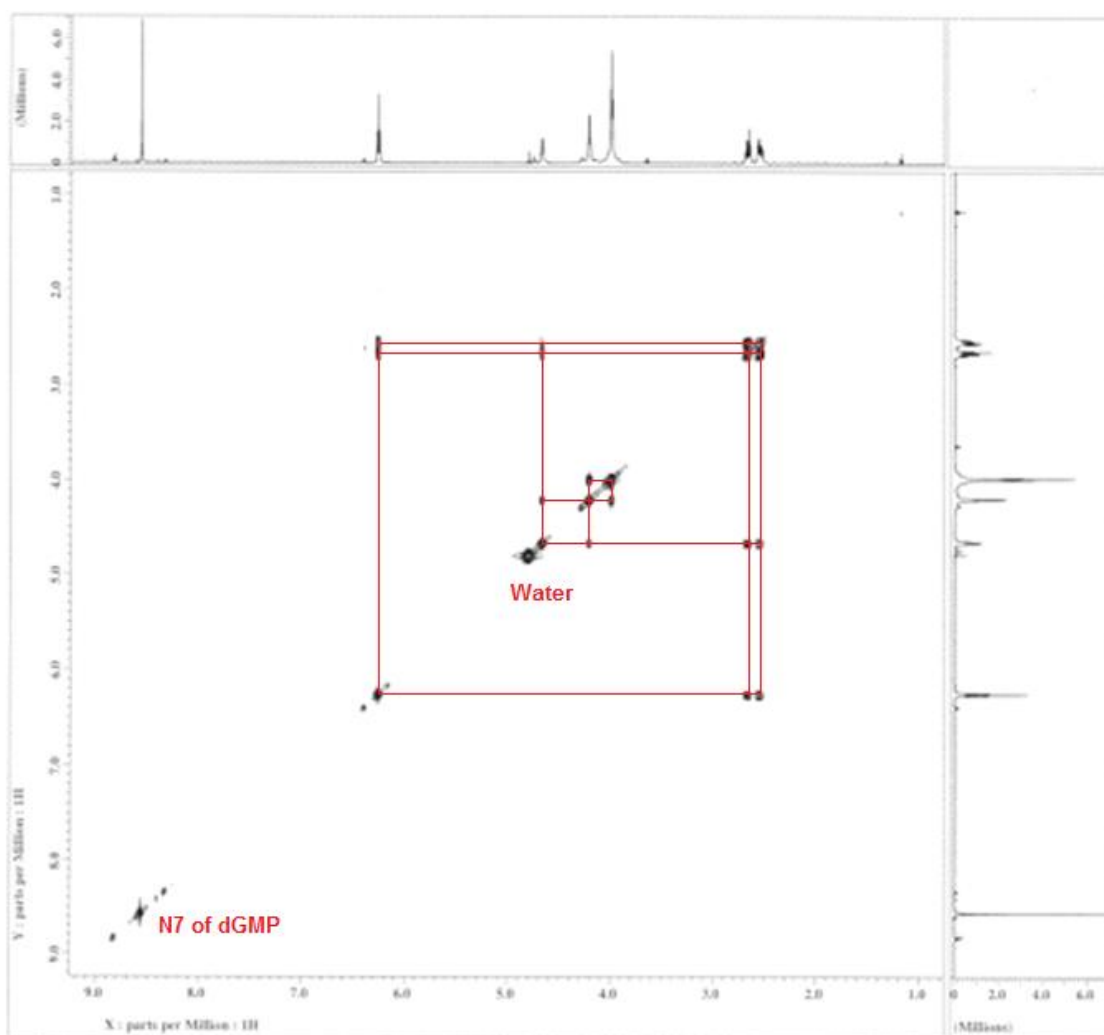


Figure A5: COSY-NMR analysis a reaction mixture of 5mM cisplatin and 10 mM dGMP dissolved in water

## **Section 2: Reaction of cisplatin with GSH**

Samples for NMR were prepared in ultrapure water. GSH was dissolved at 10 mM, and cisplatin at 5 mM. For the NMR analyses of GSH alone, samples were freeze dried then re-dissolved in 0.7 mL D<sub>2</sub>O. This was done twice. For the NMR analyses platinated GSH samples were incubated with cisplatin (2:1 molar ratio) for 72hrs, and then freeze dried and re-dissolved in D<sub>2</sub>O. This was done once.

NMR analysis of GSH was predicted to detect 7 protons, as labelled in figure A6. <sup>1</sup>H- and COSY-NMR analysis of GSH alone is shown in figures A7 and A8. <sup>1</sup>H- and COSY-NMR analysis of a reaction mixture of cisplatin with GSH is shown in figures A9 and A10.

NMR analysis of GSH alone showed 6 detectable proton peaks. These were assigned as shown in figure A6 (assignment by Professors Bernard Golding and William McFarlane). NMR analysis of a mixture of cisplatin-dGMP showed multiple peaks, though it was not possible to draw any reliable conclusions from the data.

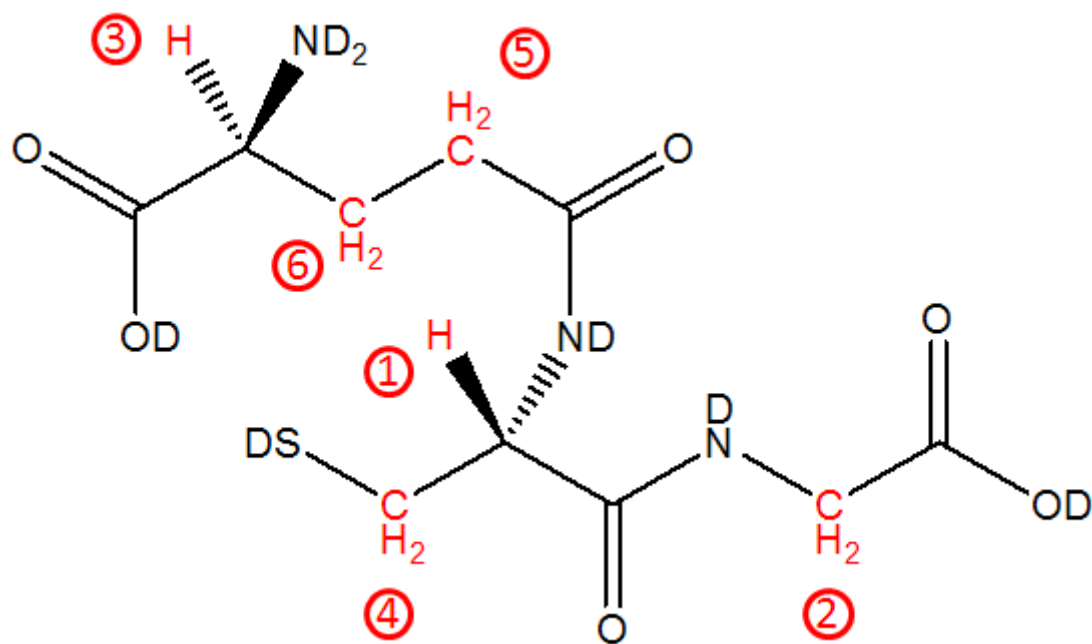


Figure A6: Structure of GSH and 6 protons predicted detected by NMR

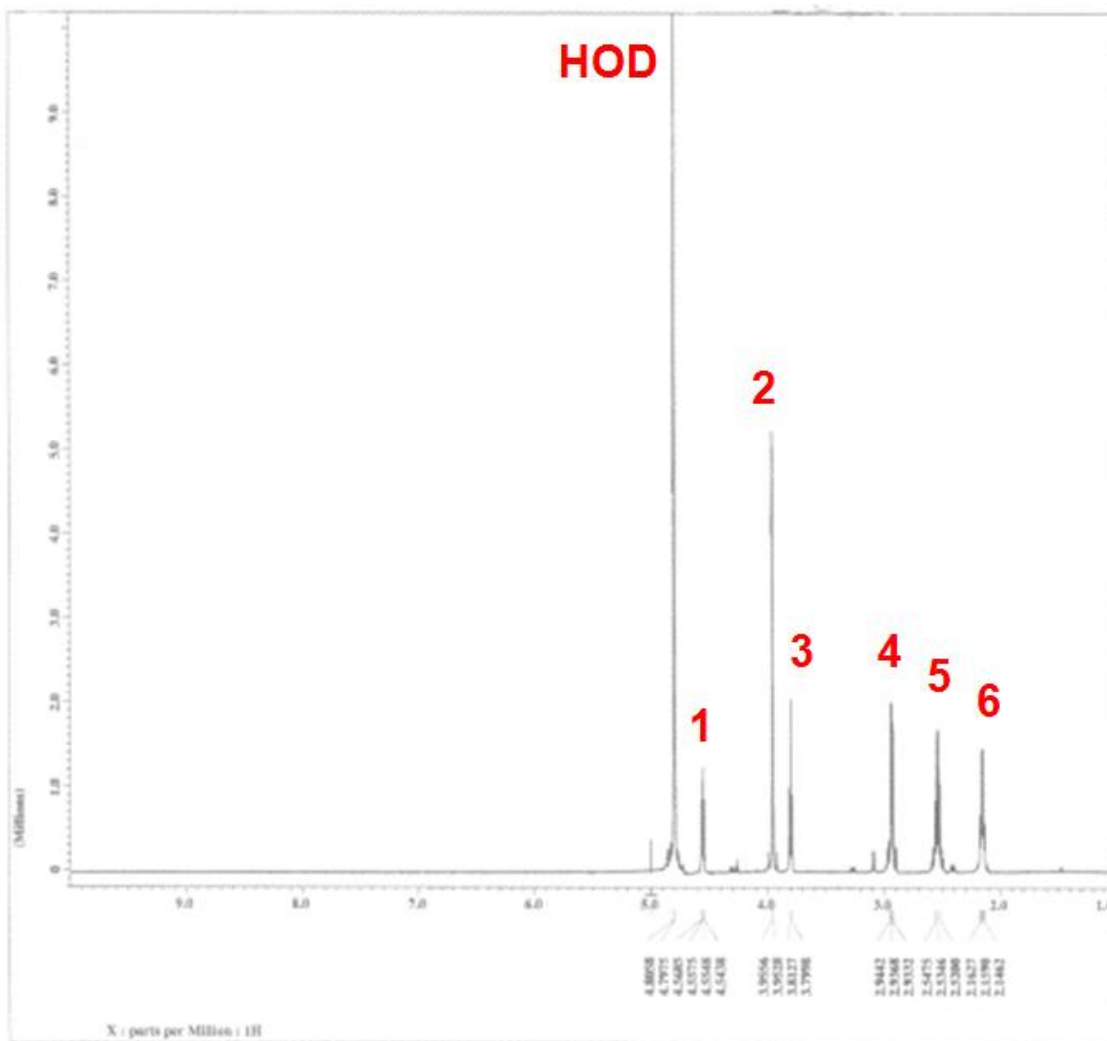


Figure A7:  $^1\text{H-NMR}$  analysis of 10 mM GSH dissolved in water

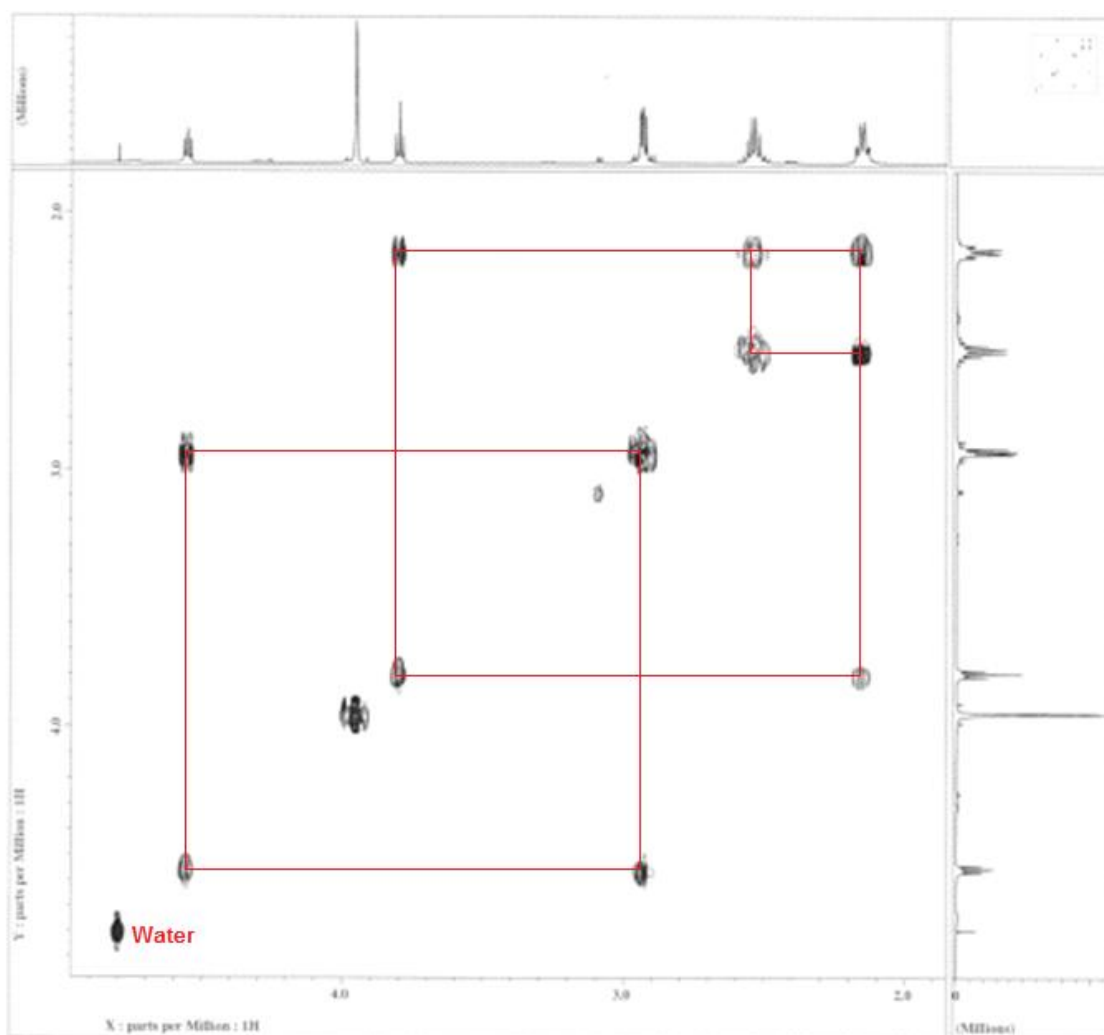
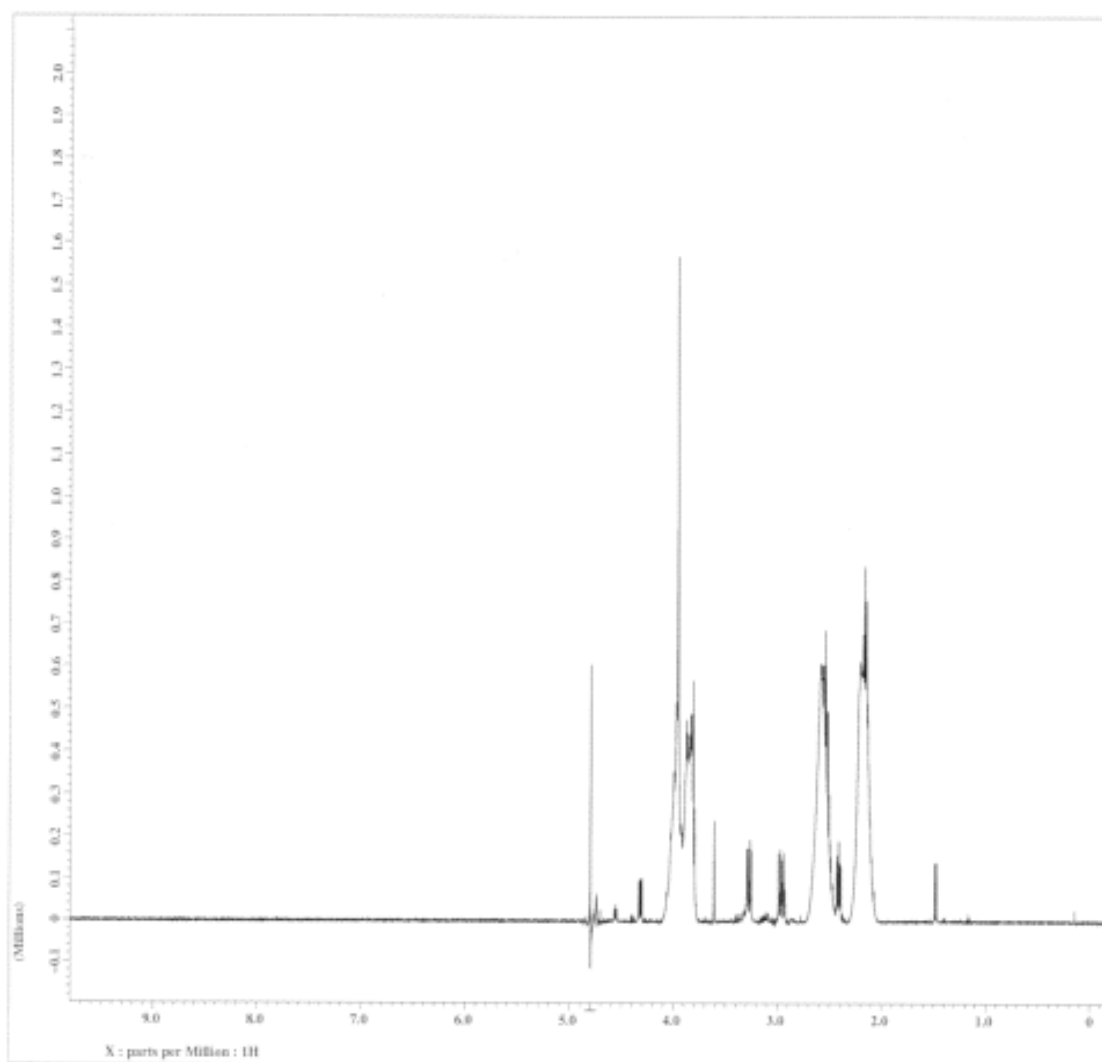


Figure A8: COSY-NMR analysis of 10 mM GSH dissolved in water



*Figure A9:  $^1\text{H-NMR}$  analysis of a reaction mixture of 5mM cisplatin and 10 mM GSH dissolved in water*

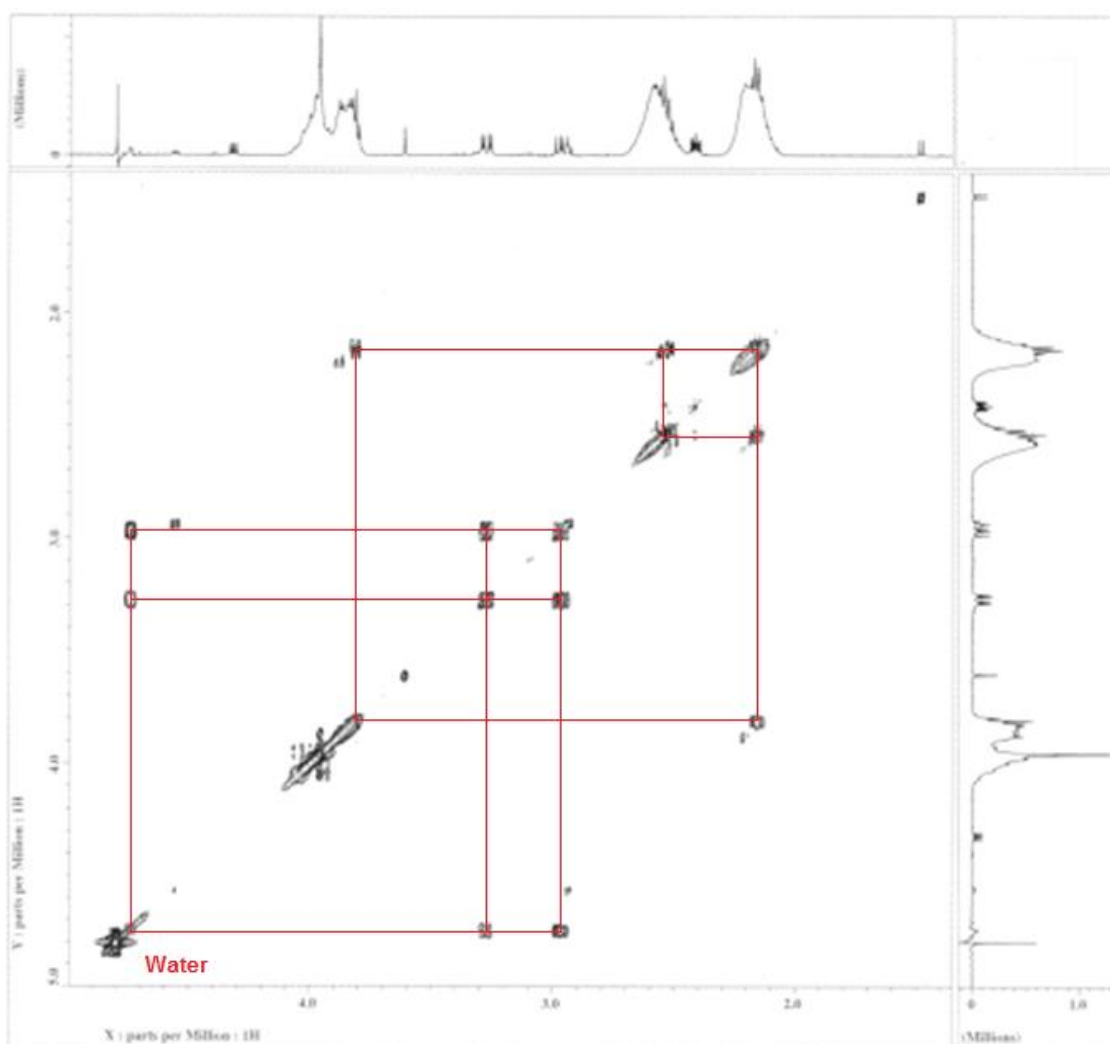


Figure A10: COSY-NMR analysis a reaction mixture of 5mM cisplatin and 10 mM dGMP dissolved in water

## Section B: FIGO Staging for Ovarian Cancer

The FIGO (International Federation of Gynaecological Oncologists) staging system is used to identify the spread of an ovarian cancer at the time of diagnosis and is used to determine appropriate therapy regimes.

Stage 1: The tumour is confined to the ovary/ovaries

- Stage 1A
  - Only one ovary is affected by the tumour, the ovary capsule is intact
  - No tumour is detectable on the surface of the ovary
  - No malignant cells are detected in the abdominal fluid
- Stage 1B
  - Both ovaries are affected by the tumour, the ovary capsule is intact
  - No tumour is detectable on the surface of the ovary
  - No malignant cells are detected in the abdominal fluid
- Stage 1C
  - The tumour occurs in one/both ovaries, the ovary capsule is ruptured
  - Tumour growth is detectable on the ovarian surface
  - Positive malignant cells are detected in the abdominal fluid

Stage 2: The tumour involves one/both ovaries and has extended into the pelvic region

- Stage 2A
  - The tumour has extended in the fallopian tubes and/or the uterus
  - No malignant cells are detected in the abdominal fluid
- Stage 2B
  - The tumour has extended into another organ in the pelvis (such as the bladder or rectum)
  - No malignant cells are detectable in the abdominal fluid
- Stage 2C
  - The tumour has extended into the pelvic region as defined in 2A/2B
  - Positive malignant cells are detected in the abdominal fluid

Stage 3: The tumour involves one/both ovaries with microscopically confirmed peritoneal metastasis (outside the pelvis) or regional lymph node metastasis

- Stage 3A
  - Microscopic peritoneal metastasis beyond the pelvis
- Stage 3B
  - Macroscopic peritoneal metastasis beyond the pelvis
  - Tumours less than 2 cm maximum diameter
- Stage 3C
  - Macroscopic peritoneal metastasis beyond the pelvis (> 2cm tumour diameter) and/or regional lymph node metastasis

Stage 4: Distant metastasis beyond the peritoneal cavity